The ‘dark side’ of tamoxifen: understanding adverse cellular response to endocrine therapy in ER+ breast cancer

A thesis submitted to Cardiff University in candidature for the degree of Doctor of Medicine (MD)

Michael David Rees

2018

Breast Cancer Molecular Pharmacology Group

Cardiff University

Declaration of Statements

This work has not been submitted in substance for any other degree or award at this or any other university or place of learning, nor is being submitted concurrently in candidature for any degree or other award.

Signed _____ (candidate) Date _____

Statement 1

This thesis is being submitted in partial fulfilment of the requirements for the degree of MD.

Signed _____ (candidate) Date _____

Statement 2

This thesis is the result of my own independent work/investigation, except where otherwise stated.
Other sources are acknowledged by explicit references. The views expressed are my own.

Signed _____ (candidate) Date _____

Statement 3

I hereby give consent for my thesis, if accepted, to be available online in the University's Open Access repository and for inter-library loan, and for the title and summary to be made available to outside organisations.

Signed _____ (candidate) Date _____

Statement 4: Previously Approved Bar on Access

I hereby give consent for my thesis, if accepted, to be available online in the University's Open Access repository and for inter-library loan after expiry of a bar on access previously approved by the Academic standards and Quality Committee.

Signed _____ (candidate) Date _____

Summary

Background: Endocrine resistance is a common problem in estrogen receptor positive (ER+) breast cancer, particularly in the advanced setting. Beyond the anticipated effects of endocrine resistance, recent evidence points towards some ER+ cancers exhibiting a counterintuitive, adverse response to endocrine treatments, particularly in the setting of E-cadherin deficiency. Here the effects of adverse cell response to endocrine therapy is explored, including responsible cellular mechanisms. The ER co-receptor PELP-1, found to be of importance in mediating a pro-invasive response to endocrine treatments, was further explored in relation to its function in ER+, as compared to triple negative breast cancer (TNBC).

Methods: The effects of endocrine treatments on the proliferative and invasive/migratory capacity of ER+ and TNBC cells, in the presence or absence of functional E-cadherin and/or PELP-1, were determined using cell counting and trans-well Boyden chamber-based assays respectively. For TNBC cells, studies were extended into 3D culture models. Mechanistic studies on endocrine-mediated modulation of cell signalling were determined by Western blotting.

Results: Tamoxifen and fulvestrant induced a pro-invasive/pro-migratory phenotype in ER+ MCF-7 cells that displayed a high basal expression of PELP-1. This effect was augmented in the setting of E-Cadherin suppression and regulated in a Src-dependent manner. In contrast, no adverse phenotype was observed with cells cultured in estrogen-deprived conditions. PELP-1 suppression reduced endocrine-induced invasion/migration in MCF-7 cells, whilst PELP-1 knockdown in TNBC cells inhibited endogenous invasion in 2D and 3D culture.

Conclusion: ER-targeting anti-estrogens may be responsible for inducing an adverse cell phenotype in ER+ breast cancers that highly express PELP-1; this effect may be more apparent in tumours that are also E-cadherin deficient. Such tumours may benefit from treatment with aromatase inhibitors as opposed to ER-targeting agents. PELP-1 may be an important target for future therapy, and act as a biomarker, predicting response to treatment in ER+ and TNBC.

Acknowledgements

My work was generously funded by the PINK Appeal, a charity founded by a remarkable group of women whose fundraising activities to support breast cancer research in Cardiff has become well established over several years. I am grateful to them for allowing me this opportunity.

I would like to take this opportunity to thank my supervisors. Firstly, I would like to thank Dr Stephen Hiscox, whose original ideas initially conceived this project, and who has guided me through the transition from surgeon to researcher over these last 3 years. I would also like to thank my clinical supervisor Professor Peter Barrett-Lee, who has been extremely supportive over this time and whose insights into aspects of this project have been invaluable. I am enormously grateful to you both.

All the members of the Breast Cancer Molecular Pharmacology Group (BCMPG) at the School of Pharmacy, Cardiff University, have been extremely helpful. I would like to thank Carol Dutkowski and Huw Mottram for their help in tissue culture, along with Richard McClelland, Sue Kyme and Pauline Finlay for their general support in the laboratory. I would like to say a special thank you to Chris Smith, as without his help, dedication and countless hours of support, I am sure I would not have been able to get to complete this work.

Outside of my own laboratory I would like to thank Dr Aled Clayton and his group, and Dr Chiara Moriconi, both at Cardiff University, for their help in optimizing and troubleshooting the 3D cell invasion assays used as part of this thesis.

Finally, I would like to take this opportunity to thank my wife, Lisa, for her unbelievable levels of understanding and support while I have completed this work, particularly after the birth of our son, Gethin. Above everyone else, I could not have done it without you!

Publications, Presentations and Posters

Papers

- Rees M, Smith C, Barrett-Lee P and Hiscox S. PELP-1 promotes adverse endocrine therapy response in ER+ breast cancer. 2018. Cancer Research. 78 (Suppl 13): 2884. (Abstract Only)
- Rees M, Smith C, Barrett-Lee P and Hiscox S. PELP-1 regulates adverse endocrine responses to endocrine therapy in Estrogen Receptor (ER) positive breast cancer. 2018. European Journal of Cancer. 92 (S121-S122). (Abstract Only)

Presentations

- M. Rees, C. Smith, P. Barrett-Lee and S. Hiscox. PELP-1 regulates adverse endocrine responses to endocrine therapy in Estrogen Receptor (ER) positive breast cancer. Royal Society of Medicine Presidents Day, Cardiff, 29th September 2017.

Posters

- M. Rees, C. Smith, P. Barrett-Lee and S. Hiscox. PELP-1 promotes adverse endocrine therapy response in ER+ breast cancer. European Breast Cancer Conference, Barcelona, 21st – 23rd March 2018

Table of Contents

1.0 Introduction

1.1 Breast Cancer

Breast cancer remains the most common form of cancer in females worldwide with an estimated 1.7 million new cases diagnosed globally in 2012 (1). The incidence of the disease varies across the world, with the highest rates reported across Northern Europe, North America and Oceania, and the lowest incidences reported in Asia and Africa (2). Within the UK there were 53,700 new cases diagnosed in 2013 alone, making it the most common form of cancer, accounting for 15% of all new cancer cases (3). Although breast cancer is predominantly a disease affecting females, 1% of all cases occur in male patients (3).

A number of key risk factors for breast cancer have been identified, including overall age, age at menarche and menopause and family history (4). In addition lifestyle factors also influence the incidence of disease, including obesity, alcohol consumption, age at first pregnancy (4), and more notably use of the combined oral contraceptive pill (5) and hormone replacement therapy (6). These risk factors are all associated with an increased lifetime exposure to estrogen, known to be a common contributing factor in the development of breast cancer (4).

Outside of estrogen exposure, genetic aspects also play an important role in the development of breast cancer, giving rise to up to 10% of all cases (7, 8). The most common of these cases are related to inheritance and expression of mutations within the BRCA1 and BRCA2 genes, which are tumour suppressor genes that play an integral role in response to cellular stress via activation on DNA repair processes, and are typically transmitted in an autosomal dominant fashion (7, 9). Inheritance of the mutated form of these genes is associated with a significant increase in risk of developing breast cancer, with the lifetime risk of breast cancer development in these individuals in the region of 45-80% (10). Outside of breast cancer mutations within the BRCA genes also correspond to an increased risk of ovarian, colonic and endometrial cancer among others (7). Tumour development

tends to occur at a younger age when compared to non-genetic breast cancers (8), with an increased tendency for breast tumours to be of basal-like or "triple negative" subtype (7)

Breast cancer incidence in the UK has been increasing over the last 30 years, a result of several factors. These include the ageing population and declining birth rate seen amongst Western societies and lifestyle factors, such as rising rates in obesity and the tendency of a sedentary lifestyle (11, 12). In addition the development of breast cancer screening programs amongst the individual nations of the UK have increased breast cancer detection rates, which has also contributed to this trend (13). Despite this increasing incidence, survival has improved significantly over this same period with age standardised 5-year survival in England and Wales improving from 53% in 1971-1972 to 87% during 2010-2011 (3). While this figure represents an improvement in the curative rate for early stage breast cancer, it also indicates an increasing proportion of patients living longer with controlled recurrent and metastatic disease.

Breast cancer is increasingly seen as a heterogeneous disease and can be classified by histological and molecular subtype. Histologically, invasive ductal carcinoma (IDC) is the most prevalent subtype, comprising around 80% of all breast cancers (14), and is mainly defined by its inability to demonstrate sufficient morphological characteristics to be classified into the other defined histological subtypes (15). The most common of these is lobular carcinoma, which accounts for around 15% of cases, and is characterised by the composition of non-cohesive cells individually dispersed or arranged in a single-file linear pattern amongst a fibrous stroma (15). Breast cancer can be further subdivided histologically, based on the tumours expression of the ER, PR and HER2 receptors. This classification is mainly based on immunohistochemistry (IHC) techniques to identify expression, is independent of the macroscopic cellular features of the tumour, and is generally a more useful classification as it helps guide treatment and prognosis on the basis of predicted response to ER and HER2 targeted therapies.

More recently reclassification of breast cancer on the basis of microarray gene expression profiling has taken place, which in addition to traditional ER, PR and

HER2 status, also takes into consideration the expression of several others elements, such as cytokeratins, basal markers and proliferative markers, including Ki-67(16). This reclassification allows tumours to be divided into six intrinsic subtypes (Table 1.1), with each subtype demonstrating a different prevalence, prognosis, response to treatment and recurrence risk (16, 17).

Intrinsic Subtype	ER	PR	HER2	Ki67	Outcome	Prevalence
Luminal A	+	+	-	-	Good	23.7%
Luminal B (HER2-)	+	+/-	-	+	Intermediate	38.8%
Luminal B (HER2+)	+	+/-	+	+	Poor	14%
HER2+ (Non-Luminal)	-	_	+	+/-	Poor	11.2%
Basal-Like	-	-	-	+/-	Poor	12.3%
Normal-Like	+	+	-	-	Intermediate	7.8%

Table 1.1 – Characteristics of the molecular subtypes of breast cancer. Adapted from (16, 17). Breast cancer may be divided on a molecular basis into 6 different subtypes based on microarray profiling. Important factors that help define the molecular subtype included ER, PR, HER2 and Ki67 expression, among others.

All luminal subtypes express the ER, demonstrate a more favourable prognosis compared to their ER- counterparts, and account for around 70% of all breast cancers (17). Within this luminal subtype, luminal B tumours tend to show a higher expression of proliferative genes and relatively poorer 5 and 10-year survival data when compared to the luminal A subtype (18). Normal-like tumours also tend to have several key similarities with luminal A tumours, including ER and PR expression, with the key differences found in alternative expression

patterns, with normal-like tumours tending to resemble normal breast profiling more closely than their luminal A counterparts (16). Meanwhile, tumours with HER2 overexpression are found in around 20% of all breast cancers, have a worse prognosis when compared with luminal A tumours, but respond well to HER2-targeted therapies (19). Within this HER2 subtype, ER+ tumours are also associated with increased disease-free survival when compared with ER- tumours (20). Meanwhile, the basal-like subtype of breast cancer, typically demonstrating a lack of ER and HER2 overexpression, is associated with the worst prognosis of all subtypes (17).

The characterisation of these breast cancer subtypes based on ER and HER2 expression is partly for simplicity purposes, as routine clinical use of molecular profiling at present is costly and impractical. Indeed, the actual picture is increasingly complex and does not always follow the patterns of expression laid out above. For example, within ER+/HER2- tumours, occurrence rates of non-luminal tumours by gene expression are found in up to 11% of cases (21). A variety of tumour types also exist within the HER2+ subgroup, which may predict the degree of response to HER2 targeted treatments (22). Meanwhile, although the terms basal-like and triple-negative breast cancer (TNBC) is commonly used interchangeably, to denote absence of ER, PR and HER2 expression, only 86% of basal-like tumours demonstrate this pattern of expression (21). Despite these variations, classification based on ER and HER2 status still offers significant advantages due to its ease of application and its usefulness in making management plans for patients based on tumour biology.

Whilst surgery to excise breast tumours and associated axillary lymph nodes remains the initial treatment of choice for most early stage breast cancers, helping to achieve local control of disease, both local and systemic non-surgical treatments are playing and ever more important role in treatment. Advances in such treatment have been primarily based on a better understanding of breast cancer biology and its associated molecular subtypes, as outlined above. This has helped by promoting the development of more personalised care, which has allowed clinicians to better define the benefits of treatments, based on tumour sub-type,

and tailor therapies appropriately. One such example is the treatment of ER+ tumours with hormone manipulation or endocrine therapy. Another is the development of HER2 targeted therapies, such as Trastuzamab (Herceptin ®), for the treatment of HER2+ disease, which given together with standard chemotherapy has improved the 3-year survival of HER2+ cancers by up to 50% (23). While systemic therapies were traditionally given to breast cancer patients in the adjuvant setting, following the completion of surgery, more recently the use of neoadjuvant chemotherapy for locally advanced and traditionally poor prognostic tumours has become more mainstream. This has allowed tumour down-staging prior to surgery (24), and in some cases may bring about a complete tumour pathological response (pCR), whereby residual tumour is no longer detectable on histology following surgical excision. This type of treatment is particularly common amongst patients with HER2+ and TNBC, due to the higher rates of pCR seen amongst these tumour subtypes as compared to luminal cancer subtypes (21). Indeed, pCR is seen in around 25-35% of TNBC patients treated with neoadjuvant anthracycline/taxane chemotherapy (25), while the more recent advent of combination Pertuzamab/Trastuzamab therapy in the neoadjuvant setting for HER2+ disease has demonstrated pCR rates of up to 66% (26).

Further advances in personalised treatment through microarray-based technology has been made through the development of commercially available prognostic signatures, such as the 70-gene MammaPrint® microarray assay, the 21-gene Oncotype DX® assay and the 50-gene Prosigna® PAM50 assay (27). These signatures are each composed of a different set of genes but all are used to determine genetic features of the tumour, including proliferation and invasion. These features are then interpreted by computer algorithm to determine a predicted patient prognosis to help determine the benefit of adjuvant chemotherapy. These signatures have shown the highest discriminatory power amongst ER+ tumours, to which their role is currently confined. Meanwhile, their use in ER- disease is relatively limited, mainly due to the inherently high expression of pro-proliferative genes in these subtypes (27).

The improved understanding of tumour biology, as highlighted above, has resulted in a dramatic change in the landscape of breast cancer treatment over recent decades. Despite this, ongoing development is still required to build on this current understanding and develop further personalised treatment regimes, including those patients with TNBC, for whom currently no proven personalised treatment options exist. This will ultimately provide breast cancer patients with the best opportunity for long term survival, whilst avoiding the unnecessary morbidity of treatment that is inappropriate for their disease.

1.2 Estrogen and the Estrogen Receptor (ER)

1.2.1 Estrogen

While estrogens influence several physiological processes, such as reproduction, cardiovascular health, bone integrity, cognition, and behaviour, they are also implicated in the development and progression of a variety of different diseases (e.g. cancer, osteoporosis, neurodegenerative diseases, insulin resistance, endometriosis etc.) (28).

In premenopausal females circulating estrogen is predominantly from secretion of 17β-estradiol (E2) by the ovaries (29), while in postmenopausal females the predominant estrogen is estrone (E1), produced from aromatase-mediated conversion of androgens via the adrenal glands, fat, muscle and breast tissue (Figure 1.1) (30). Estrone may then also be converted to estriol (E3) via a 16α-hydroxyoestrone intermediate (31).

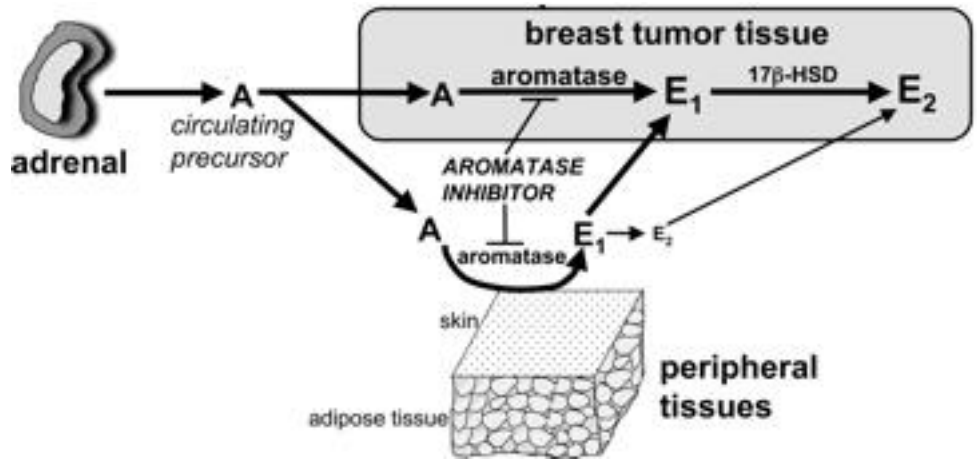

Figure 1.1 –Estrogen synthesis/conversion in post-menopausal females, including the function of aromatase. Adapted from (32). Estrone (E1) is produced by the peripheral conversion of androgens by aromatase.

The association between breast cancer and elevated levels of estrogen has been demonstrated in many studies over the last 40 years (33). This includes exposure from endogenous levels of estrogen (34), estrogen produced from endocrine associated conditions, such as obesity (35), and use of estrogens as part of

hormone replacement therapy in post-menopausal women (36). Such evidence has supported the hypothesis that increasing breast cancer risk is correlated with cumulative lifetime estrogen exposure. As such, research into estrogens mechanism of action has resulted in the development of endocrine therapies that have improved breast cancer survival significantly during this period (37, 38).

Studies in rodents have demonstrated that estrogen has carcinogenic properties in a variety of tissues in addition to the breast, including the kidneys, liver and uterus (33). While in some cases this may be related to direct DNA damage from some its oxidative metabolites (33), the main focus of interest has been its ability as a steroid hormone to permeate the cell and nuclear membrane and interact with the appropriately named estrogen receptor (ER).

1.2.2 The Estrogen Receptor (ER)

The ER and its family are a large group of nuclear receptors primarily responsible for mediating signalling related to estrogen stimulation. The ER is found in approximately 70% of all breast cancers, which are thus referred to as ER positive (ER+) cancers (39). The remainder of breast cancers lack the ER receptor and are therefore defined as ER negative (ER-). The expression of ER is closely associated with the biology of breast cancer and thus intimately linked with treatment and prognosis. Since the advent of endocrine therapies that target the ER, it's expression has generally been seen as a good prognostic factor with favourable 5-year survival data of between 80-90%, depending on corresponding HER2 expression (40).

There are two known forms of the ER, ERα and ERβ. These are coded for by separate genes (ESR1 and ESR2), found at different loci on separate chromosomes (locus 6q25.1 and locus 14q23-24.1, respectively) (41). Despite this, ERα and ERβ have some similar homologies, particularly with regards to the DNA-binding domain (42). Both receptors may also be activated by 17β-estradiol in a dose dependent manner (43), although ligand binding homology is less similar at around 55% (44). In addition ERα and ERβ can be co-expressed in cells and may

interact and dimerize with each other (45). Despite these similarities however, each receptor has differing and varying physiological functions, predominantly as a result of selective ligand binding (46). As such, ERα appears to be the predominant protein associated with breast cancer cell signalling (47, 48) and will therefore be referred to as the ER in the remainder of this work.

The ER is a 66kDa protein, consisting of 6 separate but interacting domains, and is a member of the nuclear receptor (NR) superfamily (Figure 1.2). The A/B domain of the protein is located at the N terminus and is primarily involved with protein-protein interactions and transcriptional activation of target genes via an intrinsic activation function (AF-1) (49). The C region constitutes the DNA binding domains (DBD), which is the most highly conserved region of the receptor. These DBD's are folded into a globular shape containing two zinc finger motifs, which are responsible for the binding of estrogen response elements (50). The D domain or hinge region is the most variable part of the ER and may be responsible for localisation of the ER to the nucleus (41). Finally, the E/F region of the receptor contains the ligand binding domain, or AF-2 region, located at the C terminus of the protein. This AF-2 region may undergo significant conformational changes in the presence or absence of different ligands, and therefore determines the subsequent binding of receptor co-activators or co-repressors. The AF-1 and AF-2 domains therefore control transcriptional activity of the ER (51).

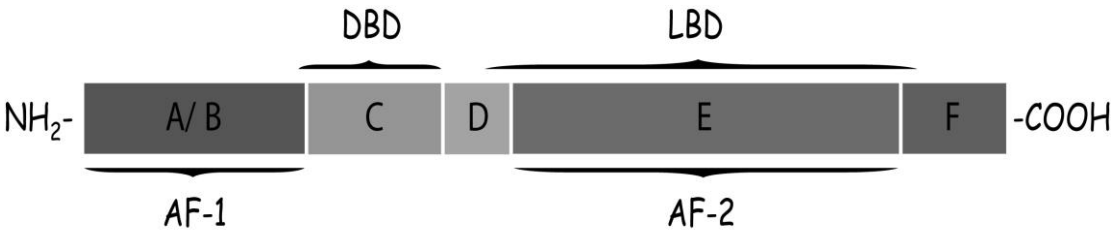

DBD: DNA binding domain

LBD: Ligand binding domain
AF-1: Ligand independent transactivation domain
AF-2: Ligand dependent transactivation domain

Figure 1.2 – Schematic representation of the ER. Adapted from (52). The ER can be divided into several domains, based on function. These include the AF-1 and AF-2 domains, which control transcriptional activity, and the highly-conserved DNA binding domain (DBD).

The ER mediates cellular signalling through two distinct mechanisms, often referred to as genomic and non-genomic signalling. In the context of genomic signalling, estrogens bind to the ER located within the cell nucleus, resulting in a conformational change in the receptor, which in turn leads to a dissociation from chaperones, receptor dimerization and subsequent activation for transcription (53). This in turn may be a result of either a classical/direct or tethered pathway. In the classical pathway ligand activation leads directly to DNA, via estrogen response elements (ERE's), allowing modulation of gene regulation to occur. Meanwhile in the tethered pathway, ligand binding results in further protein-protein interactions with other transcription factors, therefore affecting gene regulation indirectly (54). Genomic actions of the ER that are independent of ERE's include genes activated by the interaction of the ER with Fos and Jun proteins at its AF-1 binding site (55). Such genes include those for IGF-1, which is intricately involved in events that lead to pro-proliferative and anti-apoptotic effects (56), and cyclin D1, known for its role in cell cycle regulation (57). Stimulating protein-1 (SP-1) is another important mediator of ER-DNA binding, allowing the regulation of transcription for genes encoding the LDL-receptor, endothelial nitric oxide synthase (eNOS) and retinoic acid receptor-1 (58). The ER also interacts with NFkB, preventing NFkB from stimulating the expression of the cytokine IL-6, which has several pro and anti-oncogenic effects (59).

In contrast, non-genomic signalling of the ER occurs where ligand binding leads to activation of signalling cascades carried out by secondary messengers that are independent of gene transcription and regulation. Interestingly, as the ER itself

has no intrinsic kinase activity, it is reliant on the presence of co-receptors, which facilitate non-genomic signalling activity. Such proteins include Src kinase, Shc, PELP-1, the p85 subunit of PI3K and receptor tyrosine kinases, such as EGFR and IGF-1R (58, 60). As a result, the ER may form large complexes by interacting with these proteins, allowing the downstream activation of several signalling pathways, including the PLC/PKC, Ras/Raf/MAPK and PI3K/AKT pathways (58). These pathways govern several key cellular responses, such as proliferation, migration and invasion, with the resultant cellular events occurring more rapidly when compared to those related to the genomic activity of the ER (61). As such, both the genomic and non-genomic consequences of ER signalling are crucial to the development and subsequent progression of ER+ breast cancer.

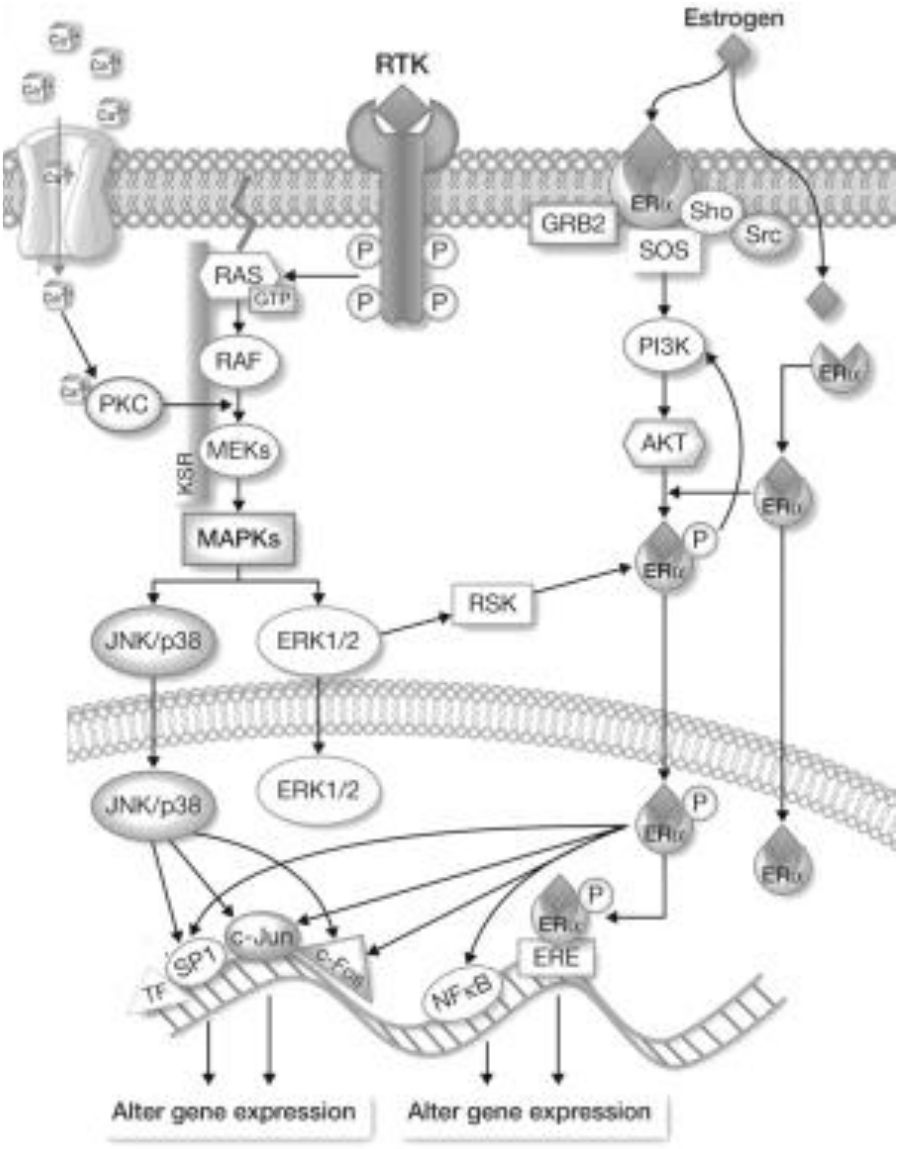

Figure 1.3 – Schematic representation of ER genomic and non-genomic signalling in breast cancer. Adapted from (62). In genomic signalling, the ER has a direct effect of transcriptional activity via either a direct or tethered pathway. In non-genomic signalling, the ER activates several signalling cascades within the cell that are independent of gene regulation and transcriptional.

1.3 Human Epidermal Growth Factor Receptor 2 (HER2)

Human epidermal growth factor 2 (HER2) is one of four members of the HER family of tyrosine kinases and is overexpressed in approximately 20% of all breast cancers (63), having originally been discovered in relation to its role in breast cancer over 30 years ago (64).

HER2 itself is a transmembrane glycoprotein, composed of 3 distinct domains; an N-terminus extracellular domain, a transmembrane domain and an intracellular tyrosine kinase domain. The N-terminus domain is the largest of these three sections of the HER2 complex and contains cysteine-rich subdomains, which are responsible for homodimerization and heterodimerization with other receptors (65). The N-terminus of the receptor may either be found in a closed (inactive), or more commonly open (active) configuration, and may switch between the two states upon ligand binding of other HER family members (63). The transmembrane domain is a single α-helix containing two dimerization motifs, thought to play a role in generating the necessary dimerization forces during receptor activation (66). The intracellular domain is composed of a juxtamembrane linker, a tyrosine kinase domains, which contains several important loops for the receptors enzyme active site, and carboxyl-terminal tail (63).

Following dimerization, HER2 may signal through several intracellular pathways, including PI3K, MAPK and Src, with the pattern of dimerization with other HER family members thought to be responsible for the production of different intracellular signalling cascades (67). HER2 signalling may disrupt E-cadherin function via phosphorylation of β-catenin, leading to a weakening in E-cadherin's tumour suppressor effects (63). In addition, estrogenic stimulation may activate HER2 signalling via cross talk with the non-genomic functions of the ER (68). Another function of HER2 is its ability to translocate to the nucleus to act as a transcription factor for several genes, including cyclin D1 and p53 (69). As such HER2 interacts with cellular controls governing proliferation, survival and invasion (70).

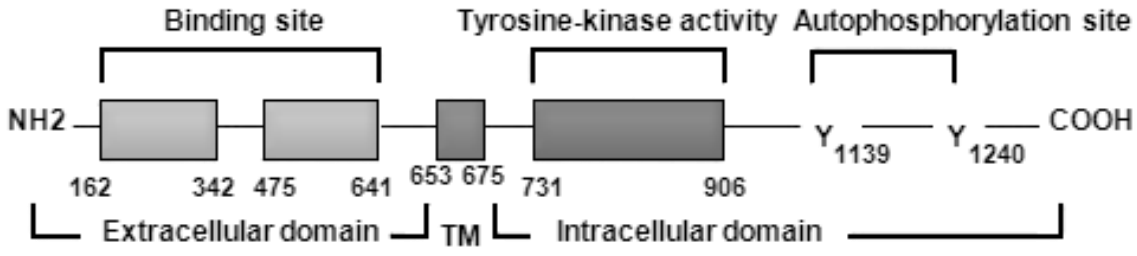

Figure 1.4 – Schematic representation of the HER2 tyrosine kinase receptor showing its distinct functional domain. Adapted from (71). The HER2 receptor may be divided into several domains based on function. These include the extracellular domain containing the receptors binding site, alongside the intracellular tyrosine kinase activity site, responsible for the receptors downstream activity.

HER2 expression appears to be inversely correlated with ER status, and usually confers a disadvantage in terms of survival outcome and pathological features (63). Despite this, drugs have been developed to target HER2 that has resulted in an improvement in patient survival. The best recognised of these is trastuzamab (Herceptin ®), which is a humanized monoclonal antibody that recognizes the external domain of HER2, currently licensed for use in the adjuvant, neoadjuvant and metastatic setting in the UK. Although it's exact mechanism of action remains unclear, it appears to inhibit downstream signalling from HER2 despite not blocking homodimerization itself (72). A newer drug that targets HER2 signalling is Pertuzamab, which is a HER dimerization inhibitor that prevents HER2 interaction with other HER family members. Pertuzamab is currently licensed in the UK for use in the neoadjuvant setting only, in combination with Trastuzamab, and to date has shown impressive results in improving the downstaging, of disease and increasing the rate of complete tumour pathological response in HER2+ tumours (26). In addition to targeted monoclonal antibody therapy alone, newer antibody-drug conjugates (ADC's) are becoming available in the setting of HER2+ breast cancer, including T-DM1 (ado-trastuzamab emtansine; T-MCC-DM-1; Kadcyla®). This drug links the HER2 targeting capability of trastuzamab with a cytotoxic moiety, in this case DM-1, and therefore has a dual action whereby

trastuzamab initially triggers receptor mediated endocytosis, followed by intracellular lysis of the complex by lysosomal degradation. This process releases DM-1 with its linker within the cell cytoplasm then allows the drug to act by inhibiting microtubule formation, which in turn initiates cell death (73). While Kadcyla® has been approved in the UK for use in HER2+ metastatic disease, trials are currently underway to assess its role in both the adjuvant and neoadjuvant setting (74)

1.4 Endocrine Therapy

Endocrine therapy is the name given to those treatments that target estrogen signalling and is a standard mode of treatment for patients with ER+ breast cancer in both the adjuvant and metastatic setting.

Treatments work by either directly antagonizing the ER itself or by inducing estrogen deprivation to reduce circulating levels of the hormone to reduce interaction with the ER. The drugs that form the mainstay of endocrine therapy in current clinical practice are outlined below.

1.4.1 Tamoxifen

Tamoxifen is a type of non-steroidal anti-estrogen, but is better described as a selective estrogen receptor modulator (SERM), because of its agonist and antagonistic properties in relation to the ER. Although first marketed in the UK as a treatment for breast cancer in 1973 (75), tamoxifen was initially developed several years earlier as a potential antifertility agent (76), while other early applications included both induction of ovulation (77) and menometrorrhagia (78).

Tamoxifen has a complex mechanism of action. While the drug competitively binds to the ligand binding domain of the ER in place of 17β-estradiol, its action is that of a partial agonist, in addition to its antagonistic properties (Figure 1.5). This paradox is complex but may be explained by the genomic signalling actions of the AF-1 and AF-2 domains of the ER (Figure 1.2). This relies on the fact that, within DNA, some promoter regions require the combined action of both the AF-1 and AF-2 domain for wild-type transcriptional activity, whereas for other promoter regions, the AF-1 and AF-2 domains may function independently (79). As Tamoxifen has been found to only activate the AF-1 region of the ER (79), tamoxifen may act as an agonist on those regions which only require AF-1 activation for transcription, as opposed to acting as an antagonist in regions that require activation of both AF-1 and AF-2. This theory alone however is unlikely to give a full explanation of tamoxifen's mechanism of action. Other studies have demonstrated for example, that the transcriptional activity produced by cell

stimulation with tamoxifen is equal to that produced by 17β-estradiol. Despite this the action of tamoxifen on the cell differs to that of estrogen and this may be due to different co-activators/suppressors that are recruited to the ER when each ligand binds (80).

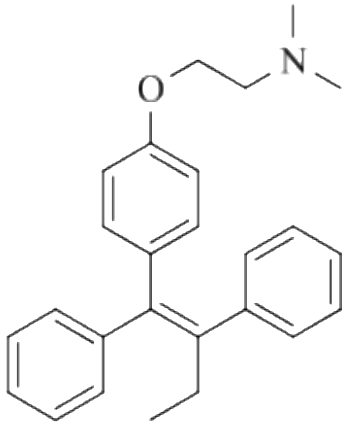

tamoxifen

Figure 1.5 – Diagram depicting the chemical configuration of tamoxifen. Adapted from (81). Tamoxifen is similar in chemical structure to the steroid hormone estrogen, allowing it to act as a competitor at the ligand binding domain of the ER.

Since its discovery, tamoxifen has remained a mainstay of treatment for both early-stage and metastatic breast cancer. In the adjuvant setting tamoxifen continues to be the first line endocrine agent for pre-menopausal women with early-stage disease (82). Its use is reserved as a second agent, after failed or poorly tolerated treatment with aromatase inhibitors, in post-menopausal patients, due to the increased risks of venous thromboembolism and endometrial carcinoma in this age group (83). The optimum duration for therapy with tamoxifen has evolved over recent years with several trials demonstrating a survival benefit when continuing tamoxifen beyond the standard 5 years of therapy (84-87). As such patients with relatively poor prognosis ER+ disease, are often offered extended endocrine therapy for up to 10 years (Figure 1.6).

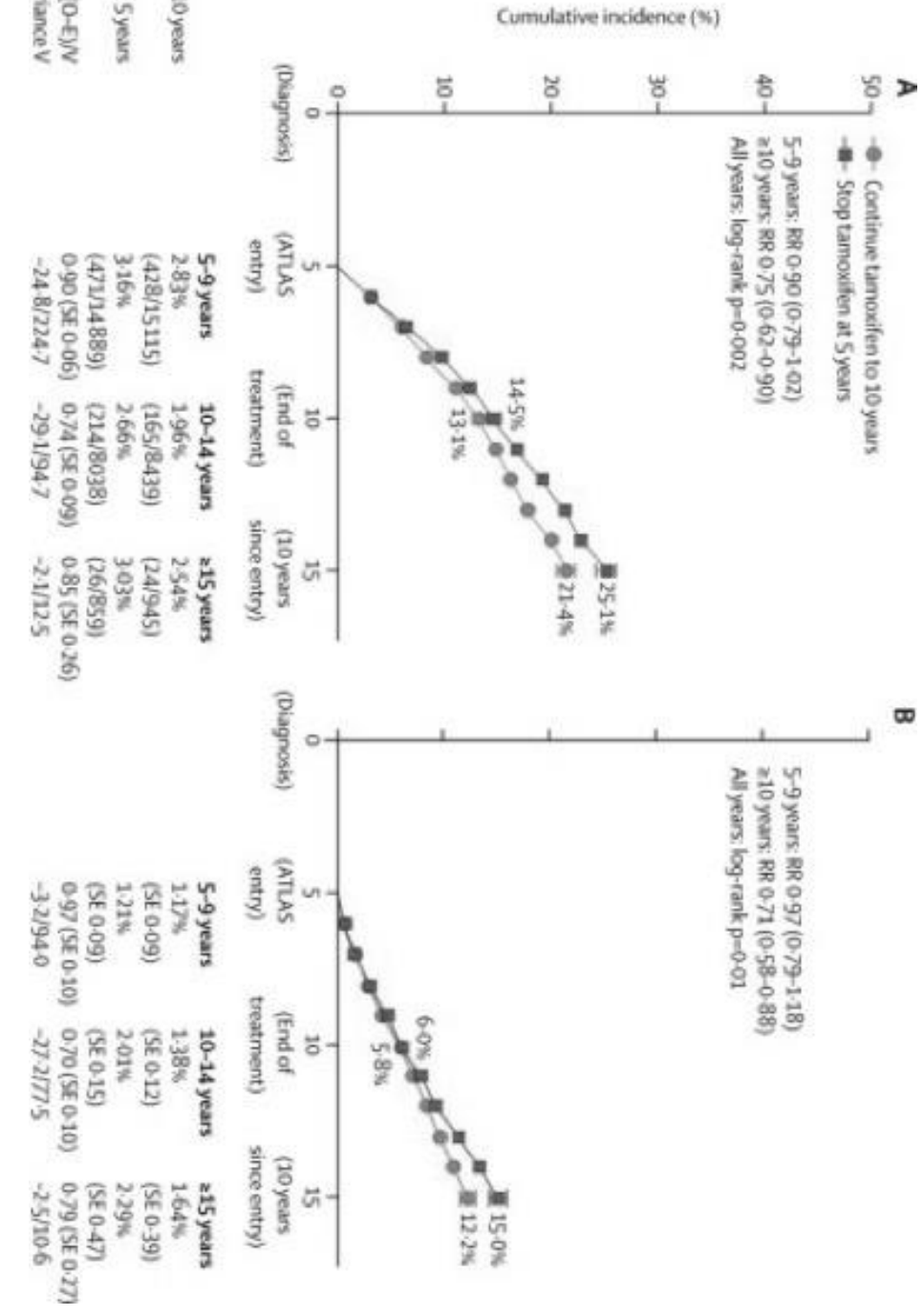

Figure 1.6 – Survival and recurrence data from the ATLAS trial. Data and graphs have been adapted from (87). Adjuvant tamoxifen therapy extended for 10 years (as compared to 5 years) results in improved (A) recurrence and (B) breast cancer survival.

In advanced breast cancer tamoxifen has been used as an effective treatment since 1969, with initial reports showing a remission rate of 22% when used as a monotherapy, despite no routine testing for ER status amongst patients (88). Later studies have also demonstrated either stability of disease or disease response in up to 53% in ER positive patients (89). This rate is of remission is often improved when combined with palliative chemotherapy. Despite this, even when treatment is successful for several years, disease often relapses due to the development of hormone resistance.

1.4.2 Fulvestrant (Faslodex ®)

Fulvestrant was originally developed as a pure ER antagonist in an attempt to overcome some of the drawbacks of tamoxifen, including the partial agonistic effects, which leads to endometrial stimulation and tumour growth, and in situations where tumours had become tamoxifen resistant (90). The structure of Fulvestrant is similar to that of estradiol, with fulvestrant having an additional alkylsulphinyl side chain, which is crucial for the antagonistic effects of the drug against the ER. Fulvestrant has a binding affinity for the ER 100 times greater than that of tamoxifen and has no agonistic effects in estrogen target tissues, including the uterus (90).

The competitive binding of Fulvestrant results in the disabling of the AF-1 and AF-2 regions of the ER, resulting in complete transcriptional inactivity. In addition, these changes also result in impaired dimerization, disrupted nuclear localization, increased turnover (91-93) and ultimately degradation of the ER (94).

While pre-clinical studies have demonstrated the relative effectiveness of fulvestrant over tamoxifen in inhibiting in-vitro growth (95, 96), results from clinical data has been more disappointing, in part due to dosing discrepancies. Current guidelines and licensing grant the use of fulvestrant as only a third-line agent in ER+ tumours in locally advanced or metastatic disease (97), given that several trials have demonstrated promising results in patients that have failed treatment with both tamoxifen and aromatase inhibitors previously (98-100).

While initial studies demonstrated a dose response effect in the range of 50-250mg of intramuscular fulvestrant (101), more recently a 500mg dose of the drug has been substantiated, based on results reported in the CONFIRM trial (102), which demonstrated improved overall survival with the higher dose. In comparison with other endocrine therapies in advanced breast cancer, the FIRST trial (103) demonstrated 500mg fulvestrant to be at least as effective as 1mg anastrozole, with the fulvestrant arm demonstrating a slightly longer time to progression than with the AI. Fulvestrant was also shown to be equally effective as tamoxifen in ER+ cancer (104), in terms of time to progression and overall response rate, although its intramuscular method of administration makes it a less practical option. The drug has also been shown to work well in combination with other agents, particularly in the metastatic setting, given the higher incidence of ER mutations, leading to hormone resistance to tamoxifen and aromatase inhibition (105). This includes combination treatment with the CDK4/6 inhibitors palbociclib® and ribociclib®, which have both impressively shown to almost double progression free survival when compared with fulvestrant therapy alone in phase III trials (106, 107).

In summary, fulvestrant is a well-tolerated third-line agent for ER+ breast cancer, whose role is mainly evident in metastatic disease. At present the role of the drug is limited, partly a result of the inconvenient monthly intramuscular dosing regimens, although it remains an important option in selected patients who have failed or are unsuitable for treatment with tamoxifen or aromatase inhibitors.

1.4.3 Aromatase Inhibitors (AI)

While the development of drugs that interact with the ER itself have played an important role in the treatment of ER+ breast cancer, the pharmacological targeting of estrogen synthesis itself has been of equal significance. This has been particularly relevant to the treatment of postmenopausal patients.

Following the menopause, approximately 90% of estrogens are produced by estradiol and oestrone biosynthesis from androgen compounds, by the cytochrome P450 enzyme aromatase (108, 109). Whilst this enzyme can be found at several sites, including the ovaries in pre-menopausal women, the placenta

during pregnancy (110), and within breast tissue itself (111, 112), its location within peripheral adipose tissue is of most crucial importance within the context of post-menopausal breast cancer.

Drug development targeting the inhibition of aromatase has been ongoing since the 1970's, with the first AI demonstrating anti-tumour effects developed for therapeutic use being aminoglutethimide (109). Since then the development of second-generation, and subsequently third-generation AI's, such as letrozole, anastrozole and examestane have demonstrated increased potency of action and improved tolerability of treatment (113). These drugs all contain imidazole or triazole rings and can therefore act as non-steroidal reversible inhibitors to aromatase (Figure 1.7).

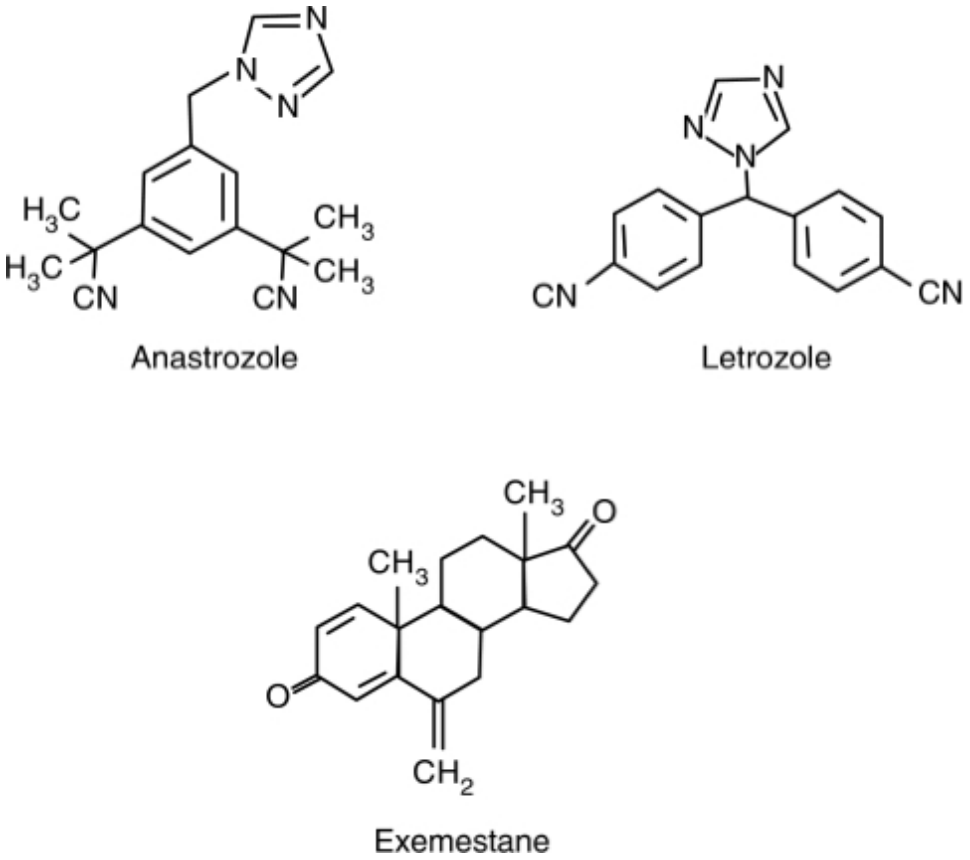

Figure 1.7 – Diagram demonstrating the chemical structures of letrozole, anastrazole and examestane. Adapted from (81). Aromatase inhibitors exhibit either a steroidal (examestane) or non-steroidal (anastrazole/letrozole) type structure.

In the UK, AI's are licensed for use as first line therapy in postmenopausal patients with ER+ breast cancer, in both the adjuvant and metastatic setting (97). Indeed, large trials have demonstrated better efficacy of AI's over tamoxifen in this age group, with AI's reducing breast cancer recurrence rates by about 30%, proportionally, over 5 years when given as adjuvant treatment (114). This advantage of AI's over tamoxifen also holds true in the metastatic setting, with improved clinical response rates (115).

One major issue with the long-term use of AI's are potential side effects and patient tolerability. Side effects include symptoms of arthralgia and hot flushes, while long term use may lead to a reduction in bone density and increased risk of osteoporosis (116). In addition, the development of resistance to AI's after sustained use also remains of significant clinical importance, as will be discussed below.

1.5 Endocrine Resistance

While endocrine therapy has played an important role in the management of ER+ breast cancer patients, clinical response, whether in the adjuvant or metastatic setting, is often finite due to the development of hormone resistance. While de-novo resistance is also of clinical relevance, with up to 20% of ER+ tumours proving refractory to first line treatment (117), it is usually acquired resistance after previous successful treatment with endocrine agents that is responsible for disease relapse or progression in most cases. In such scenarios, while second or third-line agents may be trialled, it often that the clinical benefit rate declines with each new agent given, from around 70% for first line therapies to approximately 30% when second-line agents are used (118, 119).

There are several known mechanisms as to why resistance to endocrine therapies may arise, including mutation in the ER, ER cross-talk and expression of cancer cell pathways with control independent of the ER (Table 1.2).

Cellular metabolic response	ER-related response
Decreased drug uptake	Loss or mutation of ER
Intra-cellular drug sequestration	Aberrant post-translational modification
Metabolism of tamoxifen to estrogenic compounds	Agonist action of tamoxifen
Alteration of transcription factors or ER co-regulators	Alteration of the estrogen response element
Modification of signalling pathways	Epigenetic modification
Autonomous growth factor production	ER cross-talk

Table 2.1 – Mechanisms of Endocrine Resistance in ER+ breast cancer. Adapted from (120). Endocrine resistance may be related to changes in the metabolic response to the drug, or due to inherent changes within the ER itself.

While loss ER expression itself is a relatively rare finding among hormone resistant cancers, accounting for only 10% of cases (121, 122), alternative mutations of the ESR1 gene, that merely effect the functioning of the ER, are more common. Indeed, mutations in ESR1 are relatively rare in the treatment naïve setting (123), but become more frequent, in up to 20% of metastatic and pre-treated ER+ cancer (124).

Endocrine resistance is often associated with overexpression/over-amplification of growth factor receptors, including HER2, HER3 and EGFR. These growth factors may become over-expressed through cross-talk mechanisms with the ER and tend to lead to the activation of several pathways in a Src-dependent manner, including the PI3K/AKT/mTOR and RAF/MEK/ERK pathways (125). As a result, PI3K hyper-activation may promote estrogen-independent ER transcriptional activity (126), as well as downregulating PR expression making the cell less responsive to tamoxifen (127). Meanwhile, ERK activation may phosphorylate the ER and activate various ER co-receptors to stimulate ER function despite anti-endocrine treatment (127). Outside of these mechanisms cell cycle checkpoint alterations mean cell cycle arrest is overcome by an increase in cyclin D1 and cyclin-dependent kinases, features typically associated with endocrine resistance (128).

As outlined, endocrine resistance is a significant problem in the long-term treatment of patients with ER+ breast cancer. Despite this, multiple new treatment strategies that use combination therapy are showing some signs of success in treating endocrine resistant disease (125). Such strategies include combining endocrine therapy with HER2-targeted therapy for those with HER2+ disease (129), or with an mTOR inhibitor, given that the PI3K/AKT/mTOR pathway has been shown as one of the mechanisms that confers endocrine resistance (127). In addition, given the prominent role of Src kinase expression in the context of endocrine resistance, combining endocrine therapy with a pharmacological Src inhibitor may also be a viable option, despite mixed results from clinical trials to date (130).

1.6 Adverse response to endocrine therapy

Endocrine resistance typically leads to clinical relapse and/or disease progression. Importantly, in-vitro evidence reveals that acquisition of resistance is also accompanied by the development of aggressive cellular features that can likely favour tumour progression (131, 132). Continual exposure to endocrine agents may therefore promote adaptive mechanisms that sustain cellular growth and promote cellular migratory/invasive responses. Indeed recent data has demonstrated that tamoxifen actually promotes cellular invasion in hormone responsive, MCF-7 and T47D breast cancer cells that are deficient in E-cadherin (133, 134). In addition, this invasive phenotype appeared to be related to an increase in expression of Src kinase (133, 134). Intriguingly, others have also shown that tamoxifen itself may promote cellular invasion in ER+, MCF-7 cells (135, 136), which may be linked to the association of tamoxifen treatment with FAK-mediated cytoskeletal remodeling (137) and matrix metalloproteinase expression (138). Moreover, tamoxifen has also previously been reported to promote metastases development in tumors with a variant form of the ER (139), whilst further evidence has suggested that estrogen may play a protective role in terms of the invasive and migratory capacity of breast cancer cells (140). Whilst to date there is no readily available data depicting how these findings may translate into clinical practice, under-recognition of adverse responses to endocrine therapies may be partly responsible. Indeed, it may be that some patients with ER+ cancer who experience early relapse/disease progression whilst taking endocrine therapy are wrongly attributed as having developed endocrine resistance or inherently aggressive underlying disease. As such, further work to expand knowledge in this area would seem appropriate to help define the size of this problem, understand the underlying mechanisms that may be involved in its occurrence, and helping to guide management strategies to overcome this issue.

1.7 E-cadherin

E-cadherin is one of a family of membrane-associated glycoproteins that mediate calcium-dependant cell-cell interactions (141). First described by Takeichi in 1977 in Chinese hamster V79 cells (142), E-cadherin has been found to be equally important in both normal physiological and many pathological states. By forming an important part of adherens junctions between cells, E-cadherin helps to organize and tether microfilaments to maintain cell adhesive properties and integrate both inter and intracellular signalling (143). In addition to its necessity for cells to form solid tissues, E-cadherin is also functionally important in the maintenance of cell polarity and hence is crucial in the development of the polarized epithelial cell type seen in many tissues within the human body (144, 145).

E-cadherin is a 120Kd single-pass transmembrane glycoprotein, containing an extracellular region extending from the cell surface that binds to cadherins present on adjacent cells (Figure 1.8). Meanwhile, its intracellular domain contains binding sites for interactions with members of the catenin family, and other regulatory proteins that both directly and indirectly connect E-cadherin with the actin cytoskeleton (143). The association between E-cadherin and the catenin family is important in many cell regulatory mechanisms, including endocytosis, cell survival and growth. As such, any alterations in these binding molecules can affect cell-cell interactions, resulting in increased tumour aggressiveness and cell invasion (146).

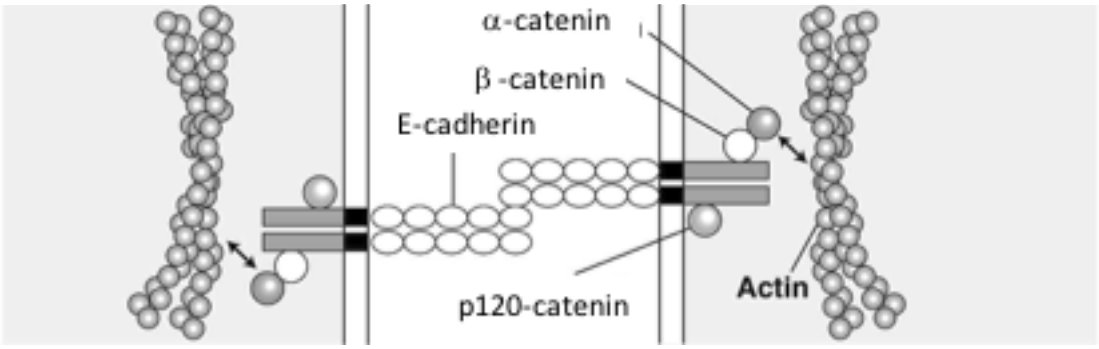

Figure 1.8 – Schematic representation of E-cadherin and its role in adherens junctions. Adapted from (147). E-cadherin associates with its counterpart on adjacent cell membranes, while being linked to the actin cytoskeleton, through its association with catenins.

One member of the catenin family of significant importance is p120 catenin, which stabilizes cadherin expression, while it's disassociation results in the endocytic internalisation of the cadherin molecule (146). Loss of p120 has also been shown to lead to increase tumour aggressiveness and is associated with high tumour grade, increased mitotic rate and the absence of ER expression in breast cancer (148). Meanwhile, α-catenin helps to strengthen the bond between adjacent E-cadherin molecules and is also found to be downregulated in cancer, with its loss associated with the reduced mechanical stability of adherens junctions, which facilitates tumour progression and metastases (149). The other prominent member of the catenin family associated with E-cadherin is β-catenin, whose expression within the cell may also have a role in tumour behaviour, and can vary depending on cancer subtype, with a more prominent nuclear as opposed to membranous localization noted amongst lobular tumours (150, 151). In addition, it is the nuclear translocation of β-catenin seen following E-cadherin loss in the process of epithelial-mesenchymal transition (EMT), that may result in the enhanced cell proliferation and oncogenic expression associated with this state (152, 153).

While EMT is a normal mechanism in many physiological events, such as embryogenesis and wound healing, it is a vital process the development of cancer metastases. During EMT, polarized epithelial cells lose their cell-cell adhesions,

along with their attachment to a basement membrane, adopting a mesenchymal phenotype, where they undergo invasion, intravasation and ultimately dissemination. Once located at a distant site, these cells reverse these cellular changes and can revert to their original epithelial subtype. During this transition, several key epithelial cell markers are suppressed, while mesenchymal markers are expressed. As a result, E-cadherin is downregulated during this process, while the mesenchymal marker N-cadherin is expressed, in a process known as the Cadherin switch (154-156).

Downregulation of E-cadherin expression is more frequently associated with basal-like, as opposed to luminal breast cancer subtypes (146), and is generally associated with a poorer prognosis, with shorter overall and disease free survival (157). This downregulation is associated with surface E-cadherin loss, changes within the cytoskeleton and subsequent changes in gene expression. These changes may then confer the dissociation and dissemination of epithelial cells and dysregulation of the cell cycle, promoting cell survival, and angiogenesis (152, 158-160).

As one might therefore expect, E-cadherin is linked to several signalling pathways that regulate cell behaviour. These include interaction with several transcription factors such as Notch1, members of the Wnt family, and TGF-β, which plays a central role in the control of EMT (161). In addition, the ErbB/EGF and EGFR pathways also play a role in downregulation of CDH1 gene expression, resulting in increased cell invasion and motility. Other molecules, such as focal adhesion kinase (FAK), β-catenin, Ras, Raf, mitogen activated protein kinase (MAPK) and PI3K/Akt also play a role in this process by up-regulating transcription suppressors such as Snail, Twist and Zeb, ultimately downregulating CDH1 expression as part of EMT (162, 163).

In summary, E-cadherin, and its associated downregulation, is a poor prognostic marker in breast cancer, and is an important component in the multi-step process in metastasis development. This appears to be related to both physical disassociation of cells through lack of adherens junctions, and through expressional and mechanistic changes within the cell itself. Despite this, its role in

the context of endocrine therapy and potential adverse cell response to such treatment is currently poorly defined, partly due to the inherent difficulty in targeting the functional absence of E-cadherin in a clinical context.

1.8 Src kinase

Src is a 60 kDa non-receptor cytoplasmic tyrosine kinase, usually activated by upstream stimulation of plasma membrane receptors (164). As the first discovered proto-oncogene (165), Src is the most widely studied member of a larger family Src kinases, which include Lyn, Fyn, Lck, Hck, Fgr, Blk, Yrk, and Yes (166, 167).

The protein is composed of several recognised domains (Figure 1.9), including a N-terminal region, involved in localization to the inner surface of the cell membrane, a unique domain specific to each member of the Src family of kinases, and a SH2 domain, which binds phosphorylated tyrosine residues of other proteins, or with other regions of the Src protein itself. In addition, a linker domain provides binding sites for intramolecular binding with the SH3 domain, while the catalytic domain contains the "activation loop", which controls substrate accessibility and harbours the kinase activity for enhanced phosphorylation of downstream molecules (166, 168).

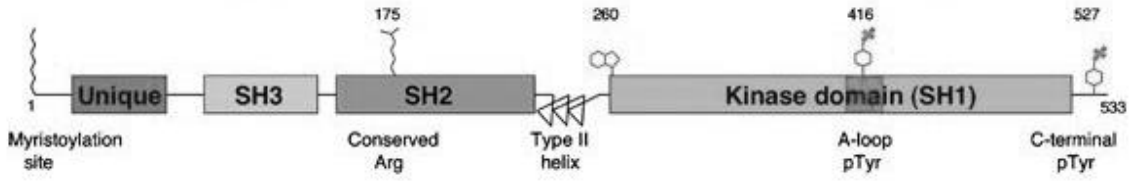

Figure 1.9 – Schematic representation of the structure of Src kinase. Adapted from (169). Src may be divided into distinct domains based on function, including the SH2 domain, which allows the proteins to interact with the ER.

The role of Src in breast cancer has become increasingly well-established over time. Elevated levels of Src activation has been demonstrated within breast cancer cells compared with normal breast tissue (170, 171). Src expression is also noted to be higher in the presence of endocrine resistance in ER+ tumours and is associated with a poorer prognosis (172). As such, Src has been implicated in several critical cellular processes for cancer cell survival and dissemination, including proliferation, angiogenesis, motility and invasion (170, 171).

Src plays an important role in signalling cross-talk between several growth promoting pathways, including those mediated by the ER, EGFR and HER2 (164). As such, Src may become activated by steroid hormones, such as estrogen (173), indirectly through this method or even by direct activation by the steroid hormone itself (174). These mechanisms allow Src to act as a mediator for the many downstream effects of EGFR and ER, whereby phosphorylation of such RTK's allows for the docking of Src. This initiates a complex set of cell-signalling pathways (Figure 1.10) that result in downstream pro-proliferative and pro-invasive effects, mediated through signalling by MAPK and AKT among others (175).

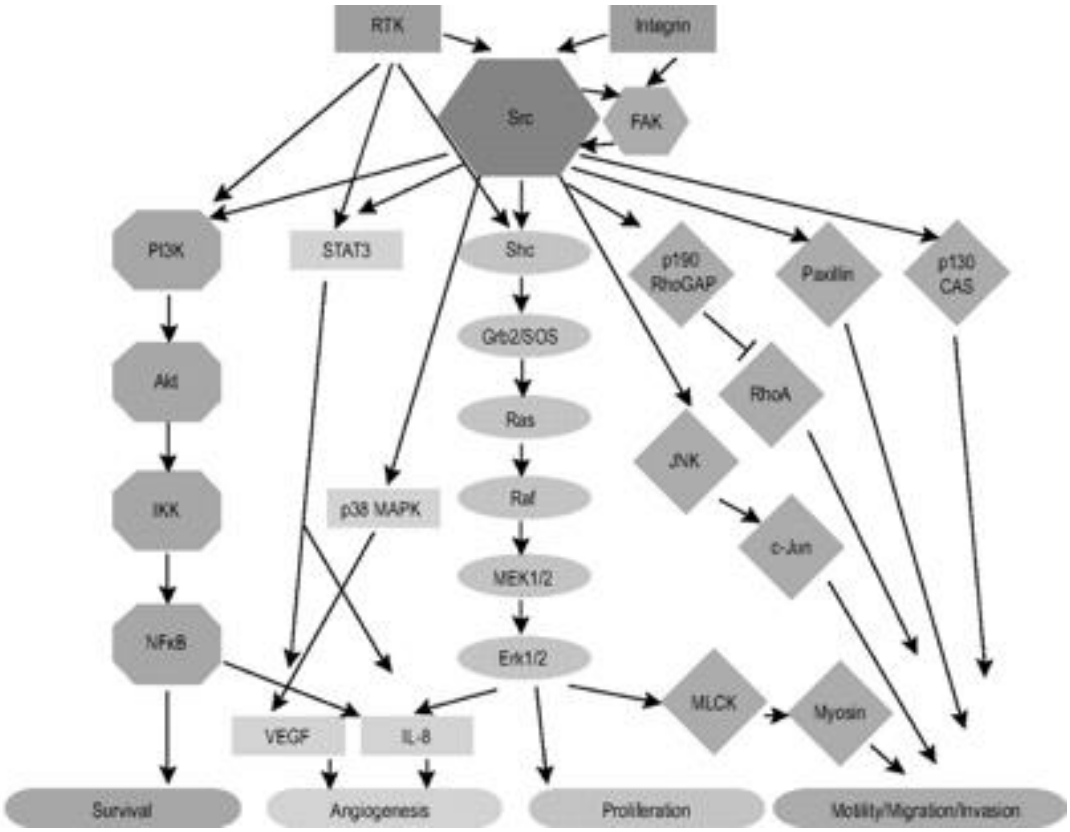

Figure 1.10 – Diagram demonstrating the downstream signalling cascades of Src kinase. Adapted from (164). Src kinase activity has many downstream effects via its interaction with cellular several signalling cascades.

Src has also been implicated in the breast cancer metastasis through its role in processes such as angiogenesis, focal adhesion and invasion, in conjunction with

EMT. In terms of angiogenesis, hypoxia has been found to activate Vascular endothelial growth factor (VEGF) through a Src dependent mechanism (176, 177). While breast cancer cell lines have shown an increase in Src activity compared with normal breast tissue (178), conversely pharmacological Src inhibition results in decreased cell motility and a less invasive cellular phenotype (179). Suppression of Src also results in a reduction of cell migration and attachment in MCF-7 cells through a FAK dependent mechanism (180), whilst also preventing cell rounding and detachment via its interaction with integrin (181).

Given the role of Src in breast cancer proliferation, invasion, angiogenesis and metastases, there has been growing interest in the development of suitable pharmacological inhibitors that may slow disease progression and be of use within the clinical environment. Indeed, preliminary pre-clinical studies have suggested Src inhibition may be a suitable therapeutic option, particularly in basal and triple-negative tumours (182, 183). One example is the small molecule multi-kinase inhibitor, Dasatinib, which inhibits several members of the SFK family (184). While its primary use lies in treating basal/triple-negative cancers (183), Dasatinib also inhibits growth of luminal cell lines to some degree, indicating a potential role amongst ER+ tumours (182, 183). In addition, AZD0530 is another potent selective inhibitor of Src and Abl kinases (175) that has been shown to inhibit Src phosphorylation in MCF-7 cells (173). AZD0530 has also been shown to suppress cellular invasion in-vitro in tamoxifen-resistant cell lines (131), while clinical trials involving its use in combination with endocrine therapies are ongoing (185).

In summary, Src kinase is a crucial component of cancer cell regulation that is central to several key pathways involved in proliferation, invasion and cancer cell metastases development. Its association with the ER and the development of endocrine resistance makes is a potential target when assessing adverse cancer cell response to endocrine agents.

1.9 3D cell culture and the tumour micro-environment

The standard methods of assessing breast cancer, or cancer cells in general, typically involves cell culture within a 2D environment. This is particularly the case where immortalised cell lines are used as the primary instrument for study. Despite this, ongoing evidence suggests that this may not necessarily always be the best way to make such assessments on cell behaviour, particularly when trying to translate findings from in-vitro studies into clinical models (186).

Traditional 2D cell culture relies on cell adherence to the flat surfaces of plastic of glassware, which provide physical support for the cells. Cells grown in such a way will have similar access to nutrients and growth factors from their surrounding medium, which results in homogenous growth and proliferation (187). While this may be a useful feature for the simplicity of scientific study, 2D culture provided no control of cell shape, which determines the biochemical cues that affects cell activity in-vivo (186). In addition, cells in our body perform activities in response to stimulation from a complex 3D microenvironment, containing the surrounding extracellular matrix (ECM), surrounding cells of similar type, as well as other cell types, such as fibroblast (188, 189). As such, natural nutrient gradients develop and waste gradients build up across such a 3D environment, affecting cell proliferation and cell death respectively (187). Given these crucial differences, interest in assessing cells in an in-vitro cell culture environment has grown over recent years.

There are several potential approaches when undertaking 3D cell culture, depending on the desired observations that are to be made (186). The majority of techniques employ embedding cells in various formation, within either an organically-derived ECM, such as collagen, or synthetic-based ECM, such as Matrigel®; a solubilized basement membrane preparation extracted from the Engelbreth-Holm-Swarm (EHS) mouse sarcoma (190). Cells are then free to interact with surrounding cells and the ECM within a 3D spatial arrangement whilst receiving nutrients from culture medium that bathes the matrix. These 3D culture systems may modified as required by changing the ECM stiffness through

changes in the BM concentration, or by co-culturing the cell of interest with other cell types, such as fibroblasts, bringing the system closer to physiological arrangements encountered in-vivo (186). Many cellular outcomes may then be studied from such culture systems, including proliferation, invasion, and also signalling changes through the extraction and separation of cells from the surrounding ECM (186).

The highlighted differences outlined above therefore make 3D cell culture a more realistic model of in-vivo conditions, particularly as significant differences have been shown to exist between cell behaviour in each type of culture system. Indeed, several studies have shown differences in cell proliferation, differentiation and gene expression between cells grown in 2D and 3D cell culture (191-193). In breast cancer, for example, the BCMPG have previously shown that culturing HER2+ breast cancer cells in a 3D environment can promote AKT to MAPK switching within the cell, causing a relative loss of therapeutic response to treatment (194). In terms of cell motion, migration has been shown to vary between 2D and 3D systems, likely due to the more complex interactions with the surrounding ECM with 3D culture and the additional obstacles created for cell movement (195, 196).

Given the above, it would therefore be of interest to study the phenotypic response of breast cancer cells to endocrine treatments as part of this thesis, assessing whether any responses seen in 2D cell culture are also evident when cells cultured in a 3D environment.

1.10 Hypothesis and Aims

Resistance to endocrine treatments is a major clinical problem, limiting the effectiveness of treatment and ultimately impacting on patient survival. Research has revealed several elements that may play a significant role with respect to resistance, which affects how breast cancers respond to endocrine therapy. Strikingly, recent data points to a loss of the cell-to-cell adhesion molecule, E-cadherin, as a mechanism by which some endocrine agents promote an adverse phenotype in hormone responsive ER+ breast cancer cells.

The primary hypothesis of this MD project is that ER-targeting endocrine agents induce an invasive phenotype in E-cadherin deficient models of ER+ breast cancer and that this response to endocrine agents may differ in 2D, compared with 3D cell culture.

The aims of this project are therefore (i) to explore endocrine agents as promoters of invasion in ER+ breast cancer under conditions of E-cadherin deficiency, (ii) explore potential regulatory pathways that may underlie this phenomenon and (iii) compare changes in cell invasion, induced by endocrine agents, in 2D and 3D cell culture systems.

2.0 Materials and Methods

2.1 Materials

Table 2.1 lists all materials used to undertake the work involved in producing this thesis, including the relevant supplier.

Material	Supplier
3-3'-Diaminobenzidine (DAB) chromogen	Dako, Stockport, UK
37% Formaldehyde	Fisher Scientific Ltd, Loughborough, UK
Acrylamide/bis-acrylamide (30%)	Sigma-Aldrich, Poole, Dorset, UK
Agarose	Bioline Ltd, London, UK
Ammonium Persulphate (APS)	Sigma-Aldrich, Poole, Dorset, UK
Amphotericin B (Fungizone)	Invitrogen, Paisley, UK
Anti-goat horseradish-peroxidase-linked IgG	Dako, Stockport, UK
Anti-mouse horseradish-peroxidase-linked IgG	Cell Signalling Technology, Leiden, Holland
Anti-rabbit horseradish-peroxidase-linked IgG	Cell Signalling Technology, Leiden, Holland
Antibiotics (penicillin/streptomycin)	Invitrogen, Paisley, UK
Aprotinin	Sigma-Aldrich, Poole, Dorset, UK
BD Cell Recovery Solution (Matrisperse®)	BD Biosciences, Oxford, UK
BD Falcon™ 50ml centrifuge tubes	BD Biosciences, Oxford, UK
Bio-Rad Dc Protein Assay Reagents	Bio-Rad laboratories Ltd, Herts, UK
Bovine Serum Albumin (BSA)	Sigma-Aldrich, Poole, Dorset, UK
Bromophenol Blue (BPB)	PDH Chemicals Ltd, Poole, Dorset, UK
Cell Culture Medium (RPMI 1640/Phenol-red-free RPMI 1640)	Invitrogen, Paisley, UK

Cell Scrapers	Greinir Bio-One Ltd, Gloucestershire, UK
Chemiluminescent (West Femto Max.)	Fisher Scientific Ltd, Loughborough, UK
Chemiluminescent Supersignal® West HRP (Dura)	Bio-Rad laboratories Ltd, Herts, UK
Chromatography Paper CHR 200	Fisher Scientific Ltd, Loughborough, UK
Corning Standard Transwell® Inserts	Fisher Scientific Ltd, Loughborough, UK
Cotton Swabs	Johnson and Johnson, Maidenhead, UK
Coulter Counter Counting Cups and Lids	Sarstedt AG and Co, Numbrecht, Germany
Dharmafect Lipid Transfection Reagent	Invitrogen, Dharmacon Inc, Chicago, USA
Di-thiotreitol (DTT)	Sigma-Aldrich, Poole, Dorset, UK
Disposable Cuvettes	Fisher Scientific Ltd, Loughborough, UK
DPX Mounting Medium	Fisher Scientific Ltd, Loughborough, UK
Eppendorf 2ml	Fisher Scientific Ltd, Loughborough, UK
Ethidium Bromide (EtBr)	Sigma-Aldrich, Poole, Dorset, UK
Ethylene Diamine Tetracetic Acid (EDTA)	Sigma-Aldrich, Poole, Dorset, UK
Filter Paper	Whatman, Maidstone, Kent, UK
Foetal Calf Serum (FCS)	Invitrogen, Paisley, UK
General Laboratory Glassware	Fisher Scientific Ltd, Loughborough, UK
Gills Haemotoxylin Solution	Sigma-Aldrich, Poole, Dorset, UK
Glass Coverslips	BDH Chemicals Ltd, Poole, Dorset, UK

Glass Slides	Fisher Scientific Ltd, Loughborough, UK
Glutamine	Invitrogen, Paisley, UK
Glycine	Sigma-Aldrich, Poole, Dorset, UK
Goat Serum 100%	DAKO Cytomation, Denmark
Histo-TEK® Cassette	Fisher Scientific Ltd, Loughborough, UK
Hydrochloric Acid (HCL)	Fisher Scientific Ltd, Loughborough, UK
Hydrogen Peroxide	Fisher Scientific Ltd, Loughborough, UK
Hyperladder™ I and IV	Bioline Ltd, London, UK
Isoton® II Azide-free Balanced Electrolyte Solution	Beckham Coulter Ltd, High Wycombe, UK
Kodak MXB Autoradiography Film (blue sensitive; 18x24cm)	Genetic Research Instrumentation (GRI), Rayne, UK
Leupeptin #L0649	Sigma-Aldrich, Poole, Dorset, UK
Lower Buffer for SDS-PAGE gels (Tris 1.5M, pH8.8	Bio-Rad Laboratories Ltd, Herts, UK
Magnesium Chloride ($MgCl_2$)	Sigma-Aldrich, Poole, Dorset, UK
Marvel® Skimmed Milk Powder	Premier International Foods, UK
Matrigel® Matrix Basement Membrane	BD Biosciences, Oxford, UK
MEK Inhibitor U0126	Cell Signalling Technology, Leiden, Holland
Micro-centrifuge Tubes	Elkay Laboratory Products, Basingstoke, UK
Molony-murine Leukaemia Virus (MMLV) Reverse Transcriptase	Invitrogen, Paisley, UK
Monoclonal Anti-b-Actin-Peroxidase clone AC-15 #A3854 200ml	Sigma-Aldrich, Poole, Dorset, UK

N,N,N',N'-tetramethylethylene-diamine (TEMED)	Sigma-Aldrich, Poole, Dorset, UK
Nitrocellulose transfer Membrane (Protran® BA85; 0.45μM Pore size)	Schleicher and Schuell, Dassell, Germany
Noble Agar	Sigma-Aldrich, Poole, Dorset, UK
ON-TARGET plus CDH1 siRNA SMARTpool	Dharmacon, GE Healthcare, Little Chalfont, UK
ON-TARGET plus Non-targeting (NT) siRNA	Dharmacon, GE Healthcare, Little Chalfont, UK
ON-TARGET plus PELP-1 (27043) siRNA SMARTpool	Dharmacon, GE Healthcare, Little Chalfont, UK
Paraplast Plus® Paraffin Wax	Sigma-Aldrich, Poole, Dorset, UK
Perifosine #14240	Cell Signalling Technology, Leiden, Netherlands
pH Calibration Buffer Tablets (pH4.7 and 10)	Fisher Scientific Ltd, Loughborough, UK
Phenylarsinine Oxide	Sigma-Aldrich, Poole, Dorset, UK
Phenylmethylsulfonyl Fluoride (PMSF)	Sigma-Aldrich, Poole, Dorset, UK
Pipette Tips	Greiner Bio-one Ltd, Gloucestershire, UK
Polyoxyethylene-sorbitan Monolaurate (Tween 20)	Sigma-Aldrich, Poole, Dorset, UK
Ponceau S Solution [0.1% (w/v) in 5% Acetic Acid]	Sigma-Aldrich, Poole, Dorset, UK
Potassium Chloride (KCL)	Sigma-Aldrich, Poole, Dorset, UK
Precision Plus Protein® All Blue Standards (10-250kDa)	Bio-Rad laboratories Ltd, Herts, UK
Protein Dye (#500-0006)	Bio-Rad laboratories Ltd, Herts, UK
Random Hexamers (RH)	Amersham, Little Chalfont, UK
Restore Plus Western Blot Stripping Agent #46430	Fisher Scientific Ltd, Loughborough, UK

RNase-free H_20	Sigma-Aldrich, Poole, Dorset, UK
RNAsin® Ribonuclease Inhibitor	Sigma-Aldrich, Poole, Dorset, UK
RPMI Medium 1640	Fisher Scientific Ltd, Loughborough, UK
Sodium Azide	Sigma-Aldrich, Poole, Dorset, UK
Sodium Chloride (NaCl)	Sigma-Aldrich, Poole, Dorset, UK
Sodium Dodecyl Sulphate (SDS)	Sigma-Aldrich, Poole, Dorset, UK
Sodium Fluoride (NaF)	Sigma-Aldrich, Poole, Dorset, UK
Sodium Hydroxide (NaOH)	Fisher Scientific Ltd, Loughborough, UK
Sodium Molybdate (Na_2MoO_4)	Sigma-Aldrich, Poole, Dorset, UK
Sodium Orthovanadate ($NaVO_4$)	Sigma-Aldrich, Poole, Dorset, UK
Solvents (i.e. Acetone, Chloroform, Ethanol, Formaldehyde, Paraformaldehyde, Isopropranol, Xylene, Methanol)	Fisher Scientific Ltd, Loughborough, UK
Sterile Phosphate Buffered Saline (PBS)	Invitrogen, Paisley, UK
Sterile Bijou Vials (5ml)	Bibby Sterilin Ltd, Stone, UK
Sterile Cell Culture Plastic ware	Nunc International, Roskilde, Denmark
Sterile Disposable Serological Pipettes (5ml, 10ml, 25ml)	Sarstedt AG and Co. Numbrecht, Germany
Sterile Falcon Tubes	Sarstedt AG and Co. Numbrecht, Germany
Sterile Syringe Filters (0.2μm)	Becton Dickinson (BD) UK Ltd, Oxford, UK
Sterile Syringe Needles	Sherwood-Davis & Geck, Gosport, Hampshire, UK

Sterile Syringes (BD Plastipak™ 2ml, 5ml, 10ml, 20ml)	Becton Dickinson (BD) UK Ltd, Oxford, UK
Sterile Universal Containers (30ml)	Greiner Bio-One Ltd, Gloucestershire, UK
Sucrose	Fisher Scientific Ltd, Loughborough, UK
Taq DNA Polymerase (Bio Taq™; 5U/μl)	Bioline Ltd, London, UK
Temed	Sigma-Aldrich, Poole, Dorset, UK
Tri Reagent	Sigma-Aldrich, Poole, Dorset, UK
Tris HCl	Sigma-Aldrich, Poole, Dorset, UK
Triton X-100	Sigma-Aldrich, Poole, Dorset, UK
Trizma (Tris) Base	Sigma-Aldrich, Poole, Dorset, UK
Trypsin/EDTA 10x Solution	Invitrogen, Paisley, UK
TWEEN-20 BioXtra	Sigma-Aldrich, Poole, Dorset, UK
Upper Buffer for SDS-PAGE Gels (Tris 0.5M, pH 6.8)	Bio-Rad Laboratories Ltd, Herts, UK
Vectorshield® Hard-set Mounting Medium inc. DAPI Nuclear Stain	Vector Laboratories Inc, Peterborough, UK
Vectorshield® Soft-set Mounting Medium inc. DAPI Nuclear Stain	Vector Laboratories Inc, Peterborough, UK
Western Blocking Reagent	Roche, Mannheim, Germany
X-ray Film Developer and Fixer Solutions (X-O-dev)	Photon Imaging Systems, Ashton Keynes, UK

Table 2.1 – Materials. All materials used to undertake the work involved in producing this thesis are listed in alphabetical order, including the relevant supplier.

2.2 Cell Lines and Cell Culture

2.2.1 Cell Media

RPMI 1640 containing phenol-red pH indicator (RPMI) was supplemented with 5% or 10% (cell line dependent) foetal calf serum (FCS), penicillin (1000units/ml), streptomycin (100ug/ml) and amphotericin B (2.5μg/ml), and used for routine cell culture (referred to at R5% or R10% respectively).

Phenol-red-free RPMI 1640 (WRPMI) was supplemented with 5% FCS, L-Glutamine (200mM), penicillin (1000units/ml), streptomycin (100ug/ml) and amphotericin B (2.5μg/ml), and was used for experimental culture (referred to as W5%).

Finally, Phenol-red-free RPMI 1640 (WRPMI) was supplemented with 5% charcoal stripped foetal calf serum (SFCS), L-Glutamine (200mM), penicillin (1000units/ml), streptomycin (100ug/ml) and amphotericin B (2.5μg/ml), and was used for experimental culture (referred to as W5%s).

2.2.2 Cell Lines

Hormone sensitive MCF-7 wild type cell line, originally from the American Type Culture Collection (ATCC©), were maintained in R5%. The T47D cell line (ATCC©) was used as an alternative luminal A breast cancer cell line and were also maintained in R5%. The BT474 and MDA-MB-361 cell lines, both ER+ve and HER2+ve (ATCC©), were maintained in R10%. The ER-ve and HER2-ve cell line, MDA-MB-231 (ATCC©) was maintained in R5%, while the alternative ER-ve, HER2-ve cell line, MDA-MB-468 (ATCC©) was maintained in R10%. Finally, the tamoxifen resistant MCF-7 cell line (TamR) is an in-house cell line derived from prolonged exposure of MCF-7 cells to Tamoxifen, allowing the development on in-situ resistance. TamR cells were grown in W5%s supplemented with 4-hydroxytamoxifen (100nM), commonly referred to as tamoxifen.

Cell Line	Routine Culture Medium	Experimental Culture Medium
MCF7	RPMI + 5%FCS	WRPMI + 5%FCS
T47D	RPMI + 5%FCS	WRPMI + 5%FCS
BT474	RPMI + 10%FCS	WRPMI + 10%FCS
MDA-MB-361	RPMI + 10%FCS	WRPMI + 10%FCS
MDA-MB-231	RPMI + 5%FCS	WRPMI + 5%FCS
MDA-MB-468	RPMI + 10%FCS	WRPMI + 10%FCS

Table 2.2 – Cell Lines and Culture Media. Cells were generally cultured in medium containing RPMI during routine culture, while WRPMI was used during experimental procedures to eliminate the potential estrogenic activity of phenol red.

2.2.3 Cell Culture Techniques

All cell culture was undertaken under sterile conditions within a MDH Class II laminar-flow safety cabinet. Equipment and consumables were either purchased as sterile for single use or sterilized at 119°C using a Denley BA852 autoclave.
Cell were maintained in 25cm^2 (T25) flasks within a Sanyo MCO-17AIC incubator at a constant temperature of 37°C and within a humidified atmosphere containing 5% CO_2. Cells were assessed using a phase contrast microscope (Nikon UK Ltd, Kingston-Upon-Thames, UK) with culture medium changed every 3-4 days and cells passaged when 70-95% confluence was achieved.
During routine passage, culture medium was removed from the incubating vessel and cells were dispersed from monolayer culture by adding 5ml of Trypsin (0.05%)/EDTA (0.02%) in PBS. Culture vessels were then incubated for 3-5 minutes until cells were in suspension before the Trypsin/EDTA was neutralised with an equal volume of culture medium and the cells suspension transferred to a universal container. Cells were then pelleted by centrifugation (Jouan C312, Thermo Fisher Scientific Inc, MA, USA) at 1000rpm for 5 minutes. The supernatant

was then decanted and the cell pellet re-suspended in culture medium before seeding to further culture vessels containing an appropriate volume culture medium (usually at a 1:10 ratio).

2.2.4 Cell Counting

For each experimental procedure, the same technique as described above was followed, but in order to obtain a single cell suspension, cells were passed through a sterile 25G needle. Assessment of cell number was then made by adding 100µl of the re-suspended cell solution in 10ml of Isoton® II solution before cell counting was determined using a Coulter™ Multisizer II (Beckman Coulter UK Ltd, High Wycombe, UK). Cells were then re-seeded into media at an appropriate density based on the experiment design.

2.2.5 3D cell culture techniques

For work involving 3D cell culture, two different culture techniques were used. These were defined as "3D embedded cell culture" and "3D on top cell culture", with both techniques described below.

2.2.5.1 3D "Embedded" cell culture

Pre-chilled culture dishes/plates were coated with an appropriate volume of phenol red free Matrigel® (Appendix 7.11), which had been thawed at 4°C overnight, using pre-chilled pipette tips. This Matrigel® coat was spread evenly across the surface of the culture vessel using a pipette tip, avoiding the development of bubbles, and the culture vessel was then incubated at 37°C for 30 minutes to allow the matrix to set.

Cells were then trypsinized and counted as per protocol and a dilution created for the desired cell concentration (0.5-0.6 x 10^6 cells/ml – cell line dependent). An appropriate volume of the diluted cell suspension (Appendix 7.11) was

transferred to a 1.5ml micro centrifuge tube, where the cells were pelleted by centrifugation at 1000rpm for 5 minutes at 4°C. The supernatant was decanted and the cells pellet carefully re-suspended in the appropriate volume of Matrigel® (Appendix 7.11). This cell/Matrigel® mix was then carefully pipetted onto the pre-coated surface of the culture vessel. The culture vessel was again incubated at 37°C for 60 minutes to allow the Matrigel® to set, before an appropriate volume of experimental medium +/- treatment was added to overlie the Matrix (Appendix 7.11). The cells were maintained in this culture at 37°C for up to a maximum of 6 days, with the medium changed every 3 days.

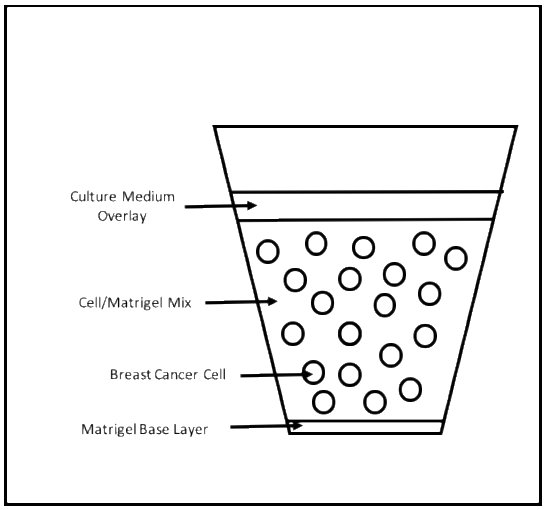

Figure 2.1– Schematic representation of 3D "embedded" cell culture. Cells were embedded within a Matrigel® matrix and bathed in the appropriate culture medium.

2.2.5.2 3D "on top" cell culture

Pre-chilled culture dishes/plates were coated with an appropriate volume of phenol red free Matrigel® (Appendix 7.11), which had been thawed at 4°C overnight, using pre-chilled pipette tips. This Matrigel® coat was spread evenly across the surface of the culture vessel using a pipette tip, avoiding the development of bubbles, and the culture vessel was then incubated at 37°C for 30 minutes to allow the matrix to set.

Cells were then trypsinized and counted as per protocol and a dilution created for the desired cell concentration (0.175-0.2 x 10^5 cells/ml – cell line dependent). Cells were then pelleted by centrifugation at 1000 rpm for 5 minutes at 4°C and then re-suspended in half the "medium volume" (Appendix 7.11) and carefully pipetted onto the pre-coated surface of the culture vessel.

The remaining medium was then chilled on ice and combined with 10% volume Matrigel® (1/10 dilution). This Matrigel®/medium mixture was then carefully added to overlay the cell layer. The cells were maintained in this culture at 37°C for up to a maximum of 6 days, with the medium changed every 3 days.

To avoid cell aggregation and ensure equal seeding of cells across the Matrigel® bed of the culture surface, agitation of the plate/dish was performed in both the x and y axes at intervals during the first hour of the incubation period.

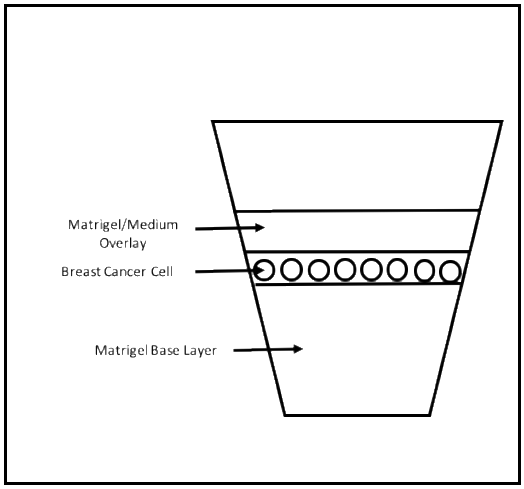

Figure 2.2 – Schematic representation of 3D "on-top" cell culture. Cells were seeded onto a Matrigel® base layer, before being sandwiched by an overlying layer of Matrigel®, diluted with culture medium.

2.2.6 siRNA Transfection

Cells were seeded in 35mm dishes (100,000 cells per well) and incubated at 37°C for 72 hours. After this period 1.5 ml micro-centrifuge tubes were labelled for both non-targeting (NT) and treatment (e.g. CDH1) siRNA variables as Tube A and Tube B. The appropriate volumes of siRNA (1µg/µl) and x1 siRNA buffer was thawed on ice and antibiotic and serum-free WRPMI was filter sterilised by passage through a 0.2µm Acrodisk® filter (Appendix 7.12).

Appropriate volumes of siRNA, x1 siRNA buffer and WRPMI was added to Tube A, while WRPMI and Dharmafect® transfection lipid was added to Tube B, for both NT and treatment arms of the experiment. Tubes were left to incubate at room temperature for 5 minutes. After this time, the contents of Tubes A and B for each variable was gently added and left for a further incubation period of 20 minutes at room temperature.

Following the incubation period this volume was aliquoted as necessary and mixed with experimental medium +/- treatments in a 1:5 ratio to create the final volume of transfection medium. The existing medium bathing the incubating cells was then removed and replaced with the appropriate volume of transfection medium. Cells were then incubated in this medium for 72 hours at 37°C to allow transfection to take place.

2.3 Analysis of Protein Expression

SDS-Page electrophoresis and Western Blotting, followed by immunoblotting with phospho-specific antibodies, were used to assess changes in intra-cellular protein expression.

2.3.1 Cell Lysis for Protein Extraction

Cells were seeded in 35mm dishes and treated under appropriate experimental conditions for the appropriate time, dependent on experiment. After this period, the medium was removed and the cells were twice washed with 1ml of ice-cold PBS before the addition of lysis buffer (Appendix 7.1 and 7.2) containing protease inhibitors (volume 50-100µl depending on cell confluency). The cell material, contained within the added lysis buffer, was then collected using a cell scraper, transferred to a 1.5ml Eppendorf tube and left to rest on ice for 20 minutes. Lysates were then isolated by centrifugation of the Eppendorf contents at 13,000rpm for 15 minutes at 4°C), followed by separation of the supernatant, which was stored at -20°C until later required.

2.3.2 Protein Concentration Assay

The concentration of soluble protein within lysate samples was determined using the Bio-Rad Micro Assay Procedure. A standard curve was created by performing multiple dilutions of a stock solution (1µg/µl) of Bovine Serum Albumin (BSA) in dH_20 (Appendix 7.3), within Eppendorf tubes. Each protein lysate sample was simultaneously diluted at a 1:400 concentration with dH_20 (i.e. 1µl of lysate with 399µl of dH_20), within Eppendorf tubes.

Subsequently, 100µl of Bio-Rad dye was added to each Eppendorf tube (i.e. standard curve and protein lysate samples) and each tube was vortexed briefly to allow thorough mixing of the solution. A 150µl of each solution was then transferred in duplicate to a 96-well plate and readings for the optical density of each well was calculated using a ELISA plate reader.

A standard curve was constructed (Appendix 7.4) using the mean optical density measurements from the BSA standard samples. The undiluted protein concentration of each lysate sample was then calculated by multiplying the concentration, determined from the mean optical density of each sample using the standard curve, by a multiplier of 400.

2.3.3 Protein Sample Preparation

To prepare each protein lysate sample for use in SDS-Page, a standard final protein concentration in all samples of 1µg/µl was obtained. An appropriate volume of lysate solution was therefore mixed with a solution of loading buffer (Appendix 7.6) containing DTT, in quantities to ensure a final solution containing 100µg of protein in 100µl volume. Each sample was gently mixed by pipette and then left at 95°C on a hot-block for 5 minutes. Samples were then briefly spun with a centrifuge, to ensure no vapour remained in the lids of the Eppendorf tubes, and the samples were then used immediately for SDS-Page, or stored at -20°C until later required.

2.3.4 SDS-Page

Sodium-Dodecyl-Sulphate-Polyacrylamide Gel Electrophoresis (SDS-Page) was performed using the Bio-Rad Mini Protean® III system, which was powered by a Powerpac® basic power pack. Gels used within this system were composed of an upper stacking gel, which held the samples within individual wells, alongside a lower resolving gel, which allowed proteins within samples to segregate based on molecular weights (Appendix 7.10). Glass plates were cleaned using ethanol and assembled in the apparatus provided. The resolving gel was then formed by the addition of the individual constituents within a universal container. The mixture was then poured between the plates, leaving an appropriate amount of space for the later addition of the upper stacking gel, overlaid with a small volume of isopropanol to prevent evaporation, and allowed to set at room temperature (approximately 20-25 minutes).

Once set, the overlying isopropanol was removed, and the stacking gel was then made by mixing the individual constituents within a universal container. The gel mixture was then added between the glass plates to overlay the resolving gel and a 10 or 15-well comb (depending on requirements) was inserted into the stacking gel mixture before allowing the gel to set at room temperature (approximately 30-35 minutes). Gels were then either used for SDS-Page immediately or stored overnight for use the following day, by wrapping the gel in water soaked tissue and cling film.

Each gel was then placed within the electrophoresis apparatus, and a x1 concentration of SDS-Page running buffer was added to both the inner and outer reservoirs of the tank, in which the gels and apparatus was inserted (Appendix 7.5). The comb for each gel was then gently removed and volumes of previously prepared cell lysates were mixed with sample loading buffer and DTT, equating to equal values of protein (usually 20μg). Samples were then inserted into each lane of the gel as required. A protein molecular weight marker (Precision Plus All Blue Standards 10-250kDa, 3μl) was added to a separate lane, and 20μl of x1 sample loading buffer containing DTT was then added to any unused lanes within the gel, to ensure all samples ran vertically once a current is applied.

Electrophoresis was then performed using a constant voltage of 120V (equating to around 80mA of current) until the sample/buffer dye front had run the length of the gel.

2.3.5 Western Blotting

Proteins were transferred from the SDS-PAGE gel to a pre-cut nitrocellulose membrane using the Bio-Rad® mini-protein system. Four pieces of filter paper and one piece of Protran® nitrocellulose membrane (pore size 0.45μm) were cut to the same size of each gel to be transferred. These were then soaked in Western blot transfer buffer (Appendix 7.7) along with Teflon sponge pads (2 pads per gel).

Upon completion of electrophoresis each gel was extracted from the electrophoresis apparatus, the upper stacking gel removed and the lower resolving gel was left to soak in Western blot transfer buffer. Each Western blot transfer cassette was then assembled with care taken to avoid the presence of air bubbles between the gel and overlying nitrocellulose membrane. Each cassette was then loaded into the transfer apparatus ensuring correct orientation of the cassette for transfer of the proteins from the gel and onto the nitrocellulose membrane. The transfer apparatus was then submerged in a tank containing Western blot transfer buffer. An ice block and magnetic flea were also added to the tank to prevent overheating of the tank during transfer. Transfer then took place with the tank placed upon a magnetic stirrer, to allow the magnetic flea to spin, by applying a constant voltage of 100V for 1 hour.

2.3.6 Immunoprobing of Western blots

Once the transfer was complete, the nitrocellulose membrane was removed from the cassette and stained with Ponceau-S solution, which would help confirm successful transfer of protein and provide an indication of the equal sample loading to each well. The membrane was then washed with Tris buffered saline containing Tween-20 (TBST, Appendix 7.9) on a rocking platform placed on a vigorous setting, until the Ponceau-S stain had been removed. The membrane was then submerged in a solution of 5% (w/v) Marvel made up in TBST and placed to rock gently on a rocking platform for 1 hour. Once blocking was complete, the membrane was incubated with the primary antibody on a roller, usually overnight at a temperature of 4°C overnight, although this was dependent on the primary antibody used.

Primary antibodies were made up by dilution (typically 1:1000) in TBST containing 5% (v/v) western blocking reagent and 0.05% (v/v) sodium azide. After incubation with the primary antibody the blot was washed with TBST on a rocking platform, placed on a vigorous setting for 20 minutes, and then incubated

with the correct horseradish peroxidase (HRP) conjugated secondary antibody on a roller for 1 hour at room temperature. Following secondary antibody incubation, the membrane was then washed with TBST on a rocking platform placed on vigorous setting for 20 minutes prior to antibody detection by chemiluminescence.

After the TBST wash, excess moisture from the blot was gently removed by blotting on absorbent paper and blots were placed within a light-proof developing cassette. An appropriate amount of the mixed chemiluminescent agent (approx. 200μl per membrane) was applied to the membrane, which was then covered with a clean sterile plastic protective sleeve, ensuring homogenous spread of the chemiluminescent agent over the membrane and avoiding the presence of bubbles. In darkness, an x-ray film was placed over the membrane and left for a variable period, to provide optimum exposure, before the x-ray film was developed in darkness using an X-O-graph compact X2 developed (X-O-graph Imaging System, Telbury, UK). Exposure time and the choice of chemiluminescent agent (Enhanced Chemiluminescent (ECL) Reagent, Clarity®, Supersignal™ West Femto) was performed depending on the levels of expression of each protein of interest. The bands obtained were scanned and analysed using a Bio-Rad imaging densitometer. Blots shown are a representative of a minimum of 3 biological replicate sample. Densitometry was used for statistical analysis.

Primary Antibody	Source	Dilution	Company

E-cadherin	Mouse	1:1000	R&D Systems
pSrc Y418	Rabbit	1:1000	Invitrogen, Paisley, UK
Src Total	Rabbit	1:1000	Invitrogen, Paisley, UK
pSTAT3	Rabbit	1:1000	Cell Signalling Technology, MA, USA
STAT3 Total	Rabbit	1:1000	Cell Signalling Technology, MA, USA
pFAK tyr397	Rabbit	1:1000	Cell Signalling Technology, MA, USA
FAK Total	Rabbit	1:1000	Cell Signalling Technology, MA, USA
pEGFR tyr1068	Rabbit	1:500	Cell Signalling Technology, MA, USA
EGFR Total	Rabbit	1:1000	Cell Signalling Technology, MA, USA
c-erbB2 Total	Rabbit	1:1000	Cell Signalling Technology, MA, USA
pAKT ser473	Rabbit	1:1000	Cell Signalling Technology, MA, USA
AKT Total	Rabbit	1:1000	Cell Signalling Technology, MA, USA
PTEN	Rabbit	1:1000	Cell Signalling Technology, MA, USA
pERK 1/2	Rabbit	1:1000	Cell Signalling Technology, MA, USA
ERK Total	Rabbit	1:1000	Cell Signalling Technology, MA, USA
pMEK 1/2	Rabbit	1:1000	Cell Signalling Technology, MA, USA
MEK Total	Rabbit	1:1000	Cell Signalling Technology, MA, USA

pERα 118 (16J4)	Mouse	1:1000	Cell Signalling Technology, MA, USA
ER Total	Rabbit	1:1000	Santa Cruz Biotechnology
PELP-1 Total	Rabbit	1:1000	Cell Signalling Technology, MA, USA
Sema 3E Total	Mouse	1:500	R&D Systems
Human Plexin D1 Total	Rabbit	1:500	R&D Systems
Neuropilin 1 Total	Rabbit	1:1000	Abcam
MMP-9	Rabbit	1:1000	Cell Signalling Technology, MA, USA
RhoA	Rabbit	1:1000	Abcam
Cdc42	Rabbit	1:1000	Abcam
Rac-1	Rabbit	1:1000	Abcam
Slug	Rabbit	1:1000	Cell Signalling Technology, MA, USA
Snail	Rabbit	1:1000	Cell Signalling Technology, MA, USA
TWIST	Rabbit	1:1000	Cell Signalling Technology, MA, USA

Table 2.3 -List of Primary antibodies used in immunoprobing of Western blots (+/- use in Immunocytochemical analysis). All primary antibodies were typically incubated at 4°C overnight.

Secondary Antibody	Source	Dilution	Company
GAPDH-HRP linked	Mouse	1:10000	Abcam, Cambridge, UK
β-Actin-HRP linked	Mouse	1:10000	Sigma-Aldrich, Poole, Dorset, UK
Anti-goat horseradish-peroxidase-linked IgG	Goat	1:10000	Dako, UK
Anti-mouse horseradish-peroxidase-linked IgG	Mouse	1:10000	Cell Signalling Technology, MA, USA
Anti-rabbit horseradish-peroxidase-linked IgG	Rabbit	1:10000	Cell Signalling Technology, MA, USA

Table 2.4 -List of secondary antibodies used in immunoprobing of Western blots (+/- use in Immunocytochemical analysis). All secondary antibodies were incubated at room temperature for 1 hour.

2.4 Cell Invasion Assays

2.4.1 2D Boyden Chamber Cell Invasion Assay

Matrigel® was defrosted on ice and diluted to a stock concentration of ~11mg/ml by mixing 1 part Matrigel with 2 parts sterile WRPMI (a 1 in 3 dilution). 50μl of this Matrigel® dilution was then carefully pipetted, using cold pipette tips, into the upper chamber of each Boyden Chamber insert (Costar® #3422, 24-well plate with 6.5mm diameter, 8μm pore inserts). The plate and associated inserts were then incubated at 37°C for 2 hours to allow the Matrigel® to set.

Once the Matrigel® had set, 650μl of experimental medium was pipetted into the lower chamber of each well. Cells were then trypsinized and 5000 cells (within a volume of 200μl) was pipetted into the upper chamber of each insert. The plate was then incubated at 37°C for 72 hours to allow invasion to take place.

After 3 days, inserts were removed from their corresponding well, the medium from the upper chamber removed by pipette and the layer of Matrigel® was carefully and gently removed from the upper chamber with a cotton bud. In a fume cabinet, the membrane of each insert was submerged in a 3.7% formaldehyde solution for 15 minutes for cell fixation. Each membrane was then twice washed by submersion in PBS and left to air dry briefly. The membrane of each insert was then carefully excised with a scalpel blade and the membrane was then mounted on a microscope slide (cell side up) with a single drop of DAPI (Vectorshield), followed by a coverslip. Slides were then left to set inside a dark room and then stored at 4°C.

For quantification cells were visualized under fluorescent microscopy using a x10 lens, with a set wavelength of 461nm. Cell counts were taken from 10 fields viewed in a systematic fashion for each membrane.
As an alternative measure of quantification using a clonal population EGFP-expressing MCF-7 cells, inserts were fixed with 3.7% formaldehyde, stained with

DAPI and mounted using a coverslip as previously mentioned, but cells were alternatively counted by detecting EGFP-expressed cells under fluorescent microscopy, with a set wavelength of 395nm. As recorded previously, cell counts were taken from 10 fields viewed in a systematic fashion for each membrane.

2.4.2 Development of a 3D cell invasion assay

The standard methods of assessing cells in-vitro typically involves cell culture within a 2D environment. This is particularly the case where immortalised cell lines are used as the primary instrument for study. Despite this, ongoing evidence suggests that this may not necessarily always be the best way to make such assessments on cell behaviour, particularly when trying to translate findings from in-vitro studies into clinical models (186).

Traditional 2D cell culture relies on cell adherence to the flat surfaces of plastic of glassware, which provide physical support for the cells. Cells grown in such a way will have similar access to nutrients and growth factors from their surrounding medium, which results in homogenous growth and proliferation (187). While this may be a useful feature for the simplicity of scientific study, 2D culture provides no control over cell shape, which determines the biochemical cues that affects cell activity in-vivo (186). In addition, cells in our body perform activities in response to stimulation from a complex 3D microenvironment, containing the surrounding extracellular matrix (ECM), surrounding cells of similar type, as well as other cell types, such as fibroblast (188, 189). As such, natural nutrient gradients develop and waste gradients build up across such an environment, affecting cell proliferation and cell death respectively (187). Given these crucial differences, interest in assessing cells in a 3D in-vitro cell culture environment has grown over recent years.

There are several potential approaches when undertaking 3D cell culture, depending on the desired observations that are to be made (186). The majority of techniques employ embedding cells in various formations, within either an organically-derived ECM, such as collagen, or synthetic-based ECM, such as

Matrigel®; a solubilized basement membrane (BM) preparation extracted from the Engelbreth-Holm-Swarm (EHS) mouse sarcoma (190). Cells are then free to interact with surrounding cells and the ECM within a 3D spatial arrangement whilst receiving nutrients from culture medium that bathes the matrix. These 3D culture systems may be modified as required by changing the ECM stiffness through changes in the BM concentration, or by co-culturing the cell of interest with other cell types, such as fibroblasts, bringing the system closer to physiological arrangements encountered in-vivo (186). Many cellular outcomes may then be studied from such culture systems, including proliferation, invasion, and also signalling changes through the extraction and separation of cells from the surrounding ECM (186).

The highlighted differences outlined above therefore make 3D cell culture a more realistic model of in-vivo conditions, particularly as significant differences have been shown to exist between cell behaviour in each type of culture system. Indeed, several studies have shown differences in cell proliferation, differentiation and gene expression between cells grown in 2D and 3D cell culture (191-193). In breast cancer, for example, the BCMPG have previously shown that culturing HER2+ breast cancer cells in a 3D environment can promote AKT to MAPK switching within the cell, causing a relative loss of therapeutic response to treatment (194). In terms of cell motion, migration has been shown to vary between 2D and 3D systems, likely due to the more complex interactions with the surrounding ECM with 3D culture and the additional obstacles created for cell movement (195, 196).

Given the above, it would therefore be of interest to study the phenotypic response of breast cancer cells to endocrine treatments as part of this thesis, assessing whether any responses seen in 2D cell culture are also evident when cells cultured in a 3D environment.

.

One may argue that the previously described Boyden chamber assay, used to assess invasion, is in effect assessing invasion in 3D, as cells invade through a 3D

layer of Matrigel®. While this may be true, this assay is a better measure of single cell invasion as cell-cell contacts are limited in this setting, as cells are initially seeded as a single cell monolayer of the surface of the Matrigel®. The idea of a true 3D invasion therefore, would be one where cells are cultured in a 3-dimensional configuration, allowing interaction with surrounding cells in a true circumferential fashion. This would be a better in-vitro representation of an in-vivo breast tumor and allow more physiological interaction of breast cancer cells with the tumor microenvironment.

As a starting point for this task, a 3D invasion assay developed by Vinci et al. (197) was utilized and subsequently modified. This assay essentially involves the culture of cells within an ultra-low adherent, U-bottom plate, which prevents cells from adhering to the well bottom, and therefore allows cells to adhere to each other within a 3D "spheroid" configuration. After a suitable period of culture to allow spheroid formation, some of the culture medium is carefully removed from the well and replaced with an equal volume of Matrigel®. Mixing of the Matrigel® with existing culture medium within the well is then aided by centrifugation of the plate, creating an ECM of desired stiffness to maintain 3D architecture whilst allowing cell invasion to occur from the central spheroid into the periphery of the surrounding ECM. Invasion can then be assessed at a suitable endpoint by light microscopy, to visualize the extent of invasion (Figure 2.3a). Quantitatively this can be represented using imaging software, such as Fiji®, to determine the relative change in either the perimeter or area (Figure 2.3b) of the spheroid during the course of the experiment.

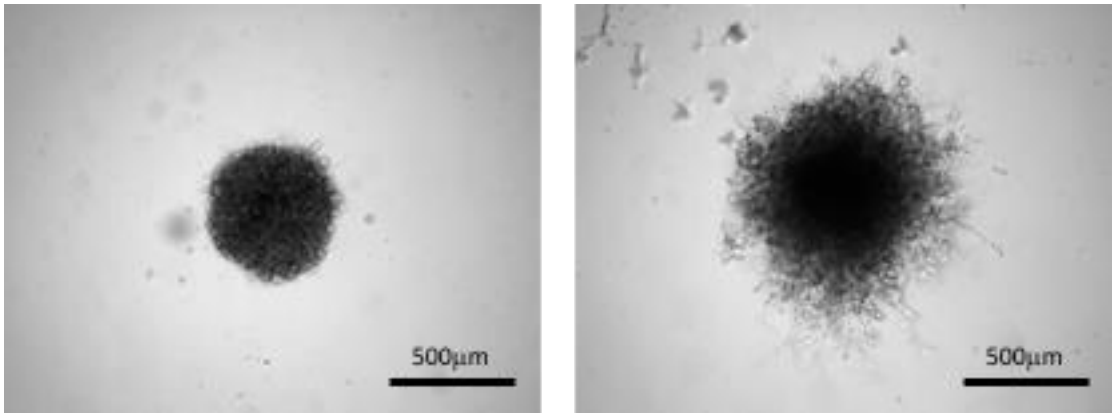

a.

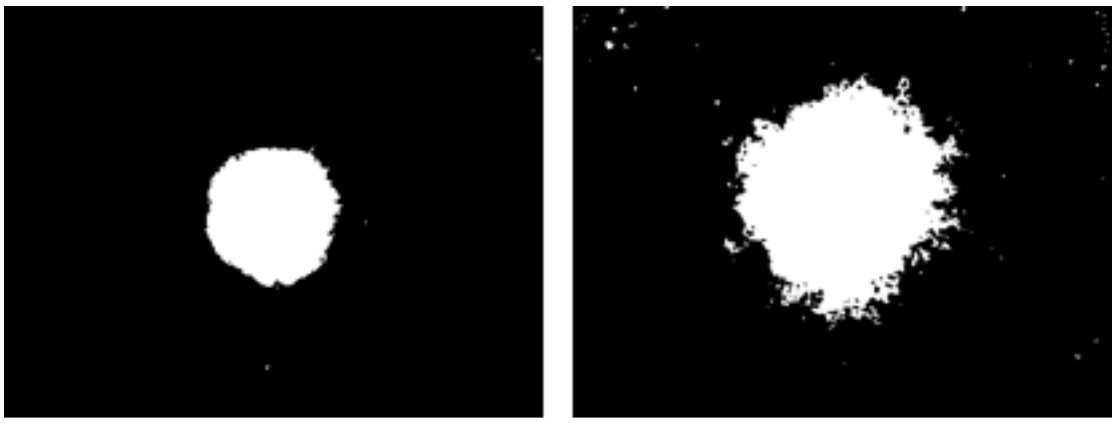

b.

Figure 2.3 – Calculation of the relative change in spheroid area using Fiji® computer software. (a) MDA-231 cells cultured within a 3D spheroid assay for 6 days imaged by 2D light microscopy (day 0 = left image, day 6 = right image). (b) The same images modified by Fiji® via the threshold adjust tool to identify the extent invasion through measurement of relative spheroid perimeter change or relative spheroid area change.

This system was trialed and optimized with several breast cancer cell lines with variable success. During the optimization period variables, such as cell seeding density, culture period for spheroid formation, Matrigel®: culture medium ratio, centrifugation settings and assay time were modified systematically to attempt to develop an assay that is rigorous, reproducible and fit for purpose. Below is a summary of the significant findings during this period of optimization for each cell line.

ER+ cell lines

1. MCF-7

MCF-7 cells formed relatively compact, non-uniform, friable spheroids when grown in ULA-plates for 3 days, using a seeding density of 5,000 cells/well. Cells were poorly invasive, and invasion could not be adequately imaged with bright field (Figure 2.4) or time-lapse microscopy (Supplemental File 1), despite attempts of optimization through adapting the Matrigel®: medium ratio, or stimulation of cells with estradiol, tamoxifen and EGF.

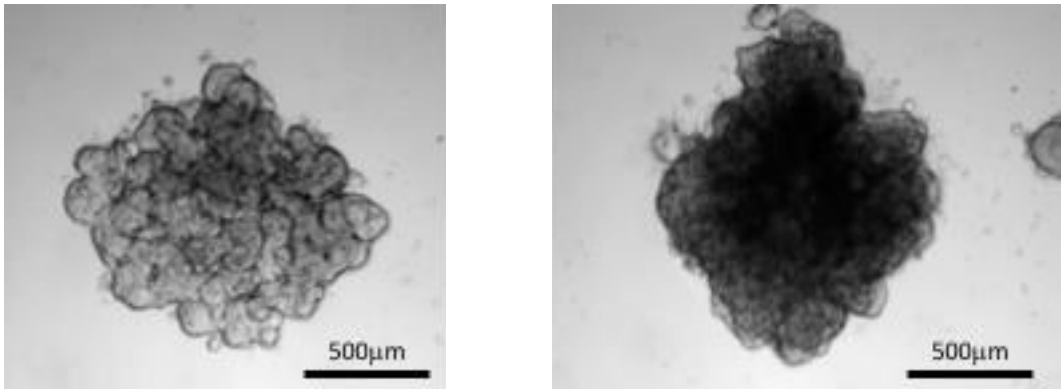

Figure 2.4 – MCF-7 spheroid invasion assay. MCF-7 cells grown within the 3D spheroid invasion assay (5000 cells/well) after day 0 (left) and day 6 (right) of cell culture.

SiRNA-mediated CDH-1 knockdown MCF-7 cells grown in ULA-plated for 3 days tended to form more uniform, but less compact spheroids, compared to their wild-type counterparts. E-cadherin knockdown cells were relatively more invasive, although this was poorly demonstrated by light microscopy due to limitations in the sensitivity of this method of detection (Figure 2.5). Attempts at optimization of the assay through adapting the Matrigel®: medium ratio, or stimulation of cells with estradiol or EGF, failed to significantly enhance invasion using this cell line.

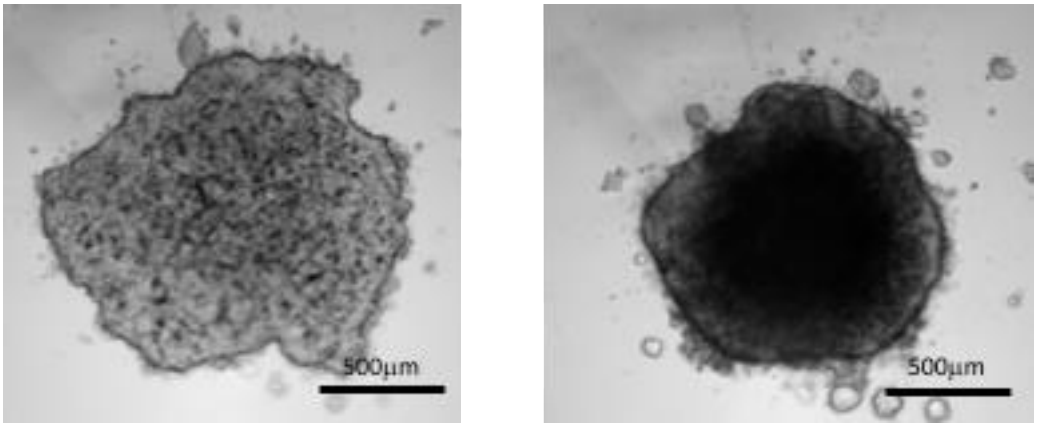

Figure 2.5 – MCF-7 cell spheroid invasion assay following treatment with CDH1 siRNA. MCF-7 cells, treated with anti-CDH1 siRNA, grown within the 3D spheroid invasion assay (5000 cells/well) after day 0 (left) and day 6 (right) of cell culture.

2. T47D

T47D cells formed relatively compact, non-uniform spheroids when grown in ULA-plates for 3 days, using a seeding density of 5,000 cells/well. In a similar fashion to MCF-7 cells, T47D cells were also poorly invasive, and invasion could not be adequately imaged using bright field microscopy (Figure 2.6). Attempts to optimize the assay, through adapting the Matrigel®: medium ratio, or stimulation of cells with estradiol or EGF, failed to demonstrate reliable cell invasion.

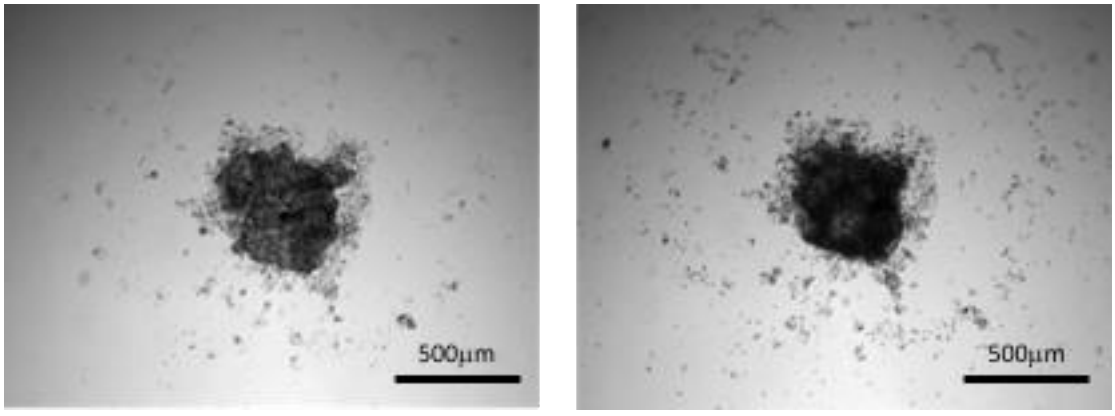

Figure 2.6 – MCF-7 spheroid invasion assay. T47D cells grown within the 3D spheroid invasion assay (5000 cells/well) after day 0 (left) and day 6 (right) of cell culture.

3. BT474

BT474 cells formed dense, compact, uniform spheroids when grown in ULA-plates for 3 days, using a seeding density of 5,000 cells/well. Cells were very poorly invasive, and invasion was not evident with bright field microscopy (Figure 2.7) after 6-days, despite attempts of optimization through adapting the Matrigel®: medium ratio, or stimulation of cells with estradiol, EGF or Heregulin.

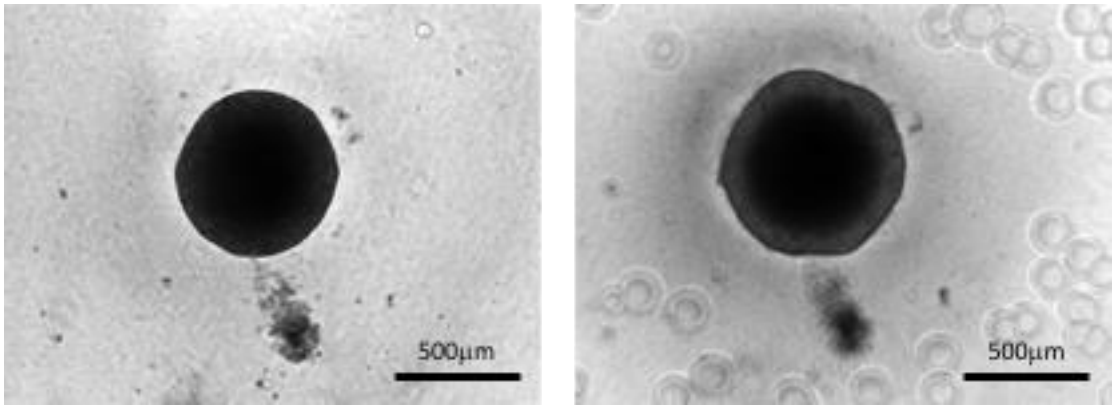

Figure 2.7 – BT474 spheroid invasion assay. BT474 cells grown within the 3D spheroid invasion assay (5000 cells/well) after day 0 (left) and day 6 (right) of cell culture.

SiRNA-mediated CDH-1 knockdown BT474 cells grown in ULA-plated for 3 days tended to form uniform, but less compact spheroids, compared to their wild-type counterparts (Figure 2.8). Despite E-cadherin knockdown, cells remained poorly invasive after 6 days, and invasion could not be significantly increased after adapting the Matrigel®: medium ratio, or stimulating of cells with estradiol, EGF or Heregulin.

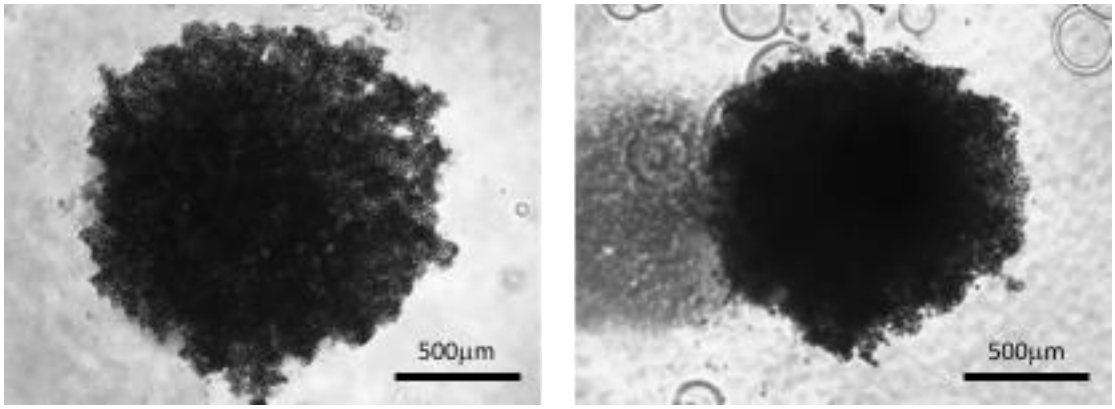

Figure 2.8 – BT474 cell spheroid invasion assay following treatment with CDH1 siRNA. BT474 cells, treated with anti-CDH1 siRNA, grown within the 3D spheroid invasion assay (5000 cells/well) after day 0 (left) and day 6 (right) of cell culture.

4. MDA-MB-361

As with the BT474 cell line, MDA-MB-361 cells formed dense, compact, uniform spheroids when grown in ULA-plates for 3 days, using a seeding density of 5,000 cells/well. These cells were also poorly invasive, and invasion was not evident with bright field microscopy (Figure 2.9) after 6-days, despite attempts of optimization through adapting the Matrigel®: medium ratio, or stimulation of cells with estradiol, EGF or Heregulin.

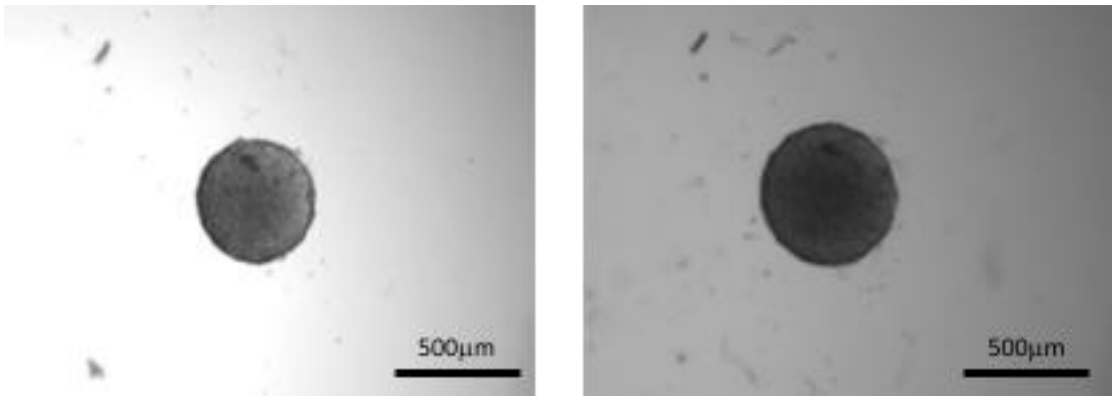

Figure 2.9 – MDA-MB-361 spheroid invasion assay. MDA-MB-361 cells grown within the 3D spheroid invasion assay (5000 cells/well) after day 0 (left) and day 6 (right) of cell culture.

ER- cell lines

1. MDA-MB-231

MDA-231 cells formed tight, compact, uniform spheroids when grown in ULA-plates for 3 days, using a seeding density of 5,000 cells/well. Invasion was evident for up to 6 days and could be imaged adequately by both bright field (Figure 2.10) and time-lapse microscopy (Supplemental File 2), using a 1:3 Matrigel®: medium ratio.

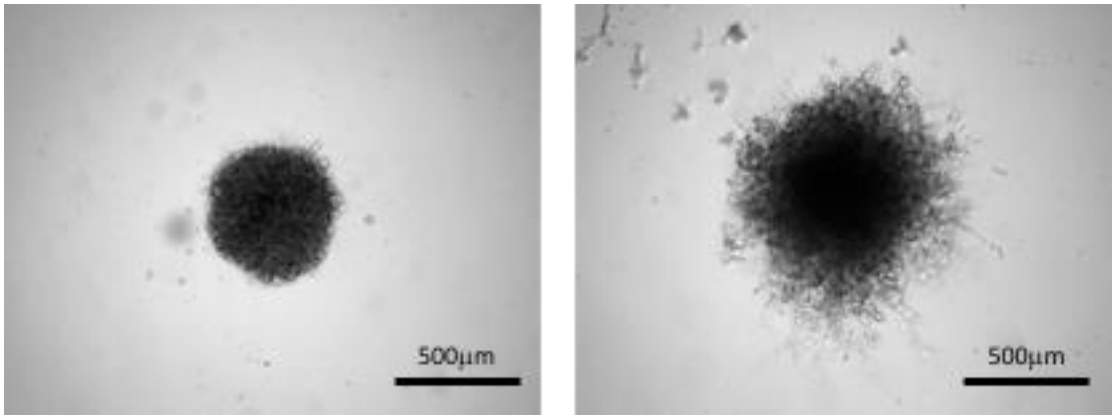

Figure 2.10 – MDA-MB-231 spheroid invasion assay. MDA-MB-231 cells grown within the 3D spheroid invasion assay (5000 cells/well) after day 0 (left) and day 6 (right) of cell culture.

2. MDA-MB-468

MDA-468 cells formed loose, friable but uniform spheroids, when grown in ULA-plates for 3 days, using a seeding density of 5,000 cells/well. Invasion was evident for up to 6 days, although was less pronounced than for MDA-231 cells, and could also be imaged by bright field microscopy (Figure 2.11), using a 1:3 Matrigel®: medium ratio.

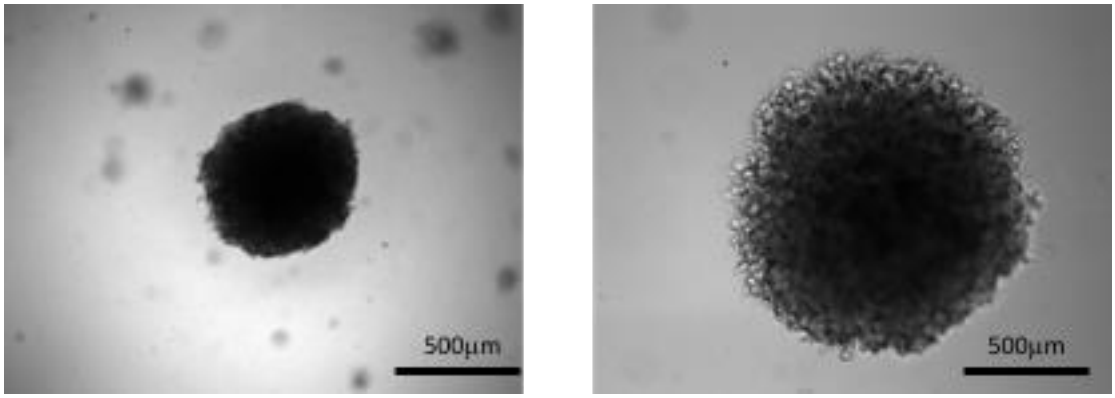

Figure 2.11 – MDA-MB-468 spheroid invasion assay. MDA-MB-468 cells grown within the 3D spheroid invasion assay (5000 cells/well) after day 0 (left) and day 6 (right) of cell culture.

In summary, given the variable success following the optimization of the above assay, reliability was demonstrated among the ER negative cell lines assessed (MDA-MB-231, MDA-MB-468), while less success found when using ER positive cell lines (MCF-7, T47D, BT474, MDA-MB-361). As a result, a variation on the above technique was trialed to see if the assay could be improved.

This technique was developed following collaboration with Dr Aled Clayton and his group, based at Cardiff University, who had experience in working with 3D cell culture in the context of assessing invasion (see acknowledgments). This technique, termed the 3D "fried egg" assay due to the appearance of the spheroid following cell invasion is based on a similar principle to the assay described above, whereby cells are cultured as spheroids within ULA plates. Within the "fried egg" assay however, after spheroid formation spheroids are carefully transferred from the ULA plates to a flat bottom 96-well plate, pre-coated with a Matrigel® bed.

After allowing the transferred spheroid to settle on the Matrigel® bed, each well was then supplemented with additional culture medium +/- treatments. Spheroids were then observed by light microscopy, daily, for a period of up to 6 days, to assess cell invasion from the central spheroid into the Matrigel® periphery. Again, in a similar manner to the original assay, quantification of

invasion can be demonstrated using imaging software, such as Fiji®, to determine the relative change in either the perimeter or area of the spheroid at the end of the assay.

This assay was again trialed and optimized using several breast cancer cell lines with the following summary highlighting the important findings for each breast cancer cell line.

ER+ cell lines

1. MCF-7

As demonstrated previously MCF-7 cells formed relatively compact, non-uniform, friable spheroids when grown in ULA-plates for 3 days, using a seeding density of 5,000 cells/well. Spheroid transfer to Matrigel® coated plates resulted in some disruption to the spheroid architecture however. Cells were also poorly invasive, and invasion could not be adequately imaged with bright field (Figure 2.12) microscopy after a period of 6 days.

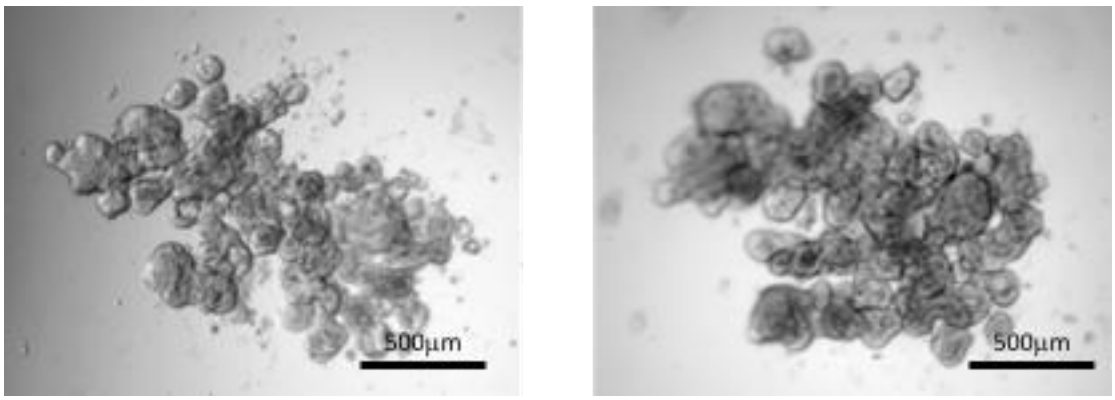

Figure 2.12 – MCF-7 "fried egg" invasion assay. MCF-7 cells grown within the 3D "Fried Egg" invasion assay (5000 cells/well) after day 0 (left) and day 6 (right) of cell culture.

siRNA-mediated knockdown of E-cadherin in MCF-7 cells led to the formation of more uniform, but less compact spheroids when grown in ULA plates. This led to

an increase in the fragility of the spheroid, which meant spheroid transfer to Matrigel® coated plates resulted in spheroid fracture and complete disruption to spheroid architecture (Figure 2.13).

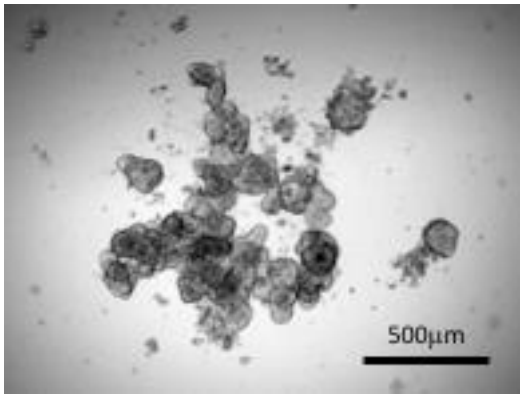

Figure 2.13 – MCF-7 spheroid fracture. Spheroid fracture occurred frequently after attempted transfer of MCF-7 spheroid, treated with anti-CDH1 siRNA, during 3D "Fried Egg" assay.

2. T47D

As shown previously, T47D cells formed relatively compact, non-uniform spheroids when grown in ULA-plates for 3 days, using a seeding density of 5,000 cells/well. Although spheroid transfer to Matrigel® coated plates did not disrupt the spheroid architecture, cells were poorly invasive, and invasion could not be adequately imaged using bright field microscopy (Figure 2.14).

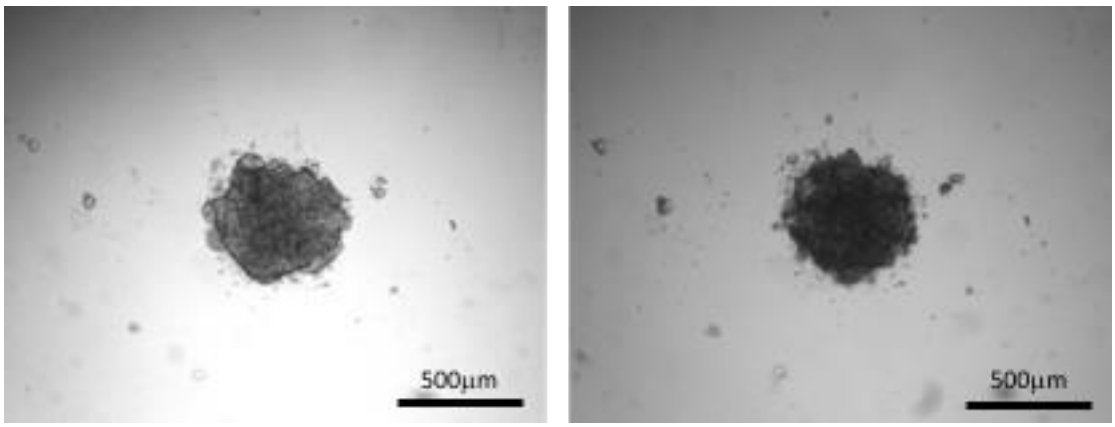

Figure 2.14 – T47D "fried egg" invasion assay. T47D cells grown within the 3D "Fried Egg" invasion assay (5000 cells/well) after day 0 (left) and day 6 (right) of cell culture.

3. BT474

As shown previously, BT474 cells formed dense, compact, uniform spheroids when grown in ULA-plates for 3 days, using a seeding density of 5,000 cells/well. Spheroid transfer to Matrigel® coated plates did not disrupt spheroid architecture, but transferred cells remained poorly invasive, and invasion was not evident with bright field microscopy after 6-days (Figure 2.15).

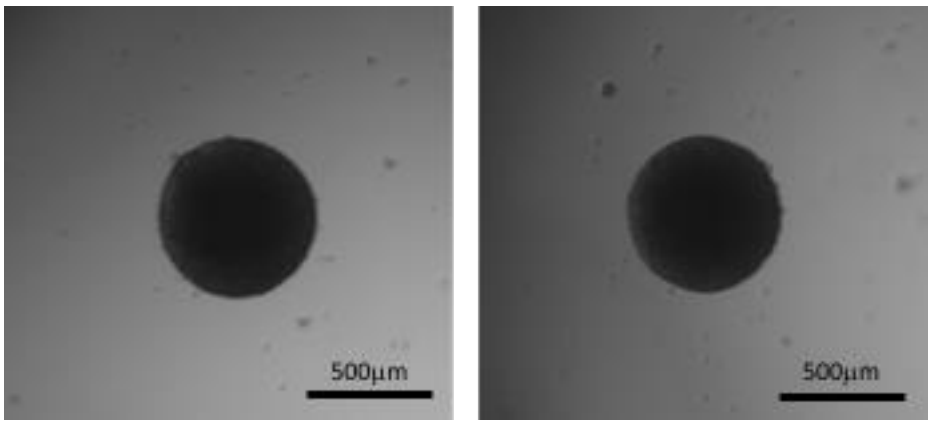

Figure 2.15– BT474 "fried egg" invasion assay. BT474 cells grown within the 3D "Fried Egg" invasion assay (5000 cells/well) after day 0 (left) and day 6 (right) of cell culture.

In a similar fashion to MCF-7 cells, siRNA-mediated knockdown of E-cadherin in BT474 cells led to the formation of uniform, but less compact spheroids. This led to an increase in the fragility of the spheroid, with transfer of the spheroid resulting in fracture and disruption to spheroid architecture (Figure 2.16).

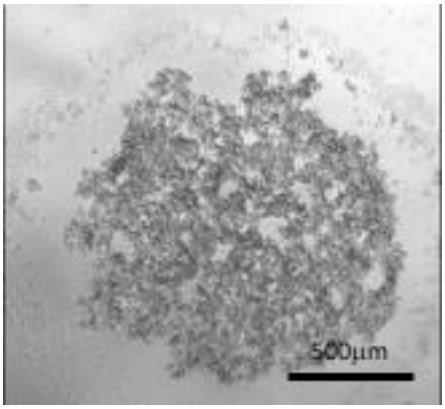

Figure 2.16 – BT474 spheroid fracture. Spheroid fracture after attempted transfer of BT474 spheroid, treated with anti-CDH1 siRNA, during 3D "fried egg" assay.

4. MDA-MB-361

MDA-MB-361 cells formed dense, compact, although slightly less uniform spheroids, when grown in ULA-plates for 3 days, using a seeding density of 5,000 cells/well. Although spheroid transfer to Matrigel® coated plates did not disrupt spheroid architecture, cells remained poorly invasive, and invasion was not evident with bright field microscopy after 6-days (Figure 2.17).

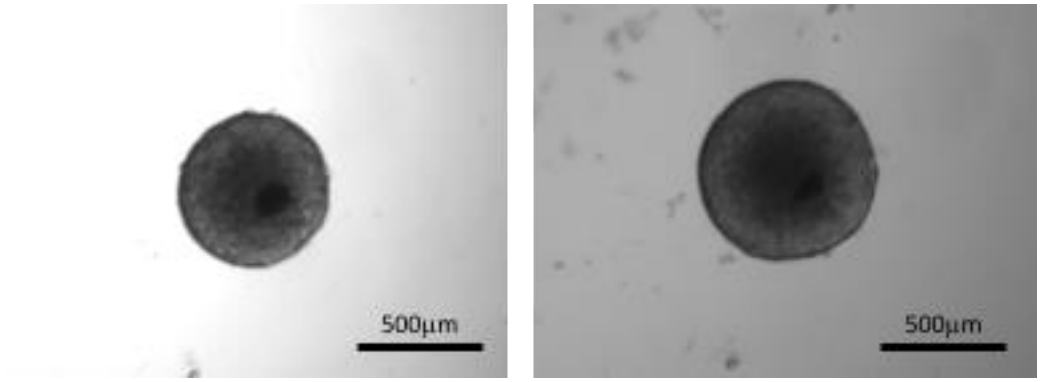

Figure 2.17 – MDA-MB-361 "fried egg" invasion assay. MDA-MB-361 cells grown within the 3D "Fried Egg" invasion assay (5000 cells/well) after day 0 (left) and day 6 (right) of cell culture.

ER- cell lines

1. MDA-MB-231

As shown previously, MDA-MB-231 cells formed tight, compact, uniform spheroids when grown in ULA-plates for 3 days, using a seeding density of 5,000 cells/well. Spheroid transfer to Matrigel® coated plates did not disrupt spheroid architecture. Invasion was evident for up to 6 days and could be imaged adequately by both bright field (Figure 2.18) and time-lapse microscopy (Supplemental File 3).

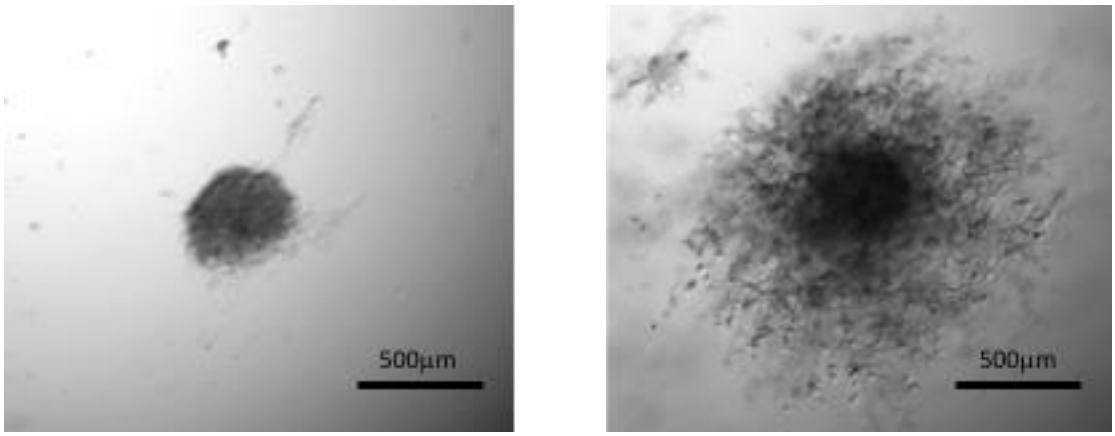

Figure 2.18 – MDA-MB-231 "fried egg" invasion assay. MDA-MB-231 cells grown within the 3D "Fried Egg" invasion assay (5000 cells/well) after day 0 (left) and day 6 (right) of cell culture.

2. MDA-MB-468

As shown previously, MDA-468 cells formed loose, friable but uniform spheroids, when grown in ULA-plates for 3 days, using a seeding density of 5,000 cells/well. Due the friable nature of these spheroids, spheroid transfer to Matrigel® coated plates resulted in spheroid fracture and complete disruption to spheroid architecture (Figure 2.19). This result meant that further use of the assay to assess invasion in this cell line was inappropriate.

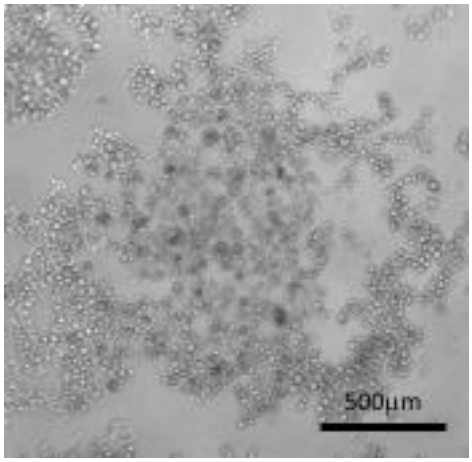

Figure 2.19 – MDA-MB-468 spheroid fracture. Spheroid fracture after attempted transfer of MDA-MB-468 spheroid, during 3D "fried egg" assay.

Following the development and optimization of both assays described above, their use was deemed suitable for assessing cell invasion in ER negative cell lines alone, as quantifiable cell invasion was demonstrable and reliable with MDA-MB-231 and MDA-MB-468 cells. Their use for assessing invasion in ER+ cells meanwhile was deemed unsuitable as invasion could not be reliably confirmed using any of the cell lines tested. This was partly due to the relatively friable nature of ER positive spheroids, as compared to spheroids using the MDA-MD-231 cell line, making calculation of the spheroid area (both assays) and spheroid transfer ("fried egg" assay) difficult. The lack of demonstrable invasion using these assays was also felt to be due to the inherent poor invasive phenotype of the ER+ cell lines relative to their ER- counterparts, as can be demonstrated using the previously described Boyden chamber invasion assay. This relative poorly invasive phenotype for ER+ cell lines may mean the sensitivity of the described 3D invasion assays are not sufficient to demonstrate invasion in this context. As such, use of these assays within this research are focused on assessing ER negative breast cancer cell line alone based upon the following formalized protocols.

Cell Line	ER/HER2 status	Spheroid Description	Invasion in Spheroid assay	Invasion in Spheroid assay
MCF-7	ER+, HER2-	compact, non-uniform, friable	No	No
T47D	ER+, HER2-	compact, non-uniform	No	No
BT474	ER+, HER2+	dense, compact, uniform	No	No
MDA-MB-361	ER+, HER2+	dense, compact, uniform	No	No
MDA-MB-231	ER-, HER2-	tight, compact, uniform	Yes	Yes
MDA-MB-468	ER-, HER2-	loose, friable, uniform	Yes	No

Table 2.5 – Summary of outcomes following optimisation of the 3D Spheroid invasion and 3D "fried egg" invasion assays. MDA-MB-231 cells showed signs of invasion in both assays, whiles MDA-MB-468 cells were deemed only suitable for use in the spheroid invasion assay. ER+ cell lines were poorly invasive and showed no evidence of invasion in either assay.

2.4.2.1 3D Spheroid Cell Invasion Assay

Cells were trypsinized and seeded (5000 cells per well in 150µl of W5% +/- treatments) into an Ultra-Low Adherent (ULA) round-bottom 96-well plate and incubated at 37°C for 72 hours to allow for spheroid formation.

After 72 hours, the plate was inspected by light microscopy to assess the success of spheroid formation. Within chosen wells, 50µl of medium was carefully removed ensuring not to damage the spheroid and was replaced with 50µl of

Matrigel®, which had been previously defrosted on ice, being careful to avoid the introduction of air bubbles. The plate was kept on ice throughout this procedure and then subsequently spun by centrifugation at 500/min for 10 minutes at 4°C to allow adequate mixing of the Matrigel® with the medium and help create a central location for the spheroid within the well. The plate was then incubated at 37°C for 2 hours to allow the Matrigel® to set before 100µl of medium +/- treatments was added to each well to overlie the Matrigel® layer. The plate was again then incubated at 37°C for a further 6 days. Wells were visually inspected by light microscopy using a x5 lens at 24 hour periods for signs of invasion of cells from the spheroid into the surrounding matrix.

To quantify invasion, the total area of the spheroid (in pixels) on day 0 and day 6 was calculated from still light microscopy images taken with a x5 lens, using Fiji version 2.0. To compare the invasion between replicates and different treatment conditions, the relative change in spheroid area was expressed by dividing the spheroid area at day 6 by the calculated spheroid area at day 0.

2.4.2.2 3D "Fried Egg" Cell Invasion Assay

Cells were trypsinized and seeded (5000 cells per well in 150µl of W5% +/- treatments) into an Ultra-Low Adherent (ULA) round-bottom 96-well plate and incubated at 37°C for 72 hours to allow for spheroid formation.
After 72 hours, the plate was inspected to assess the success of spheroid formation. Matrigel® was thawed on ice, and in a separate flat-bottom 96-well plate, 50µl of Matrigel® was carefully added to coat the bottom of each well to be used, ensuring even coverage and avoiding the creation of air bubbles. This plate was then incubated at 37°C for 2 hours to allow this Matrigel® coating to set.

Once the Matrigel® had set, chosen spheroids were carefully transferred, using a 1ml pipette, from the ULA round-bottomed plate into the Matrigel® coated wells of the flat-bottom plate, along with the accompanying medium. Care was taken to avoid spheroid fracture during this procedure. The plate was then incubated for a further 2 hours at 37°C to allow the spheroid to settle and embed into the

Matrigel® base of each well before supplementing each well with a further 150µl of experimental medium +/-treatments. The plate was then incubated at 37°C for a further 6 days. Wells were visually inspected by light microscopy using a x5 lens at 24 hour periods for signs of invasion of cells from the spheroid into the surrounding matrix.

To quantify invasion, the total area of the spheroid (in pixels) on day 0 and day 6 was calculated from still light microscopy images taken with a x5 lens, using Fiji version 2.0. To compare invasion between replicates and under different treatment conditions, the relative change in spheroid are was expressed by dividing the spheroid area at day 6 by the calculated spheroid area at day 0.

2.4.3 3D spheroid fixation, sectioning and staining

As part of developing the above 3D invasion assays, cells were observed via time-lapse microscopy during the spheroid formation phase of the procedure, following cell seeding in ULA round bottom wells. This was initially done to observe how cells became uniformly configured within a 3D spheroid structure from the initial random configuration of cells seen within the well immediately after cell seeding (Figure 2.20). These time lapse microscopy images, using the MCF-7, T47D and BT474 cell lines respectively (Supplemental Files 4-6), were taken over a 72-hour period following cell seeding within the ULA round bottom well and demonstrated an initial gradual congregation of cells within the centre of the well. In addition to this however, these congregated cells appeared to demonstrate a more complex interaction with one another, whereby cells present on the outside of the spheroid appeared to move centrally via a “folding” action. This was most notable during the formation on MCF-7 cell spheroids (Supplemental File 4) and contributed to high density appearance of the resultant spheroid.

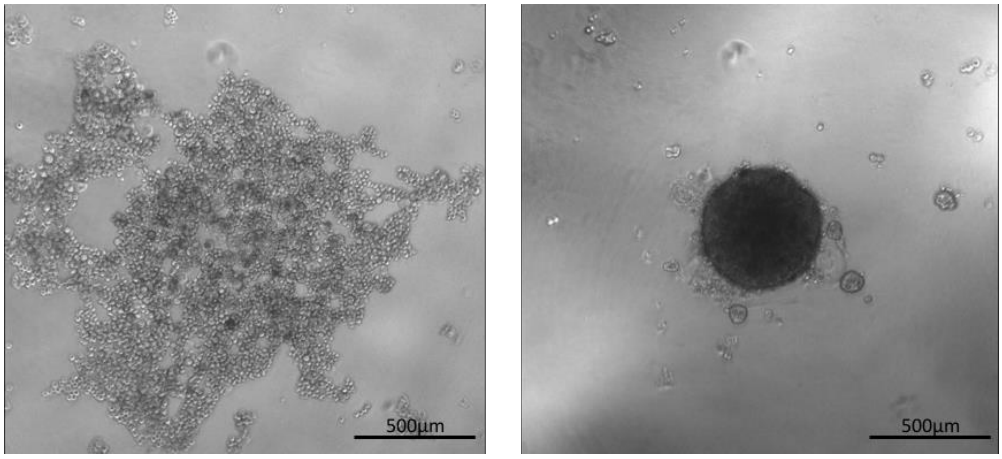

Figure 2.20 – T47D cell spheroid formation. T47D cells seeded into ULA round bottom wells (5,000 cells/well) on day 0 (left) formed a relatively compact central spheroid on day 3 (right).

Following this observation of complex cell-cell interactions, it was decided to design a process that may help further explore the structure of these 3D spheroids. This process would involve cell fixation, agar embedment, sectioning and staining of the spheroid, without compromising its 3D architecture, allowing its structure to be examined in cross-section by microscopy. To achieve this a suitable protocol was developed and optimised as described.

Cells were seeded into ULA round bottom wells (5,000 cells/well), as previously described, and cultured at 37°C for 72 hours to allow spheroid development. Following visual inspection by light microscopy to determine spheroid formation, spheroids were carefully retrieved from each well using a 1ml pipette, ensuring not to disrupt the spheroid architecture, transferred into a sterile Eppendorf containing 3.7% formaldehyde in PBS and left to incubate at 40°C for 1 hour. Meanwhile, a vial of agar was left to melt within a water bath at 37°C and a 1ml syringe was prepared, by cutting off the tip using a scalpel and partly withdrawing the plunger to the 1ml mark, allowing the barrel to fill with air. Following incubation, the supernatant was gently decanted from the Eppendorf and the spheroids gently transferred using a 1ml pipette into the cut 1ml syringe. Molten agar was then quickly transferred to fill the remaining volume of the syringe barrel and the plunger gently depressed to remove any excess air. The syringe

containing the embedded spheroids were refrigerated at 4°C overnight to allow the agar to set fully.

The following day the set agar was removed from the 1ml syringe, 3-4mm slices were sectioned using a blade before mounting these slices within a cassette. This cassette was then submerged in a tank 3.7% formaldehyde for 2 hours at room temperature. Following this period, the cassette was removed from the formaldehyde and submerged in 10% ethanol for 45 minutes. Subsequently, the cassette was transferred through increasing concentration ethanol solutions (i.e. 20%, 30% etc.) for 45 minute periods each time, until a final concentration solution of 70% was reached, where cassettes were left submerged overnight.

The following day the cassettes were again re-submerged in increasing concentrations of ethanol solution for 45 minutes each time, until a final concentration of 100% ethanol was reached. The cassette was then submerged in 100% xylene for a total of 150 minutes, refreshing the xylene solution every 30 minutes before embedding the cassette into 3 consecutive beakers, containing molten wax, for 30 minutes each time. A wax mould was then filled with molten wax and the pellets transferred from the cassettes into the wax mould before allowing the mould to set overnight at room temperature.

The next day 3μm sections were cut from the wax mould and were assessed for the presence of spheroids by polarised, high contrast light microscopy. Sections showing evidence of spheroids were retained and dewaxed by submergence in xylene for 14 minutes. These sections were then hydrated by passage through graded ethanol solutions (100-70%) being washed in water then finally PBS. Sections were then stained in haematoxylin for 5 minutes, washed under running tap water for 5 minutes and differentiated in 1% acid alcohol (1% HCl in 70% ethanol) for a further 5 minutes. These sections were then again washed under running tap water, dipped in ammonia water and then again washed under tap water for 5 minutes. Sections were then stained with 1% eosin for 10 minutes before undergoing a final wash with running tap water for 5 minutes. Sections

were left to air dry and mounted in DPX mounting media before being viewed by light microscopy.

The above process was carried out on spheroids grown using a panel of ER+ breast cancer cell lines (MCF-7, T47D, BT474 and MDA-MB-361). Images obtained through H+E staining of these spheroids (Figures 2.21 and 2.22) demonstrated some intrinsic differences between each cell line. Interestingly, images appeared to suggest that spheroids formed from MCF-7 cells (Figure 2.21) have a more complex and less compact architecture, with evidence of acellular spaces within the spheroids structure. In contrast, spheroids formed from T47D, BT474 and MDA-MB-361 cells (Figure 2.22) appeared to form more compact homogenous spheroids with a relative lack of acellular spaces contained with the spheroid architecture.

While these images and the underlying process involved helps to provide a better understanding of spheroid architecture, it may also have potential future practical applications. This may include allowing a cross section of the spheroid to be examined by ICC in future assays, allowing for the assessment of differential protein expression, based on cellular response to its environment, including the location of the cell within this 3D structure.

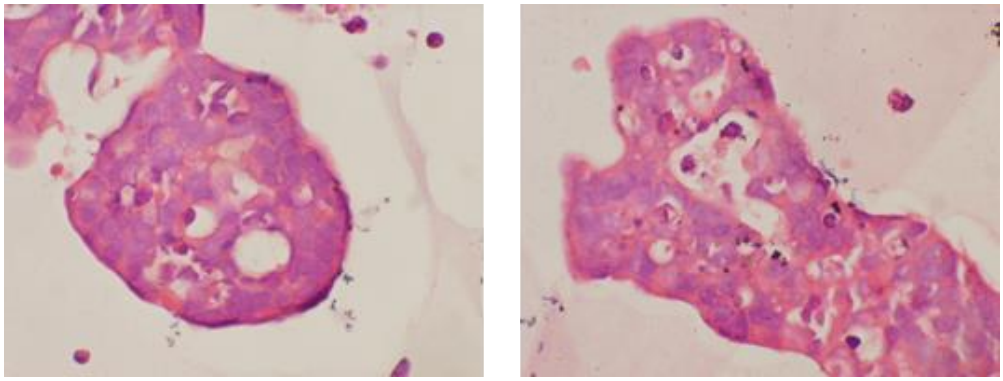

Figure 2.21 – MCF-7 spheroid cross section architecture. MCF-7 cell spheroids grown for 72 hours before being fixed, sectioned and stained with H+E. MCF-7 cell spheroids demonstrated a complex architecture with acellular areas contained within the spheroid structure.

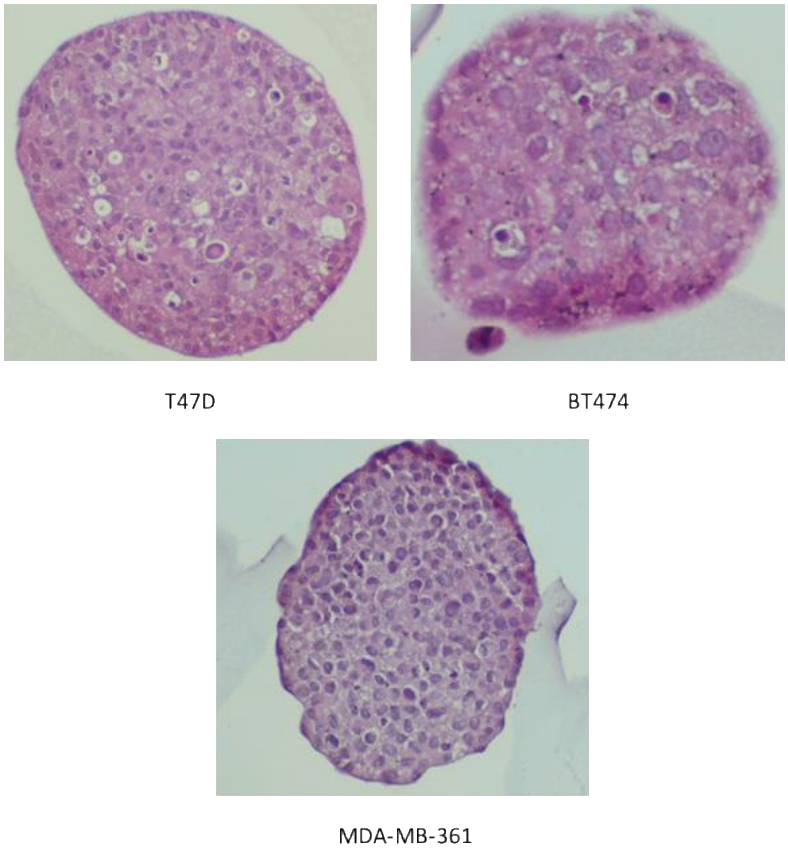

Figure 2.22 – Cross sectional architecture of alternative ER+ cell line spheroids. T47D, BT474 and MDA-MB-361 cell spheroids grown for 72 hours before being fixed, sectioned and stained with H+E. T47D, BT474 and MDA-MB-361 cell spheroids demonstrated a compact homogenous architecture.

2.5 Cell Migration Assays

2.5.1 2D Boyden Chamber Cell Migration Assay

The bottom surface of Boyden Chamber inserts (Costar® #3422, 24-well plate with 6.5mm diameter, 8μm pore inserts) were submerged in a 1/100 dilution of fibronectin in WRPMI (10μg/ml, 300μl per well) and incubated for 2 hours at 37°C to achieve a fibronectin coating of the porous membrane of the insert. After 2 hours, the inserts were removed and the fibronectin allowed to air dry by being placed upside down within a sterile cabinet for 15 minutes.

Once dry the inserts were then returned into the empty wells of the 12-well plate and 650μl of experimental medium was pipetted into the lower chamber of each well. Cells were then trypsinized and 4000 cells (within a volume of 200μl) was pipetted into the upper chamber of each insert. The plate was then incubated at 37°C for 24 hours to allow cell migration to take place.

After 24 hours, inserts were removed from their corresponding well, the medium from the upper chamber removed by pipette and remaining cells within the inside of the insert carefully and gently removed with a cotton bud. In a fume cabinet, the membrane of each insert was submerged in a 3.7% formaldehyde solution for 15 minutes for cell fixation to take place. Each membrane was then twice washed by submersion in PBS and left to air dry briefly. The inserts were then submerged in 0.5% crystal violet solution for 15 minutes for staining. Following this step, the inserts were twice washed by submersion in PBS, followed by a final wash with distilled water before being allowed to air dry.

For quantification, cells were visualized under light microscopy using a x10 lens. Cell counts were taken from 10 fields viewed in a systematic fashion for each membrane.

2.6 Cell Growth Assays

2.6.1 MTT Cell Proliferation/Metabolism Assay

The MTT cell proliferation/metabolism assay relies on the metabolism of 3-(4,5-dimethylthiazol-2-yl)-2,5-diphenyl-2H-tetrazolium dehydrogenase enzymes within cellular mitochondria to produce formazan crystals. The cells are then lysed to release these crystals, which are dissolved within the lysate solution. The optical density of the solution is then measured to produce a figure that is considered proportional to cellular metabolism for comparison between variables.

Cells were harvested and seeded into a 96-well plate at a density of 5000 cells/well and maintained under experimental conditions over a period of 6 days. The medium from each well was then removed and wells were washed gently with warm PBS (150μl per well), taking care not to disrupt cells attached to the bottom of the well. The PBS was then removed and replaced with 3-(4,5-dimethylthiazol-2-yl)-2,5-diphenyl-2H-tetrazolium dehydrogenase (MTT). The plate was then incubated at 37°C for 4 hours. After this time, the MTT was removed and replaced with Triton-X-100 (100μl/well) and the plate kept in a sealed plastic bag at 4°C overnight. Data was obtained by recording the optical density (wavelength 560nm) of each well using an ELISA plate reader (mean of eight separate wells per condition), with experiments repeated using a minimum of three biological replicates.

2.6.2 Cell Counting Assay

Cells were harvested and seeded in 35mm dishes at a density of 100,000 cells/dish and maintained under experimental conditions to grow over a period of 6 days. The medium from each dish was then removed and cells were incubated with 1ml of Trypsin (0.05%)/EDTA (0.02%) in PBS for 3-5 minutes at 37°C. The cell/trypsin suspension was then neutralised with an equal volume of culture medium and the cells suspension transferred to a universal container. Cells were then pelleted by centrifugation (Jouan C312, Thermo Fisher Scientific Inc, MA, USA) at 1000rpm for 5 minutes.

The cell pellet was then re-suspended in 1ml of warm culture, before being passed through a 25G syringe needle, to create a single cell suspension. Assessment of cell number was then made by adding 100µl of the re-suspended cell solution in 10ml of Isoton® II solution before cell counting was determined using a Coulter™ Multisizer II (Beckman Coulter UK Ltd, High Wycombe, UK). Total cell number within the initial dish was then calculated by determining the number of cells per ml of cell suspension.

2.7 Immunocytochemistry Analysis

2.7.1 Estrogen Receptor Immunocytochemistry Analysis (ER-ICA) Fixation

Cells were seeded in 35mm dishes (100,000 cells per dish), containing 3-triethoxysilylpropylamine (TESPA) coated coverslips, and incubated at 37°C for the desired time-course of each individual experiment, with and without appropriate treatments.

For ER-ICA fixation coverslips were removed from the growth medium and inserted into a coverslip rack, which was immediately submerged in a tank of 3.7% formaldehyde at room temperature for 15 minutes. The rack was then removed and submerged in a tank of PBS, at room temperature, for 5 minutes. Following this PBS wash the rack was transferred and submerged into a tank of methanol for 5 minutes, followed by a tank of acetone for 3 minutes, both maintained at a temperature of -10°C to -30°C by surrounding each tank with dry ice. Finally, the rack was submerged for a further 5 minutes in a tank of PBS kept at room temperature for a final wash, before storing each of the coverslips in sucrose storage medium, at -20°C, ready for future use.

2.7.2 ICC staining of TESPA coated coverslips for Total ER

Following ER-ICA fixation of coverslips (see method above), coverslips were washed three times by submersion in PBS for 3 minutes each. The coverslips were then blocked by submersion in a solution of 0.03% PBS/Tween for 3 minutes. Excess solution was then removed prior to application of the primary antibody. The NCL ER clone 6F11 (Mouse) antibody was then added to each to each coverslip (1:150 dilution on PBS, 50µl per coverslip) and left to incubate at room temperature for 60 minutes. The coverslips were then rinsed with PBS and washed twice, for 5 minutes, with a solution of 0.03% PBS/Tween. A drop of DAKO Mouse Envision secondary antibody was then added to each coverslip and left to incubate at room temperature for 60 minutes, before again rinsing with PBS,

followed by two washes with 0.03% PBS/Tween for 5 minutes each. 50µl of DAKO DAB Chromogen (1 drop of DAB combined with 1ml of substrate) was then applied to each of the coverslips and left to incubate at room temperature for 10 minutes. Coverslips were then washed twice with distilled water, for 5 minutes each. Counterstaining was subsequently performed by applying 4% Ehrlich's haematoxylin, followed by two washes with tap water, for 2 minutes each. Coverslips were left to air dry completely before mounting on slides using DPX mounting medium.

2.7.3 ICC staining of TESPA coated coverslips for PELP-1

Following ER-ICA fixation of coverslips (see method above), coverslips were washed three times by submersion in PBS for 3 minutes each. The coverslips were then blocked by submersion in a solution of 0.03% PBS/Tween for 3 minutes. Excess solution was then removed prior to application of the primary antibody. The PELP-1 polyclonal (Rabbit) antibody was then added to each to each coverslip (1:100 dilution on PBS, 50µl per coverslip) and left to incubate at room temperature for 60 minutes. The coverslips were then rinsed with PBS and washed twice, for 5 minutes, with a solution of 0.03% PBS/Tween. A drop of DAKO Rabbit Envision secondary antibody was then added to each coverslip and left to incubate at room temperature for 60 minutes, before again rinsing with PBS, followed by two washes with 0.03% PBS/Tween for 5 minutes each. 50µl of DAKO DAB Chromogen (1 drop of DAB combined with 1ml of substrate) was then applied to each of the coverslips and left to incubate at room temperature for 10 minutes. Coverslips were then washed twice with distilled water, for 5 minutes each. Counterstaining was subsequently performed by applying 4% Ehrlich's haematoxylin, followed by two washes with tap water, for 2 minutes each. Coverslips were left to air dry completely before mounting on slides using DPX mounting medium.

The intensity of staining by ICC for PELP-1 (and ER) was determined by calculating a Histoscore (H-score) for each slide examined. This would allow for an objective comparison when assessing protein expression between different

experimental variables. To determine a H-score the proportion of cells in each slide examined that stained (1) weakly, (2) moderately, and (3) strongly for PELP-1 (or ER) was manually assessed. The H-score for each slide was then calculated using the following equation (giving a score within a range of 0-300):

H-score = (3 x % strongly staining cells) + (2 x % moderately staining cells) + (1 x % weakly staining cells)

2.7.4 Use of confocal microscopy to detect protein co-localization

MCF7 cells were grown in the presence and absence of endocrine agents to 70% confluency on size 0 coverslips. Coverslips were then fixed in 4% (vol./vol.) formaldehyde/PBS for 15 minutes, followed by ice-cold (-20C) methanol for 5 minutes and ice cold (-20C) acetone for 3minutes. Cells were then further permeabilized with 2% (vol./vol.) Triton-X-100 for 5 minutes. An overnight incubation at 21°C was performed with a mixture of rabbit anti-PELP1 (1:100 Cell Signalling Technology, clone D5Q4W in PBS) and monoclonal anti-ER (1:100 Vector, clone 6F11,) antibodies. After primary antibody incubation, cells were left for 90 minutes to incubate at room temperature with the secondary antibody (ER = goat anti mouse-594 antibody, PELP-1 = Alexa-fluor goat anti-rabbit-488 antibody) (1:1000 vol/vol in PBS). Cells were then washed and mounted on glass slides. Confocal fluorescence microscopy analysis was conducted on a Leica SP5 inverted confocal laser scanning microscope equipped with a 63x oil-immersion objective, 488/633 nm excitation laser lines and 545 nm beam-splitter. Images were recorded using the sequential scanning mode to prevent fluorescence channel crosstalk/ bleed-through. Images were scanned at 100 Hz with a line average of three to reduce noise. Co-localization of PELP1 and ER was visualized as areas of yellow/orange within the microscopic field.

2.8 GM generation of stable EGFP-expressing MCF-7 cell line

2.8.1 Plasmid Preparation

The bacteria containing the plasmid of interest were purchased within an agar slab (Figure 2.23). Bacteria were retrieved from the slab and streaked across an agar plate using an inoculation loop. The plates were then incubated overnight at 37°C with 5% CO_2.

The following morning a single colony from the agar plate was selected and placed within a starter culture, containing 5ml of Lysogeny broth (LB) medium with the appropriate selective antibiotic (ampicillin). This starter culture was then incubated for 8 hours at 37°C within an orbital shaker set at a frequency of 300rpm. The starter culture was then diluted into a larger volume of selective LB medium (200µl of starter medium into 100ml LB broth – 1/500 dilution), which was then incubated overnight at 37°C within an orbital shaker set at a frequency of 300rpm.

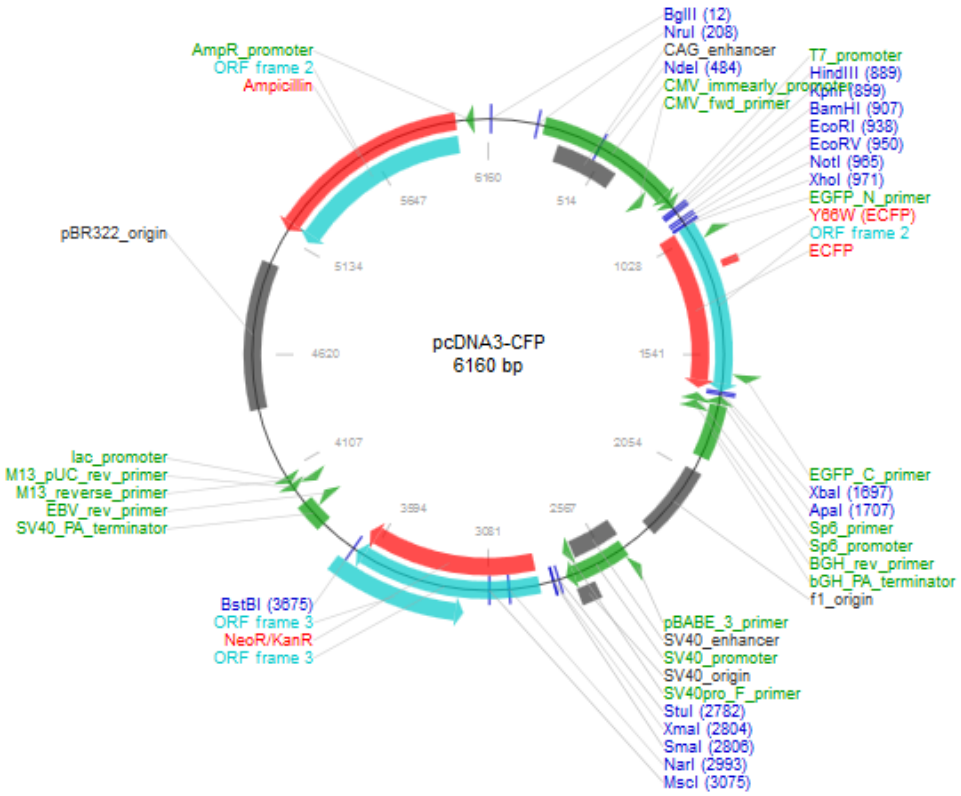

Figure 2.23 – Representation of the pcDNA3-EGFP plasmid used in the creation of EGFP-expressing MCF-7 breast cancer cells. The plasmid consists of 6160bp, with a 5446bp backbone. Contained within the plasmid are a 700bp EGFP insert, along with sites corresponding to ampicillin and geneticin (G418) resistance for use as selectable markers.

2.8.2 Plasmid Purification

Plasmid Purification was performed via the Endofree® Plasmid Purification Kit (Qiagen®). The bacterial cells produced from the previously mentioned overnight culture were harvested by centrifugation of the flask at 6000xg for 15 minutes at 4°C. The supernatant was then discarded and the bacterial cells re-suspended in 10ml of Buffer P1 (with added RNAase A) to induce cell lysis. The lysate was then transferred from the culture flask to a 50ml Falcon® tube. Once the cells had been completely re-suspended, 10ml of buffer P2 was added and mixed thoroughly by vigorous inverting and the suspension was then left to incubate at room temperature for 5 minutes. During this incubation period the QIAfilter Maxi Cartridge was prepared within a separate 50ml Falcon® tube. Chilled buffer P3 (10ml) was then added to the lysate and mixed immediately by vigorous inverting to aid precipitation of genomic DNA, proteins and cell debris. The lysate was then carefully poured into the barrel of the QIAfilter cartridge and left to incubate at room temperature for 10 minutes, allowing a precipitate containing proteins, genomic DNA and detergent to float to the top of the cartridge. The cap at the bottom of the QIAfilter Maxi Cartridge was then removed and the plunger gently inserted to filter the lysate into the 50ml Falcon® tube. At this stage, a 120μl sample of the filtered lysate (Sample 1) was collected and saved for later assessment on an analytical gel to determine whether growth and lysis conditions were optimal.

The QIAfilter Maxi Cartridge was then disposed of and 2.5ml of Buffer ER was added to the filtered lysate (containing the plasmid of interest) and the lysate left to incubate on ice for 30 minutes. During this incubation period the Qiagen-tip 500 was equilibrated by applying 10ml of Buffer QBT to the column and allowing this to empty completely by gravity flow. After incubation, the filtered lysate was then passed through the Qiagen-tip 500 and allowed to empty by gravity flow, allowing the plasmid DNA to be trapped by passing through the QIAGEN resin at the bottom of the device. At this stage, a 120μl sample of the flow through was collected and saved (Sample 2) for later assessment by the analytical gel, to determine the efficiency of plasmid binding to the QIAGEN resin. The Qiagen-tip was then twice

washed by passing 30ml (x2) of Buffer QC through its column, removing all contaminants within the resin. At this point a 240μl sample from the combined fractions of the wash was taken and saved for the analytical gel (Sample 3).

The plasmid DNA was then eluted from the Qiagen resin by passing 15ml of Buffer QN through the column and collected in an endotoxin free tube, with a 60μl sample of the eluate kept for analysis by the analytical gel (Sample 4).
The DNA plasmid was then precipitated by adding 10.5ml of room-temperature isopropanol, which was mixed, and then the solution immediately centrifuged at 15000xg for 30 minutes at 4°C. The supernatant was then carefully decanted to leave a pellet of Plasmid DNA, which was washed with 5ml of endotoxin-free, 70% ethanol and again centrifuged at 15000xg for 10 minutes (ensuring all traces of isopropanol are removed) and the supernatant carefully decanted. The pellet was then air dried for 10 minutes and re-dissolved in endotoxin-free Buffer TE.

To determine the plasmid yield, DNA concentration was determined by UV spectrophotometry at 260nm. Qualitative analysis was determined by running the plasmid on an agarose gel, after cleavage with the restriction enzymes BamH1 and EcoR1 respectively, at variable dilutions (Figure 2.24). On the same gel, the samples taken and stored (1-4) during the various steps of the purification process, were analyzed to assess the efficiency of each step of the technique. Following adequate quantitative and qualitative assessment, the dissolved DNA plasmid was aliquoted and stored at -20°C until needed.

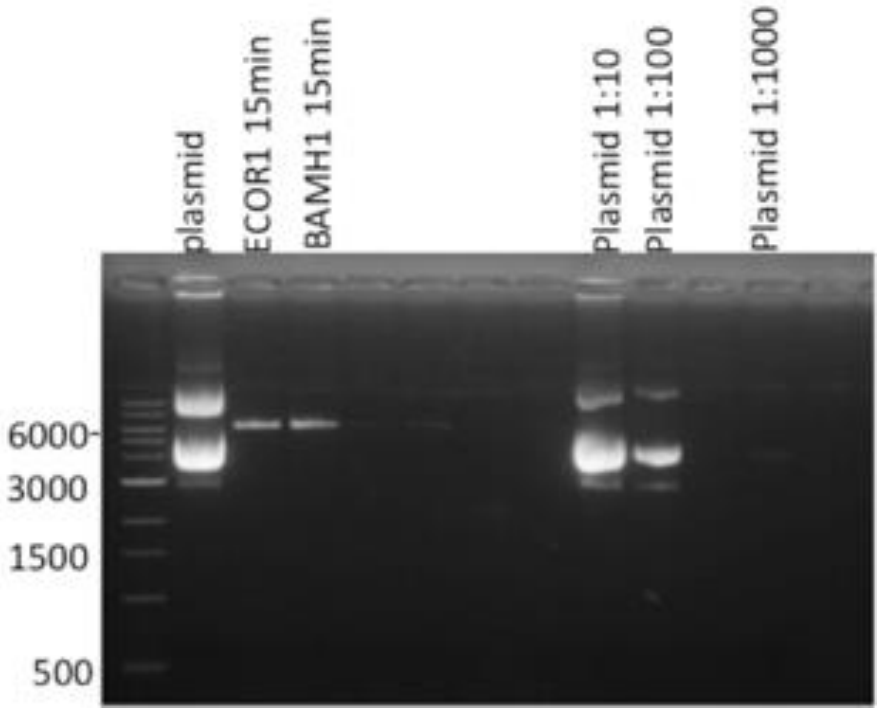

Figure 2.24 – Agarose gel demonstrating expression on non-cleaved EGFP plasmid at 1:10, 1:100 and 1:1000 dilution, alongside cleaved form of EGFP plasmid using restriction enzymes BamH1 and EcoR1. The non-cleaved form of the plasmid demonstrates several bands on the gel, based upon migration of its folded and un-folded forms. The plasmid signal becomes weaker with dilution. Cleavage forms of the plasmid, using restriction enzymes BamH1 and EcoR1, reveal a single band, corresponding to the 6160bp plasmid size.

2.8.3 Plasmid Transfection

Plasmid transfection was performed using the lipid based Fugene 6® transfection reagent. The appropriate volume(s) of plasmid DNA, transfection reagent and medium used for each transfection were identified using the table shown in Appendix 7.14. The transfection procedure was initially optimised for the MCF-7 cell line by varying the Fugene 6®: plasmid DNA ratio and transfection incubation time. Following this period of optimization, the final transfection protocol was as follows:

Initially, the Fugene 6® reagent was diluted with an appropriate volume of serum-fee medium within an Eppendorf tube, by pipetting the Fugene 6® reagent directly into the medium without allowing contact with the walls of the tube. The Eppendorf was then tapped to allow mixing and then the Eppendorf incubated at room temperature for 5 minutes. An appropriate volume of plasmid DNA was the then added to the diluted Fugene 6® reagent using a 3:1 ratio (i.e. 1μg of plasmid DNA for every 3μl of concentrated Fugene 6® reagent). The Eppendorf contents were then mixed once more by tapping the tube gently and left to incubate at room temperature for 15 minutes.

MCF-7 cells grown to 70% confluence within 35mm dishes, in preparation for transfection were then removed from the incubator and the lipid/Plasmid DNA complex added in a dropwise manner whilst swirling the plate/flask to ensure coverage of the entire surface. The cells were then returned to the incubator for culture at 37°C for 72 hours prior to identification of successful transfection, through detection of EGFP expression by fluorescent microscopy.

2.8.4 Selection and Clonal Expansion of Transfected EGFP Cell Line

Selection of EGFP-expressing cells within the transfected cohort of MCF-7 cells was performed by culturing cells in the antibiotic Geneticin (G418). This would cause cellular toxicity and cell death of wild-type MCF-7 cells, while preserving EGFP-expressing cells due to the presence of a G418 resistant gene encoded on the transfected plasmid.

The optimum G418 dose was determined by constructing a kill curve using wild-type MCF-7 cells. To do this MCF-7 cells were seeded in 35mm culture dishes (100,000 cell/dish) and cultured in W5% medium overnight at 37°C. The following day medium was replaced with W5% medium containing staggered doses of Geneticin (G418) antibiotic (0 – 1.1mg/ml) in duplicate, and cells were cultured at 37°C for a further 6 days, with the medium replaced every 3 days. Cells were then trypsinized and counted using a Coulter counter to determine the surviving cell number. Based on the resulting kill-curve (Figures 2.25), the

Geneticin dose necessary to produce relative cell survival of less than 20% was determined as 0.6mg/ml. This dose was also confirmed by repeating the experiment using an MTT assay in place of cell counting.

Transfected cells were cultured in W5% medium containing 0.6mg/ml of Geneticin, changing the culture medium every 3 days, for 7 days in total, after which the cells were maintained in routine culture of R5% medium containing a lower dose of 0.1mg/ml Geneticin.

To develop a clonal cell line of uniformly expressing EGFP-transfected MCF-7 cells, this heterogeneous group of cells was trypsinized, diluted and re-seeded into a 96-well plate at a density of 1 cell per well. Cells were maintained in culture at 37°C in R5% medium, containing 0.1mg/ml of G418, with the culture medium changed every 3 days. Each well was then inspected after 24 hours using both bright-field and fluorescent microscopy to identify wells containing a single EGFP-expressing cell. These wells were marked and then observed daily to visually assess the rate of cell proliferation and cell number. After 7-days incubation in this environment these wells were again visualised with fluorescent microscopy to detect 3 wells containing cells with the brightest expression of EGFP, determined visually. Cells within each of these 3 wells were trypsinized and re-suspended in culture flasks containing R5% medium, containing 0.1mg/ml G418, labelled as clones 1, 2 and 3 respectively, and grown and maintained in routine cell culture at 37°C until needed (Figure 2.26).

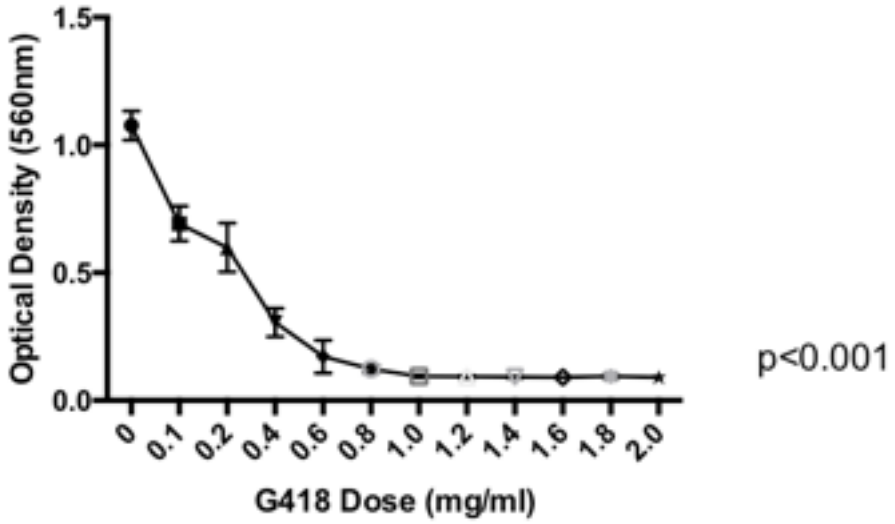

a.

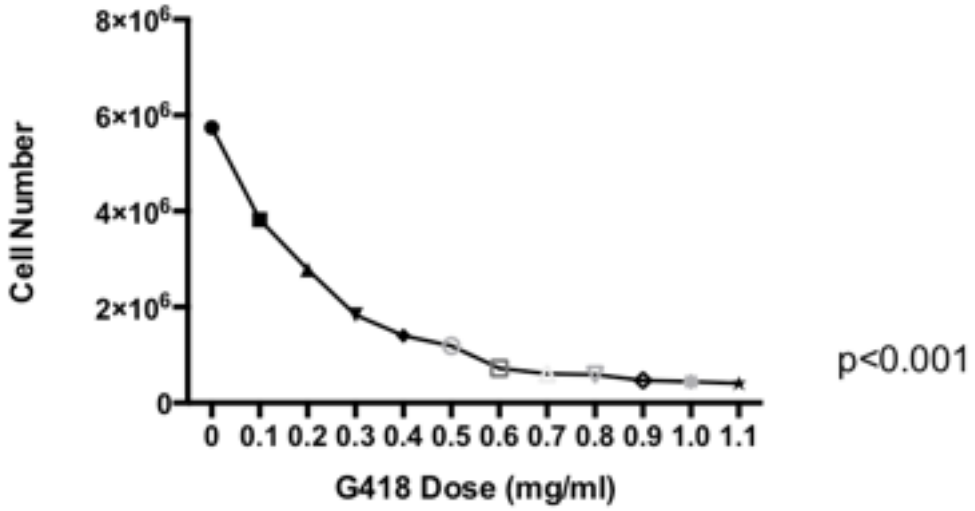

b.

Figure 2.25 – Kill curve demonstrating survival effect of MCF-7 cells following treatment with a varying dose of G418, assessed using (a) MTT and (b) cell counting assays. Cell survival is reduced as the dose of G418 increased.

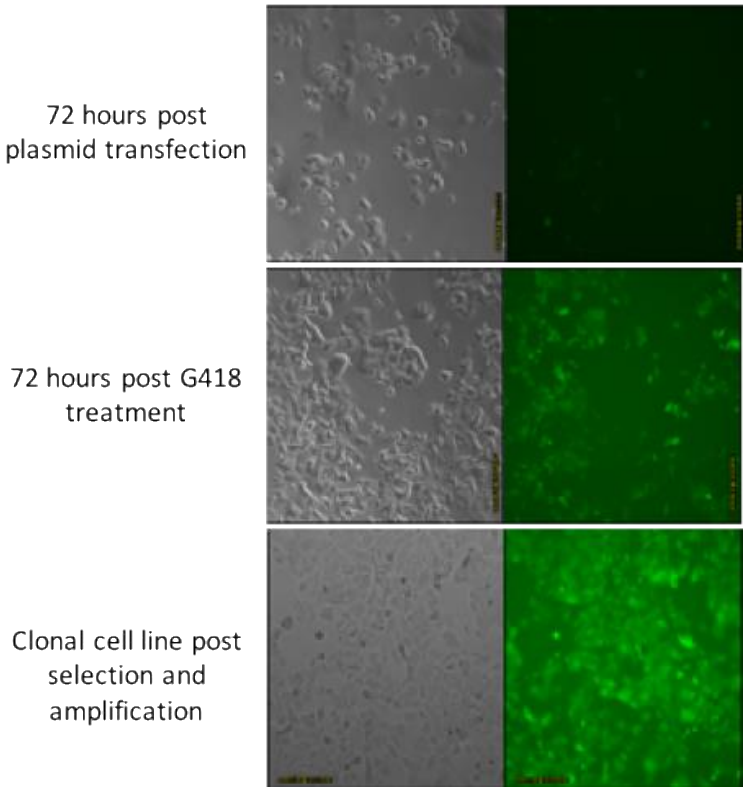

Figure 2.26 - Evidence of EGFP expression at each stage of cell line development. EGFP-transfected MCF-7 cells were diluted and re-seeded into a 96-well plate (1 cell/well). Cells were maintained in culture and each inspected to detect wells containing cells with the brightest expression of EGFP.

2.9 Graphics and Statistical Analysis

All graphical data is presented using Prism Graphpad® version 6 statistical software. Pictorial data, such as cell counting from still images and 3D spheroid analysis, was assessed using ImageJ ® version 2.0.0. Densitometry of Western blotting data was performed using Image Studio®. Statistical analysis was performed using SPSS® 20. Statistical significance was determined by a p-value of <0.05. For analysis of data comparing two independent variables an independent samples t-test was performed where data followed a normal distribution, while a Mann-Whitney test was performed in cases where the data was deemed to be non-parametric. For comparison of multiple variables, a one-way ANOVA test was performed to assess for a significance across the dataset, with a post-hoc Bonferroni test used to assess significance between two of the variables within the dataset.

3.0 Results

3.1 Exploring the effect of endocrine therapies in an E-cadherin deficient model of Luminal A breast cancer

3.1.1 Introduction

Previous work from the BCMPG intriguingly revealed that (i) endocrine agents consistently stimulate a modest increase in cellular invasion and migration in endocrine-responsive, ER+ breast cancer cells and that (ii) these effects are greatly augmented when E-cadherin expression is lost (133, 134).

These observations have potential clinical ramifications as they demonstrate that the response to endocrine therapy is variable amongst endocrine responsive, ER+ tumours. Further to this, they may represent that at least a subset of ER+ tumours demonstrate an adverse response to some endocrine therapy, such as tamoxifen, and patients with such tumours may be better served with an alternative endocrine therapy. If so, further knowledge of this response along with any underlying mechanisms involved would be invaluable in trying to optimise and personalise adjuvant therapy based on tumour biology.

The initial aim of this thesis was therefore to establish a model of E-cadherin deficiency in ER+ MCF-7 breast cancer cells with which to explore, at a mechanistic level, the processes underlying this phenomenon. Prior to this however, the response to endocrine therapies as described above would need to be validated, both within the MCF-7 cell line and amongst other ER+ breast cancer cell lines, to determine the relative generality/specificity of these findings.

3.1.2 Establishment of an E-Cadherin deficient ER+ breast cancer cell model using siRNA mediated knockdown of the CDH1 gene

To investigate the response of breast cancer cells to endocrine therapy in the setting of E-Cadherin deficiency, gene-silencing technology using siRNA was used to create E-Cadherin knockdown in ER+ breast cancer models.

A 72-hour lipid-based transfection system was utilized using Dharmafect smartpool® CDH1 siRNA (methods 2.2.6). Initially, transfection was optimized using a range of concentrations of siRNA (100nm, 150nm, 200nm) to determine the most effective dose of siRNA for knockdown of the target (assessed by Western blot analysis). siRNA dose-optimization was performed initially using the luminal A, MCF-7 cell line (Figure 3.1), where Western blot data revealed successful knockdown of E-cadherin at all doses tested; no difference was seen in the level of suppression when using the 100nm, 150nm or 200nm siRNA concentrations. Successful knockdown of E-cadherin was also achieved using the ER+, HER2+, BT474 cell line (Figure 3.2). Western blot data again confirmed no significant difference in the level of E-cadherin knockdown between siRNA doses. Based on this data, experiments would proceed using the 100nm anti-CDH1 siRNA to produce optimum knockdown of E-cadherin, whilst avoiding the potential consequences of cellular siRNA toxicity from using a higher dose.

Given that some of the proposed assays to be completed in this work required a prolonged treatment time, it was next necessary to determine whether E-cadherin knockdown could be sustained for an appropriate period, using the siRNA transfection method described. A time course experiment was therefore designed where cells, transfected with control (non-targeting/NT) or CDH1-specific (CDH1) siRNA, were lysed for analysis by Western blot on 6 sequential days from the end of the 72-hour transfection period, to evaluate if suppression of E-cadherin expression was sustained over this period. This experiment was again performed again using both the MCF-7 and BT474 cell lines (Figures 3.3 and 3.4).

Results for both cell lines showed that E-Cadherin expression continued to be suppressed using this method for up to 6 days following siRNA withdrawal, indicating the suitability of this method for use in future assays of a similar time course.

As a further aim of this work was to explore the consequences of E-cadherin deficiency and endocrine response in a 3D matrix-enriched context, it was next appropriate to determine that this siRNA approach was suitable for this. MCF-7 cells, transfected with NT and CDH1-specific siRNA, were cultured in 3 different conditions before cells were lysed for analysis with Western blotting (Figure 3.5). The three conditions were: (i) cells lysed immediately following the 72hrs siRNA transfection period; (ii) cells harvested following siRNA transfection and re-seeded in 2D culture for a further 6 days and (iii) cells harvested after 72hrs siRNA treatment and used in Matrigel© 3D embedded cell culture for a further 6 days prior to cell lysis and Western blotting. Results showed that knockdown of E-cadherin was adequately sustained for 6 days in both 2D and 3D cell culture, indicating this method of knockdown is also suitable for use in similar future 3D cell culture experiments.

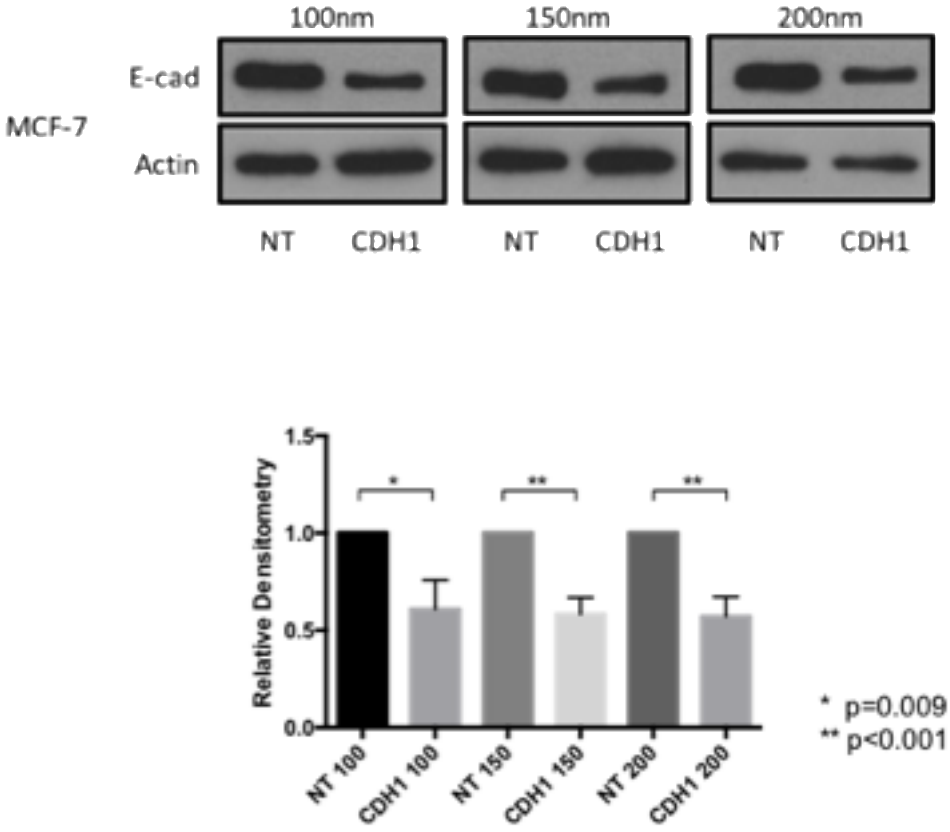

Figure 3.1 – E-cadherin expression in MCF-7 cells following CDH1 siRNA treatment. Western blotting and densitometry data demonstrating the expression of E-cadherin and Actin in MCF-7 cells, 72 hours after NT and CDH1 siRNA transfection, using 100nm, 150nm and 200nm dose of siRNA respectively. E-cadherin expression is suppressed using 100nm, 150nm and 200nm dose of CDH1 siRNA in MCF-7 cells.

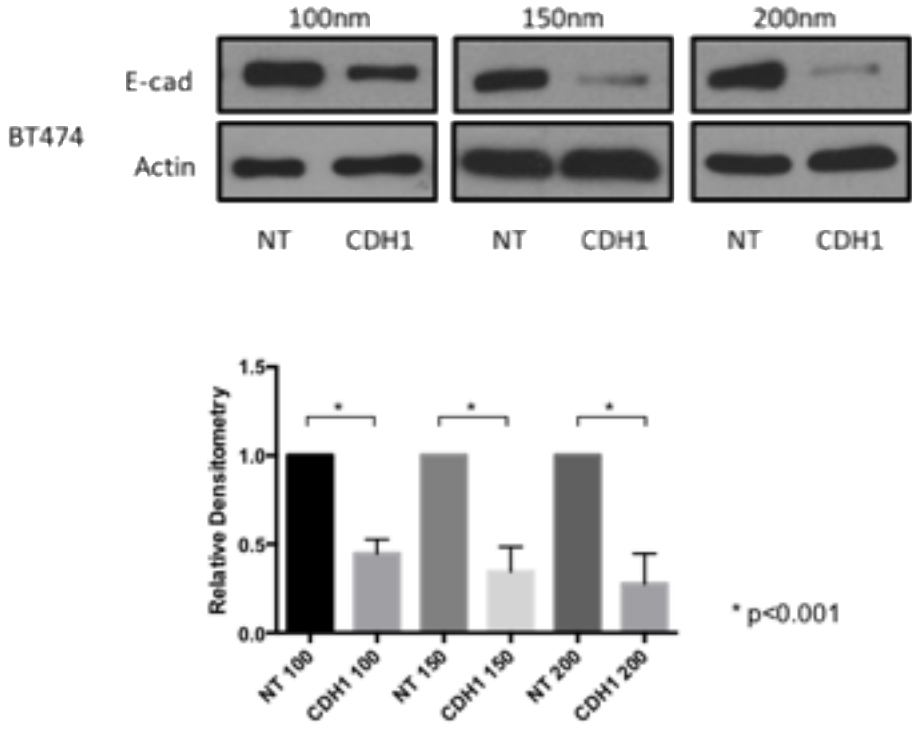

Figure 3.2 – E-cadherin expression in BT474 cells following CDH1 siRNA treatment. Western blotting and densitometry data demonstrating the expression of E-cadherin and Actin in BT474 cells, 72 hours after NT and CDH1 siRNA transfection, using 100nm, 150nm and 200nm dose of siRNA respectively. E-cadherin expression is suppressed using 100nm, 150nm and 200nm dose of CDH1 siRNA in BT474 cells.

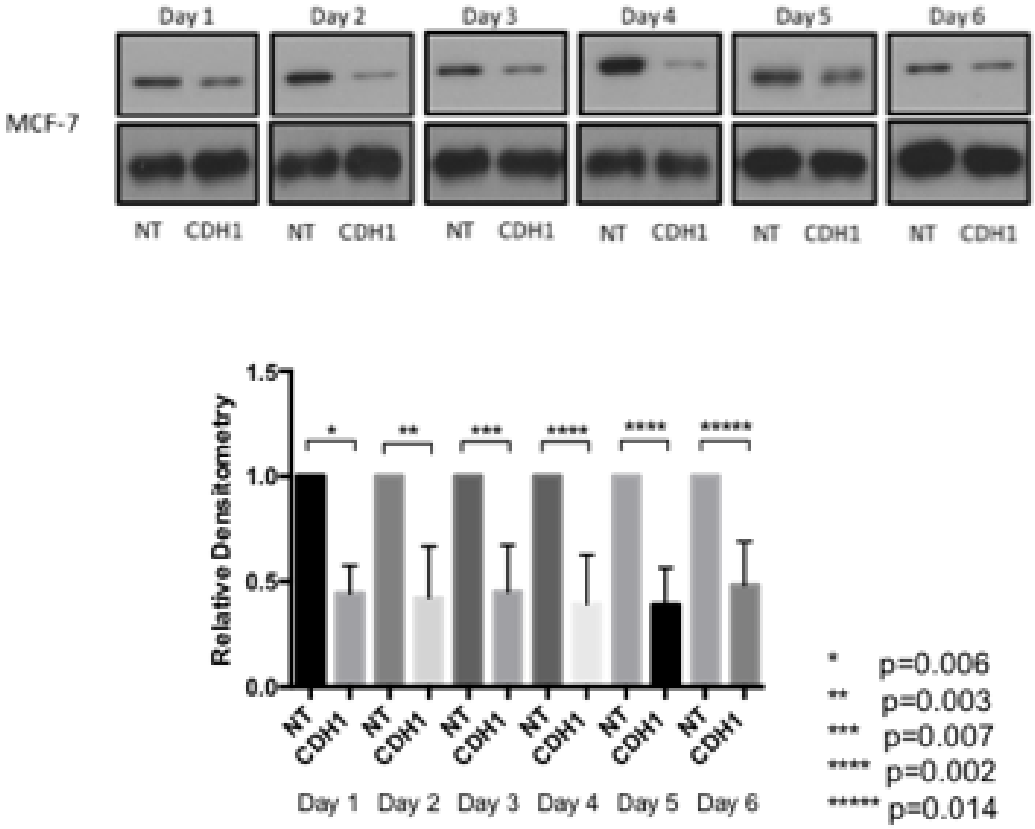

Figure 3.3 – Time course of E-cadherin expression in MCF-7 cells following CDH1 siRNA treatment. Western blotting and densitometry data demonstrating the expression of E-cadherin and Actin in MCF-7 cells on 6 consecutive days following the withdrawal of NT and CDH1 siRNA treatment (100nm). E-cadherin suppression is maintained for up to 6 days following withdrawal of siRNA treatment in MCF-7 cells.

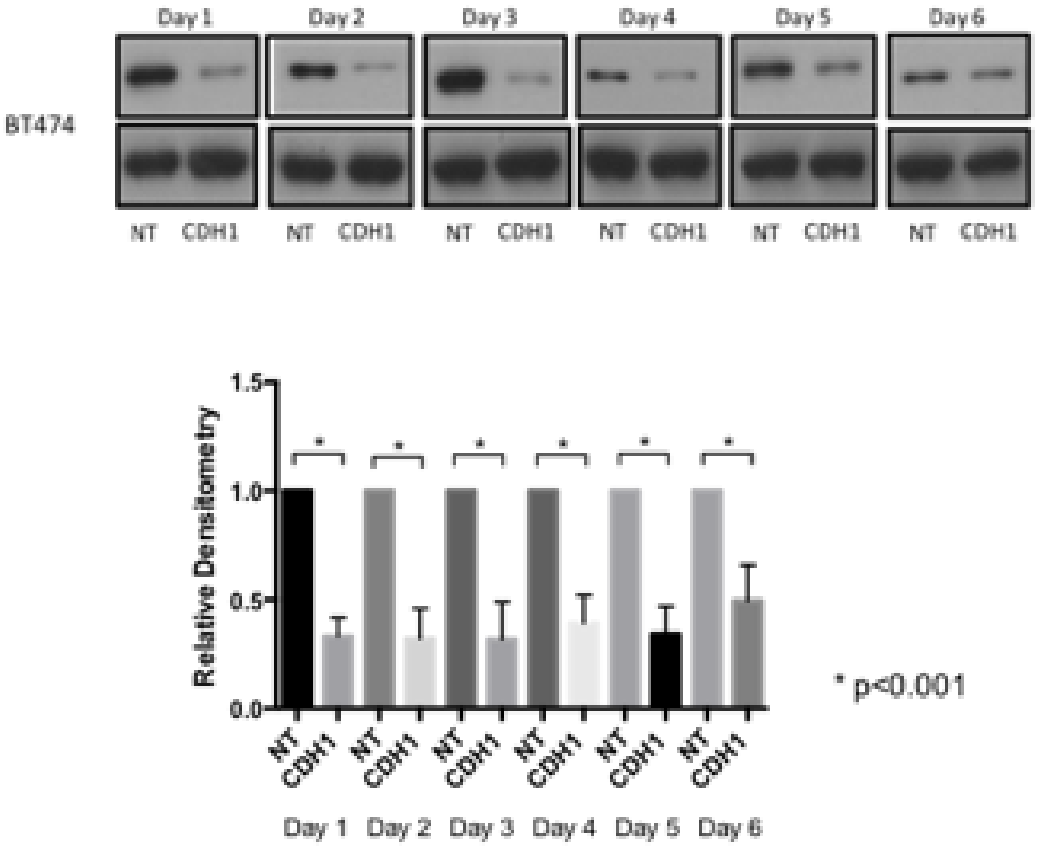

Figure 3.4 - Time course of E-cadherin expression in BT474 cells following CDH1 siRNA treatment. Western blotting and densitometry data demonstrating the expression of E-cadherin and Actin in BT474 cells on 6 consecutive days following the withdrawal of NT and CDH1 siRNA treatment (100nm). E-cadherin suppression is maintained for up to 6 days following withdrawal of siRNA treatment in BT474 cells.

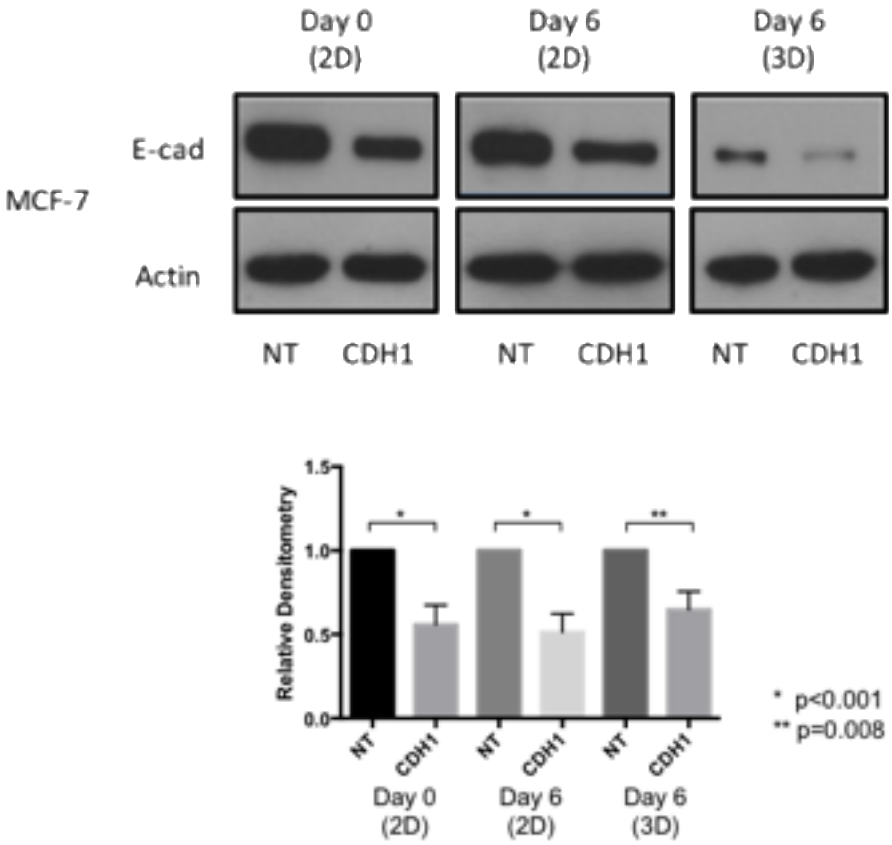

Figure 3.5 - Time course of E-cadherin expression in MCF-7 cells maintained in 2D and 3D cell culture following CDH1 siRNA treatment. Western blotting and densitometry data demonstrating the expression of E-cadherin and Actin in MCF-7 cells grown in 2D and 3D cell culture following the withdrawal of NT and CDH1 siRNA treatment (100nm). E-cadherin suppression is maintained for up to 6 days following withdrawal of siRNA treatment in in both 2D and 3D cell culture, in MCF-7 cells.

3.1.3 Tamoxifen induces invasion in wild type and E-cadherin (CDH1) deficient MCF-7 cells

After establishing a model of E-cadherin deficiency in MCF-7 cells, the next step was to confirm the findings previously described by the BCMPG (134), whereby tamoxifen therapy increased the invasiveness of E-cadherin deficient MCF-7 cells, and subsequently to expand on these observations by exploring additional endocrine treatments. To assess this, E-cadherin expression was suppressed in MCF-7 cells (+/-endocrine treatment) and the cells seeded into Matrigel®-coated trans-well invasion chambers, with invasion assessed after 3 days.

These data revealed that wild-type MCF-7 cells were poorly invasive (Figure 3.6), although intriguingly tamoxifen treatment consistently resulted in a modest, yet statistically significant, increase in invasion ($p=0.015$) compared with untreated cells. In contrast, E-cadherin knockdown resulted in a significant gain in the number of cells invading, compared to cells transfected with NT siRNA ($p=0.002$); this increase in invasiveness was dramatically augmented in the presence of tamoxifen ($p<0.001$) with more than a 20-fold increase in the number of invading cells seen compared to control.

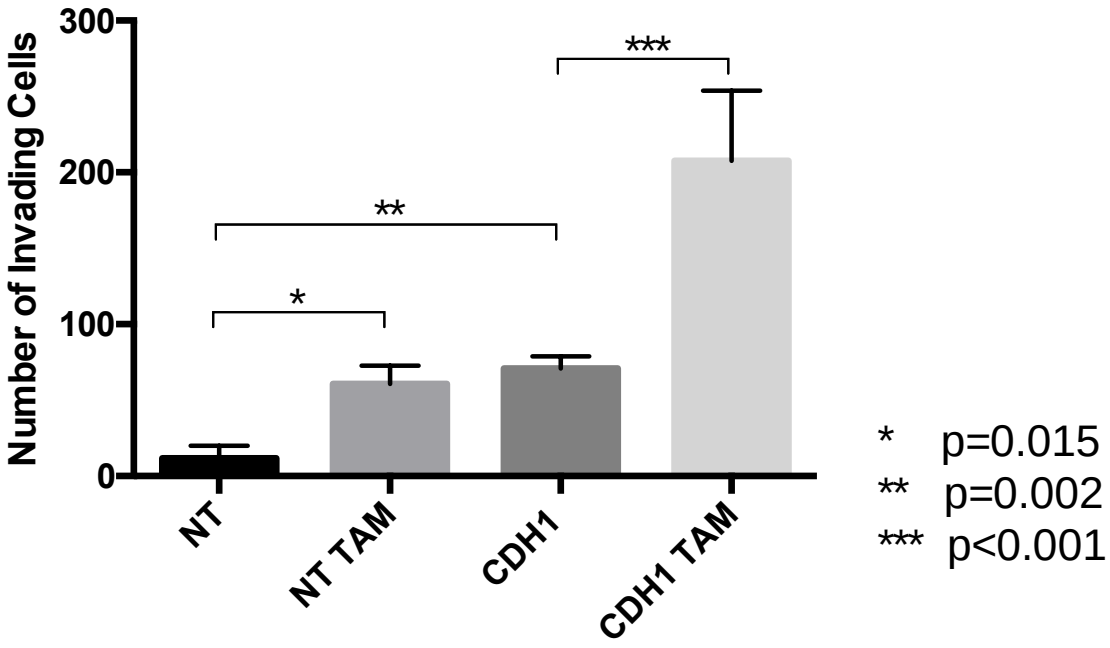

Figure 3.6 – Cell invasion in MCF-7 cells treated with tamoxifen (TAM) +/- CDH1 siRNA. MCF-7 cells were treated with non-targeting (NT) or CDH1 targeting (CDH1) for 72 hours before assessing their invasive capacity in control or tamoxifen ($1x10^{-7}M$) containing medium. Both wild-type (NT) and E-cadherin deficient (CDH1) cells treated with tamoxifen promoted an increase in cell invasion through Matrigel©. The graph shows the results for the mean of three separate experiments.

3.1.4 Establishment and optimization of a new 2D cell invasion assay, utilizing a stably transfected EGFP-expressing MCF-7 cell line

Whilst the trans-well invasion assay used described above (Methods 2.4.1) demonstrated reliable results when investigating the effect of endocrine therapy on breast cancer cell invasion, an assessment as to whether this assay could be further improved was undertaken. The original assay involved assessing the number of cells invading through an ECM within the setup of a Boyden Chamber. The final part of this assay involved fixing and then staining the invasive cells within the Boyden chamber insert with DAPI to visualize the nuclei of cells using fluorescent microscopy, which allowed for cell counting.

Whilst this was an effective assay, in an aim to improve the assay efficiency, particularly by avoiding the need for nuclei staining as part of this final step, an alternative method for cell counting was trialed. This involved the generation and maintenance of a stable fluorescent MCF-7 cell line, whereby cells could be individually counted using fluorescent microscopy set at the appropriate wavelength, avoiding the need for fixing and staining altogether. A stable clonal EGFP-tagged MCF-7 cell line was therefore developed for this purpose (Methods 2.8).

To assess the effectiveness of this method of cell counting, as compared to cell counting via DAPI staining, an invasion assay to assess the capacity of EGFP-tagged MCF-7 cells, grown in 2D cell culture, to invade through a Matrigel® matrix over a 48-hour period, was employed. As previously described, E-cadherin knockdown cells (CDH1) were compared with wild-type cells (NT) grown in the presence and absence of 6-day tamoxifen treatment ($1x10^{-7}M$). To clarify the accuracy and effectiveness of the different methods of cell counting, invasive cells present of the underside of the Boyden chamber insert after 72 hours of invasion was initially counted using fluorescent microscopy to detect EGFP expression (wavelength 488nm) of live cells, prior to formaldehyde fixation, following gentle

removal of the overlying Matrigel® matrix with a cotton bud. Inserts were then fixed with 3.7% formaldehyde, stained with DAPI, and mounted as previously described (Methods 2.4.1), before cell counts were again taken by fluorescent microscopy, using settings to detect both EGFP (wavelength 488nm) and DAPI (wavelength 358nm) expression. Results using all three methods for cell detection and counting in the context of this assay were then compared (Figure 3.7).

Results demonstrated that while all 3 methods of counting appeared to provide a similar pattern of results as described previously (Results 3.2), it was clear that there was an undercounting of cells using techniques that utilized EGFP expression. Reasons for this relative undercount can be explained by difficulty in assessing and differentiating cell numbers when cells are located in clusters using the EGFP technique, as opposed to the more defined nuclear staining using DAPI. In addition, due to the convexity of the Boyden chamber membrane, counting in-situ EGFP-expressed cells required constant re-focusing of the microscope depending which part of the membrane is visualized, which could account for some cells not being counted. While this was not a problem when the cells were fixed and the membrane mounted using a coverslip, fixation in 3.7% formaldehyde did have a delayed bleaching effect on EGFP-expression, which required slides to be counted within 24 hours of fixation. While the relative undercounting of cells using the EGFP technique would not preclude this method being used in future parts of the project, as the trend in invasion was not dissimilar to the DAPI-staining technique, due to the time delay from optimization of EGFP cell counting, and for consistency purposes, the original DAPI-staining technique was chosen for the remainder of the project.

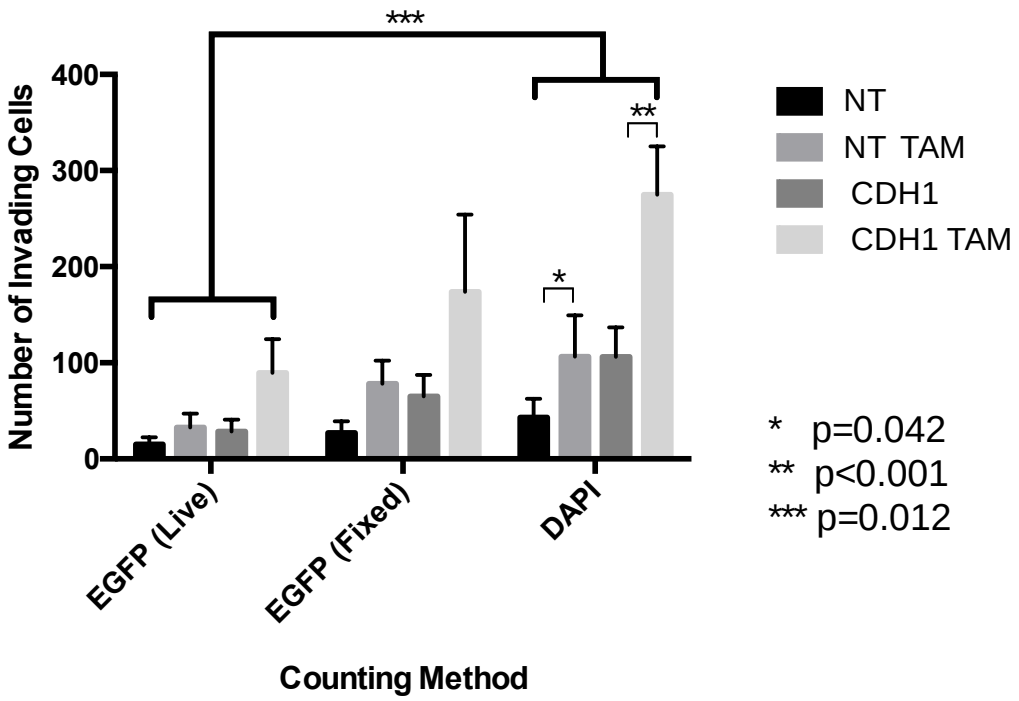

Figure 3.7 – Cell invasion in MCF-7 cells treated with tamoxifen (TAM) +/- CDH1 siRNA, determined by cell counting methods utilizing EGFP and DAPI expression. MCF-7 cells were treated with non-targeting (NT) or CDH1 targeting (CDH1) siRNA for 72 hours before assessing their invasive capacity in control or tamoxifen containing medium. Both wild-type (NT) and E-cadherin deficient (CDH1) cells treated with tamoxifen promoted an increase in cell invasion through Matrigel©. Counting via EGFP-tagged cells showed similar results to DAPI staining, but led to relative undercounting of the cell number. The graph shows the results for the mean of three separate experiments.

3.1.5 Tamoxifen induces migration in wild type and E-cadherin (CDH1) deficient MCF-7 cells

In addition to assessing the consequences of E-cadherin loss on the invasive response of ER+ breast cancer cells to tamoxifen, it was also desirable to determine whether tamoxifen could induce a migratory phenotype in cells lacking E-cadherin. To do this trans-well chambers with membranes coated with fibronectin were employed.

Non-migratory wild-type MCF-7 cells were seen to shown an increase in their migratory capacity in response to tamoxifen (Figure 3.8; $p=0.017$), and when E-cadherin expression was suppressed ($p<0.001$). The combined action of E-cadherin suppression and tamoxifen treatment resulted in a dramatic increase in cellular migration (~5-6 fold vs. control; $p<0.001$).

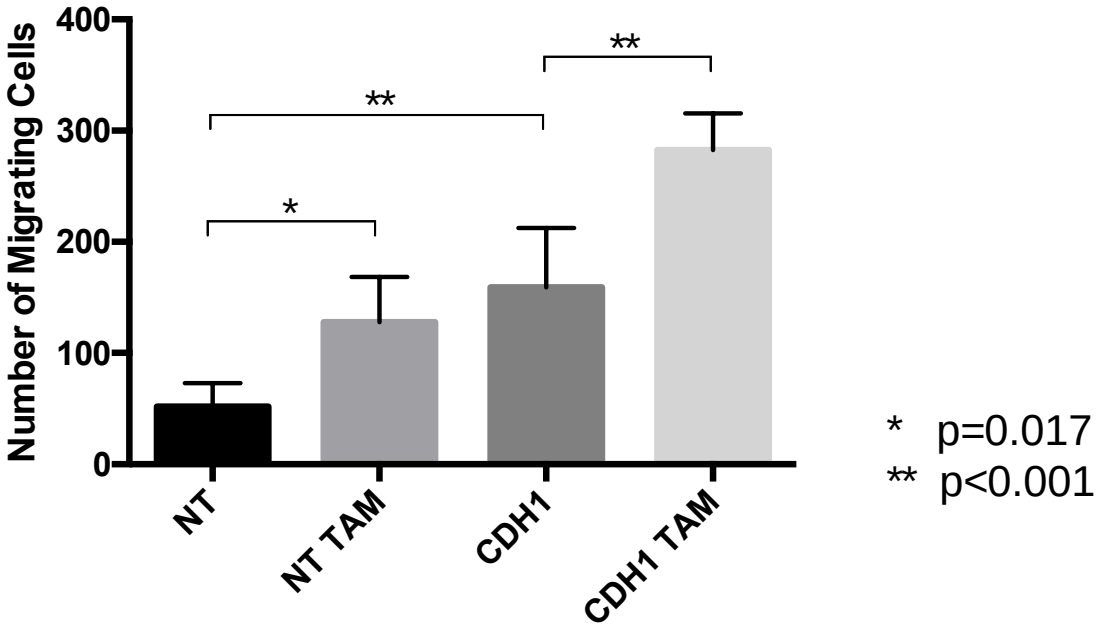

Figure 3.8 - Cell migration in MCF-7 cells treated with tamoxifen (TAM) +/- CDH1 siRNA. MCF-7 cells were treated with non-targeting (NT) or CDH1 targeting (CDH1) siRNA for 72 hours before assessing their migratory capacity in control or tamoxifen ($1x10^{-7}M$) containing medium. Both wild-type (NT) and E-cadherin deficient (CDH1) cells treated with tamoxifen promoted an increase in cell migration. The graph shows the results for the mean of three separate experiments.

3.1.6 Tamoxifen inhibits proliferation in wild-type and E-Cadherin deficient MCF-7 cells

One possible explanation for the increase in invasion and migration seen with tamoxifen treatment of E-cadherin deficient cells is that tamoxifen induces cellular proliferation, which accounts for the increase in observed cell numbers. To explore whether this hypothesis was true, the effects of tamoxifen on cellular proliferation +/- CDH1 knockdown was investigated using two different approaches.

The hypothesis was initially investigated by assessing 3-day cellular growth in the presence and absence of tamoxifen +/- CDH1 knockdown within a 96-well plate using an MTT assay (Figure 3.9a). This data showed no significant difference in cellular proliferation between E-cadherin competent and E-cadherin deficient MCF-7 cells. In both cases however, tamoxifen treatment resulted in a reduction in growth compared to control ($p<0.0001$).

MTT data was further confirmed using cell counting experiments. Cells were grown for 3 days in 35mm culture dishes under each of the studied conditions in duplicate, with formal cell counts taken using a Coulter counter. When using this technique, we see similar results to that produced by the MTT assay (Figure 3.9b), whereby there is no significant difference in final cell number when comparing wild-type with E-cadherin deficient cells both with and without tamoxifen. A suppression in the final cell number was again seen with tamoxifen therapy in both arms of the experiment however ($p<0.0001$).

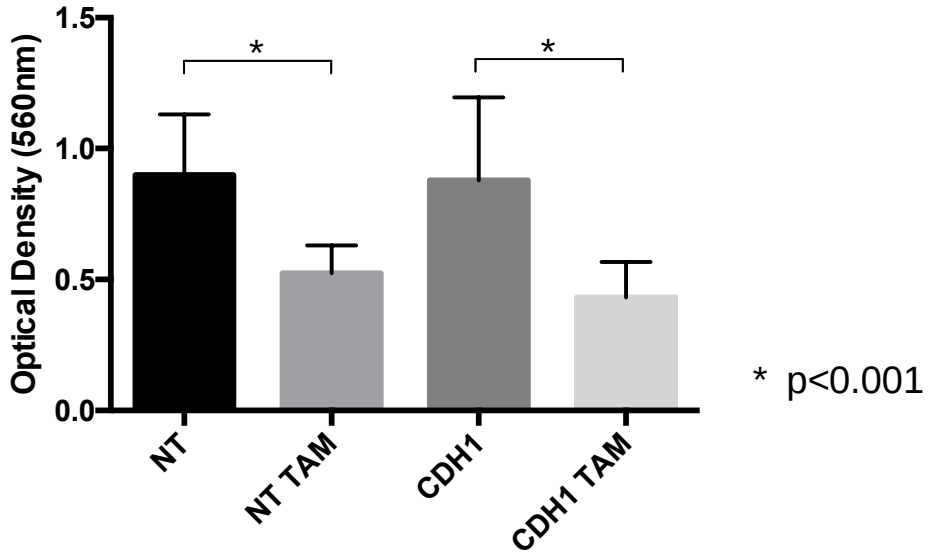

a.

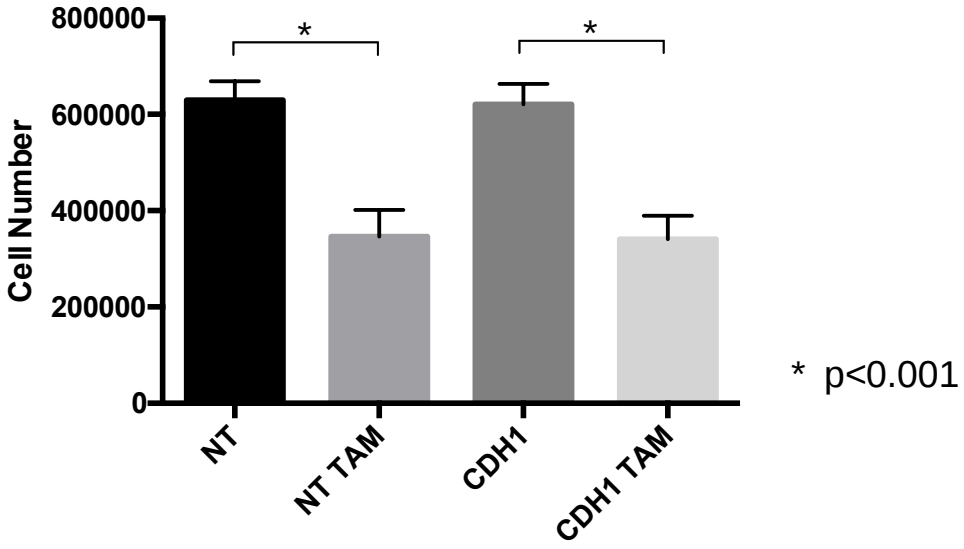

b.

Figure 3.9 - Cell proliferation in MCF-7 cells treated with tamoxifen (TAM) +/- CDH1 siRNA, determined by (a.) MTT and (b.) cell counting assays. MCF-7 cells were treated with non-targeting (NT) or CDH1 targeting (CDH1) siRNA for 72 hours before assessing 3-day proliferation in control or tamoxifen ($1x10^{-7}$M) containing medium via MTT and cell counting assays. Tamoxifen therapy resulted in a reduction in cellular proliferation in both wild type and E-cadherin knockdown MCF-7 cells.

3.1.7 Fulvestrant (Faslodex ®) therapy induces invasion and migration in the MCF-7 cell line, in the presence and absence of E-Cadherin expression

After noting the effect of tamoxifen therapy on the phenotype of MCF-7 cells, it was decided to extend these observations to a second endocrine agent, fulvestrant (FAS); a pure ER antagonist.

Invasion was again assessed by comparing E-cadherin deficient (CDH1) with wild-type cells (NT) grown in the presence and absence of fulvestrant. In a similar manner to that previously seen with tamoxifen, these data again demonstrated a small, yet significant, increase in invasion amongst wild-type cells treated with fulvestrant (Figure 3.10a, $p<0.001$). In addition, this invasive response was notably augmented when cells deficient in E-cadherin were treated with fulvestrant as compared to the control ($p<0.001$).

The effect of fulvestrant on cell migration was also investigated as before, using trans-well chambers with fibronectin coated membranes. Again, it was observed that fulvestrant treatment resulted in a small but significant increase in migration in wild-type cells (NT) (Figure 3.10b, $p=0.001$), with a more dramatic increase in migration observed with treatment in E-cadherin deficient cells ($p<0.001$).

To confirm the observed effects of fulvestrant treatment on cell invasion and migration is not a consequence of unintended effects of cell proliferation, these effects were assessed using an MTT assay (Figure 3.11). As demonstrated previously, E-cadherin knockdown alone had no significant effect on proliferation, while fulvestrant therapy had a negative effect on proliferation in both wild-type and E-cadherin deficient cells ($p<0.001$).

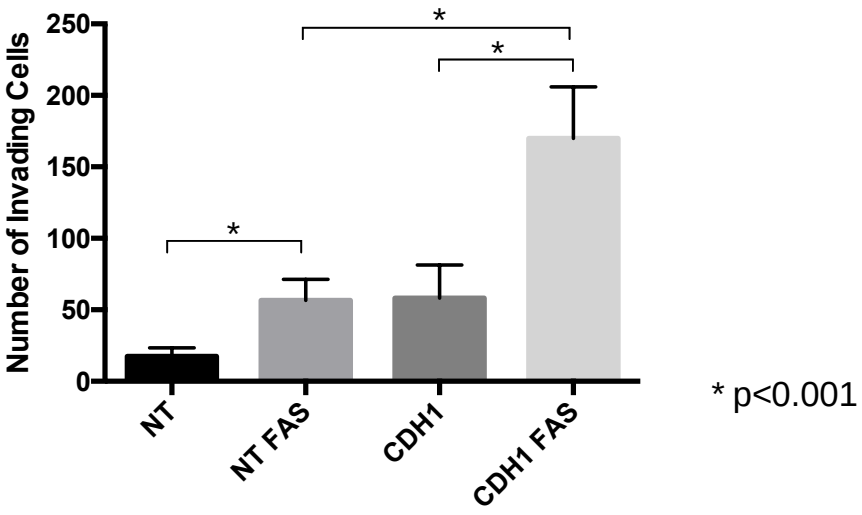

a.

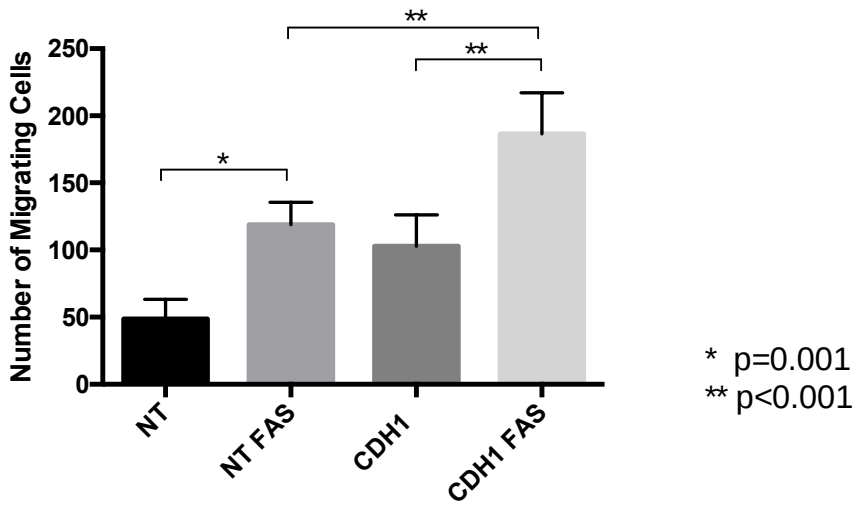

b.

Figure 3.10 - Cell (a.) invasion and (b.) migration in MCF-7 cells treated with fulvestrant (FAS) +/- CDH1 siRNA. MCF-7 cells were treated with non-targeting (NT) or CDH1 targeting (CDH1) siRNA for 72 hours before assessing their (a.) invasive, (b.) migratory capacity in control or fulvestrant ($1x10^{-7}M$) containing medium. Both wild-type (NT) and E-cadherin deficient (CDH1) cells treated with fulvestrant promoted an increase in cell invasion and migration. The graphs show the results for the mean of three separate experiments.

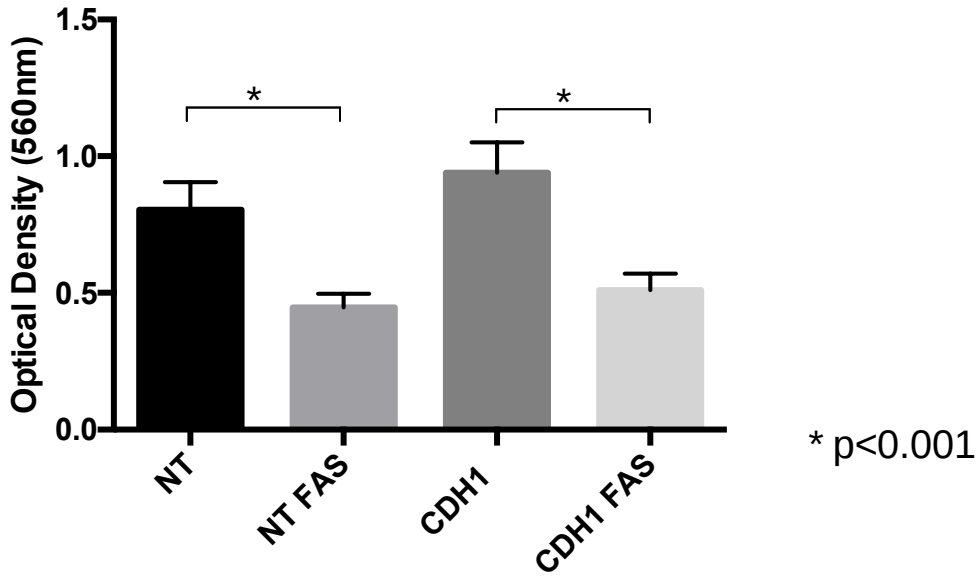

Figure 3.11 - Cell proliferation in MCF-7 cells treated with fulvestrant (FAS) +/- CDH1 siRNA. MCF-7 cells were treated with non-targeting (NT) or CDH1 targeting (CDH1) siRNA for 72 hours before assessing proliferation in control or fulvestrant ($1x10^{-7}M$) containing medium via MTT assay. Both wild-type (NT) and E-cadherin deficient (CDH1) cells treated with fulvestrant demonstrated suppressed proliferation as compared to controls. The graph show the results for the mean of three separate experiments.

3.1.8 Estradiol (E2) therapy results in an increase in invasion, migration and proliferation in MCF-7 cells, in the presence and absence of E-cadherin expression

Following the above findings with regards to the effects of tamoxifen (a selective ER modulator) and fulvestrant (a pure ER antagonist) on cell invasion and migration, it was felt appropriate to next assess the effects of a pure ER agonist, by treating cell with estradiol (E2).

As described previously, invasion was first assessed using Matrigel® coated trans-well invasion chambers, assessing the invasive response of wild-type (NT) or E-cadherin deficient (CDH1) MCF-7 with or without estradiol therapy. Results demonstrate a significant increase in invasion amongst wild-type cells treated with E2 (Figure 3.12a), when compared to control ($p<0.001$). In addition, the number of invading cells was greatly increased with E2 treatment in the E-cadherin deficient cell model ($p<0.001$).

The effect of E2 on migration was similar (Figure 3.12b), whereby a significant increase in cell migration was observed amongst wild-type cells treated with E2, as compared to controls ($p=0.031$). Again however, a larger and more exaggerated pro-migratory response was observed when E2 treatment was given to E-cadherin deficient cells ($p<0.001$).

The effect of E2 therapy on cell proliferation was also investigated by MTT assay (Figure 3.13). Here, results demonstrated a small yet significant increase in cellular metabolism with E2 treatment in E-cadherin competent ($p<0.001$) and E-cadherin deficient cells ($p<0.001$).

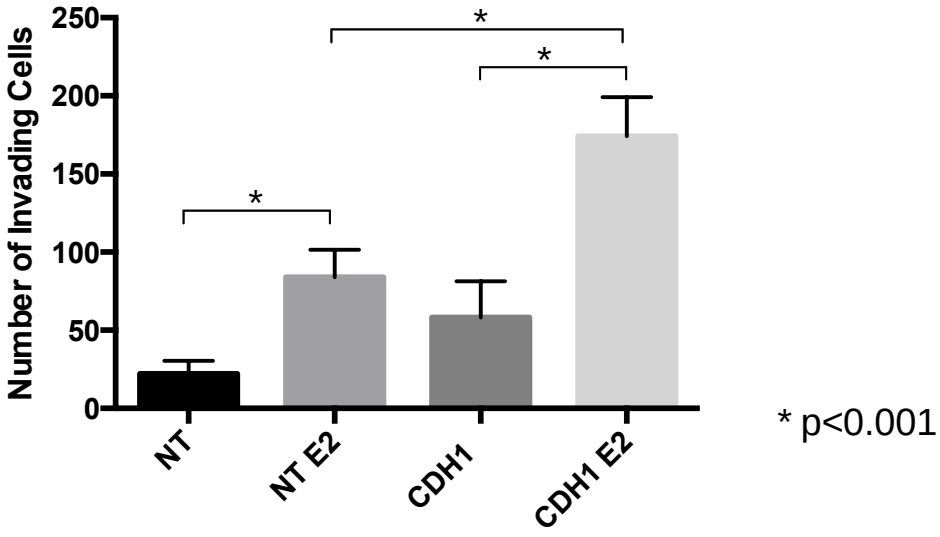

a.

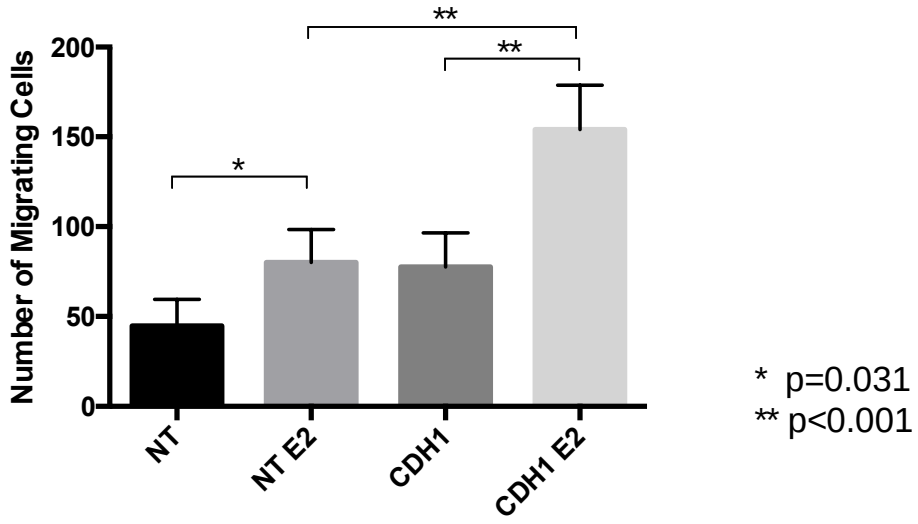

b.

Figure 3.12 – Cell (a.) invasion and (b.) migration in MCF-7 cells treated with estradiol (E2) +/- CDH1 siRNA. MCF-7 cells were treated with non-targeting (NT) or CDH1 targeting (CDH1) siRNA for 72 hours before assessing their (a.) invasive and (b.) migratory capacity in control or estradiol ($1x10^{-6}M$) containing medium. Both wild-type (NT) and E-cadherin deficient (CDH1) cells treated with estradiol promoted an increase in cell invasion and migration. The graphs show the results for the mean of three separate experiments.

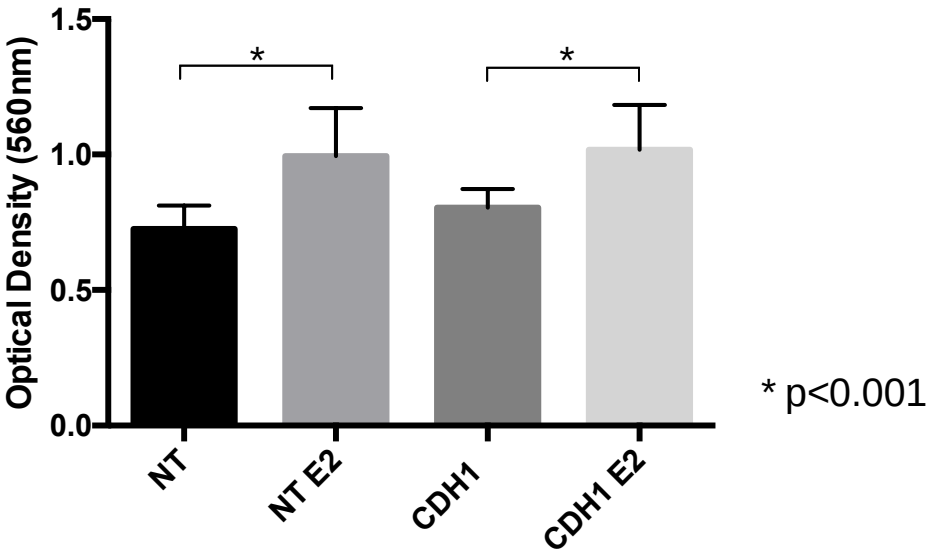

Figure 3.13 – Cell proliferation in MCF-7 cells treated with estradiol (E2) +/- CDH1 siRNA. MCF-7 cells were treated with non-targeting (NT) or CDH1 targeting (CDH1) siRNA for 72 hours before assessing their proliferative capacity in control or estradiol ($1x10^{-6}M$) containing medium, via MTT assay. Both wild-type (NT) and E-cadherin deficient (CDH1) cells treated with estradiol promoted an increase in cell proliferation. The graphs show the results for the mean of three separate experiments.

3.1.9 Estrogen withdrawal (-E2) suppresses cell invasion and migration in the MCF-7 cell line, in the presence and absence of E-cadherin expression

The above results have suggested that targeting the ER with either estradiol, fulvestrant or tamoxifen results in increased invasion and migration within the MCF-7 cell line, an effect more pronounced in in the setting of E-cadherin suppression. It was therefore decided to assess the effects of aromatase inhibitors (AI), which as opposed to targeting the ER directly, work by depriving the ER of stimulation by estrogens. To achieve the effects of AI in-vitro, cells were maintained during culture in wRPMI medium containing 2% glutamine and 5% charcoal-stripped fetal calf serum (SFCS). This would effectively mimic the effects of AI, by removing all estrogen and estrogenic stimuli (e.g. arising from phenol red) within the cell culture environment.

This model for AI treatment was used as part of the trans-well chamber invasion assay, to assess the effects of estrogen withdrawal (-E2) in conjunction with that of E-cadherin deficiency, as described previously (Figure 3.14a). Interestingly, these data demonstrated that invasion is suppressed amongst cells grown in –E2 conditions as compared to controls, both in the presence and absence of E-cadherin expression ($p<0.001$).

In a similar fashion, the effects of –E2 conditions on cell migration was also investigated (Figure 3.14b). Correspondingly, these data also demonstrate a significant suppression in migration amongst both wild-type ($p=0.036$) and E-cadherin deficient cells ($p<0.001$) grown in –E2 conditions, as compared to controls.

Once again, MTT (Figure 3.15) and cell counting (Figure 3.15b) assays were used to assess the effects of –E2 conditions on cell proliferation. This time however, a further arm to the experiment was added to assess the combined effects of culture in –E2 conditions with tamoxifen therapy. This was to assess whether

combination treatment may lead to a compounding effect on cell proliferation. Results from these data a significant suppression in cell proliferation with both tamoxifen treatment ($p<0.001$) and culture in –E2 conditions ($p<0.001$). Meanwhile the effect of tamoxifen therapy in combination with –E2 conditions had no significant additional effect on cell proliferation as compared to –E2 conditions alone.

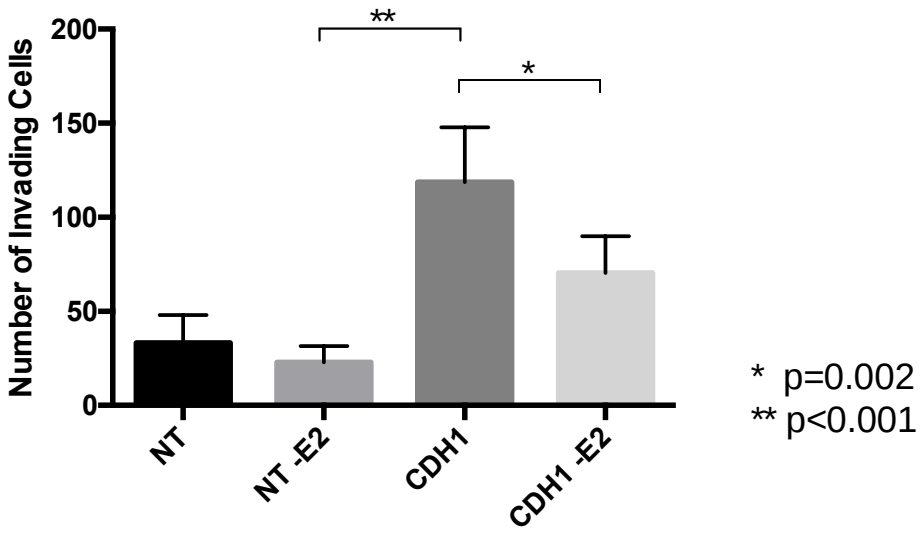

a.

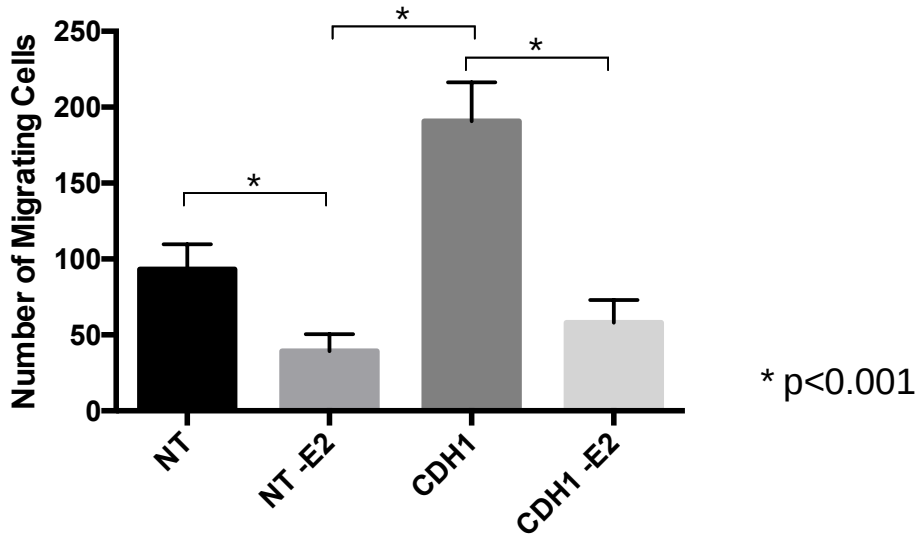

b.

Figure 3.14 – Cell (a.) invasion and (b.) migration in MCF-7 cells cultured in estrogen-deprived conditions (-E2) +/- CDH1 siRNA. MCF-7 cells were treated with non-targeting (NT) or CDH1 targeting (CDH1) siRNA for 72 hours before assessing their (a.) invasive and (b.) migratory capacity in control or estrogen withdrawal containing medium. Both wild-type (NT) and E-cadherin deficient (CDH1) cells treated with estrogen withdrawal demonstrated suppressed cell invasion and migration. The graphs show the results for the mean of three separate experiments.

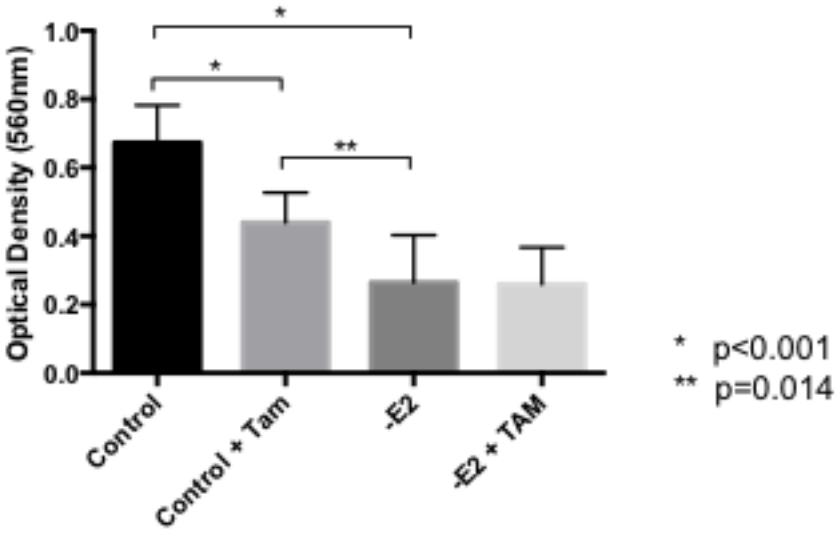

a.

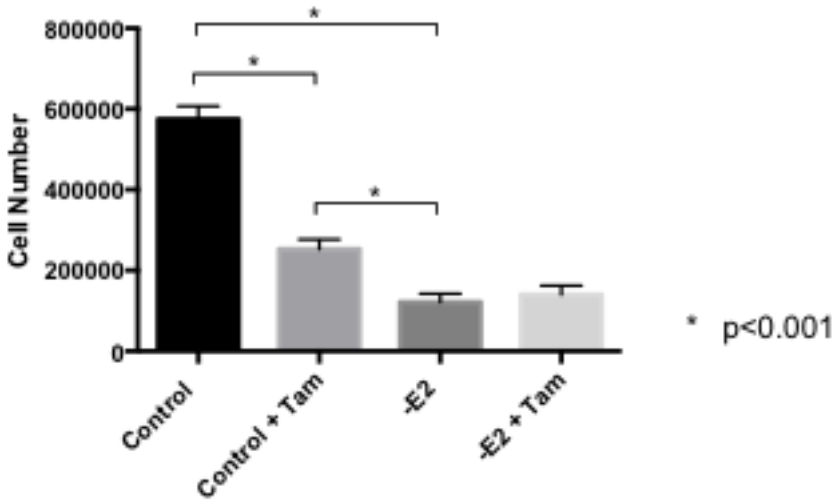

b.

Figure 3.15 – Cell proliferation in MCF-7 cells cultured in estrogen-deprived conditions +/- CDH1 siRNA, assessed by (a.) MTT and (b.) cell counting assays. MCF-7 cells were treated with tamoxifen and/or cultured in estrogen deprived conditions (-E2) before assessing cell proliferation by (a.) MTT and (b.) cell counting assays. Cells cultured in –E2 conditions showed suppressed levels of proliferation as compared to control. Proliferation after combined tamoxifen/-E2 treatment was similar cells cultured in –E2 conditions alone. The graphs show the results for the mean of three separate experiments.

3.1.10 Tamoxifen has no significant effect on invasion and migration within a panel of alternative ER+ cell lines

The results in this chapter to date have demonstrated that endocrine agents that target the ER, result in increased invasion and migration in MCF-7 cells. It was therefore of interest to assess whether similar findings could also be demonstrated in other ER+ breast cancer cell lines, to determine the generality/specificity of this adverse endocrine response. A panel of alternative ER+ cell lines were therefore chosen for this purpose. The cell lines chosen within this panel included an alternative luminal A breast cancer cell line (T47D), alongside two ER+, HER2+ cell models (BT474, MDA-MB-361).

As was the case with MCF-7 cells, the previously described invasion and migration assays were employed to assess the invasive and migratory response to E-cadherin suppression (+/- tamoxifen treatment) in each of these cell lines.

When examining invasion in these cell lines, it was interesting to note that the observed pattern of invasion appeared to differ compared to that observed in MCF-7 cells. With regards to the HER2+ cell lines (BT474, MDA-MB-361) we see that there appears to be a trend towards an increase in invasion in E-cadherin deficient cells compared to wild-type cells (Figures 3.16a and 3.16b), although this fails to reach statistical significance. Meanwhile, there was a non-statistical trend suggesting tamoxifen may have more of a suppressive effect on invasion in both wild-type and E-cadherin deficient cells. Similar results were also seen in the alternative luminal A cell line (T47D), whereby there was a non-statistical trend towards increased invasion amongst E-cadherin knockdown cells, whilst tamoxifen appeared to have suppressive effect (Figure 3.16c).

When examining cell migration in the same panel of alternative ER+ cell lines, a different pattern of results was again observed in comparison to MCF-7 cells. In BT474 and MDA-MB-361 cells there was a trend towards increased migration with E-cadherin deficiency (Figures 3.16d and 3.16e), while tamoxifen had no

significant effect on migration. A similar pattern was also observed in T47D cells with E-cadherin deficiency leading to a non-significant increase in migration (Figure 3.16f), while tamoxifen treatment had no significant effect on cell migration.

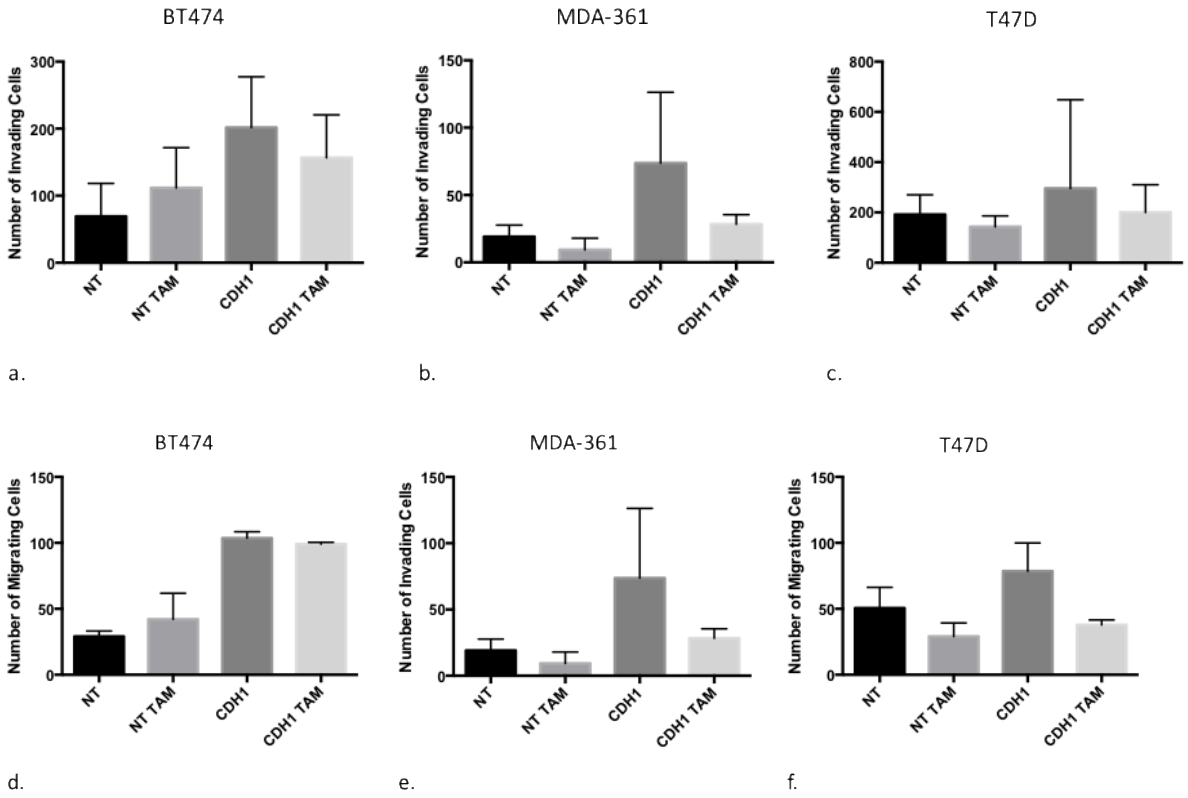

Figure 3.16 – Cell invasion and migration in BT474, MDA-MB-361 and T47D cells treated with tamoxifen (TAM) +/- CDH1 siRNA. BT474, MDA-MB-361 and T47D cells were treated with non-targeting (NT) or CDH1 targeting (CDH1) siRNA for 72 hours before assessing their (a-c.) invasive, (d-f.) migratory in control or tamoxifen containing medium. Tamoxifen treatment had no significant effect on cell invasion and migration in any of these 3 cell lines. The graphs show the results for the mean of three separate experiments.

3.1.11 Discussion

In this section, we demonstrate that (i) some endocrine agents may enhance the ability of ER+ breast cancer cells to migrate over, and invade through, extra-cellular matrix components and (ii) that these adverse responses are significantly augmented in the absence of E-cadherin expression.

While these results may be somewhat surprising, given the desired intent of tamoxifen therapy clinically, they perhaps should not be completely unexpected as it is becoming clearer that administering such endocrine agents may have effects that go beyond their originally described mechanism of action. As such, while the selective estrogen receptor modulatory functions of tamoxifen may cause changes in the cell that result in suppressed proliferation, it may also be possible that tamoxifen inadvertently promotes pathways that promote migration and invasion. Evidence supporting this rationale, for example, suggests tamoxifen may induce FAK-mediated cytoskeletal remodeling (137) and expression of matrix metalloproteinases (138). In addition, while the majority of signaling changes induced following estrogen stimulation are largely felt to be repressive in nature (198), tamoxifen and other anti-hormones may promote re-expression of genes, including those linked with resistance such as EGFR and HER2 (199). These changes may ultimately lead to undesired consequences within the cell (200), including the potential development of a pro-invasive phenotype. Finally, with some evidence suggesting a protective role of estrogen on the invasive and motility properties of breast cancer cells (140), although not demonstrated here, it may be logical to suggest anti-hormone therapy would have an opposing effect.

Others have also shown an increase in single cell migration with tamoxifen, as assessed by Boyden chamber assay (135), along with increased healing in MCF-7 cell wounds with tamoxifen (136), while the BCMPG have previously demonstrated a pro-invasive effect with tamoxifen in MCF-7 cells (134), yet only in the setting of poor cell to cell contact. In this current project however a smaller, but still significant, increase in invasion and migration is evident with tamoxifen therapy alone in MCF-7 cells. The difference between these findings therefore

raise the question as to whether a specific set of signaling events occur in cells with low E-cadherin expression treated with tamoxifen, which subsequently promote invasion. Alternatively, it may be possible that tamoxifen alone is responsible for the underlying signaling changes that drive invasion, while the downregulation of E-cadherin simply creates an environment where these signaling changes are more effective in bringing about cell invasion, through removal of a "physical barrier" in the form of adherens junctions.

E-cadherin loss may be present in up to 40% of all non-lobular breast cancers (201), and is a marker of poor clinical prognosis (202, 203). The downregulation of E-cadherin reduces the strength of intercellular homophillic adhesion, which enhances cell motility (158), and is a crucial step during the process of epithelial to mesenchymal transition. Adherens junction disruption alone however is not sufficient to facilitate this process, as loss of E-cadherin has been shown to be associated with several other functional changes that are crucial in this process. These include changes in β-catenin, along with the expression of multiple transcription factors, such as Twist and ZEB-1(204). In addition, loss of E-cadherin has been found to activate other pathways responsible for a higher migratory/invasive phenotype in cells, through a similar mechanism, involving both the T cell factor (TCF) and lymphocyte enhancer factor (LEF) signaling pathways (205). Meanwhile an increase in cytoplasmic p120 catenin levels is also observed, through the dissociation of the E-cadherin-catenin complex, resulting in activation of Rac1 and Cdc42 and inhibition of RhoA (206, 207), promoting the function of lamellopodia and inhibiting cell adhesion. As a result, the mechanism explaining the invasive phenotype demonstrated by tamoxifen in E-cadherin negative breast cancer cells may be more complex than it first appears.

In addition to tamoxifen treatment, fulvestrant also revealed similar results, whereby a pro-invasive/pro-migratory phenotype was demonstrated with treatment, which was more pronounced amongst MCF-7 cells with suppressed E-cadherin expression. Again, previous results by the BCMPG (134) revealed a similar picture, although a significant increase in invasion was again only demonstrated amongst E-cadherin deficient MCF-7 cells treated with fulvestrant.

In a similar manner to that shown previously with tamoxifen, fulvestrant therapy resulted in a suppression in cell proliferation, a result which would suggest, if anything, the pro-invasion/pro-migratory effects observed may be under-represented by the results of these experiments. Fulvestrant-induced invasion in breast cancer is less clearly documented in the literature. While some of those that have addressed this issue previously have found no difference in cell migration with fulvestrant, it is notable that fulvestrant (and tamoxifen) appeared to reverse the protective effect of E2 in cell invasion (135). In addition, both fulvestrant (and tamoxifen) may facilitate invasion through the modulation of matrix metalloproteinases (MMP's) and activation of the transcription factor snail (135). In a similar fashion, antiestrogens may also reduce the number of cell-cell contacts through the loss of intercellular junctions, desmosomes (208) while others have noted that anti-estrogen therapy results in increased expression of P-cadherin, which may increase cell invasion (209).

As was the case with both tamoxifen and fulvestrant, a pro-invasive and pro-migratory effect in MCF-7 cells was demonstrated using estradiol therapy. This response was again more exaggerated in the setting of poor cell-cell contact through E-cadherin knockdown. This result was perhaps surprising as evidence in the literature has supported a suppressive role for estradiol in invasion and migration amongst several breast cancer cell lines (210-214). Estradiol was found to inhibit invasion by 2-fold in ER-transfected MDA-231 cells (215, 216), an effect reversed by tamoxifen. These results suggest that some estrogen-regulated genes negatively influence invasion, including the matrix degradation protein 1-anti-chymotrypsin and E-cadherin (210).

While the results from this project appear to contrast these findings, demonstrating a pro-invasive and pro-migratory effect of estradiol, there are several potential explanations for this. Firstly, it is noticeable from the results of the MTT analysis that estradiol exerts a pro-proliferative effect on MCF-7 cells, a finding that is heavily supported in the literature (140). As a result, it may be that the pro-proliferative effects of estradiol act to increase cell number during the time-course of experiments, falsely elevating the number of invasive/migratory

cells demonstrated at the end-point of the assay(s). Secondly, as noted previously, the effect of ER signaling on E-cadherin may have a key role in the inhibitory effects on invasion. In our assay, E-cadherin knockdown may therefore prevent the normal suppressive effect of estradiol and instead promote invasion and migration through an alternative means of signaling, such as EGFR or Src kinase (175).

Cell culture under conditions of estrogen withdrawal was used to mimic the effects aromatase inhibitors within an in-vitro environment. This was achieved by cell culture in WRPMI media, containing 5% charcoal-stripped fetal calf serum (SFCS), removing all estrogen/steroidal compounds which may stimulate ER signaling. Cells cultures under these conditions demonstrated suppressed invasion and migration in both wild-type and E-cadherin knockdown MCF-7 cells, in contrast to the effects of all other endocrine therapies.

These findings would correspond with those of others (134), who have previously suggested a potential clinical benefit in treating ER+ tumors with low E-cadherin expression, with aromatase inhibitors as opposed to tamoxifen or other ER modulators/antagonists. These findings may be the result of inhibitory effects of ER signaling, independent of ligand binding, a result of the first zinc finger of the DNA-binding domain (140). Other studies have also confirmed an inverse correlation between ER expression and invasion in hormone-deprived conditions among MCF-7, ZR75.1 and T47D breast cancer cell lines (216). In addition, pure anti-estrogens which decrease total ER levels within MCF-7 cells, such as fulvestrant may increase levels of invasion (216, 217).

To identify whether the invasive/migratory response to tamoxifen seen in MCF-7 cells is representative across all ER+ breast cancers, we repeated the initial invasion and migration assays using a panel of alternative ER+ cell lines. These included an alternative luminal A cell line (T74D), the closest direct comparison to MCF-7 cells, along with two ER+, HER2+ cell lines (BT474 and MDA-MB-361). While there was a trend towards an increase in invasion and migration with E-cadherin knockdown amongst these alternative cell lines, albeit not to a level of

statistical significance, tamoxifen therapy had no statistical effect and tended to inhibit invasion and migration if anything. This variable effect of tamoxifen implies that that the pro-invasive/migratory response is not generic across all ER+ breast cancers, and may be more specific to a subset of ER+ disease. While a pro-invasive response with tamoxifen has been demonstrated by several others in MCF-7 cells (134-136, 218, 219), reports of a similar effect in other cell lines are less well recognized. While there is limited evidence supporting a similar pro-invasive response with tamoxifen in T47D cells (134, 216, 217), there appears to be little evidence demonstrating an effect in HER2+ cell lines, such as BT474 and MDA-MB-361.

While the presence of HER2 signaling, and subsequent cross-talk with the ER in HER2+ cell lines, may represent an obvious reason for a differing response in invasion and migration to tamoxifen, significant differences between MCF-7 and T47D cells are subtler. Although 2D gel analysis of these cell lines are similar, T47D cells were found to express a higher number of proteins, compared to the MCF-7 cell line, with several proteins identified as specific to one single cell line (220). In addition, T47D cells have been noted to have a differential response to estradiol, as compared to MCF-7 cells. As such, this may lead one to speculate that there is likely to be a similar differential response to other ER-targeting agents, such as tamoxifen and fulvestrant.

In summary, this chapter demonstrates that endocrine agents may invoke an adverse pro-invasive/pro-migratory response in subtypes of ER+ breast cancer and that this phenotype is augmented in the presence of E-cadherin loss. This response is not demonstrated in conditions of estrogen deprivation and does not appear to be generic across all ER+ breast cancer cell lines. The signaling that drives this response, and whether this signaling is (i) specific to the endocrine effects on the ER, (ii) related to signaling through E-cadherin, or (iii) is secondary to a combination of these effects, is unclear and will therefore be explored further. In addition, the cell line specific effects of tamoxifen that have been demonstrated lead to questions about potential differences in signaling between these cell lines

that may result in a different response to treatment and should therefore also be explored in greater detail.

3.2 Exploring the mechanisms of endocrine-induced invasion and migration if ER+ breast cancer

3.2.1 Introduction

The previous section presented intriguing data that ER-targeting anti-hormone therapies promote a pro-invasive and pro-migratory phenotype in ER+ MCF-7 breast cancer cells, and that this response is more exaggerated amongst cells lacking E-cadherin.

While there are several known signalling pathways that govern invasion and migration in breast cancer, the cellular mechanisms that underlie the above response to anti-hormone therapy are less clearly understood. Moreover, the data suggests one of two hypotheses may be relevant:

(i) that the combined effect of E-cadherin loss and endocrine treatment activates specific pro-migratory/invasive pathways that are not activated/fully activated in the context of either E-cadherin loss or endocrine treatment alone,

or

(ii) endocrine treatments activate signalling pathways that govern cell aggressiveness but the cellular consequence of this is not fully seen until the physical barrier to migration/invasion (i.e. cadherin-mediated cell-cell adhesion) is removed.

As part of this chapter, these hypotheses were investigated as follows:

(i) Interrogation of microarray data, made available through from previous work by the BCMPG, was performed. This microarray data represented expressional changes of a large panel of cellular proteins in both wild-type and E-cadherin deficient MCF-7 cells treated with/without tamoxifen. This data, along with a review of all available relevant literature, was used to identify potential cellular targets

responsible for changes in cell migration and invasion that were influenced by E-cadherin expression and/or tamoxifen therapy in MCF-7 cells.

(ii) Cellular targets identified through this process were chosen for further assessment by Western blotting, using cell lysates from wild-type and E-cadherin deficient cells treated with a range of endocrine treatments.

(iii) The phenotypic effects on invasion, migration and proliferation of key cellular targets, confirmed by Western blotting to have altered expression with either E-cadherin deficiency and/or endocrine treatment, were tested by the introduction of pharmacological inhibitors to manipulate the relevant cell pathway(s).

(iv) These expressional changes of these same key cellular targets, in response to E-cadherin manipulation and endocrine therapy, were assessed in an alternative ER+ cell line that does not exhibit the same adverse response to tamoxifen reported in the previous chapter.

3.2.2 Src kinase mediates endocrine-induced ER+ cell invasion and migration

As previous studies had suggested a possible role of Src kinase in mediating tamoxifen induced invasion within MCF-7 cells (134), it was decided to assess this relationship further in the context of findings within this project.

Western blot data revealed increased levels of Src phosphorylation at Y148 in both wild-type and E-Cadherin knockdown MCF-7 cells treated with both tamoxifen and fulvestrant (Figure 3.17) after culture for 6 days, while total-Src expression remained unaltered. Conversely, 6-day culture of MCF-7 cells under conditions of estrogen withdrawal led to a suppression in Src activity, independent of E-cadherin status (Figure 3.17).

Given these findings, it was decided to assess the functional relevance of Src kinase in relation to cell invasion and migration by pathway manipulation with a pharmacological inhibitor. The pharmacological Src inhibitor, Sarcanitib (AZD0530) (221), was therefore chosen for treatment in MCF-7 cells within the context of the invasion and migration assays previously described.

Prior to assessing the functional effects of Src inhibition, dose optimization of Sarcanitib was conducted by performing 6-day treatment in MCF-7 cells, with and without tamoxifen therapy, analyzed by Western blotting (Figure 3.18a). The effect of the pharmacological inhibitor on cellular proliferation was also assessed on MCF-7 cells, treated with and without tamoxifen, by MTT assay (Figure 3.18b). From these data, a Sarcanitib dose of 1μg/ml was chosen as the minimum dose required to achieve a knockdown of Y418 p-Src expression, while having the least possible impact in terms of its effect of cellular proliferation.

Invasion and migration of MCF-7 cells was then re-examined to assess the impact of 6-day treatment with Sarcanitib. These results showed that the addition of the pharmacological inhibitor suppressed both invasion ($p=0.015$, Figure 3.19a) and migration ($p<0.0001$, Figure 3.19b) in E-cadherin knockdown cells treated with

tamoxifen. The effect in this arm of the experiment appears to be independent to the anti-proliferative effect of Sarcanitib, shown by the effect of this inhibitor on proliferation with subsequent MTT assays. Here we see that while the pharmacological inhibitor had a suppressive effect on proliferation in both wild-type and E-cadherin knockdown MCF-7 cells, when combined with tamoxifen therapy the effect on proliferation is similar to that seen where cells are treated with tamoxifen alone (Figure 3.20).

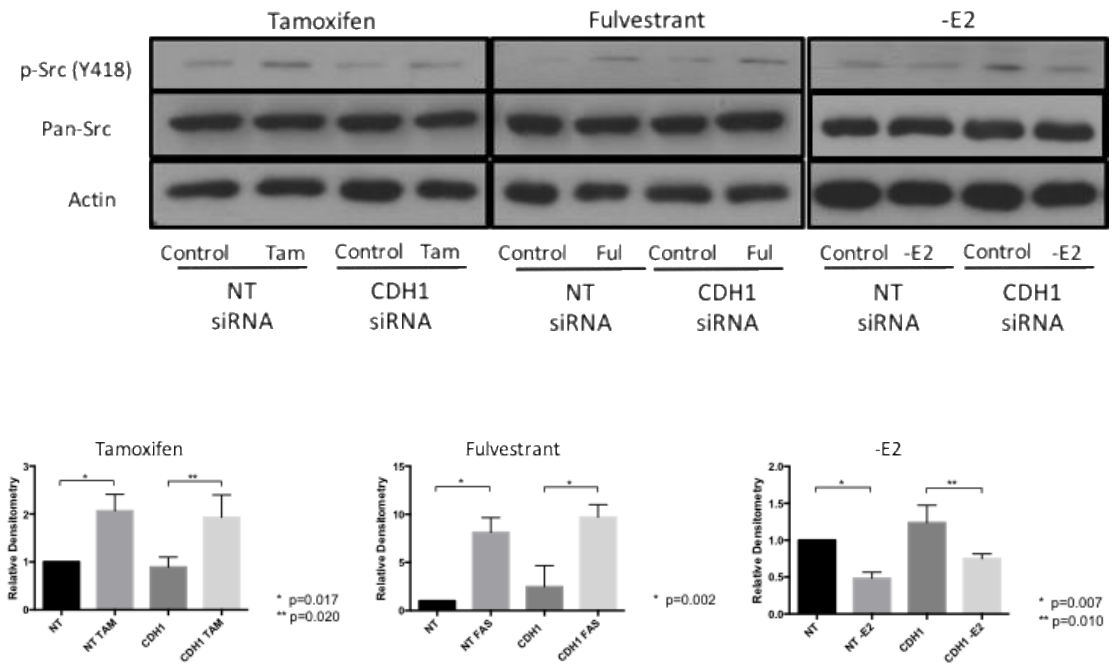

Figure 3.17 – Src expression in MCF-7 cells treated with tamoxifen and fulvestrant, or cultured under conditions of estrogen withdrawal, +/- CDH1 siRNA. Western Blot Analysis of pSrc, pan-Src and Actin expression in MCF-7 cells under conditions of 6-day estrogen withdrawal, tamoxifen or fulvestrant therapy, with and without E-cadherin suppression. Tamoxifen and fulvestrant promote an increase in pSrc expression, while Estrogen withdrawal suppresses pSrc expression, in MCF-7 cells. E-cadherin knockdown has no effect of pSrc expression. Differences in expression were assessed formally by densitometry.

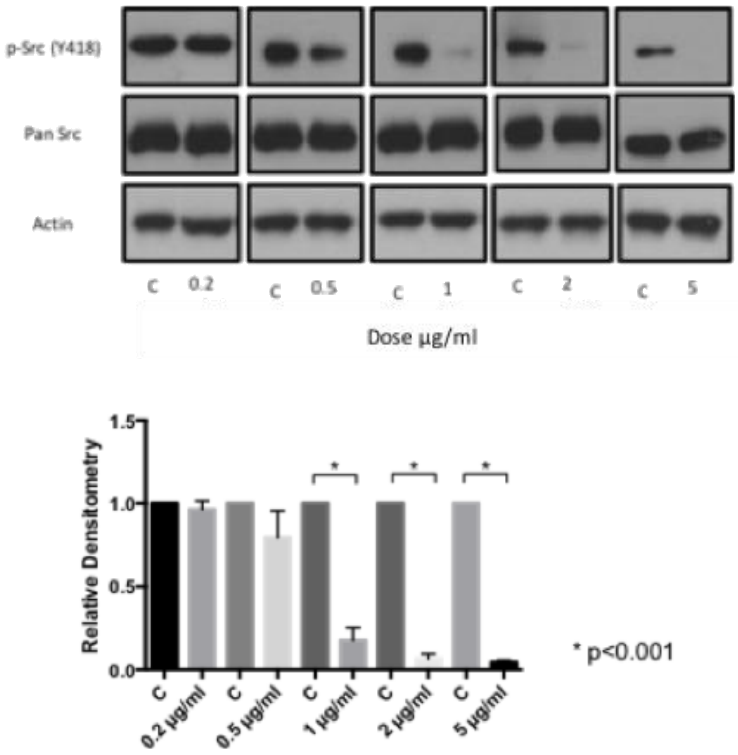

a.

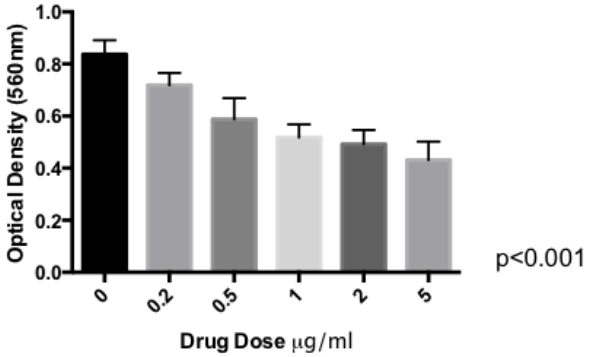

b.

Figure 3.18 – Dose effect of sarcanitib treatment on (a.) pSrc expression and (b.) cellular proliferation in MCF-7 cells. Western Blot Analysis of pSrc, pan-Src and Actin expression in MCF-7 cells was performed following 6-day treatment with Sarcanitib, at an incremental dose. Differences in expression were assessed formally by densitometry. Cellular proliferation following Sarcanitib treatment, using the same dosing regimen, was also assessed by MTT assay. Sarcanitib treatment suppresses pSrc expression and cellular proliferation in a dose dependent manner.

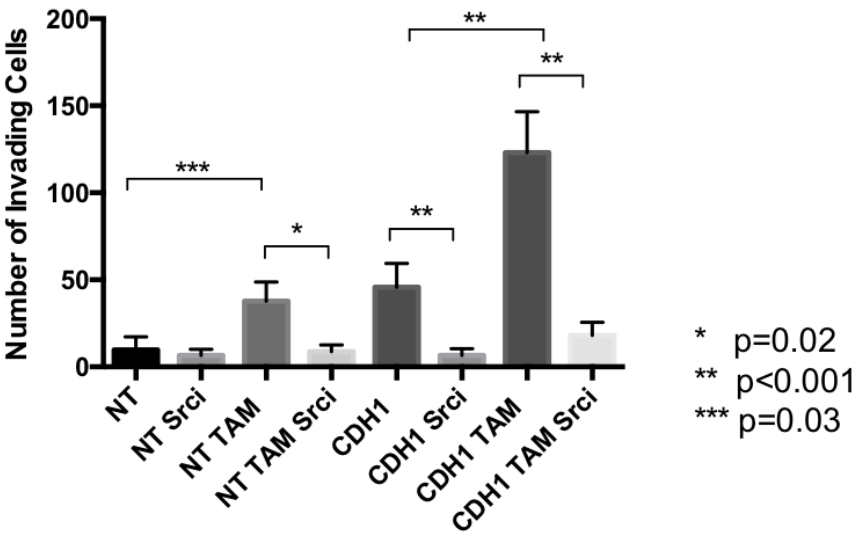

a.

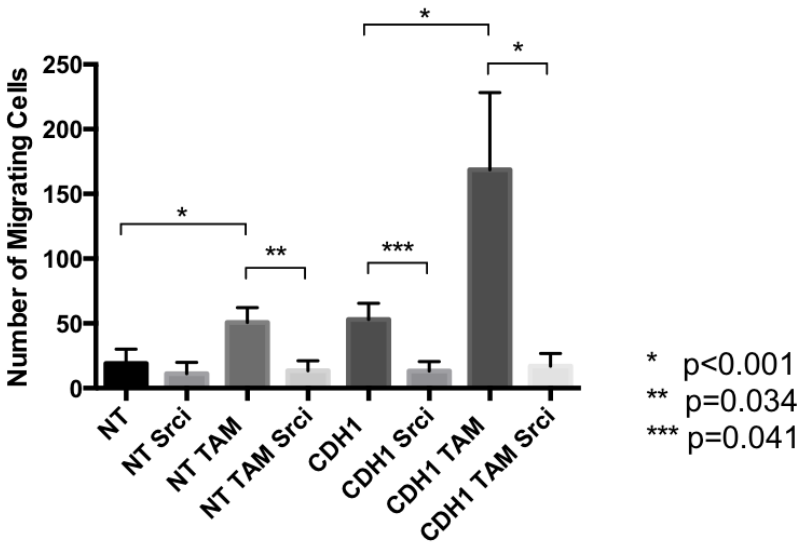

b.

Figure 3.19 – The effect of sarcanitib treatment on (a.) cell invasion and (b.) cell migration in MCF-7 cells treated with tamoxifen +/- CDH1 siRNA. MCF-7 cells were treated with non-targeting (NT) or CDH1 targeting (CDH1) siRNA for 72 hours before assessing their (a.) invasive and (b.) migratory capacity in response to 6-day tamoxifen ($1x10^{-7}M$) and/or Sarcanitib (1μg/ml) treatment. Sarcanitib therapy reversed the previously observed pro-invasive/pro-migratory response to tamoxifen. The graphs show the results for the mean of three separate experiments.

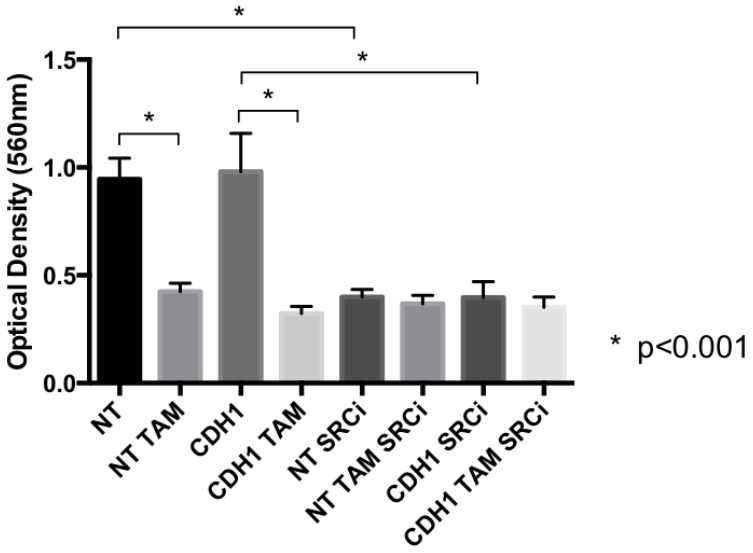

Figure 3.20 – The effect of sarcanitib treatment on cellular proliferation in MCF-7 cells treated with tamoxifen +/- CDH1 siRNA. MCF-7 cells were treated with non-targeting (NT) or CDH1 targeting (CDH1) siRNA for 72 hours before assessing cell proliferation, via MTT assay, in response to 6-day tamoxifen ($1x10^{-7}M$) and/or Sarcanitib (1μg/ml) treatment. Sarcanitib treatment suppresses cellular proliferation. The effect of combined tamoxifen/sarcanitib treatment on cellular proliferation is similar to that of either treatment given in isolation.

3.2.3 Exploring Src-based signaling pathways involved in endocrine-induced ER+ breast cancer cell invasion/migration

Given that Src kinase appears to be a key component in endocrine-induced invasion/migration, it was next decided to explore the substrates of Src in broader detail. As part of this analysis the intra-cellular kinases ERK 1/2 and AKT were next assessed.

3.2.3.1 ERK 1/2 mediates endocrine-induced ER+ cell invasion and migration

As outlined above, one area of interest within the remit of Src-related substrates is the Ras-Raf-MEK-ERK pathway, which is mediated by Src activation of RTK's (164). Within this pathway, the role of ERK 1/2 in relation to several key cellular processes, such as proliferation and actin cytoskeletal migration (222), was of particular interest.

When exploring this pathway, data from Western Blotting revealed an increased expression of phospho-ERK 1/2 with tamoxifen therapy (Figure 3.21) in both wild-type and E-cadherin deficient MCF-7 cells (while total ERK 1/2 expression remained unchanged). The functional relevance of this increased expression, in relation to invasion and migration, was therefore explored in a similar manner to that of Src, by pharmacological manipulation. The pharmacological MEK inhibitor, U0126 (223), was chosen to inhibit downstream ERK 1/2 phosphorylation and assess the effect introduction of this had on the pattern of endocrine-induced invasion and migration. Dose optimization of U0126 was first determined by giving MCF-7 cells 6-day treatment with a range of doses, with the suppression of pERK 1/2 expression determined by Western Blotting (Figure 3.22a). The effect of U0126 on cellular proliferation was also assessed by MTT assay (Figure 3.22b). From these assays, a dose of 10μg/ml was chosen as the minimum dose required

to provide adequate suppression of pERK 1/2, while minimizing unwanted effects of the inhibitor on cellular proliferation.
Once this optimization of the MEK inhibitor was complete, Boyden chamber invasion and migration assays were again used to assess the effect of the inhibitor on invasion and migration in MCF-7 cells following 6-day tamoxifen therapy with and without E-cadherin knockdown.

From these experiments the results from the invasion (Figure 3.23a) and migration (Figure 3.23b) assays revealed a significant decrease in invasion/migration amongst all treatment conditions using the MEK inhibitor, reversing the previously seen effects of tamoxifen, E-cadherin knockdown and combination treatment.

The effect of using the MEK inhibitor in combination with tamoxifen therapy and E-cadherin knockdown on cellular proliferation was also assessed by MTT assay (Figure 3.24). Interestingly, while MEK inhibitor treatment resulted in reduced cellular proliferation amongst both wild-type ($p=0.003$) and E-cadherin knockdown MCF-7 cells ($p=0.002$), there appeared to be no additional effect on cellular metabolism when the combination of the MEK inhibitor and tamoxifen was used when compared to the anti-proliferative effect of tamoxifen therapy alone.

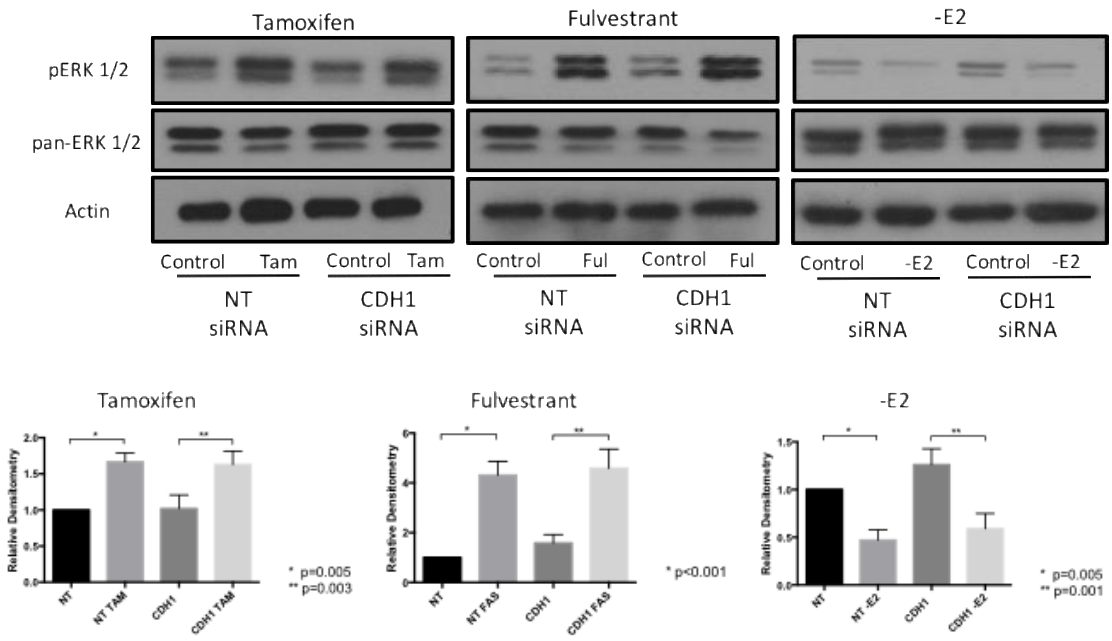

Figure 3.21 – ERK 1/2 expression in MCF-7 cells treated with tamoxifen and fulvestrant, or cultured under conditions of estrogen withdrawal, +/- CDH1 siRNA. Western Blot Analysis of pERK 1/2, pan-ERK 1/2 and Actin expression in MCF-7 cells under conditions of estrogen withdrawal, tamoxifen or fulvestrant therapy, with and without E-cadherin suppression. Tamoxifen and fulvestrant promote an increase in pERK 1/2 expression, while estrogen withdrawal suppresses pERK 1/2 expression, in MCF-7 cells. E-cadherin knockdown has no effect of pERK 1/2 expression. Differences in expression were assessed formally by densitometry.

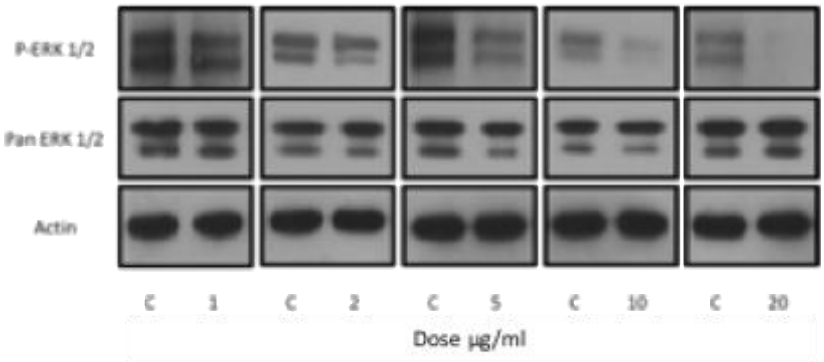

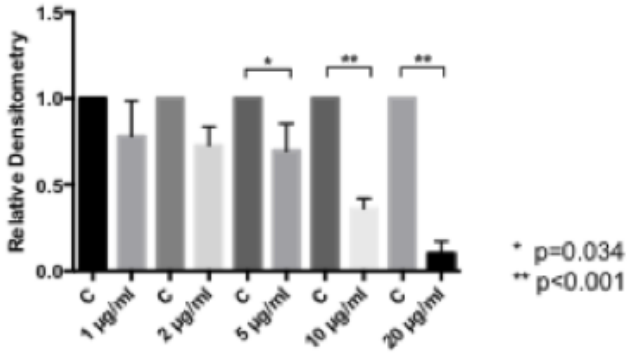

a.

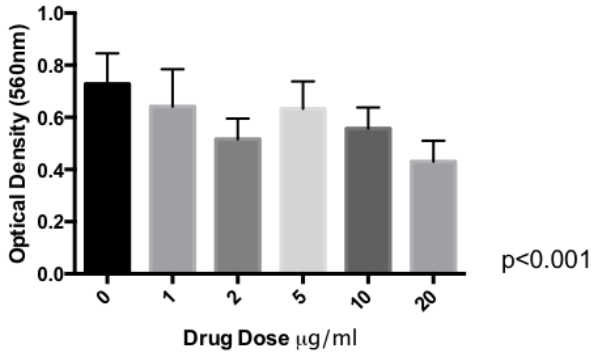

b.

Figure 3.22 – Dose effect of U0126 treatment on (a.) pERK expression and (b.) cellular proliferation in MCF-7 cells. Western Blot Analysis of pERK 1/2, pan-ERK 1/2 and Actin expression in MCF-7 cells was performed following 6-day treatment with U0126, at an incremental dose. Differences in expression were assessed formally by densitometry. Cellular proliferation following U0126 treatment, using the same dosing regimen, was assessed by MTT assay. U0126 treatment suppresses (a) pERK 1/2 expression and (b) cellular proliferation in a dose dependent manner.

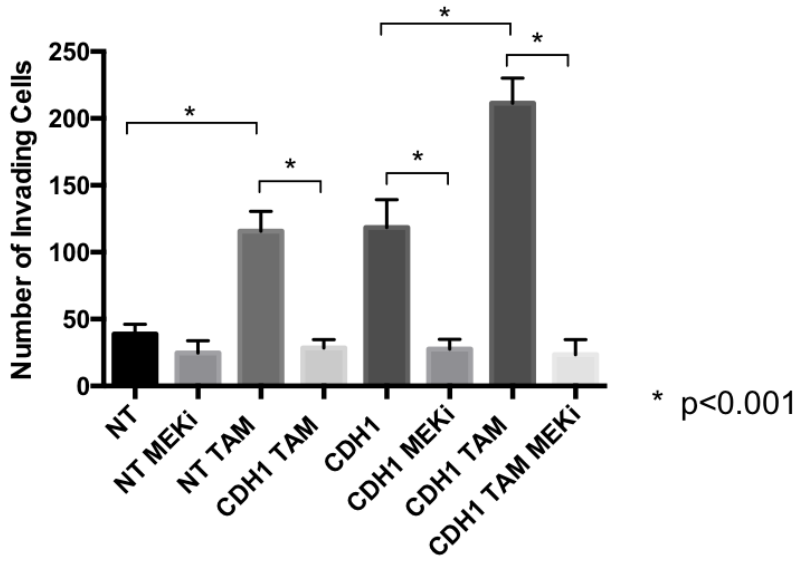

a.

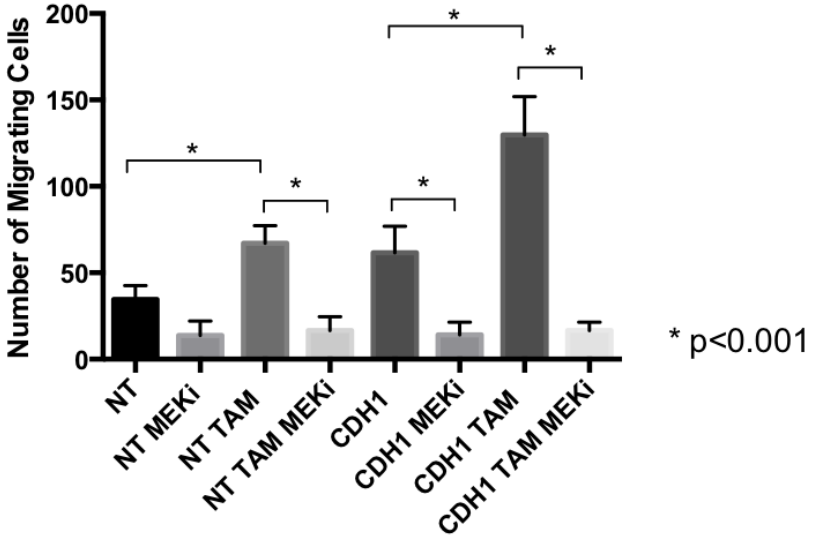

b.

Figure 3.23 – The effect of U0126 treatment on (a.) cell invasion and (b.) cell migration in MCF-7 cells treated with tamoxifen +/- CDH1 siRNA. MCF-7 cells were treated with non-targeting (NT) or CDH1 targeting (CDH1) siRNA for 72 hours before assessing their (a.) invasive and (b.) migratory capacity in response to 6-day tamoxifen ($1x10^{-7}M$) and/or U0126 (10μg/ml) treatment. U0126 therapy reversed the previously observed pro-invasive/pro-migratory response to tamoxifen. The graphs show the results for the mean of three separate experiments.

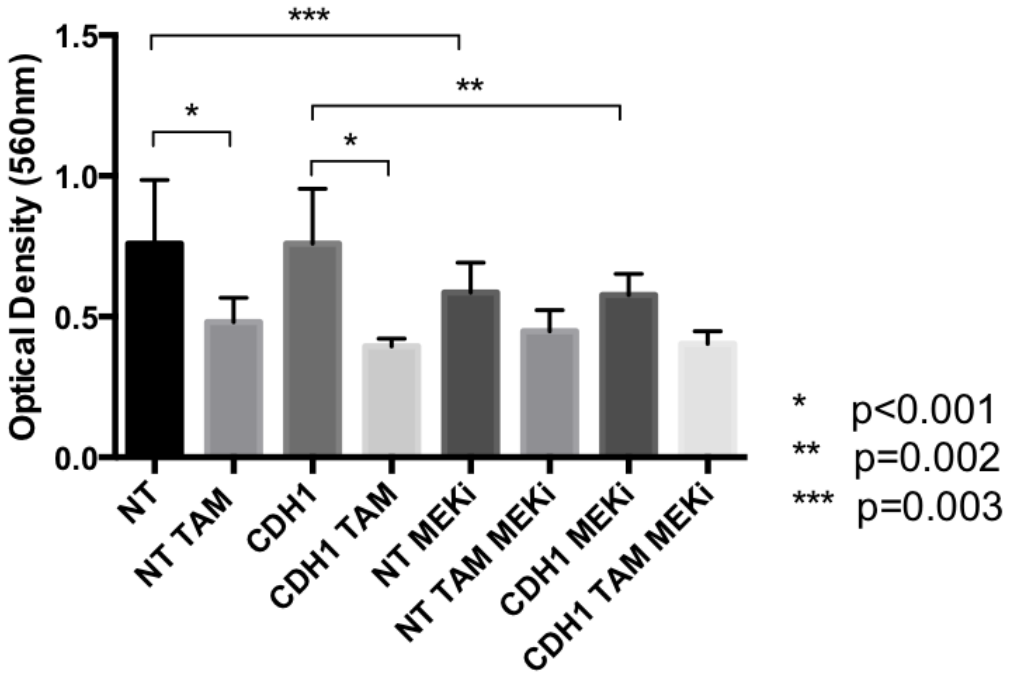

Figure 3.24 – The effect of U0126 treatment on cellular proliferation in MCF-7 cells treated with tamoxifen +/- CDH1 siRNA. MCF-7 cells were treated with non-targeting (NT) or CDH1 targeting (CDH1) siRNA for 72 hours before assessing cell proliferation, via MTT assay, in response to 6-day tamoxifen ($1x10^{-7}M$) and/or U0126 ($10\mu g/ml$) treatment. U0126 treatment suppresses cellular proliferation. The effect of combined tamoxifen/ U0126 treatment on cellular proliferation is similar to that of either treatment given in isolation.

3.2.3.2 AKT has no significant effect on endocrine-induced cell invasion/migration in ER+ breast cancer

Another pathway of interest that is closely associated with Src signaling is the PI3K-AKT pathway (164). AKT itself is known to play a critical role in cancer development as a key regulator of cell survival, proliferation (224) and may also play a role inhibiting cancer cell motility via the transcription factor Nuclear Factor of Activated T Cell (NFAT) (225).

From exploration of this pathway by Western Blotting, expression of phospho-AKT (Ser 473) was found to be suppressed by tamoxifen and fulvestrant therapy, in addition to conditions of estrogen withdrawal, in both wild-type and E-cadherin MCF-7 cells (Figure 3.25a). Reciprocally, expression of Phosphatase and Tensin Homolog (PTEN), a tumour suppressor gene whose loss usually leads to AKT activation (226), was increased by tamoxifen in keeping with the changes in AKT (Figure 3.25b).

Given these findings the role of AKT within a potential pathway contributing to the pro-invasive effect of tamoxifen in E-cadherin knockdown MCF-7 cells was explored. This was initially performed by the introduction of a pharmacological AKT inhibitor and assessing the effect on invasion and migration within the previously used cell models. For this purpose, the AKT inhibitor Perifosine (227), which inhibits AKT at both Ser 473 and Thr308, was chosen.

As was the case previously in relation to the pharmacological inhibitors for Src kinase and MEK, dose optimization of Perifosine was determined by giving 6-day treatment to MCF-7 cells, using a range of doses, and assessing the suppression of pAKT expression using Western Blotting (Figure 3.26a). Similarly, the effect of Perifosine on cellular metabolism was also assessed by MTT assay (Figure 3.26b). Following the results from both assays, a dose of 10μm was chosen as the minimum dose perifosine required to provide adequate suppression of pAKT, while aiming to minimize the effects on cellular proliferation.

Following this period of optimization, the effect of perifosine on invasion and migration was studied in MCF-7 cells in the context of tamoxifen therapy and E-cadherin knockdown. From assessing these results, it was interesting to note that Perifosine appeared to have no significant effect of either invasion (Figure 3.27a) and migration (Figure 3.27b) in MCF-7 cells, with preservation of a pro-invasive/pro-migratory phenotype with tamoxifen therapy in both wild-type and E-cadherin knockdown cells.

In conjunction with this data, the effect of perifosine therapy, in tandem with tamoxifen and E-cadherin knockdown, on cellular metabolism was assessed by MTT assay (Figure 3.28). Results demonstrated a significant reduction in cellular metabolism with perifosine in both wild-type ($p<0.001$) and E-cadherin knockdown ($p<0.001$) MCF-7 cells. When perifosine was combined with tamoxifen therapy however, the effect on cellular metabolism was not significantly different to that caused by tamoxifen therapy alone.

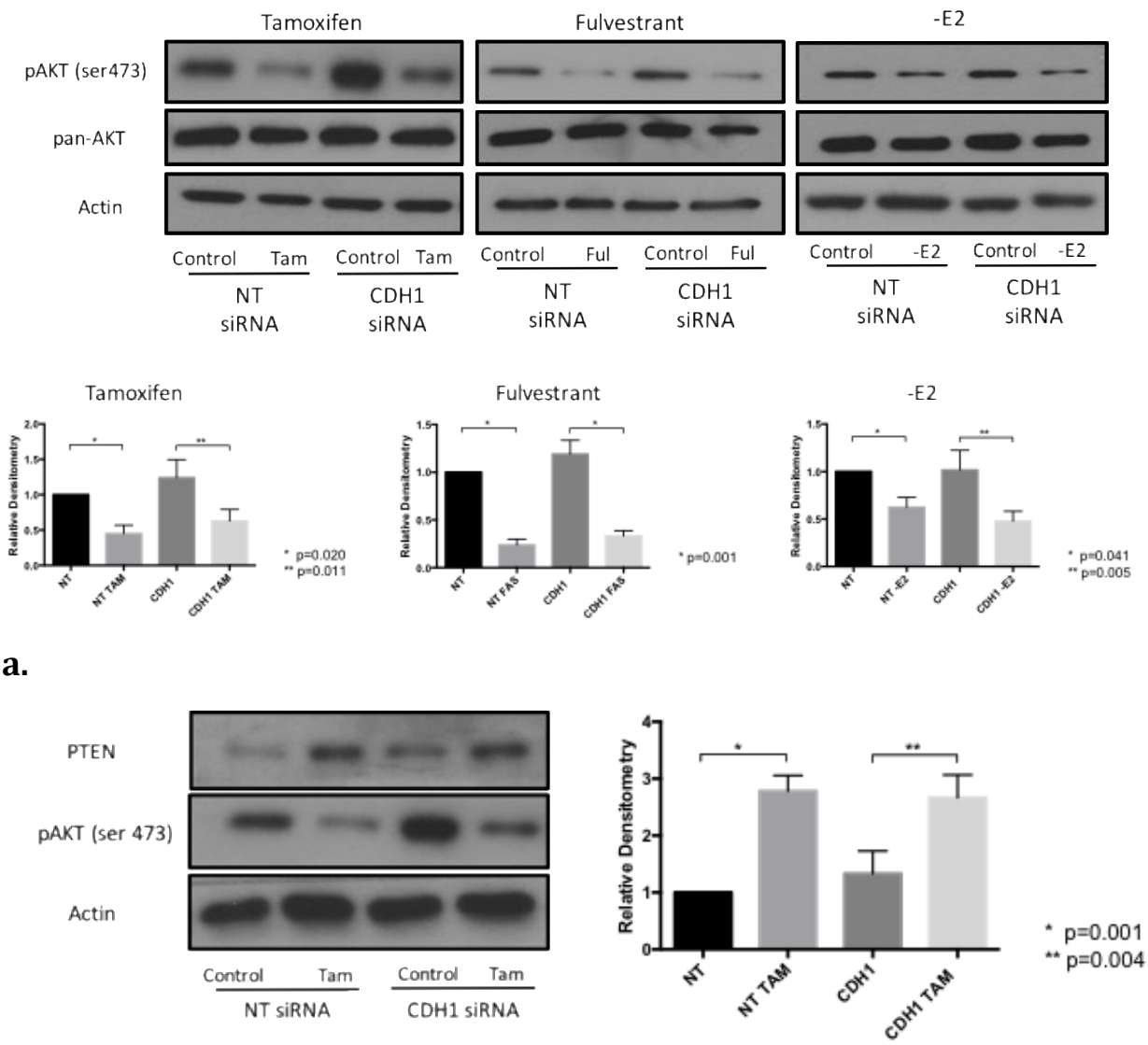

Figure 3.25 – AKT and PTEN expression in MCF-7 cells treated with tamoxifen and fulvestrant, or cultured under conditions of estrogen withdrawal, +/- CDH1 siRNA. Western Blot Analysis of pAKT, pan-AKT, PTEN and Actin expression in MCF-7 cells under conditions of estrogen withdrawal, tamoxifen or fulvestrant therapy, with and without E-cadherin suppression. Tamoxifen, fulvestrant and estrogen withdrawal (a) suppress pAKT expression and (b) tamoxifen increases PTEN expression in MCF-7 cells. E-cadherin knockdown has no effect of pAKT or PTEN expression. Differences in expression were assessed formally by densitometry.

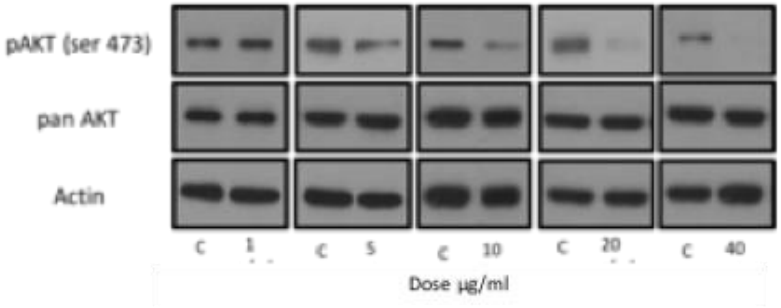

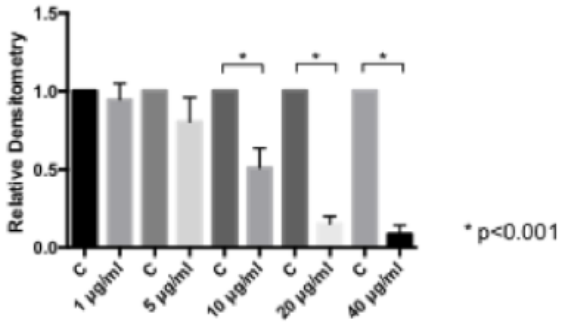

a.

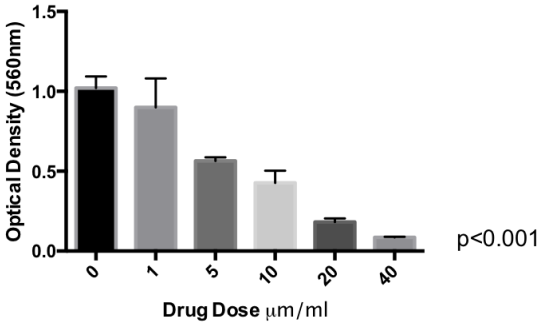

b.

Figure 3.26 – Dose effect of perifosine treatment on (a.) pAKT expression and (b.) cellular proliferation in MCF-7 cells. Western Blot Analysis of pAKT, pan-AKT and Actin expression in MCF-7 cells was performed following 6-day treatment with Perifosine, at an incremental dose. Differences in expression were assessed formally by densitometry. Cellular proliferation following Perifosine treatment, using the same dosing regimen, was assessed by MTT assay. Perifosine treatment suppresses (a) pAKT expression and (b) cellular proliferation in a dose dependent manner.

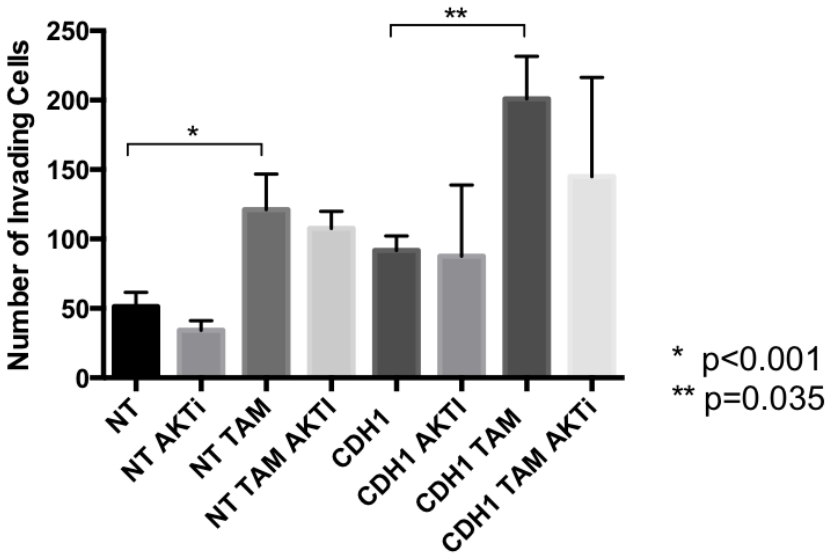

a.

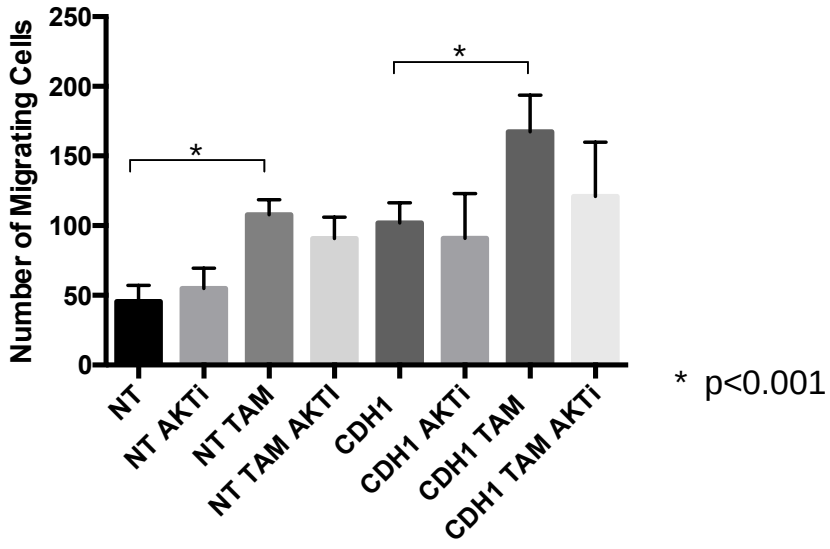

b.

Figure 3.27 – The effect of perifosine treatment on (a.) cell invasion and (b.) cell migration in MCF-7 cells treated with tamoxifen +/- CDH1 siRNA. MCF-7 cells were treated with non-targeting (NT) or CDH1 targeting (CDH1) siRNA for 72 hours before assessing their (a.) invasive and (b.) migratory capacity in response to 6-day tamoxifen ($1x10^{-7}M$) and/or Perifosine ($10\mu g/ml$) treatment. Perifosine therapy had no significant effect on cell invasion of migration. The graphs show the results for the mean of three separate experiments.

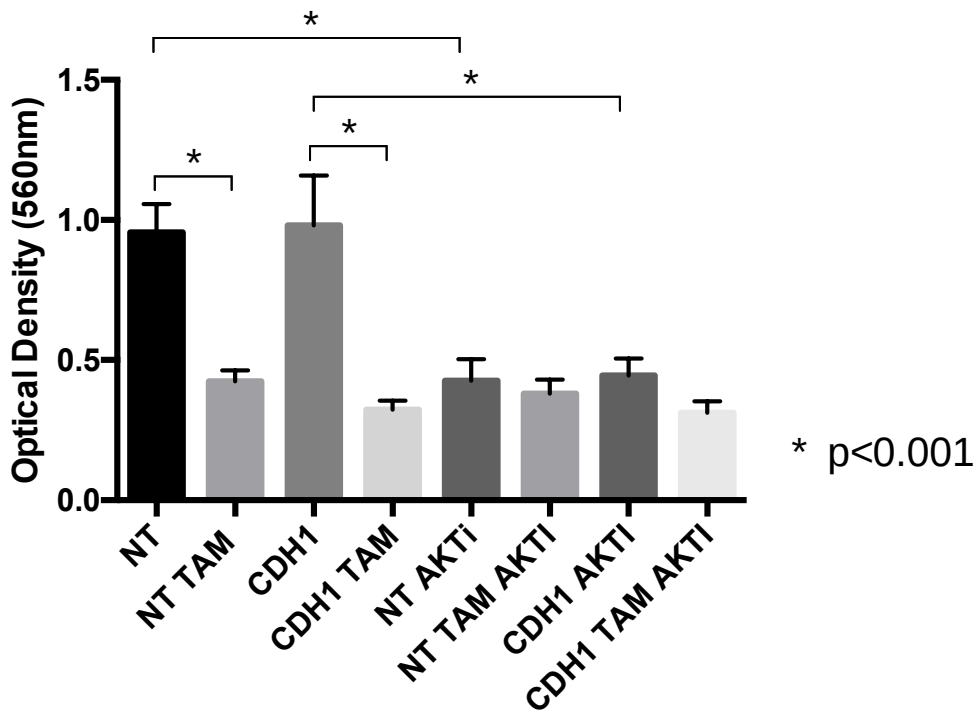

Figure 3.28 – The effect of perifosine treatment on cellular proliferation in MCF-7 cells treated with tamoxifen +/- CDH1 siRNA. MCF-7 cells were treated with non-targeting (NT) or CDH1 targeting (CDH1) siRNA for 72 hours before assessing cell proliferation, via MTT assay, in response to 6-day tamoxifen ($1x10^{-7}M$) and/or Perifosine ($10\mu g/ml$) treatment. Perifosine treatment suppresses cellular proliferation. The effect of combined tamoxifen/Perifosine treatment on cellular proliferation is similar to that of either treatment given in isolation.

3.2.4 The effect of endocrine agents and E-cadherin suppression on EMT markers and cytoskeletal regulators in ER+ breast cancer

Outside of Src kinase and its substrates within the Ras-Raf-MEK-ERK and PI3K-AKT pathways, several other targets were assessed for potential expressional changes related to endocrine-induced invasion.

One such group are potential markers of epithelial to mesenchymal transition (EMT), which include the transcription factors Snail, Slug and Twist (152, 153). As previously mentioned, loss of E-cadherin expression is one of the hallmarks of EMT (121-123). In addition, Src kinase is also known to be a regulator of breast cancer (228) and may therefore also play a role in the expression of these transcription factors. As such it would be interesting to see if the expression of this panel of EMT markers would be affected by endocrine therapy or induced E-cadherin loss. When exploring the expression of these transcription factors in this way, by Western blotting (Figure 3.29), we see that there was a significant increase in the expression of all these transcription factors with tamoxifen therapy. Meanwhile, E-cadherin expression appeared to have no significant effect on the expression of any of these transcription factors.

A second group of protein targets are a group of intracellular kinases known for their underlying role in cellular invasion and migration as part of several signaling pathways, including the Wnt signaling pathway. These include GTPase's such as RhoA, Rac1 and Cdc42. The Wnt signaling pathway and its associated intracellular kinases have previously been an area of interest for the BCMPG research group, and were also shown to be over-expressed by tamoxifen in the groups microarray data. Given that the Wnt pathway also has strong links with EMT (229) and that some of these intracellular kinases have been shown to be regulated by both Src and MEK signaling (230), these targets were felt to be of interest to explore further with Western blotting. When doing so, in a similar manner to that previously mentioned, data revealed an increase in expression of all three kinases with

tamoxifen therapy (Figure 3.30). Contrastingly, E-cadherin expression had no significant effect on the expression of these proteins.

The semaphorin pathway encompasses a complex set of cell surface and secreted proteins, which have a role in axon guidance and cell migration (231). Interestingly some elements of this pathway appear to be regulated by Src kinase and the PI3K-AKT pathway (232), while certain GTPase activity, whose expression has already been shown above to be regulated by tamoxifen, have been shown to interact with Semaphorin family members (233). Interestingly the BCMPG dataset also demonstrated an increase in expression of some members of this pathway with tamoxifen. As a result, the expression of both Sema 3E and Neuropilin 1, two components of the pathway upregulated on this microarray data were assessed by Western blotting (Figure 3.31). Results confirmed an increase in expression of both proteins with tamoxifen therapy, with expression unaltered by E-cadherin status.

The expression of matrix metalloproteinases (MMP's) was also assessed in the above context given its important role in the digestion and degradation of the cell's surrounding ECM as part of cell invasion (234). Several of the MMP members, including MMP-9 showed evidence of increased expression with tamoxifen therapy on microarray data, while MMP-9 is also noted to be regulated by MAPK (235). Western blotting data for MMP-9 (Figure 3.32) revealed that tamoxifen therapy increased its expression, while E-cadherin expression had no significant effect on detected levels.

Finally, the expression of the two other cytoskeletal regulators, the cytoplasmic non-receptor tyrosine kinase FAK, and transcription factor STAT3, were assessed given their respective roles in cell invasion and migration (132, 236), relationship with Src (132, 237), and regulation of MMP synthesis (238). Through the same assessment as described above, using Western blotting, it was notable that both FAK and STAT3 expression was upregulated by tamoxifen therapy (Figure 3.33). Meanwhile, E-cadherin expression again had no significant effect on the detected levels of either protein.

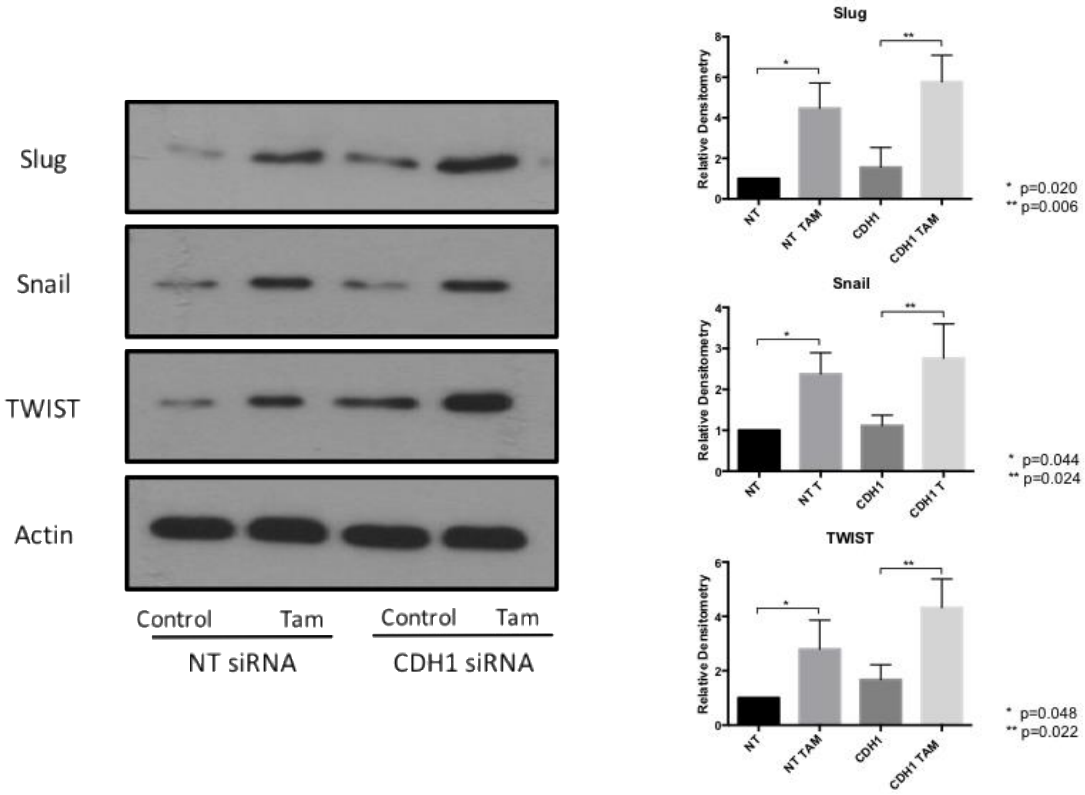

Figure 3.29 – Changes in the expression of Slug, Snail and TWIST in MCF-7 cells treated with tamoxifen +/- CDH1 siRNA. Western Blot Analysis of Slug, Snail, TWIST and Actin expression in MCF-7 cells under conditions of 6-day tamoxifen treatment, with and without E-cadherin suppression. Differences in expression were assessed formally by densitometry. Tamoxifen promotes an increase in EMT-associated transcription factor expression in MCF-7 cells. E-cadherin knockdown has no effect on the expression of EMT transcription factors.

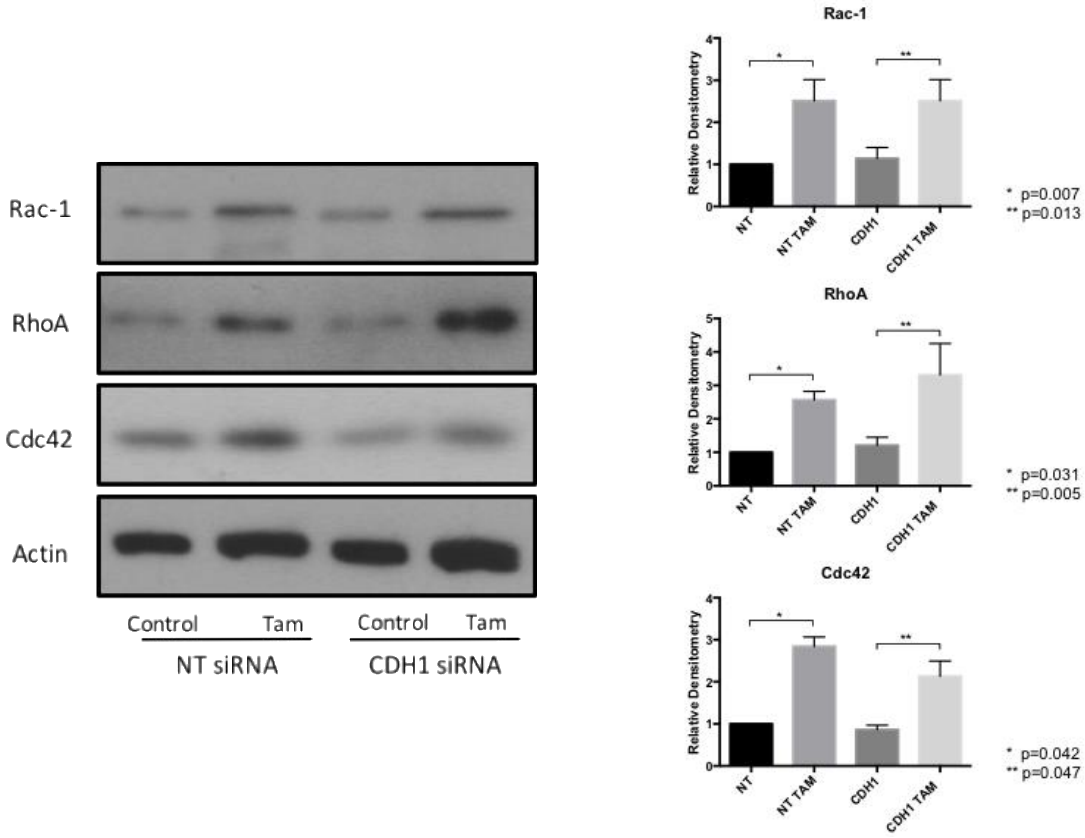

Figure 3.30 – Changes in the expression of Rac-1, RhoA and Cdc42 in MCF-7 cells treated with tamoxifen +/- CDH1 siRNA. Western Blot Analysis of Rac1, RhoA, Cdc42 and Actin expression in MCF-7 cells under conditions of 6-day tamoxifen treatment, with and without E-cadherin suppression. Differences in expression were assessed formally by densitometry. Tamoxifen promotes an increase in the expression of intracellular kinases in MCF-7 cells. E-cadherin knockdown has no effect intracellular kinase expression.

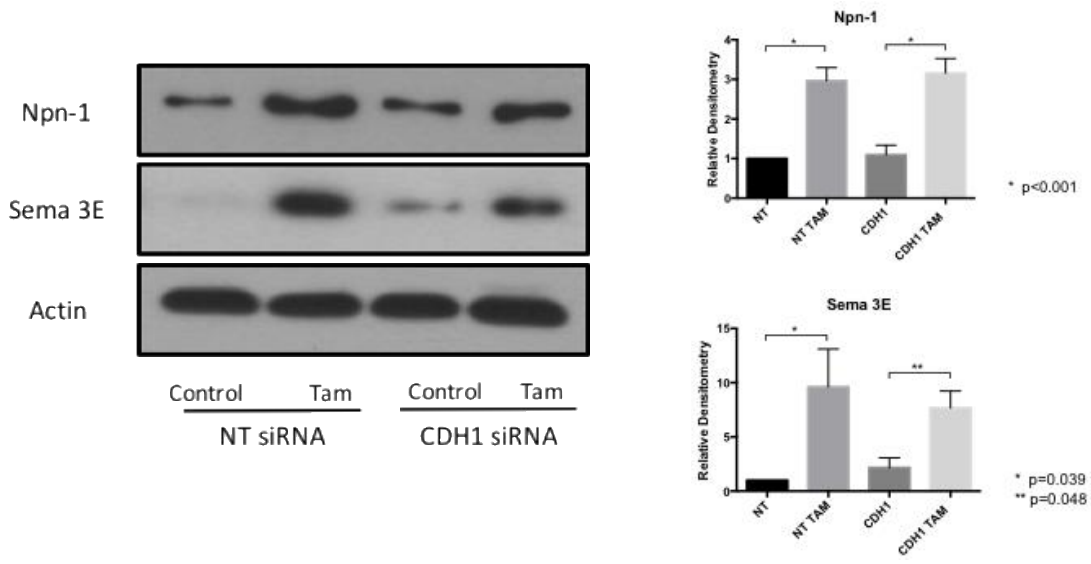

Figure 3.31 – Changes in the expression of Npn-1 and Sema 3E in MCF-7 cells treated with tamoxifen +/- CDH1 siRNA. Western Blot Analysis of Npn-1, Sema 3E and Actin expression in MCF-7 cells under conditions of 6-day tamoxifen treatment, with and without E-cadherin suppression. Differences in expression were assessed formally by densitometry. Tamoxifen promotes an increase in the expression of semaphorin family members in MCF-7 cells. E-cadherin knockdown has no effect of semaphorin expression.

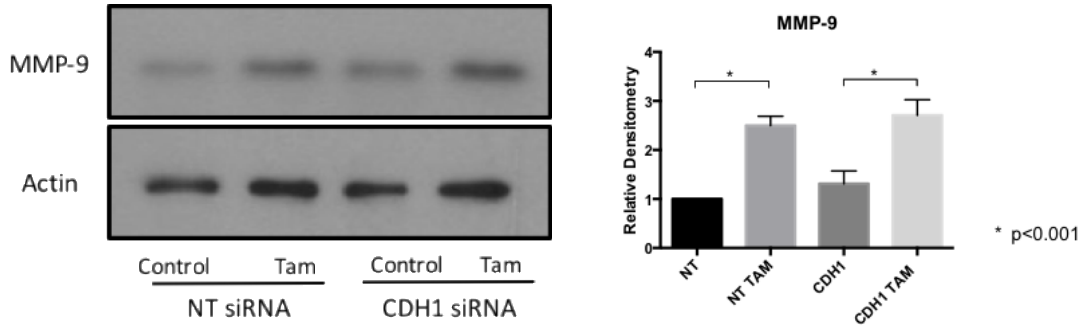

Figure 3.32 – Changes in the expression of MMP-9 in MCF-7 cells treated with tamoxifen +/- CDH1 siRNA. Western Blot Analysis of MMP-9 and Actin expression in MCF-7 cells under conditions of 6-day tamoxifen treatment, with and without E-cadherin suppression. Differences in expression were assessed formally by densitometry. Tamoxifen promotes an increase in the expression of MMP-9 in MCF-7 cells. E-cadherin knockdown has no effect on MMP-9 expression.

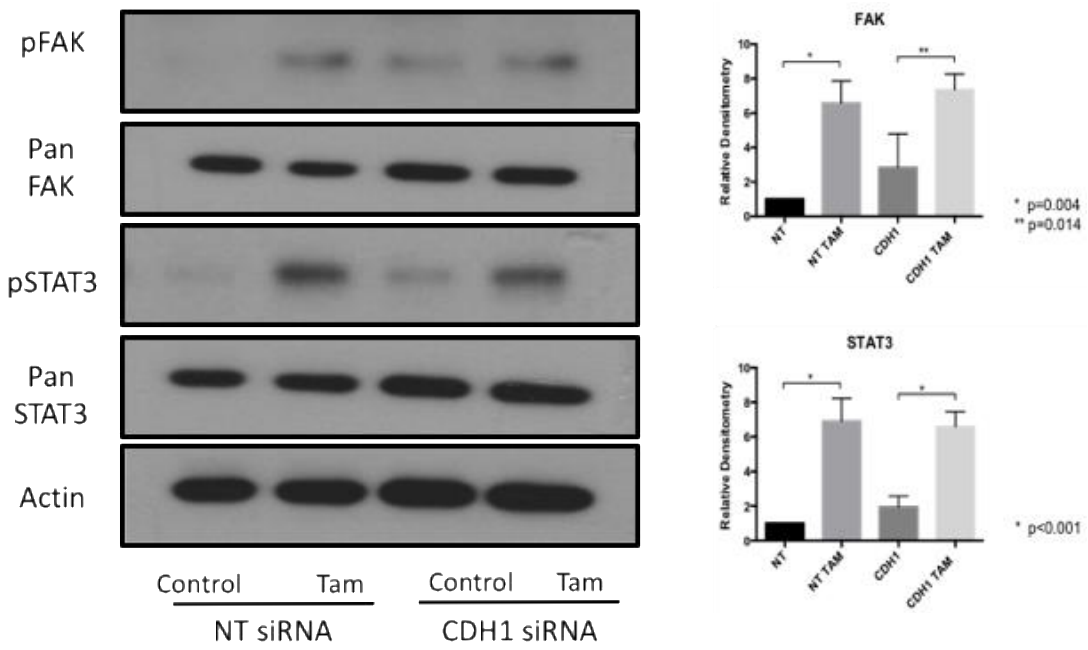

Figure 3.33 – Changes in the expression of pFAK and pSTAT3 in MCF-7 cells treated with tamoxifen +/- CDH1 siRNA. Western Blot Analysis of pFAK, pSTAT3 and Actin expression in MCF-7 cells under conditions of 6-day tamoxifen treatment, with and without E-cadherin suppression. Differences in expression were assessed formally by densitometry. Tamoxifen promotes an increase in the expression of pFAK and pSTAT3 in MCF-7 cells. E-cadherin knockdown has no effect on pFAK and pSTAT3 expression.

3.2.5 Discussion

This section has explored some of the signaling pathways that may be associated with the pro-invasive response found when treating ER+ breast cancer cells with ER-targeting endocrine treatment, particularly when cells exhibited low expression of E-cadherin. Specifically, the chapter has aimed to address the two hypotheses, drawn from results so far, that may explain this phenomenon:

(i) that the combined effect of E-cadherin loss and endocrine treatment activates specific pro-migratory/invasive pathways that are not activated/fully activated in the context of either E-cadherin loss or endocrine treatment alone,

or

(iii) endocrine treatments activate signalling pathways that govern cell aggressiveness but the cellular consequence of this is not fully seen until the physical barrier to migration/invasion (i.e. cadherin-mediated cell-cell adhesion) is removed.

The initial focus of this investigation involved the protein kinase Src, which is intimately involved in cancer invasion (164) and whose expression has previously been shown to be upregulated by tamoxifen in ER+ breast cancer in the context of an adverse response to such treatment (134). Indeed, results here also demonstrated a significant increase in Src expression with both tamoxifen and fulvestrant therapy, while estrogen suppression appeared to have the opposite effect. Interestingly, while previous reports suggest that the combination of tamoxifen with E-cadherin suppression results in elevated Src expression to a greater degree than with either treatment alone (134), findings in this chapter demonstrated no difference in Src expression based on E-cadherin status.

Src is a non-receptor tyrosine kinase, whose overexpression or aberrant activation is reported in a variety of tumors, including breast cancer (239-242), and plays an important role in many cellular processes, such as proliferation, survival, motility, invasion and angiogenesis (166, 242). Src kinase activity is known to be increased in breast cancer as compared to normal breast tissue (171)

and is intimately involved in breast cancer progression and metastasis development (243). Indeed, cell lines expressing higher levels of Src have been found to be more invasive in-vitro (244).

Underlying these findings is the importance of Src in ER-mediated gene transcription (245-248) and cross talk with growth factor signaling pathways, such as EGFR (249). Elevated Src expression has been associated with endocrine resistance, enhancing cell invasion (131), while tamoxifen itself has also previously been shown to increase Src expression in endocrine-sensitive cells (134, 172, 250), as has been demonstrated in this chapter. Interestingly, whether this change in Src expression is a result of the agonistic or antagonistic properties of tamoxifen appears controversial, with both potential mechanisms observed by others (250, 251). Results from this chapter would suggest however that it may be the antagonistic actions of tamoxifen that results in this increase in Src signaling, as similar results were also observed when replacing tamoxifen with fulvestrant, a pure ER antagonist. In addition, it is interesting to note that culture in estrogen deprived conditions, hence a relative lack of ER activation as opposed to ER antagonism, led to the opposite effect whereby Src activation was suppressed.

Given the apparent role of Src kinase in the described adverse response to endocrine treatment, it was next felt appropriate to investigate some substrates of Src. This included the role of MAPK, and specifically ERK 1/2 (175, 252), particularly given its known functions in cell migration and invasion (253). In a similar fashion to Src, ERK 1/2 signaling was activated by both tamoxifen and fulvestrant, but suppressed with estrogen withdrawal, which corresponds the invasion/migration data obtained with these treatments in the previous chapter. Again, these changes in expression appeared to be independent of E-cadherin status.

In breast cancer, the ER is known to be a major regulator of ERK expression, with previous reports demonstrating that estradiol (E2) and the ER complex activates ERK expression in several cell line models (252, 254). In MCF-7 cells this

activation is brought about by phosphorylation of Shc and p190, both substrates of Src (252, 255). As such, it is therefore likely that a similar method of activation is initiated through the binding of tamoxifen and fulvestrant to the ER, modulating this signaling pathway as previously described. Indeed, ERK expression has also been shown to be influenced by pharmacological Src and MEK inhibition in this chapter, which had subsequent negative effects on cell invasion and migration. The ERK 1/2 pathway is then ultimately activated by growth factors through Ras-Raf-MEK phosphorylation or via the PKC-Raf-MEK pathway (235). Activation of MAPK by these methods ultimately result in its translocation to the nucleus, where it may activate additional transcription factors, such as activating protein 1 (AP-1), through their phosphorylation (256, 257). Signaling from tyrosine kinases, involving the Ras/MAPK pathway (258, 259), also implicate a direct role for ERK 1/2 in activating the intracellular motility machinery through myosin light-chain kinase (MLCK) activation (260).
Via these processes, ERK 1/2 has been previously shown to be associated with tumor invasion, migration and metastasis development through several cellular processes. As such, ERK activity has been reported to be higher in metastatic, as compared to non-metastatic cancer cells (261-263).

A second pathway under the regulation of Src is the PI3K-AKT pathway (166). As such, AKT expression was also explored in relation to the endocrine-induced pro-invasive/migratory MCF-7 cell phenotype. While the PI3K-AKT pathway has been shown to be implicated in breast cancer, it is traditionally associated with deregulated cell growth and proliferation, as opposed to cell invasion/migration (224, 225). Indeed, results from this chapter demonstrated a suppression in AKT signaling with endocrine therapies, while pharmacological inhibition of AKT resulted in suppressed cell proliferation, whilst having no significant effect on migration and invasion.

AKT may be influenced by ER signaling through several mechanisms. The ER itself promotes the transcription of several genes that are upstream effectors of the PI3K/AKT/mTOR pathway, such as receptor ligands, RTK's, including Src, and several signaling adaptors (264, 265). In addition, PI3K/AKT signaling may be

activated through extra-nuclear functions of the ER, by the ER itself binding to the p85a subunit of PI3K (266), or via ER-mediated activation of IGF-1R (267). Considering this, the influence of tamoxifen and fulvestrant on AKT expression may therefore be anticipated. Consistent with this, estrogen deprivation, which has been used to mimic the effect of in-vivo aromatase inhibition, also suppressed AKT activity in a similar manner to that reported by others, both in-vitro and within clinical trials (265, 268, 269).

It is interesting to note from the results concerning Src, ERK and AKT in this chapter that there appears to be somewhat of an inverse relationship with respect to ER-targeting agents, which upregulate Src and ERK, while downregulating AKT expression, in comparison with estrogen deprivation, which suppresses the expression of all three proteins. In contrast, the effect of an agonistic agent on the ER would tend to promote increased signaling through Src, MAPK and PI3K/AKT (270, 271). This complex relationship between Src, MAPK and AKT, in response to changes within the ER from its ligands may therefore be critical to understanding the adverse response to endocrine treatments that has been observed. It is interesting to note that while this adverse response promotes a pro-invasive phenotype, proliferation is at the same time suppressed. It would therefore be interesting to know the clinical effects this may have on patient disease, particularly as to whether this may be in part responsible for the late development of distant metastatic disease several years after the initial treatment of patients with ER+ disease.

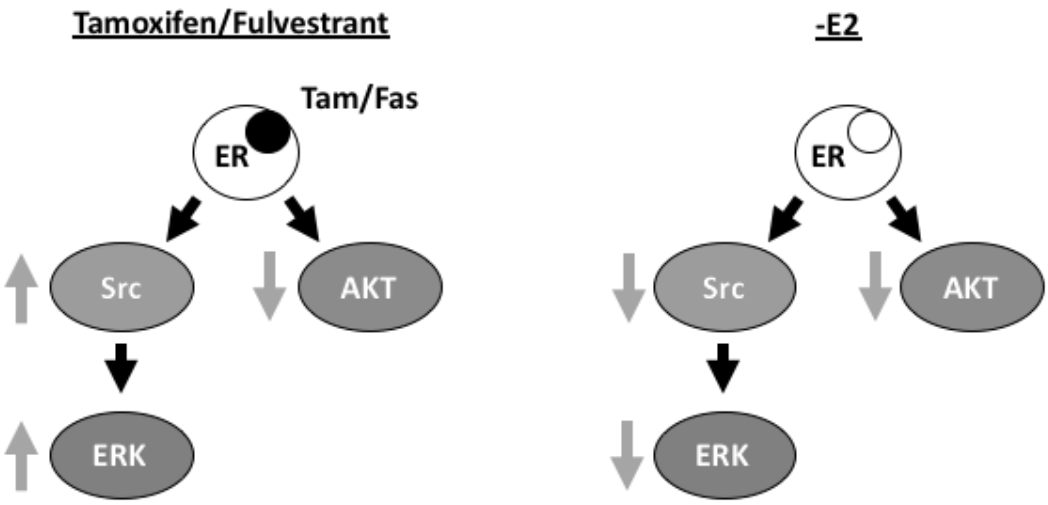

Figure 3.34 – Diagram demonstrating signaling pattern in MCF-7 cells with tamoxifen and fulvestrant treatment, as compared to culture under conditions of estrogen withdrawal (-E2). Treating cells with ER targeting agents resulted in an increase in Src and ERK expression, while AKT was suppressed. Meanwhile, estrogen withdrawal (-E2) resulted in reduced expression of all 3 proteins.

Following the identification of Src and some of its substrates as potential regulators of endocrine induced invasion, the effects of tamoxifen on the expression of FAK and STAT3 was assessed, given their known roles in cancer cell invasion/migration (272, 273), and regulation through Src-mediated signalling (274, 275). Interestingly, expression of both these elements were increased with tamoxifen treatment.

FAK is a cytoplasmic non-receptor tyrosine kinase that is activated by several growth factor receptors and integrins in several types of cancer (276). In cancer cell migration and invasion, FAK activation through ECM-induced integrin clustering promotes necessary cytoskeletal re-organisation (272, 273), which is partly mediated by FAK/Src complex formation and subsequent kinase activity (274, 275). Part of this actin remodelling is also mediated through the effect of FAK on several GTPases, including RhoA, Rac1 and Cdc42 (277-280). Indirectly through these methods, FAK signalling is responsible for the production and release of MMP's via its activation of Rac1, which in turn activates JNK protein

(277, 281). In addition, FAK activation and FAK/Src complex formation may drive the interruption of E-cadherin-mediated adherens junctions, therefore having a role in EMT (282, 283), although interestingly FAK expression appeared unaltered by E-cadherin expression from the results within this chapter.

STAT3 is a member of the STAT family of transcription factors, which is generally located within the cytoplasm in resting cells, and becomes activated by tyrosine residue phosphorylation, allowing its translocation to the nucleus (238). In normal physiology, it has essential functions in embryonic development, cell differentiation and immune response (284), while in cancer its aberrant activation is associated with cell proliferation, survival, invasion, angiogenesis and metastasis development (285). Activation of STAT3 can be brought about through multiple routes, including phosphorylation by EGFR and VEGFR (238). Importantly however, in the context of this current work, STAT3 may also be activated through non-receptor tyrosine kinases, such as Src (286), and several serine kinases, including MAPK (237), via serine 727 phosphorylation. Once activated the transcriptional activity of STAT3 has several important effects, including the regulation of MMP expression, which governs an important aspect of cell invasion (238), as well as the regulation of microtubule dynamics (287) and expression of intracellular kinases, such as Rac-1 (236), which help control cell migration.

Both FAK and STAT3 regulate the production of matrix metalloproteinases (MMP'S), which are responsible for ECM degradation as part of cell invasion (235). Interestingly, ERK 1/2 also plays a role in basement membrane degradation, acting on several of these proteolytic enzymes, including MMP-1, MMP-9, MMP-11 and urokinase-type plasminogen activator (uPA) (235), all of which have been implicated in cancer progression and invasion (288, 289). Given that microarray data also demonstrated a potential upregulation in some MMP members, this area was further investigated. Indeed, it was therefore interesting to note the results within this chapter suggesting a correlation between tamoxifen therapy, ERK 1/2, FAK and STAT3 phosphorylation, and an upregulation of MMP-9 in MCF-7 cells.

The semaphorin pathway, which has also been associated with cell migration in cancer as multi-faceted guidance proteins (231), was also investigated given that a number of proteins that function within this pathway appeared to have altered expression on microarray data. Interestingly, semaphorin pathway members may also have an element of cross talk with E-cadherin in their role as supplementary regulators of epithelial junctions (290), while some elements of this pathway also appear to be regulated by Src and AKT (232).Whilst the semaphorin pathway itself is complex and relatively poorly understood, it was interesting to note the expression of Sema 3E and neuropilin 1, both known pro-metastatic components of the pathway which derive their effects through binding with Plexins (231, 291, 292), were unaffected by E-cadherin expression but again appeared to be upregulated by tamoxifen.

Until this point, all the investigated targets have tended to show a relationship in their expression with endocrine treatments and signaling that involves targeting of the ER. Meanwhile E-cadherin expression appeared to have no significant effect on the signaling events in any of these pathways. As such, an assessment of several subsequent target proteins was undertaken, all of which have traditionally been associated with E-cadherin itself, or with the process of EMT, of which E-cadherin loss is usually a key feature (121-123).
E-cadherin has been inherently linked with tumor invasiveness and metastases development in multiple cancers and is hence associated with poor prognosis (293-295). Whilst it forms the core of the epithelial adherens junction, at its cytoplasmic domain E-cadherin associates with several proteins, such as catenins, which link it to the actin cytoskeleton. Therefore, while E-cadherin loss allows for disaggregation of tumour cells from one another, it may also mediate intracellular signaling functions via some of these associated proteins (296-299).

E-cadherin may interact functionally with both RhoA and Rac1 intracellular kinases, through its association with p120, which in turn play a role in coupling receptor signaling to changes in the actin cytoskeleton and cell contractility (300). E-cadherin may also indirectly interact with the Wnt signaling pathway, via its association with β-catenin (301), resulting in cell migration mediated through

several components, including intracellular kinases RhoA, Rac1 and Cdc42. It is interesting to note however that several of these intracellular kinases studied in this chapter appear to show no significant change in expression with E-cadherin status and instead appear to be upregulated by tamoxifen.

E-cadherin loss has also been associated with the upregulation of several transcription factors associated with epithelial to mesenchymal transition (EMT), such as Slug, Snail and Twist (302-305), which are also known to play a role in tumour progression (306). In addition, other mesenchymal markers affected by E-cadherin loss include N-Cadherin, vimentin, fibronectin and ZEB-1 (204). Despite these findings by others E-cadherin loss alone is insufficient to induce EMT in cells, with several other factors required (156). Indeed, within the context of this chapter several markers of EMT appeared unaffected by E-cadherin loss, while some transcription factors, including Slug and Snail, appeared to be again upregulated by tamoxifen and fulvestrant.

The fact that expression of several of the above targets, which one would normally associate with signaling related to E-cadherin, appear to be influenced by ER-targeting endocrine treatment as opposed to E-cadherin modulation itself, may be due to overriding control of these elements from ER, or more specifically Src signaling. To confirm this however, it would be helpful to assess the expressional response of these signaling elements following treatment with a pharmacological Src inhibitor, which would be a potential avenue for ongoing work.

In the context of current findings, it would therefore appear that E-cadherin itself may not necessarily play a significant role in pro-invasive signaling changes within this cell model. Instead, it may be more likely that E-cadherin loss creates a permissive environment, where cell signaling resultant from ER-targeting endocrine treatments is able to have a more significant effect on cell phenotype.

A further interesting point to note from this chapter is that all the data on signaling events outlined above come from assessing the MCF-7 cell line, in which a pro-invasive response to endocrine treatments were previously described. It would

therefore be interesting to compare signaling changes to endocrine treatment in an alternative ER+ cell line to assess if similar expressional changes would be seen. As a result, the T47D cell line, which was previously shown to not exhibit the same pro-invasive response to tamoxifen in the previous chapter, was chosen for supplementary analysis. As such, the expressional changes of Src, ERK 1/2 and AKT were assessed in T47D cells, in response to tamoxifen therapy +/- E-cadherin suppression, with Western blotting (Figure 3.34). It was interesting to note from this data that the expressional changes of these targets appeared different to what was seen in MCF-7 cells, with Src and ERK signaling unaltered by tamoxifen treatment, while AKT expression was still suppressed.

These findings appear to reinforce the idea that an adverse response to endocrine therapy is not a generic phenomenon across all ER+ breast cancer. Instead, there must be some key elemental differences within certain ER+ tumours, outside of ER expression alone, which promote signaling associated with an adverse response to treatment. As such, the attention of this thesis will turn to addressing this hypothesis in the next section.

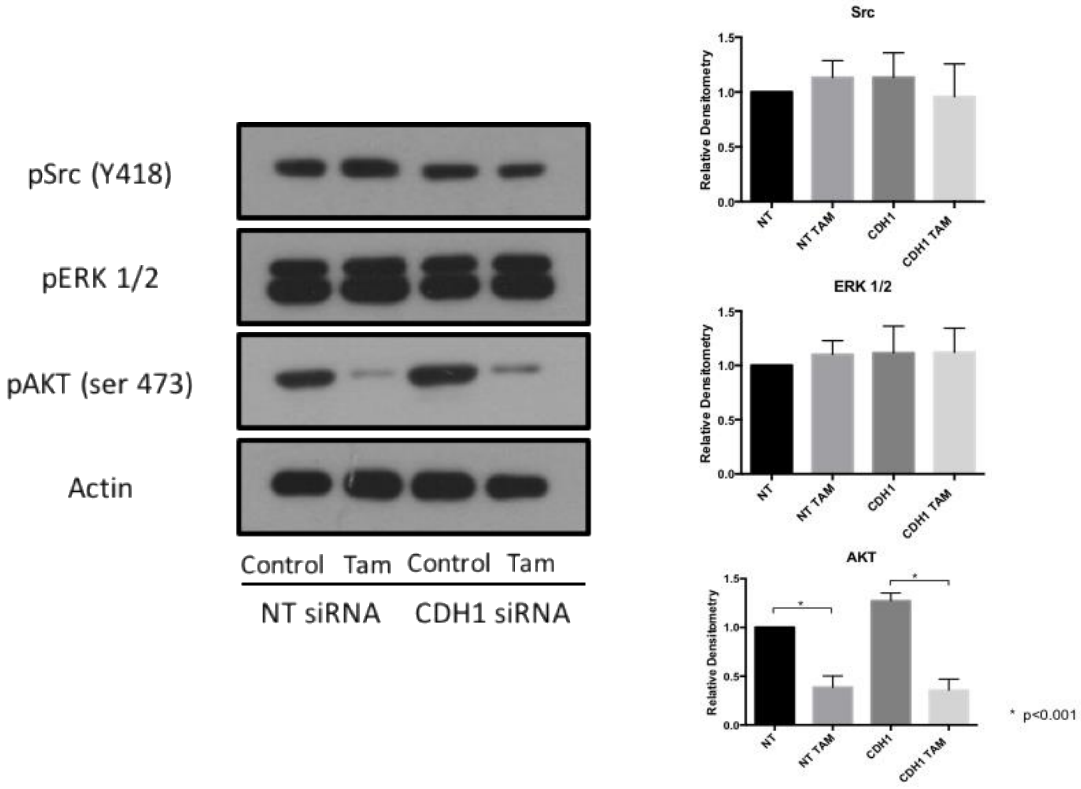

Figure 3.35 – Changes in the expression of pSrc and pERK 1/2 and pAKT in T47D cells treated with tamoxifen +/- CDH1 siRNA. Western Blot Analysis of pSrc, pERK 1/2, pAKT and Actin expression in T47D cells under conditions of 6-day tamoxifen treatment, with and without E-cadherin suppression. Differences in expression were assessed formally by densitometry. Tamoxifen has no effect on the expression of pSrc and pERK 1/2, but suppresses pAKT expression in T47D cells. E-cadherin knockdown has no effect on expression.

3.3 Exploring the role of proline, glutamate and leucine rich protein 1 (PELP-1) in ER+ breast cancer

3.3.1 Introduction

Data within the previous chapters pointed to the ability of ER-targeting agents to induce cellular invasion and migration in ER+ MCF-7 breast cancer cells. This did not appear to be a generic effect however, as a similar response was not observed in a second model of ER+ breast cancer (i.e. T47D cells). As such, the aim of this chapter is to attempt to identify key molecular determinants of an adverse response to endocrine agents in ER+ breast cancer.

To achieve this, a review of the literature was undertaken, using the National Center for Biotechnology Information (NCBI) online search engine (307), to identify key molecular differences between MCF-7 and T47D cells. Search terms used included combination of, "MCF-7", "T47D", "breast cancer" and "molecular differences". Searches conducted using these terms revealed a total of 92 results, which were further assessed by reviewing the abstract of each paper where available, followed by a review of the full paper itself in those results deemed to be of suitable interest. Results from this literature review revealed over 100 potential molecular targets demonstrating variable expression between MCF-7 and T47D cell (Appendix 7.15).

To refine the number of valid molecular targets suitable for further investigation, several criteria were applied to the expanded list, based on findings drawn from the data presented within previous chapters. These criteria stipulate that a suitable target for further investigation would be one which:

i. Demonstrates a significant differential in expression between the MCF-7 and T47D cell lines
ii. Has a body of evidence that suggests a role in direct/indirect regulation of cell invasion and/or migration
iii. Is regulated by conformational changes of the ER

iv. Regulates/is regulated by changes in expression of Src kinase

When taking these criteria into consideration, one protein of potential interest that conforms to these ideals was the proto-oncogene, proline-, glutamic acid- and leucine-rich protein 1 (PELP-1).

PELP-1, also known as modulator of non-genomic activity of estrogen receptor (MNAR) or transcription factor HMX3, is a large multi-domain protein which plays an important role in the modulation of several signalling cascades, including mediating the non-genomic actions of the ER (308). The protein has several known functions, such as interaction with nuclear receptors via its nuclear receptor (NR)-interacting boxes (LXXLL motifs) (309), and histone activation, through a histone binding regions located at the C-terminus (310, 311). Importantly, PELP-1 contains several PXXP motifs which facilitate interaction with proteins containing Src homology 3 (SH3) domains (308) permitting PELP-1-mediated activation of Src family kinases. Through this interaction PELP-1 can interact with several proteins that control the cell cytoskeleton, cell migration and metastases (312). In addition, basal expression of PELP-1 has been noted to be significantly higher amongst MCF-7 cells, compared with the T47D cell line (309). These facts would therefore appear to make PELP-1 an ideal candidate for investigation as a potential regulator of the adverse invasive response to ER-targeting endocrine agents, as previously described. As such, this chapter will explore the role of PELP-1 within ER+ breast cancer, concentrating of the following aspects:

i. The differential expression of PELP-1 among ER+ breast cancer cell lines
ii. The contribution of PELP-1 expression on the invasive and migratory capacity of ER+ breast cancer in response to endocrine treatments and/or E-cadherin suppression
iii. The effect of PELP-1 expression on key cellular signalling pathways found previously to be implicated in the adverse cell response to ER-targeting endocrine treatments

3.3.2 Basal PELP-1 expression in MCF-7 cells is high when compared to a panel of alternative ER+ cell lines

Basal levels of total PELP-1 expression was determined by Western Blot among the previously examined panel of ER positive cell lines, grown in standard experimental conditions for 6 days (Figure 3.35). These findings indicated a higher expression of PELP-1 amongst MCF-7 cells compared to the T47D, BT474 and MDA-MB-361 cell lines.

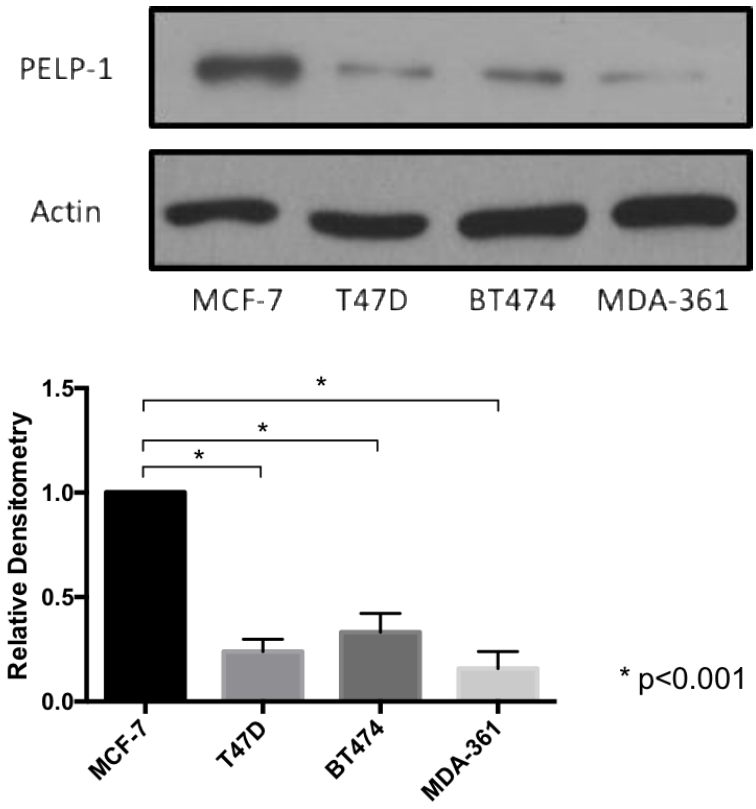

Figure 3.35 – Variation in the basal expression of total PELP-1 amongst a panel of ER+ cell lines. Western Blot Analysis of PELP-1 and Actin expression in MCF-7, T47D, BT474 and MBA-MB-361 cells. Differences in expression were assessed formally by densitometry. Total PELP-1 expression is significantly higher amongst MCF-7 cells, as compared to the T47D, BT474 and MDA-MB-361 cell lines.

3.3.3 Endocrine therapy alters PELP-1 expression in MCF-7, but not T47D cells

Once the basal level of PELP-1 expression was established, the influence of endocrine therapies, in the presence and absence of E-cadherin, was assessed by Western Blotting (Figure 3.36). These results confirmed that 6-day tamoxifen therapy appears to be associated with an increase in total PELP-1 expression, both in the presence and absence of E-cadherin expression. These results were also replicated when tamoxifen was replaced with 6-day fulvestrant therapy. Meanwhile, 6-day cell culture in conditions of estrogen withdrawal (-E2) led to a suppression of total PELP-1 expression, both in the presence and absence of E-cadherin expression.

In contrast, in the T47D cell line, total PELP-1 expression was not significantly affected by 6-day tamoxifen or fulvestrant therapy, either in the presence or absence of E-cadherin expression (Figure 3.37). Similarly, 6-day culture of T47D cells in conditions of estrogen withdrawal (-E2) had no significant effect of total PELP-1 expression, independent of E-cadherin expression.

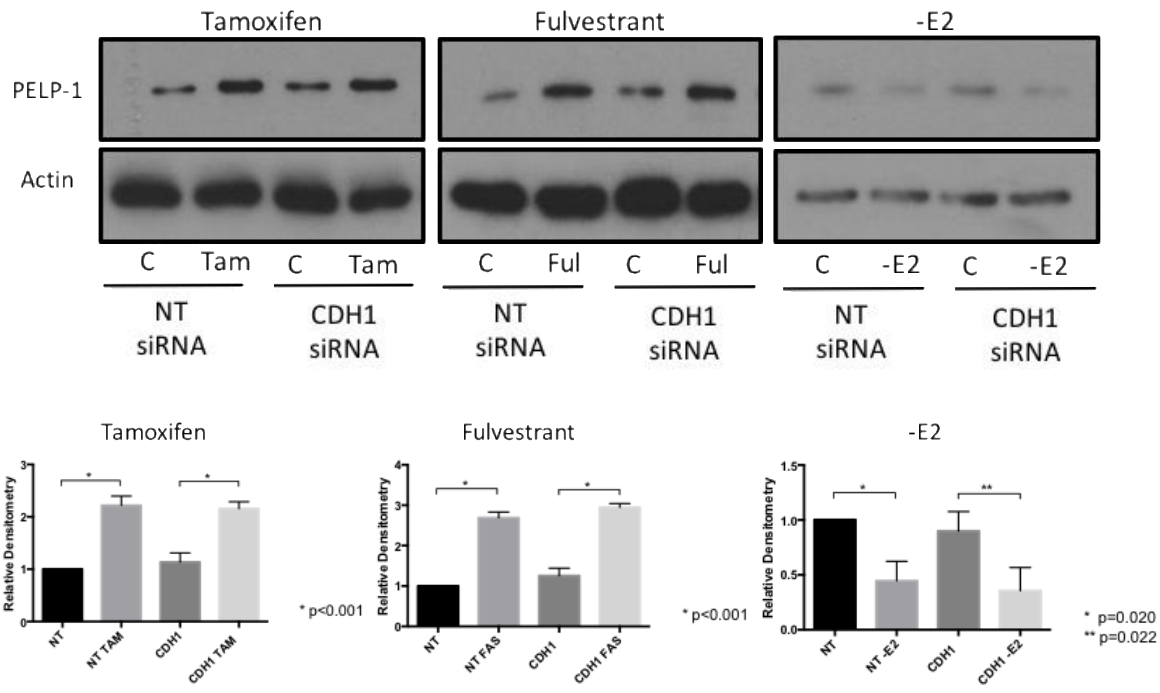

Figure 3.36 – Changes in PELP-1 expression in MCF-7 cells with tamoxifen, fulvestrant or estrogen withdrawal +/- CDH1 siRNA. Western Blot Analysis of PELP-1 and Actin under conditions of 6-day estrogen withdrawal, tamoxifen or fulvestrant treatment, with and without E-cadherin suppression. Differences in expression were assessed formally by densitometry. Tamoxifen and fulvestrant increase total PELP-1 expression, while estrogen withdrawal suppresses total PELP-1 expression in MCF-7 cells.

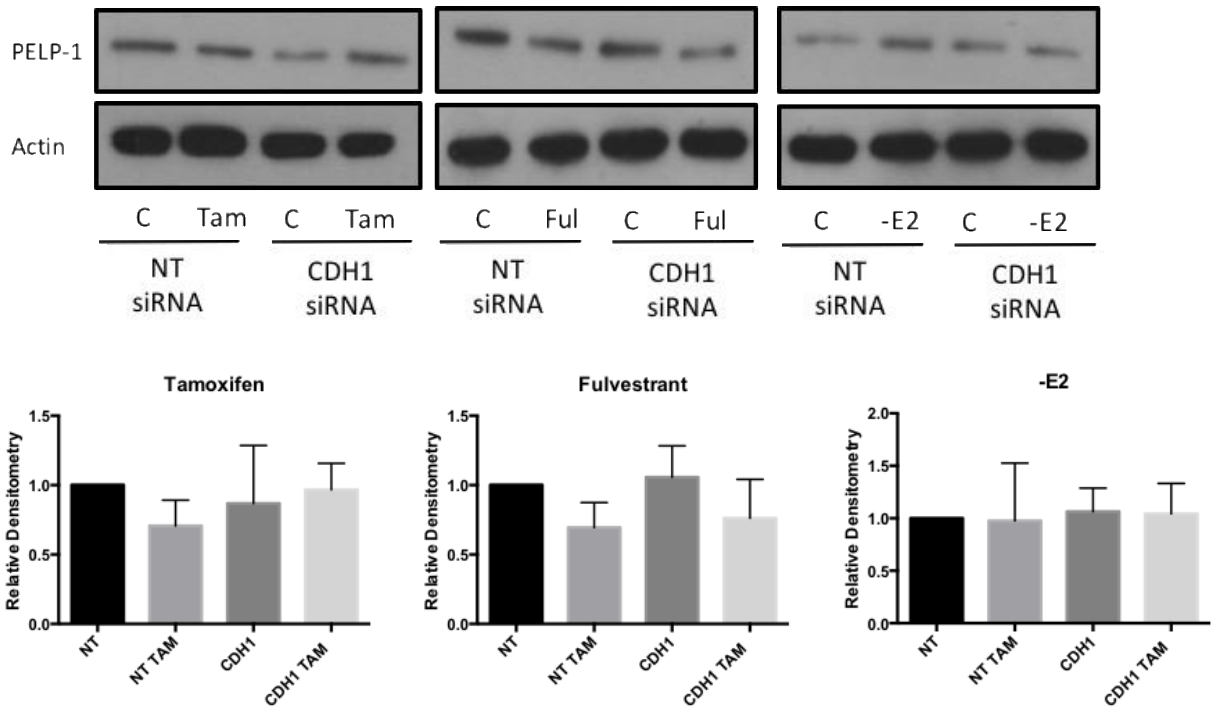

Figure 3.37 – Changes in PELP-1 expression in T47D cells with tamoxifen, fulvestrant or estrogen withdrawal +/- CDH1 siRNA. Western Blot Analysis of PELP-1 and Actin under conditions of 6-day estrogen withdrawal, tamoxifen or fulvestrant treatment, with and without E-cadherin suppression. Differences in expression were assessed formally by densitometry. Tamoxifen, fulvestrant and estrogen withdrawal has no effect on total PELP-1 expression in T47D cells.

3.3.4 Optimization of siRNA-mediated PELP-1 knockdown in MCF-7 cells

Prior to investigating the effects of PELP-1 suppression in relation to cell invasion and migration, optimization of the siRNA transfection protocol was required.

A 72-hour lipid-based transfection system was again utilized using Dharmafect smartpool® PELP-1 siRNA (Methods 2.2.6). The transfection procedure was optimized using a range of concentrations of anti-PELP-1 siRNA (100nm, 150nm, 200nm) to determine the dose that would achieve most efficient knockdown of PELP-1, assessed by Western blotting. Optimization was performed using the MCF-7 cell line, given its high basal level of PELP-1 expression. Data from Western blotting revealed no significant difference in knockdown of PELP-1 between the 100nm, 150nm and 200nm dose of siRNA (Figure 3.38). As a result, the 100nm dose of PELP-1 siRNA for all future experiments, as this produced adequate knockdown of PELP-1, while avoiding potential cellular siRNA toxicity from higher dose.

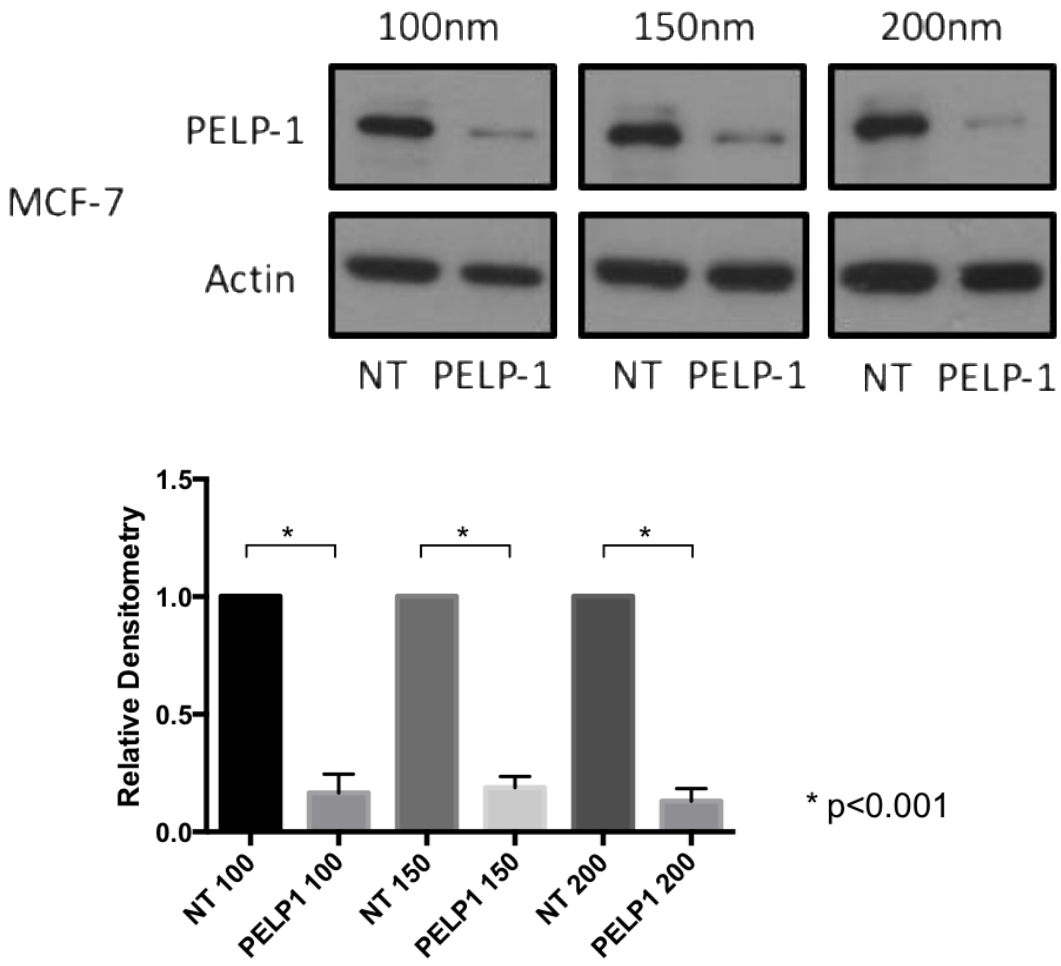

Figure 3.38 – Dose effect of PELP-1 siRNA on PELP-1 expression in MCF-7 cells. Western blotting and densitometry data demonstrating the expression of PELP-1 and Actin in MCF-7 cells, 72 hours after NT and PELP-1 siRNA transfection, using 100nm, 150nm and 200nm dose of siRNA respectively. PELP-1 expression is suppressed using 100nm, 150nm and 200nm dose of CDH1 siRNA in MCF-7 cells.

3.3.5 PELP-1 suppression reduces the pro-invasive effects of tamoxifen and fulvestrant in MCF-7 cells

The effect of PELP-1 expression in relation to cell invasion was assessed by investigating the invasive capacity of MCF-7 cells, grown in 2D cell culture, to invade through a Matrigel® matrix, as performed in earlier chapters.

Initially, the effects of tamoxifen on cell invasion were compared in PELP-1 positive (NT) and PELP-1 deficient (PELP-1) cells (Figure 3.39a). Results from this assay demonstrated a significant increase in the invading number of cells with tamoxifen treatment, both with ($p=0.002$) and without ($p<0.001$) PELP-1 knockdown. Knockdown of PELP-1 in cells treated with tamoxifen did however result in a decrease in cellular invasion compared to wild-type (NT) counterparts ($p<0.001$), while no significant difference in invasion was observed when comparing PELP-1 knockdown with wild-type cells (NT) in the absence of endocrine therapy.

In a similar fashion, the effects of fulvestrant on cell invasion were also compared in PELP-1 positive (NT) and PELP-1 deficient (PELP-1) cells (Figure 3.39b). As seen in the case of tamoxifen, fulvestrant treatment resulted in a significant increase in the invading number of cells, both with and without PELP-1 knockdown ($p<0.001$). Knockdown of PELP-1 in fulvestrant-treated cells did result in a decrease in cellular invasion compared with fulvestrant-treated wild-type (NT) cells ($p=0.002$). Meanwhile, as was the case previously, no significant difference in invasion was observed when comparing PELP-1 knockdown alone with wild-type cells (NT) in the absence of endocrine therapy.

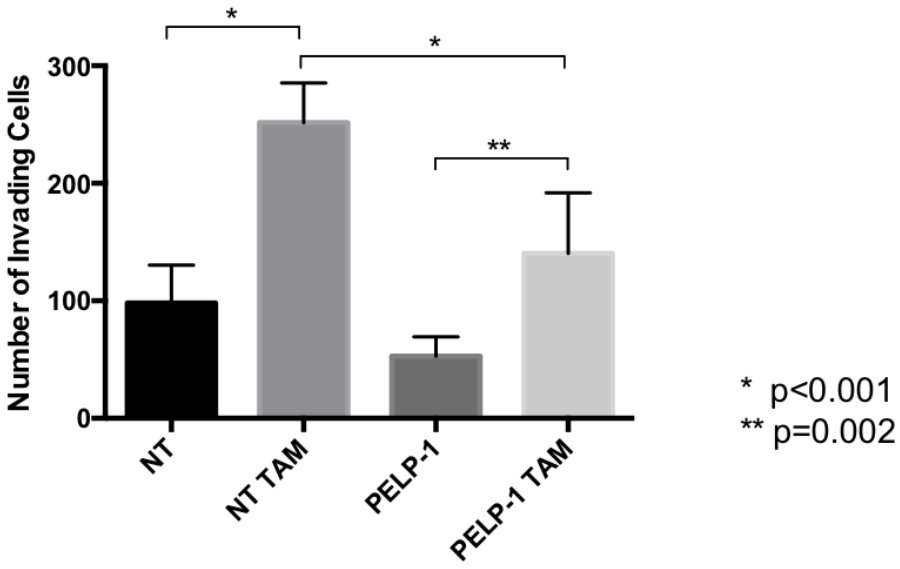

a.

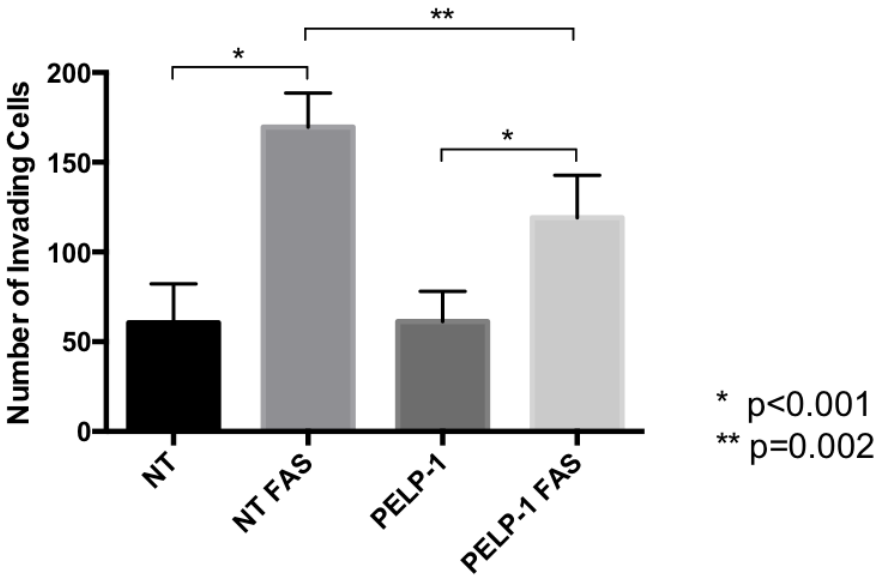

b.

Figure 3.39 – Cell invasion in MCF-7 cells treated with (a.) tamoxifen and (b.) fulvestrant +/- PELP-1 siRNA. MCF-7 cells were treated with non-targeting (NT) or PELP-1 targeting (PELP-1) siRNA for 72 hours before assessing their invasive capacity in response to 6-day (a) tamoxifen ($1x10^{-7}M$) and (b) fulvestrant ($1x10^{-7}M$) treatment. PELP-1 suppression reduced the previously observed pro-invasive response to endocrine treatments. The graphs show the results for the mean of three separate experiments.

3.3.6 PELP-1 suppression reduces the pro-migratory effects of tamoxifen and fulvestrant in MCF-7 cells

To assess migration, the capacity of MCF-7 cells grown in 2D cell culture, to migrate through a fibronectin coated membrane, was assessed in the same manner as previously described in earlier chapters.

In a similar fashion to when investigating changes in invasion, the effects of 6-day tamoxifen treatment on cell migration were compared in PELP-1 positive (NT) and PELP-1 deficient (PELP-1) cells (Figure 3.40a). These results again demonstrated a significant increase in migration amongst wild-type (NT) cells treated with tamoxifen ($p<0.001$), as described previously. In addition, while PELP-1 knockdown alone had no significant effect on migration when compared to wild-type cells (NT), a significant reduction the number of migratory cells was observed in PELP-1 knockdown cells treated with tamoxifen, compared to wild-type cells (NT) treated with tamoxifen ($p=0.014$). In contrast to the results seen when investigating invasion however, there was no observed difference in migration between PELP-1 knockdown cells treated with and without tamoxifen, indicating that PELP-1 knockdown may have a more potent effect on cell migration as compared to cell invasion in this respect.

The effect of fulvestrant on cell migration was also compared in PELP-1 positive (NT) and PELP-1 deficient (PELP-1) cells (Figure 3.40b). As seen previously, fulvestrant treatment resulted in a significant increase in the number of migratory cells ($p<0.001$). Knockdown of PELP-1 in fulvestrant-treated cells did result in a decrease in cellular migration ($p<0.001$). Meanwhile, no significant difference in migration was found when comparing PELP-1 knockdown alone with wild-type cells (NT) in the absence of any endocrine therapy.

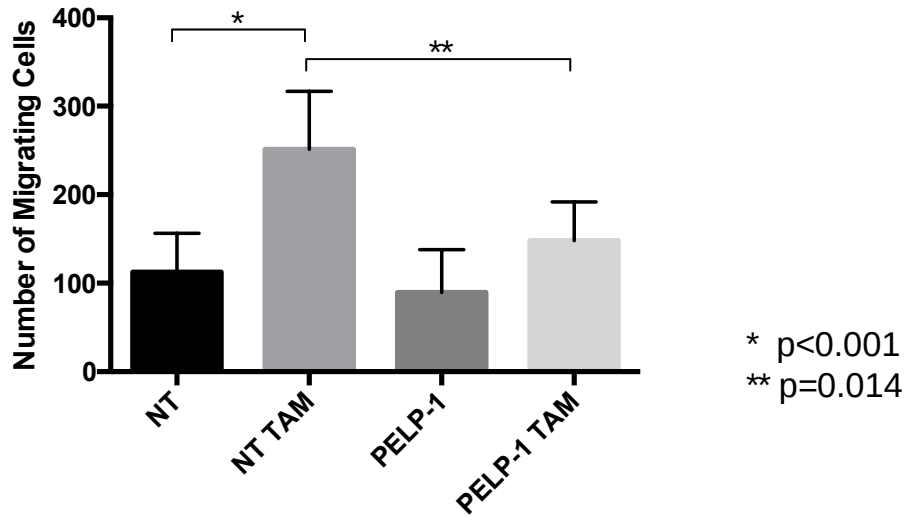

a.

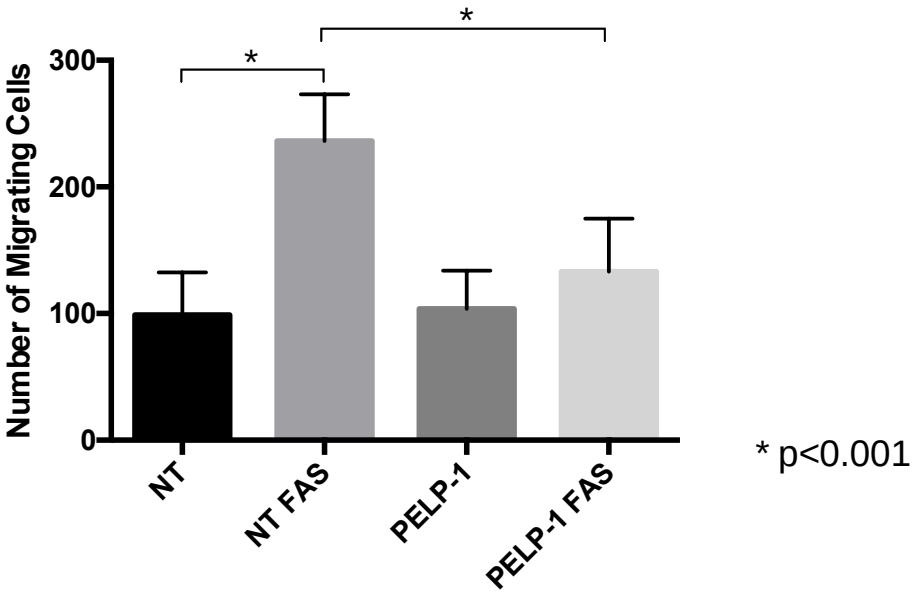

b.

Figure 3.40 – Cell migration in MCF-7 cells treated with (a.) tamoxifen and (b.) fulvestrant +/- PELP-1 siRNA. MCF-7 cells were treated with non-targeting (NT) or PELP-1 targeting (PELP-1) siRNA for 72 hours before assessing their migratory capacity in response to 6-day (a) tamoxifen ($1x10^{-7}M$) and (b) fulvestrant ($1x10^{-7}M$) treatment. PELP-1 suppression reduced the previously observed pro-migratory response to endocrine treatments. The graphs show the results for the mean of three separate experiments.

3.3.7 PELP-1 suppression has no effect on proliferation in MCF-7 cells

While previous results suggest PELP-1 suppression has a significant effect in inhibiting endocrine induced invasion and migration, it may be possible that incidental effects on cellular proliferation could mask the results of these assays.

To assess the effects of PELP-1 knockdown on cell proliferation therefore, a 6-day cell growth assay was performed, assessed by MTT assay (Figures 3.41a and 3.41b). This compared the proliferation of wild-type (NT) and PELP-1 knockdown MCF-7 cells, treated with and without tamoxifen or fulvestrant. Results from this assay demonstrated that while, as seen previously, both tamoxifen and fulvestrant therapy resulted in reduced cellular proliferation ($p<0.001$), PELP-1 knockdown had no effect in both endocrine-treated and untreated MCF-7 cells.

These results were confirmed by performing a 6-day growth assay, assessed by end-point cell counting (Figures 3.42a and 3.42b). This again compared the proliferation of wild-type (NT) and PELP-1 knockdown MCF-7 cells, treated with and without tamoxifen or fulvestrant. Results mirrored those of the MTT assay, whereby both tamoxifen and fulvestrant therapy reduced cellular proliferation ($p<0.001$), while PELP-1 knockdown had no effect on proliferation in endocrine-treated and untreated MCF-7 cells.

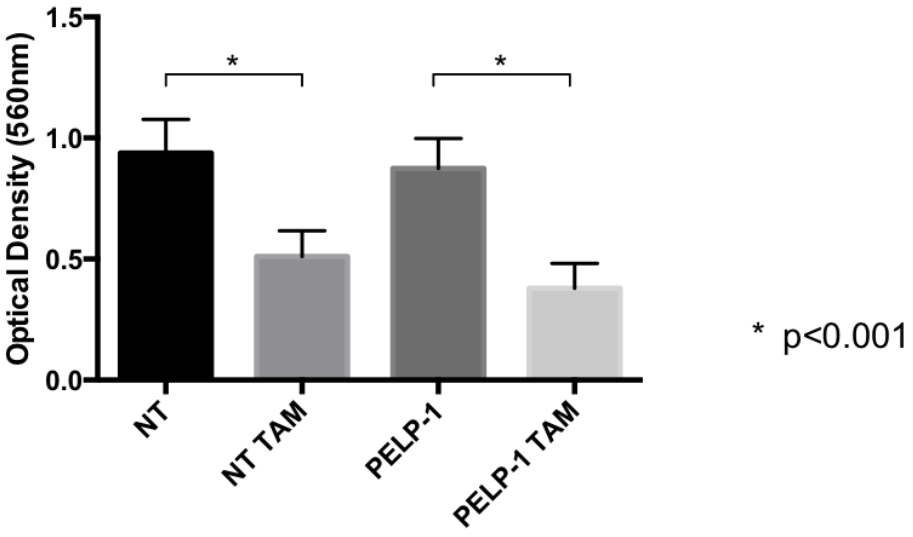

a.

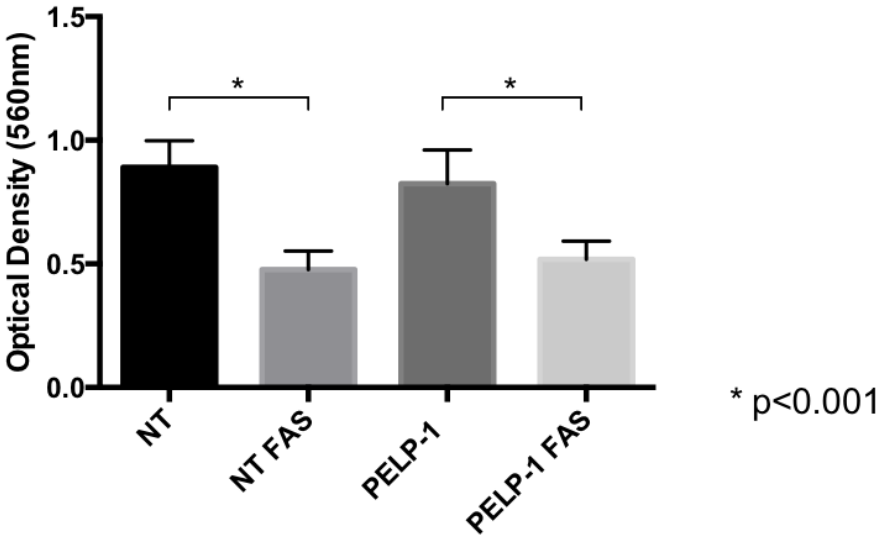

b.

Figure 3.41 – Cell proliferation in MCF-7 cells treated with (a.) tamoxifen and (b.) fulvestrant +/- PELP-1 siRNA. MCF-7 cells were treated with non-targeting (NT) or PELP-1 targeting (PELP-1) siRNA for 72 hours before assessing cell proliferation after either 6-day (a) tamoxifen ($1x10^{-7}M$) or (b) fulvestrant ($1x10^{-7}M$) treatment. PELP-1 suppression had no significant effect of cell proliferation. The graphs show the results for the mean of three separate experiments.

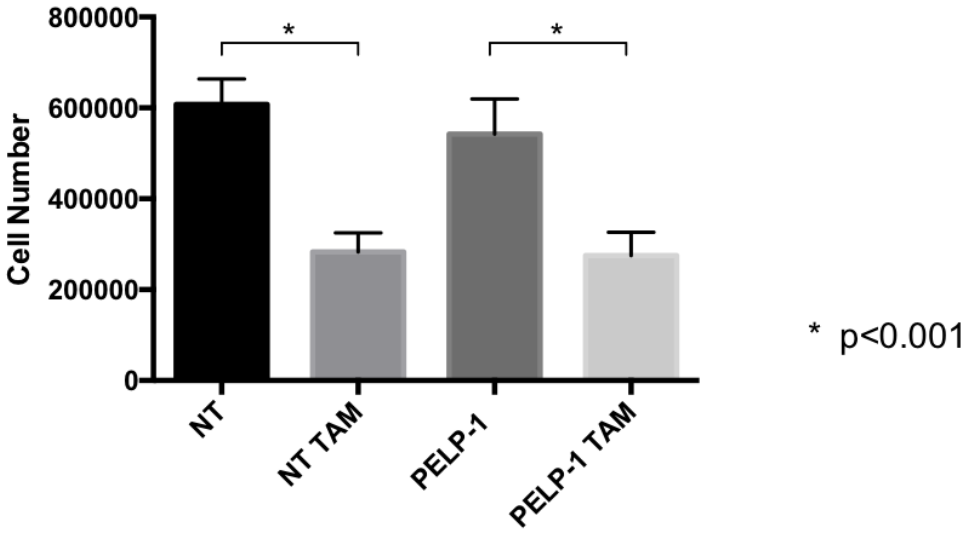

a.

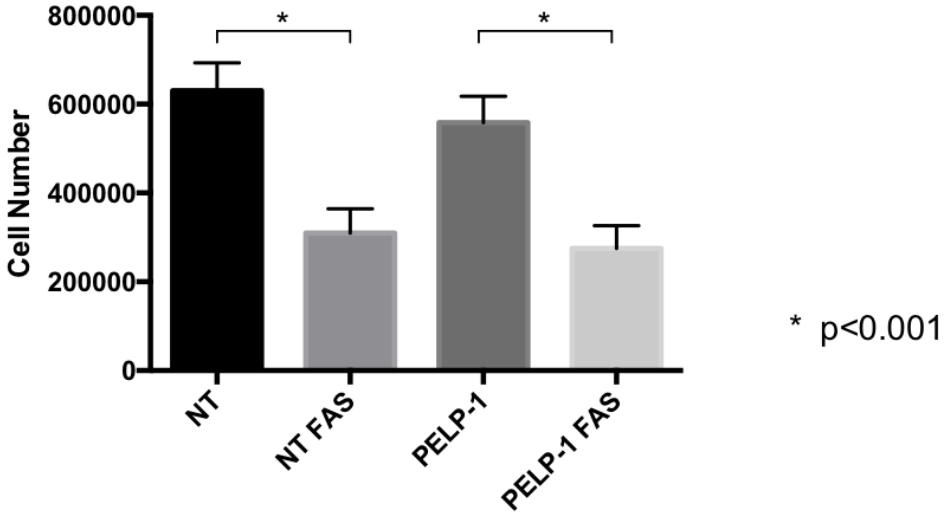

b.

Figure 3.42 – Cell proliferation in MCF-7 cells treated with (a.) tamoxifen and (b.) fulvestrant +/- PELP-1 siRNA MCF-7 cells were treated with non-targeting (NT) or PELP-1 targeting (PELP-1) siRNA for 72 hours before assessing cell proliferation after either 6-day (a) tamoxifen ($1x10^{-7}M$) or (b) fulvestrant ($1x10^{-7}M$) treatment. PELP-1 suppression had no significant effect of cell proliferation. The graphs show the results for the mean of three separate experiments.

3.3.8 PELP-1 suppression reduces the pro-invasive and pro-migratory effects of tamoxifen in MCF-7 cells within a low cell-cell contact environment

Having established that siRNA mediated PELP-1 knockdown inhibits invasion and amongst MCF-7 cells treated with tamoxifen and fulvestrant, the next step was to assess whether this effect would also be evident in the setting of E-cadherin suppression, given that a more dramatic pro-invasive/pro-migratory response to endocrine agents was demonstrated under these conditions previously.

To assess this a double-knockdown (E-cadherin/PELP-1) experiment was first designed and optimized. A double siRNA transfection with anti-CDH1 and anti-PELP-1 siRNA was performed using the same transfection protocol as previously used for each siRNA individually. In the case of double-transfection however, the siRNA dose for CDH1 and PELP-1 was halved to allow the total siRNA dose (and lipid dose) to remain the same. To assess the effectiveness of knockdown MCF-7 cells grown in antibiotic-free experimental medium was transfected with 100nm (50nm CDH1, 50nm PELP-1), 150nm (75nm CDH1, 75nm PELP-1) and 200nm (100nm CDH1, 100nm PELP-1) respectively, for 72 hours. Dishes were then lysed for protein extraction and lysates analyzed by SDS-PAGE and Western Blotting to determine the effectiveness of knockdown of E-cadherin and PELP-1. Results demonstrated effective knockdown of both E-cadherin and PELP-1 using the 100nm, 150nm and 200nm doses of combined siRNA (Figure 3.43). As a result, the 100nm combined siRNA dose was used in future experiments.

Following this period of optimization, this siRNA transfection protocol was incorporated into the Boyden chamber invasion and migration assays, to assess the functional effects of the double-knockdown of both proteins. Therefore, to assess invasion, siRNA mediated wild-type (NT), E-cadherin knockdown and PELP-1/E-cadherin knockdown MCF-7 cells were compared in the presence and absence of 6-day tamoxifen treatment (Figure 3.44a). The results from this assay revealed, as shown previously, the pro-invasive response of cell treated with

tamoxifen ($p=0.020$), augmented by E-cadherin suppression ($p<0.001$). Interestingly however, combined PELP-1/E-cadherin knockdown cells treated with tamoxifen showed no significant change in invasion, suggesting a reversal in the previously seen tamoxifen-induced pro-invasive response.

In similar fashion, to assess migration, siRNA mediated wild-type (NT), E-cadherin knockdown and PELP-1/E-cadherin knockdown MCF-7 cells were compared in the presence and absence of 6-day tamoxifen treatment (Figure 3.44b). As was the case when assessing invasion, results from this assay revealed the previously seen pro-migratory response of cell treated with tamoxifen, again augmented by E-cadherin suppression ($p<0.001$). Meanwhile, combined PELP-1/E-cadherin knockdown cells treated with tamoxifen revealed suppressed cell migration, as compared to corresponding tamoxifen-treated E-cadherin knockdown cells. Again, this result suggests that the incorporation of PELP-1 suppression within the assay results in inhibition of tamoxifen-induced migration.

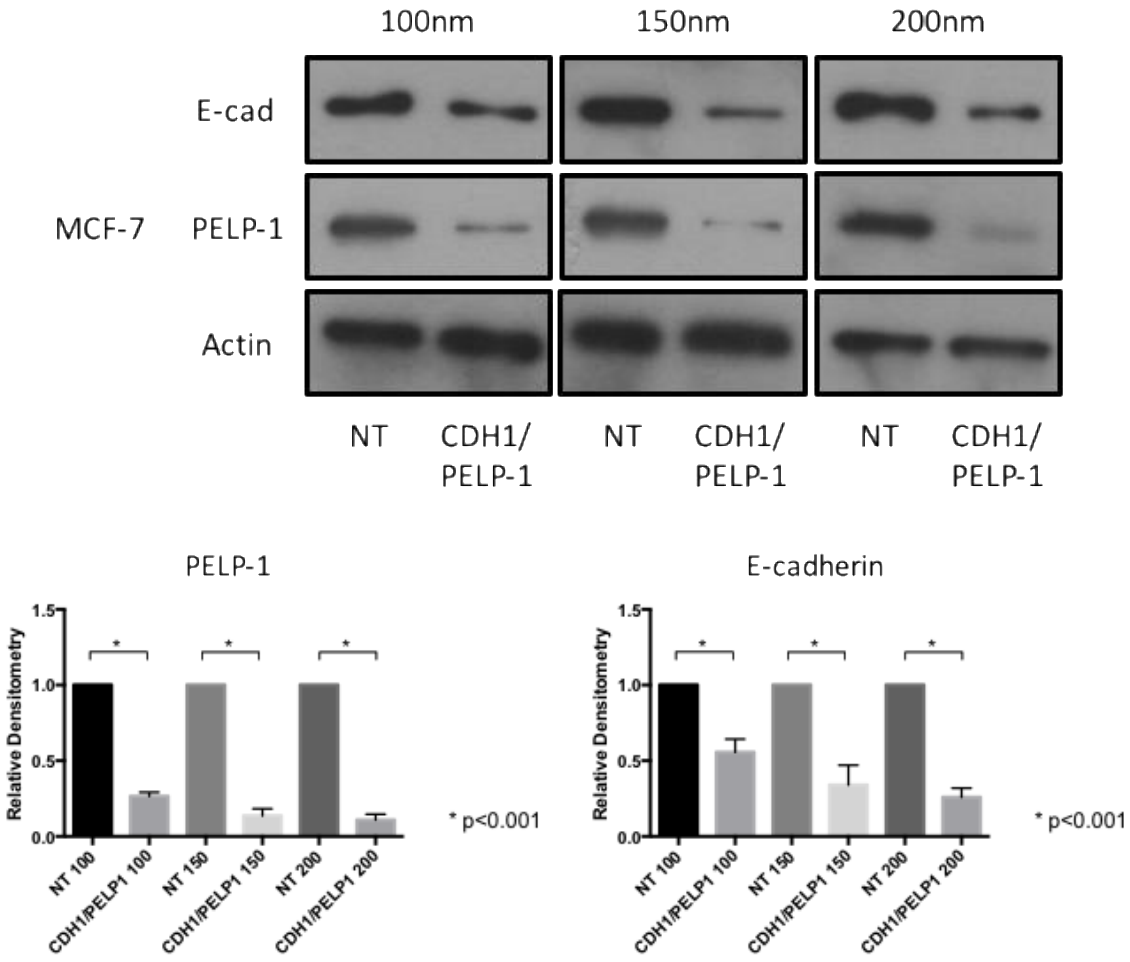

Figure 3.43 – Dose effect of combined CDH1/PELP-1 siRNA on E-cadherin and PELP-1 expression in MCF-7 cells. Western blotting and densitometry data demonstrating the expression of PELP-1, E-cadherin and Actin in MCF-7 cells, 72 hours after NT and CDH1/PELP-1 siRNA transfection, using 100nm, 150nm and 200nm dose of siRNA respectively. Both E-cadherin and PELP-1 expression is suppressed using combined 100nm, 150nm and 200nm dose of CDH1/PELP-1 siRNA in MCF-7 cells.

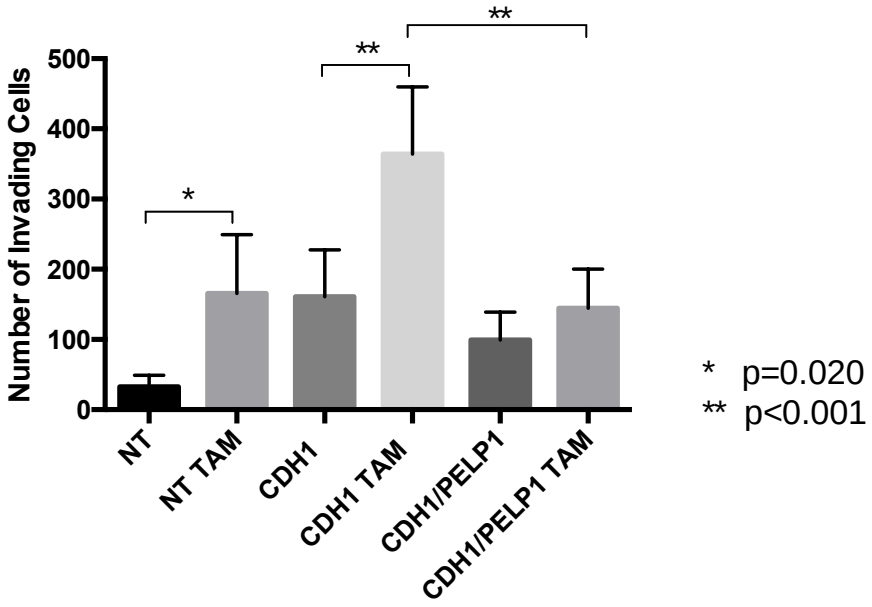

a.

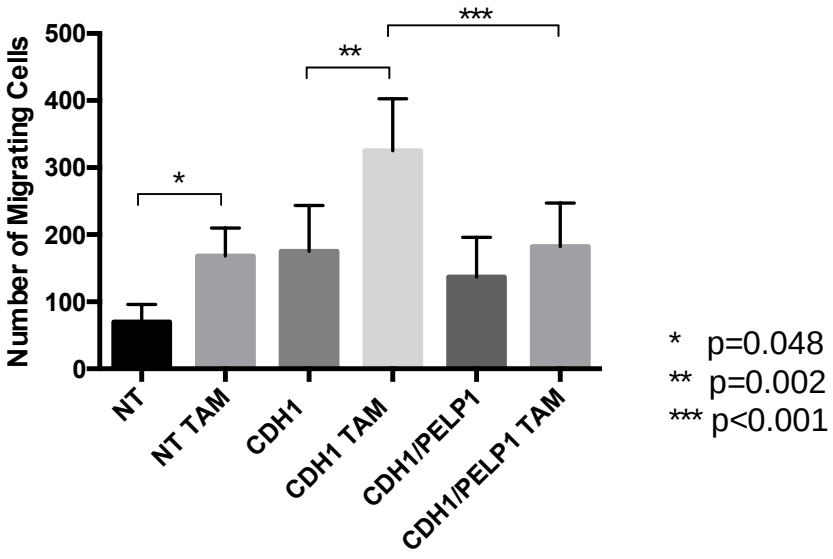

b.

Figure 3.44 - Cell (a.) invasion and (b.) migration in MCF-7 cells treated with tamoxifen +/- CDH1 siRNA or combined CDH1/PELP-1 siRNA. MCF-7 cells were treated with non-targeting (NT) or combined CDH1/PELP-1 targeting (CDH1/PELP-1) siRNA for 72 hours before assessing their (a.) invasive and (b.) migratory capacity following 6-day tamoxifen ($1x10^{-7}M$) treatment. PELP-1 suppression reduces the (a) pro-invasive and (b) pro-migratory effects of tamoxifen in MCF-7 cells within a low cell-cell contact environment. The graphs show the results for the mean of three separate experiments.

3.3.9 Endocrine therapy has no effect on PELP-1 subcellular localization in MCF-7 cells

Results from this chapter to date indicate that PELP-1 signaling is implicated in the observed pro-invasive and pro-migratory response to ER-targeting endocrine agents in MCF-7 cells, and that endocrine agents themselves may be involved in up-regulation of PELP-1 expression, which may drive this response.

In addition to this however, given that others have noted that subcellular localization of PELP-1 may have an implication on function (313), it was decided to investigate whether endocrine therapies themselves may also play a role in regulating PELP-1 localization. To address this a time-course experiment was conducted whereby MCF-7 cells were grown on TESPA coated coverslips under control conditions, conditions of estrogen deprivation (mimicking aromatase inhibition), or treated with tamoxifen (1×10^{-7}M) or fulvestrant (1×10^{-7}M). Cells were cultured under these conditions for 3, 6, 9 and 12 days respectively and then fixed and stained for PELP-1 and ER by ICC. Cells were then visualized for PELP-1 and ER sub-cellular localization by light microscopy.

The results from this assay demonstrated that the sub-cellular location of PELP-1 was almost exclusively nuclear, with particularly high density within nucleoli, within the control arm of the study at all time points (Mean H-Score=280 [SD 5.1]; Figure 3.45a). This nuclear distribution of PELP-1 was also evident, and overall appeared unaltered, where cells were treated with tamoxifen (Mean H-score=275 [SD 5.1]; p=ns), fulvestrant (Mean H-score=280 [SD 8.22]; p=ns) or grown under conditions of estrogen deprivation (Mean H-score=275 [SD 6.2]; p=ns; Figure 3.3.9 a). Interestingly however, with tamoxifen and fulvestrant treatment, there were occasional cells showing a cytoplasmic staining pattern for PELP-1 at all time points (Figure 3.45b), albeit at a very low frequency (approx. 1:500-1:1000 cells). In contrast the pattern of staining amongst cells cultured in conditions of estrogen deprivation appeared to be entirely nuclear.

Staining for ER was also performed to determine ER expression amongst cells treated under each condition over the 12-day time course. ER localization was predominantly nuclear in each experimental arm, with minimal staining in the cytoplasm (Figure 3.46). While tamoxifen had little effect of ER expression over the experiments time course (Mean H-score=290 [SD 5.2]; p=ns), treatment with fulvestrant resulted in reduced expression of ER from 6 days of treatment onwards (Day 3 H-score=290 [SD 7.6]; Day 12 H-score=190 [SD 15.1]; $p<0.01$), although sub-cellular location remained unaltered (Figure 3.46).

Finally, given the predominant nuclear staining of both PELP-1 and the ER, confocal microscopy was used to try to identify potential interaction between the two proteins. To do this, MCF-7 cells were cultured under control conditions or treated with tamoxifen for 6 days, followed by fixation and ICC staining for PELP-1 and ER. Cells were then visualized by confocal microscopy to determine co-localization of PELP-1 and the ER. Results from this assay demonstrated a moderate level of PELP-1/ER co-localization (Figure 3.47a), which did not alter significantly with tamoxifen therapy (Figure 3.47b).

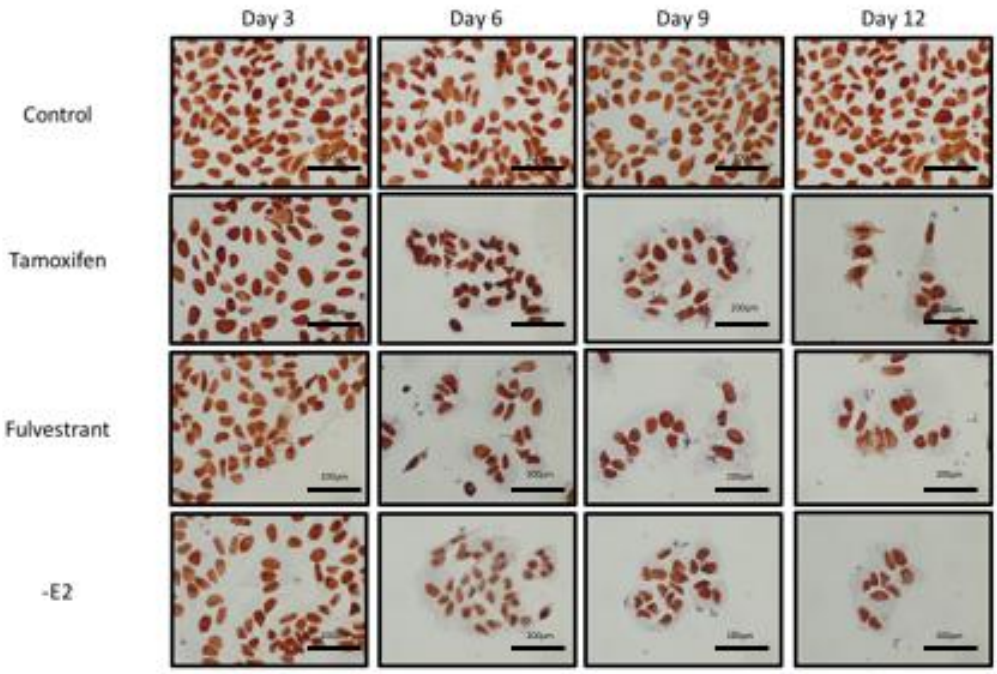

a.

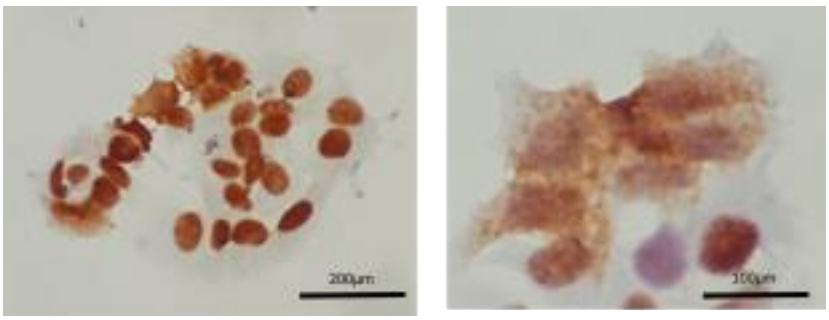

b.

Figure 3.45 – PELP-1 subcellular localization in MCF-7 cells treated with tamoxifen, fulvestrant or under conditions of estrogen withdrawal.

(a.)MCF-7 cells were cultured under control conditions or treated with tamoxifen ($1x10^{-7}$M), fulvestrant ($1x10^{-7}$M), or estrogen withdrawal for 3, 6, 9 and 12 days before being fixed and stained for PELP-1 expression. PELP-1 staining is uniform and predominantly nuclear under all treatment conditions. (b.) Occasional cytoplasmic staining for PELP-1 was identified amongst MCF-7 cells treated with tamoxifen and fulvestrant.

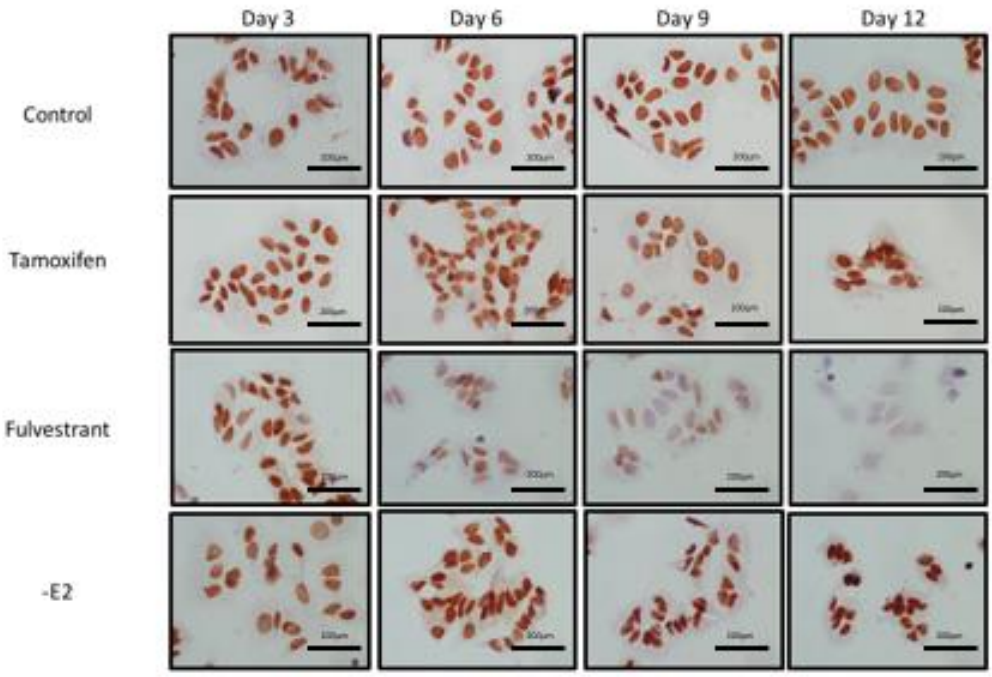

Figure 3.46 – ER subcellular localization in MCF-7 cells treated with tamoxifen, fulvestrant or under conditions of estrogen withdrawal. MCF-7 cells were cultured under control conditions or treated with tamoxifen ($1x10^{-7}M$), fulvestrant ($1x10^{-7}M$), or estrogen withdrawal for 3, 6, 9 and 12 days before being fixed and stained for ER expression. ER staining is predominantly nuclear under all treatment conditions. ER staining was weaker in MCF-7 cells treated with fulvestrant, as compared to control conditions, in a time-dependent manner.

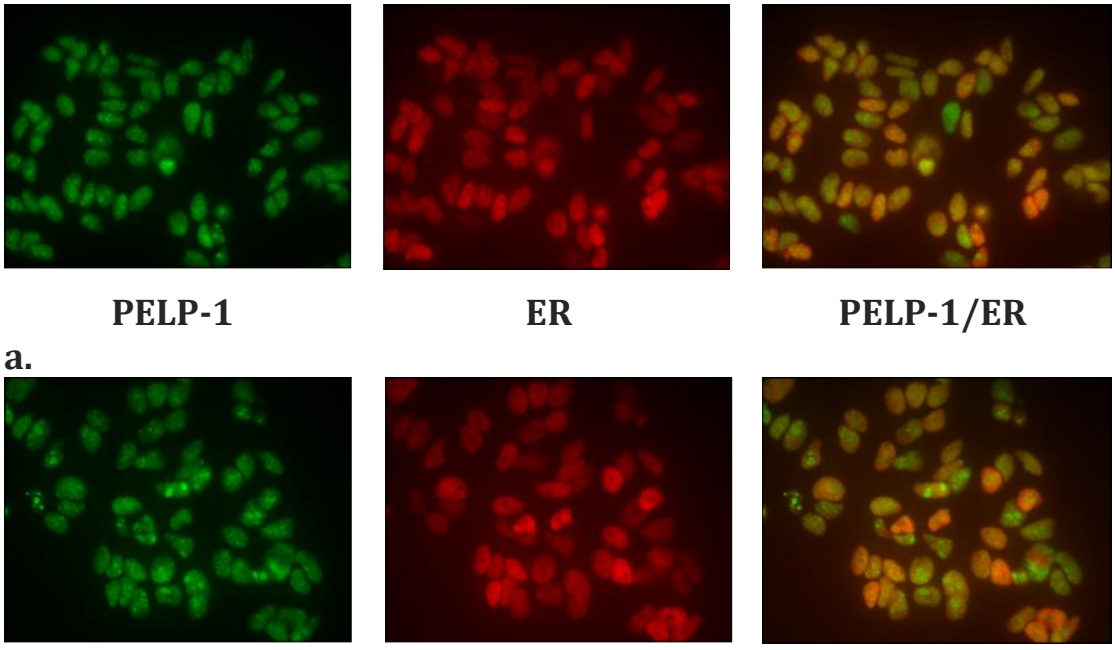

Figure 3.47 – Evidence of ER/PELP-1 co-localization under (a.) control and (b.) tamoxifen treated conditions. MCF-7 cells were cultured under control conditions or treated with tamoxifen ($1x10^{-7}M$) or estrogen withdrawal 6 days before being fixed and stained for ER (red) and PELP-1(green) expression. Cells were then imaged with confocal microscopy to assess for the co-localization of both proteins. ER and PELP-1 demonstrate a predominantly nuclear distribution. High PELP-1 signal is evident within cell nucleoli. Co-localization between ER and PELP-1 is moderate and not significantly affected by tamoxifen therapy.

3.3.10 PELP-1 suppression reverses endocrine-induced intra-cellular signaling changes in MCF-7 cells

The previous chapter demonstrated that tamoxifen and fulvestrant induced a series of intra-cellular signaling changes in MCF-7 cells, which were associated with an adverse cellular phenotype. Given that siRNA-mediated PELP-1 suppression inhibited this pro-invasive/pro-migratory phenotype, it was decided to re-assess these signaling pathways in the context of PELP-1 suppression, to assess whether these signaling pathways would be altered.

To achieve this, the effects of siRNA mediated knockdown of PELP-1 on MCF-7 cells was explored by Western Blot analysis, in the presence and absence of 6-day tamoxifen therapy (1×10^{-7}M). The signaling pathways explored in the previous chapter were then re-examined, using phospho-specific antibodies, to re-examine targets of interest.

When performing this analysis, the pathways involving the axis of Src kinase, AKT and ERK 1/2 were initially re-investigated by assessing changes in total and phosphorylated expression of these proteins in MCF-7 cells treated with and without tamoxifen for 6-days, and with non-targeting (NT) or anti-PELP-1 (PELP-1) siRNA for 72 hours (Figure 3.48). While tamoxifen had previously resulted in an increase in pSrc kinase expression, a suppression in Src was seen with PELP-1 knockdown. In addition, a similar picture was seen with ERK signaling, whereby a suppression in pERK 1/2 was seen with PELP-1 knockdown, as opposed to the previously seen increase in signaling with tamoxifen. Meanwhile, AKT signaling, which was previously suppressed by tamoxifen therapy, was further suppressed by PELP-1 knockdown.

In addition to these proteins of interest, alternative targets that were previously shown to be modulated by tamoxifen therapy were also interrogated. These included the regulatory protein focal adhesion kinase (FAK) and transcription factor STAT3. As such, changes in total and phosphorylated expression of these proteins were examined in MCF-7 cells treated with and without tamoxifen for 6-

days, and with non-targeting (NT) or anti-PELP-1 (PELP-1) siRNA for 72 hours (figure 3.49). Results showed that while tamoxifen had previously resulted in an increase in pFAK and pSTAT 3 expression, reduced expression in the phosphorylated forms of both these proteins was observed with PELP-1 suppression.

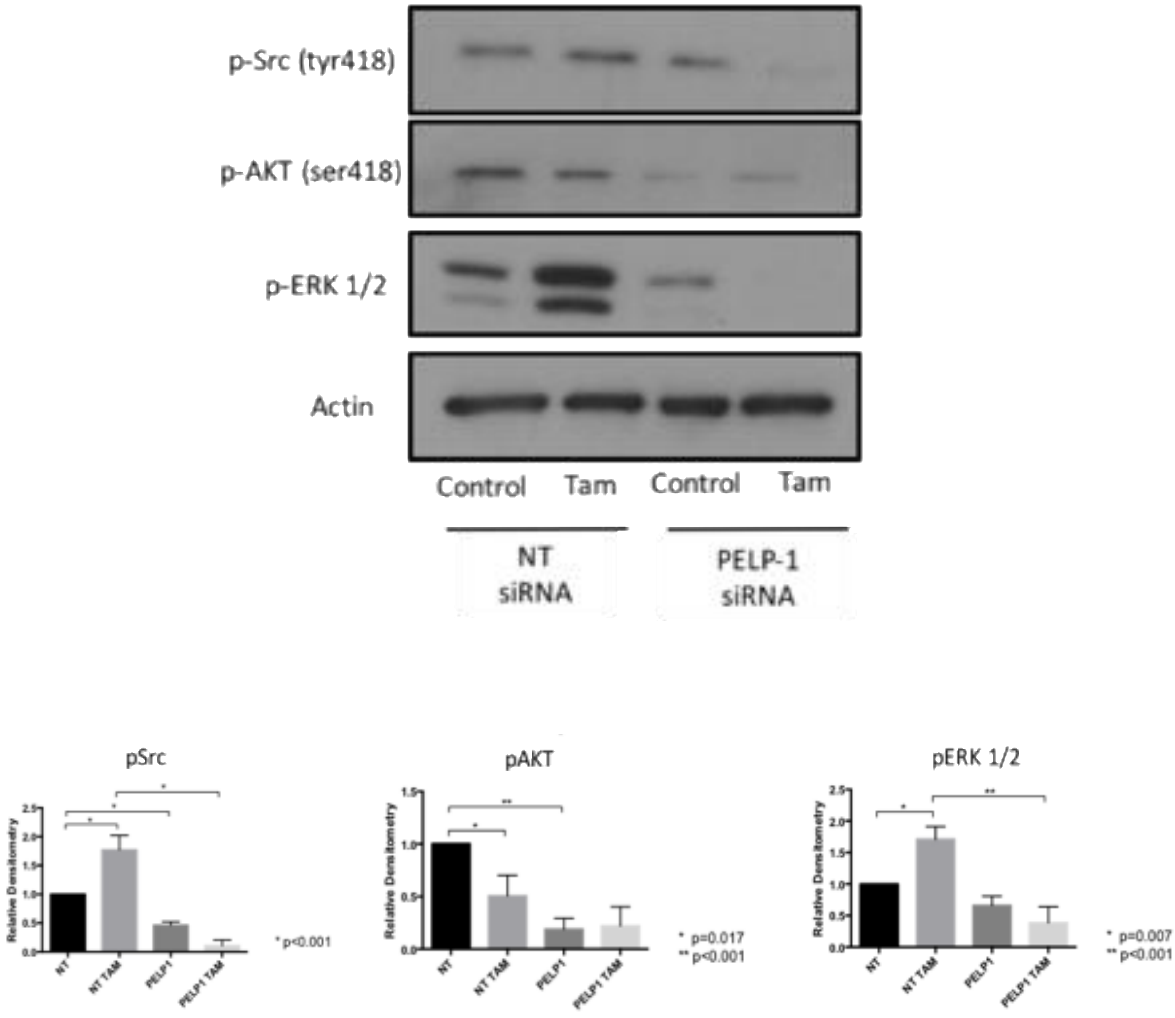

Figure 3.48 – Src, AKT and ERK 1/2 expression in MCF-7 cells treated with tamoxifen +/- PELP-1 siRNA. Western Blot Analysis of pSrc, pAKT, pERK 1/2 and Actin expression in MCF-7 cells grown under conditions of 6-day tamoxifen therapy, with and without PELP-1 suppression. PELP-1 knockdown suppresses Src, AKT and ERK 1/2 expression in tamoxifen treated MCF-7 cells.

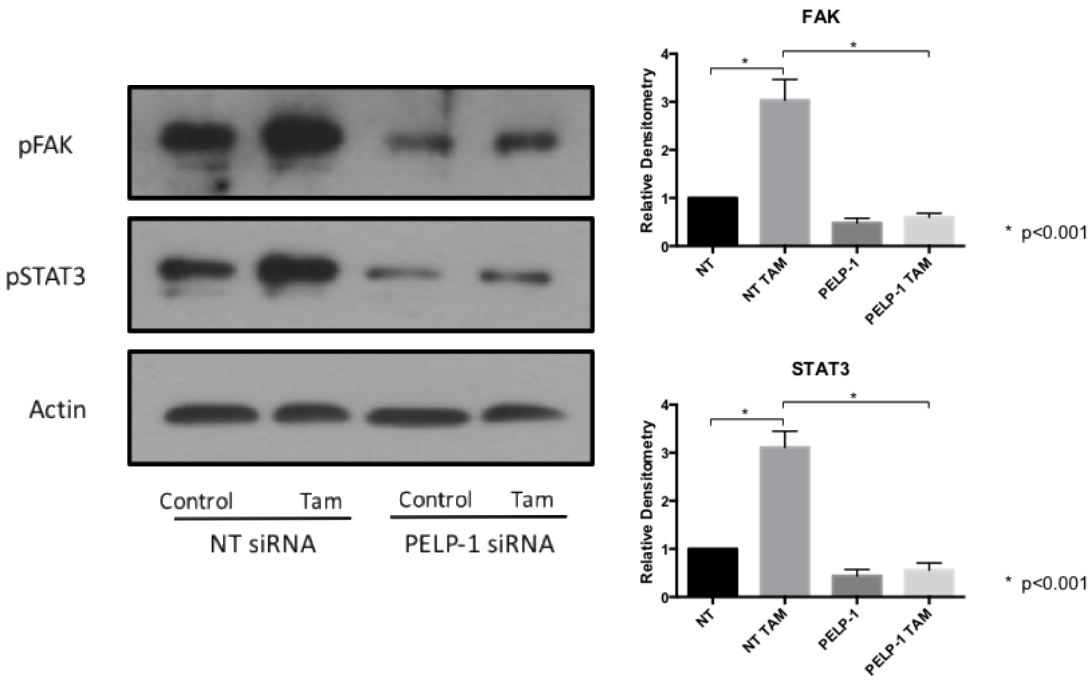

Figure 3.49 – FAK and STAT3 expression in MCF-7 cells treated with tamoxifen +/- PELP-1 siRNA. Western Blot Analysis of pFAK, pSTAT3 and Actin expression in MCF-7 cells grown under conditions of 6-day tamoxifen therapy, with and without PELP-1 suppression. PELP-1 knockdown suppresses FAK and STAT3 expression amongst tamoxifen treated cells.

3.3.11 Discussion

The aim of this chapter was to try and identify key molecular determinants of an adverse response to endocrine agents in ER+ breast cancer cells. Driving this was the observation that tamoxifen and fulvestrant induced an invasive phenotype in MCF-7, but not T47D cells, despite both cell lines being ER+ and endocrine sensitive.

Following a literature review, numerous molecular differences were found between the MCF-7 and T47D cell lines (Appendix 7.15). Potential determinants for the observed adverse response to endocrine treatments in MCF-7 cells were identified from this list by applying criteria designed to refine this selection based on findings described in previous chapters. This included identifying targets that may be implicated in the regulation of cell invasion/migration, regulated by conformational changes of the ER, and has an association with Src kinase signaling. Following the application of these criteria to the extended list of expressional differences, PELP-1 was identified as a potential target.

PELP-1 is a large multi-domain proto-oncogene (314), that functions as a co-regulatory protein that confers cancer cells with a growth and survival advantage (315, 316). PELP-1 related signalling has been identified in the progression of several cancers in-vitro (317-321), including breast (322, 323). As such, overexpression of PELP-1 in transgenic mice has been shown to contribute to the development of mammary tumours (324). In relation to breast cancer, PELP-1 was initially reported as an estrogen receptor co-activator in relation to the non-genomic functions of the ER, hence its alternative name of non-genomic action of estrogen receptor (MNAR) in some parts of the literature. PELP-1 has been shown to be exhibit high expression in >60% of both ER positive and ER negative tumours (314). Expression has been shown to be an independent prognostic predictor for poor breast cancer-specific and disease-specific survival (308), and predicts poor response to tamoxifen in ER positive tumours (325). Node-positive and metastatic tumours have also been shown to have greater PELP-1 expression than node negative specimens (314), and as such PELP-1 may be considered a useful biomarker to predict poor outcome (326, 327). PELP-1 expression also correlates

with tumour stage in non-small cell lung cancer (320) and may also be of use a prognostic marker in astrocytic tumours (328) and colorectal cancer (329).

PELP-1 contains a total of 10 nuclear receptor (NR)-interacting boxes (LXXLL motifs), which facilitate the proteins interaction with nuclear receptors (330). The protein also contains a 70 acidic amino acid chain located at the C-terminus, which functions as a histone binding region (310, 311). In addition, PELP-1 contains several PXXP motifs, which importantly facilitate the interaction with proteins containing the Src homology 3 (SH3) domain. Finally, the protein contains a number of other conserved protein-protein interaction motifs that allows binding with the domains of other proteins, including forkhead associated (FHA) domain, Src homology 2 (SH2), SH3, PDZ and WW domains (308), while 2 nucleolar domains are also found, which play an important role in ribosomal functions (331). Interestingly, mass spectrometry data appears to suggest that PELP-1 remains as a stable component of several multi-complex formations (332, 333), indicating that the protein lacks enzymatic activity and instead is more likely to act as a scaffold protein that brings other proteins in contact with both transcription factors and nuclear receptors. Importantly, these factors allow PELP-1 to interact with both with the ER and the SH3 domain of Src kinase. This interaction may propagate signalling between the ER and Src kinase, via the SH2 domain of the Src molecule, in cells where PELP-1 is highly expressed.

PELP-1 may be activated by phosphorylation from several hormonal and growth factor signals, which allows the signals from these mechanisms to be transferred to both nuclear receptors and transcription factors. These signalling molecules include epidermal growth factor (EGF) (313), protein kinase A (PKA) (334) and glycogen synthase kinase 3 β (GSK3β) (335). PELP-1 may also be phosphorylated by cyclin dependent kinases (CDK's) in a cell cycle dependent manner (336), while the DNA damage induced kinases ATM and ATR may also phosphorylate PELP-1, helping to mediate the p53-mediated DNA damage response (337). PELP-1 primarily acts as a co-regulator of several nuclear receptors, including the ER (309, 317), as outlined above. The protein also functions as a co-regulator of several transcription factors, including activator protein 1 (AP1), specificity protein 1 (SP1), nuclear factor κB (NF-κB) (310) and signal transducer and

activator of transcription (STAT3) (338). While the LXXLL motifs help the interaction of PELP-1 with liganded steroid receptors, PELP-1 may also interact with non-liganded steroid receptors suggesting protein-protein interactions independent of the LXXLL motifs. Indeed, results in this chapter demonstrate the negative effect of PELP-1 suppression on ER-dependent, Src-mediated signalling.

This project has demonstrated that PELP-1 is variably expressed amongst different ER+ breast cancer cell lines and that this differential expression may have an implication in its function. MCF-7 cells were found to have a relatively high basal level of PELP-1 expression, whereas an alternative luminal A cell line, T47D, alongside BT474 and MDA-MB-361, both of which over-express HER2, had much lower levels of expression. This is consistent with the findings of others, who have previously demonstrated high PELP-1 expression amongst a similar panel of breast cancer cell lines, with T47D cells contrastingly showing very little in the way of basal expression (309). Meanwhile, clinical breast tumour samples report PELP1 overexpression in 60-80% of all tumours (339), with high expression associated with tumour grade, proliferation, node positivity and metastasis development, equating to poorer disease free survival (314, 325, 339). What is less clear from reviewing the literature however, is whether this variability in PELP-1 expression may have an impact on the significance of its function.

In addition to variable expression amongst different breast cancer cell lines, this project also reports that endocrine therapies may influence total levels of PELP-1 expression in MCF-7 cells, with tamoxifen and fulvestrant increasing PELP-1 expression, while estrogen deprivation (mimicking aromatase inhibition) supressing levels of PELP-1. From reviewing the literature, while this finding appears to be novel, others have found that PELP-1 may regulate estrogenic effects through autocrine estrogen synthesis and local aromatase expression (340, 341). In MCF-7 cells, PELP-1 has been shown to increase aromatase expression as mediated by PI3K and Src, which may regulate estrogen levels (309). It may therefore be possible that a similar relationship between the ER/estrogen and PELP-1 holds true in reverse, whereby exogenous stimulation of the ER, through estrogen or drugs targeting the ER, positively influence PELP-1 levels, which in turn dampens local estrogen synthesis via a feedback loop. Alternatively, it may

be possible that either PELP-1 is directly activated through an unanticipated effect of ER modulation and antagonism and/or that total levels PELP-1 levels are upregulated via a nuclear function of the ER cascade. Interestingly, tamoxifen and fulvestrant appeared to have no effect on total levels of PELP-1 in T47D cells, indicating that such a relationship is not generic and may be determined by basal PELP-1 expression.

Results within this chapter implicate PELP-1 as a regulator of the invasion and migration in MCF-7 cells, a finding corroborated by other studies. For example, invasive breast cancer and metastatic tumours have been shown to have increased levels of PELP-1 expression, as compared to node-negative tumours (314). In addition, PELP-1 alters several EMT markers, including those that govern cell adhesion, migration and motility. In lung cancer, PELP-1 knockdown reduced the development of metastatic lung nodules in xenografts (342), while in endometrial cancer, PELP-1 suppression led to significant reduction in invasion and migration (343).

In-vitro studies in breast cancer have shown that motility of MCF-7 cells stimulated with E2 is increased compared to control, while siRNA PELP-1 knockdown resulted in suppression of this aggressive phenotype (270). Metastases in ZR75 and MCF-7 cells, overexpressing PELP-1, was also greater than in controls, within tail vein and cardiac injection models (270). Additionally, PELP1 expression has been found to have a positive correlation with metastatic potential in MCF10A cells (314).

Interestingly, while these mentioned studies have all implicated the involvement of PELP-1 alone in cancer metastases, through its effects on invasion and migration, the findings expressed in this project are subtly different. While PELP-1 suppression alone often led to a small yet non-significant reduction in cell invasion and migration in the previous experiments, PELP-1 knockdown had a significant effect on reversing enhanced invasion and migration induced by endocrine therapies; a finding which to date is unique. This was also the case in the context of corresponding E-cadherin deficiency, where the invasion and migration response of cells to tamoxifen/fulvestrant was previously shown to be

enhanced. As such, it would seem logical that loss of PELP-1 within the cell may either result in the reversal of some of the endocrine-induced pro-invasive/migratory signalling events within the cell, or alternatively induce a set of competing changes within the cell.

Whilst this project has demonstrated that PELP-1 suppression has a negative effect on breast cancer cell invasion and migration, it appears that there was no effect on cell proliferation metabolism as assessed by cell counting and MTT assay. Interestingly, this result appears to contrast with findings reported elsewhere where PELP-1 has been shown to play a role in estrogen dependent and independent proliferation in several tumour types (314, 342-345). In endometrial cancer, PELP-1 downregulation was found to significantly suppress cell proliferation (343). Others have also demonstrated that PELP-1 contributes to estrogen-mediated G1/S-phase cell cycle progression, increasing the rate of inherent proliferation in breast tumours (346). Additionally, PELP-1 expression was correlated with tumour size and mitotic count in ER+ breast tumours (339). Meanwhile, knockdown of PELP-1 reduced growth in both ER positive and ER negative breast and ovarian cancer (342, 344, 345). The finding of increased PELP-1 expression within normal breast tissue during pregnancy, where cell proliferation is known to be higher, also supports a role for PELP-1 in estrogen mediated cell cycle progression (309). More specifically in MCF-7 cells, PELP-1 overexpression has been shown by others to result in increased cell proliferation (314).

While these findings appear to conflict with the results in this project there may be several reasons for this. Firstly, although siRNA knockdown of PELP-1 was robust, it may be that the level of knockdown required to promote a phenotypic response in cell proliferation was not achieved and that a change in siRNA dosage may have given rise to different results. Secondly, a more prolonged cell growth assay may have been more likely to show a change in underlying proliferation. Finally, while others may have shown overexpression of PELP-1 promotes increased proliferation in MCF-7 cells, the opposite effect need not hold true. Indeed, it may be the case that under conditions of PELP-1 suppression alternative

pathways, that promote proliferation, are activated that compensate for the absence of PELP-1.

Although PELP-1 is predominantly localized within the nucleus of cells, localization within the cytoplasm has also been observed in a subset of breast cancers (313, 347). Within the cytoplasm, PELP1 may interact with steroid receptors, such as the ER, and trigger signalling cascades involving previous proteins of interest, such as G proteins (348) and Src (349). As such, overexpression of cytoplasmic PELP-1 has been shown to result in enhanced, hormone-independent, AKT and MAPK signalling (313, 347) as part of the non-genomic functions of the ER.

While it therefore seems apparent that sub-cellular localization may define PELP-1 function, what is less clear is whether treatment with endocrine therapies can affect the distribution of PELP-1 within the cell and lead to potential changes in signalling, which will later be discussed. Results within this chapter demonstrated that neither treatment with tamoxifen, fulvestrant or estrogen withdrawal appeared to significantly affect PELP-1 localization, which was predominantly with the nucleus of MCF-7 cells. Results within the literature suggest that PELP-1 expression is inversely associated with ER, PR and luminal cytokeratins , whilst being positively associated with basal cytokeratins and P53 expression (339). While PELP-1 is therefore found localized to the nucleus in normal breast tissue, aberrant cytoplasmic localization has been shown in some breast tumours however (313, 325). In this chapter, while cytoplasmic staining for PELP-1 was also seen, albeit less frequently, endocrine treatment did not significantly affect its occurrence. Despite these findings, there are reasons why these results alone may be inconclusive, as PELP-1 has been shown to interact with both the genomic and non-genomic functions of the ER in MCF-7 cells. One such reason may be that cytoplasmic re-location of PELP-1 may be a transient, dynamic process within the cell, such that simple end-point ICC staining is insufficient to demonstrate. Secondly, while endocrine therapy may not significantly alter subcellular localization of PELP-1, cytoplasmic PELP-1 is still expressed at sufficient levels, albeit much lower than nuclear PELP-1 levels, to play a role in non-genomic ER

signalling. As such, it's interaction with the ER, and it's downstream signalling components within the cytoplasm, may still be crucial.

Given the role that PELP-1 suppression played in reversing the pro-invasive/migratory effect of tamoxifen and fulvestrant on MCF-7 cells, one might also expect PELP-1 suppression to reverse the signalling changes that were previously thought to be associated with such a change in cell phenotype. Indeed, when explored with Western blotting there were changes in patterns associated with both the genomic and non-genomic signalling of the ER.

While results in the previous section revealed that tamoxifen and fulvestrant therapy increased Src kinase and MAPK activity in MCF-7 cells, PELP-1 suppression appeared to reverse these effects. These findings would fit with reports that PELP-1 acts as a scaffolding protein required for extra nuclear actions of the ER (270), which links the ER with Src kinase, resulting in activation of the ER-Src-MAPK pathway (313, 350). PELP-1 was initially identified as a Src SH3 domain-binding protein (351) via its N terminus PXXP motif. The ER is then able to interact with Src's SH2 domain at phosphotyrosine 537, while the PELP-1/ER interaction further stabilizes interaction, sequestering PELP-1 in the cytoplasm, leading to MAPK activation (352). As such, others have shown that mutations in the PXXP domains in PELP-1 result in loss of interaction between ER and Src and reduce estrogen-induced MAPK activation (353), meanwhile it has been demonstrated that overexpression of PELP-1 results in rapid stimulation of MAPK though this route (313, 352). Outside of its functions through MAPK, PELP-1 also modulates ER-Src-ILK1 signalling, promoting cytoskeletal arrangements, motility and subsequently metastases (270), while it has also been shown to interact and activate mTOR signalling (315).

Meanwhile, data from this chapter reveals that AKT signalling, which was previously shown to be suppressed by tamoxifen, fulvestrant and estrogen withdrawal, was further suppressed when levels of PELP-1 were reduced. Again, this finding may be explained through the known extra-nuclear functions of PELP-1, where it facilitates E2 and growth factor-mediated formation of multiprotein complexes with the ER (344), resulting in activation and signalling through PI3K

(354, 355). Indeed, overexpression of cytoplasmic PELP-1 has been shown by others to increase AKT signalling (313, 352).

Outside of the axis of the ER, Src kinase/MAPK and PI3K/AKT results in this chapter demonstrate that PELP-1 suppression negatively influences signalling involving STAT3 and FAK. These findings would be consistent with the previously described PELP-1 interactions as a co-regulator of several transcription factors, including activator protein 1 (AP1), specificity protein 1 (SP1), nuclear factor κB (NF-κB) (310), STAT3 and FAK (338). Growth factor signals have also been shown to promote PELP1- interactions with STAT3, and PELP-1 mediated genomic and non-genomic functions play a role in STAT3 transactivation functions (356). In addition, FAK signalling may be affected by limiting FAK activation via Src kinase, as previously described (357).

Interestingly, changes in PELP-1 are also implicated in endocrine resistance. Tumours with predominantly cytoplasmic localization of PELP-1 has been shown to contribute to tamoxifen resistance in breast tumours (313, 325, 326), while PELP-1 and Src have been shown to form complexes in prostate cancer that demonstrates androgen independence. Clinically, as determined by recurrence-free survival, ER positive breast cancer patients with high cytoplasmic levels of PELP-1 responded poorly to tamoxifen treatment, as compared to those with low cytoplasmic PELP-1 levels (325).

In conclusion, PELP-1 is a crucial co-regulator, which interacts with multiple nuclear regulators and transcription factors, providing cancer cells with several survival advantages, including enhanced invasion. Here we demonstrate that its expression may also be a determinant for adverse response to endocrine therapies in ER positive breast tumours and have postulated its non-genomic interactions with Src, MAPK and AKT as an explanation for this. Since PELP-1 itself lacks enzymatic activity, there is a need to develop therapeutic agents that interfere with the interactions of PELP-1, thus developing novel targets for future therapies. In addition, PELP-1 itself may be useful as a prognostic marker in breast cancer patients and may help determine optimal endocrine therapy, aiding clinicians in decision making.

3.4 Exploring the role of proline, glutamate and leucine rich protein 1 (PELP-1) in triple negative breast cancer

3.4.1 Introduction

The previous section identified PELP-1 as a key regulator of invasion and migration in the context of ER+ breast cancer. While the importance of PELP-1 in ER+ disease may be anticipated, given that the proteins function as an ER co-receptor, it is also important to note that PELP-1 has several other roles, many outside of its relationship with the ER itself (308, 342). It was therefore of interest to assess whether these alternative functions of PELP-1 may also relate to its role in invasion and migration, by assessing PELP-1 in ER negative disease. This would help to clarify some of the functions and mechanistic behavior of PELP-1, as well as to assess its importance outside of ER+ disease.

Subsequently, it was decided to explore the role of PELP-1 in the context of cell models depicting "triple negative" breast cancer (TNBC). To achieve this, two appropriate TNBC cell lines, MDA-MB-231 and MDA-MB-468, were chosen for investigation. From the use of these cell lines this chapter aims to assess:

(i) The variability of basal PELP- expression amongst "triple negative" breast cancer cell lines
(ii) The effect of PELP-1 modulation on cell invasion and migration in the context of "triple negative" disease
(iii) The underlying mechanisms associated with phenotypic changes in cell invasion and migration

A secondary aim of this thesis at the outset was to assess observed cellular responses in the context of 3D cell culture, given previous work from the BCMPG that identified cell signaling and cell phenotype in response to treatments may be

altered when culturing cells in a 3D, as opposed to 2D environment (194). As such, assays to assess invasion in response to cell treatment were developed and optimized (Methods 2.4.2). Whilst this optimization period proved unable to develop an assay suitable for use with ER+ cell lines that may have been implemented in previous chapters, an assay that produced reliable results using triple negative breast cancer cell lines was developed. As such this assay will be utilized here to assess the invasive response of PELP-1 modulation in 3D cell culture, in the context of TNBC.

3.4.2 Basal PELP-1 expression is higher among MDA-MB-231 cells, when compared to MDA-MB-468 cells

Given that results contained within the previous chapter demonstrated that the basal expression of total PELP-1 was variable amongst a panel of ER+ breast cancer cell lines, it was of interest to assess if a similar picture is seen amongst TNBC cell lines.

As a result, the basal expression of PELP-1 amongst MDA-MB-231 and MDA-MB-468 cells, grown under standard cell culture conditions for 6 days, was assessed by Western blotting (Figure 3.50a). Results demonstrated a variable expression in PELP-1 between cell lines, with PELP-1 expression found to be significantly higher amongst MDA-231 cells. Interestingly, in direct comparison to MCF-7 cells, basal PELP-1 expression appeared higher amongst MDA-MB-231 cells. In contrast PELP-1 expression in MDA-MB-468 cells was significantly less, as compared to MCF-7 cells (Figure 3.50b).

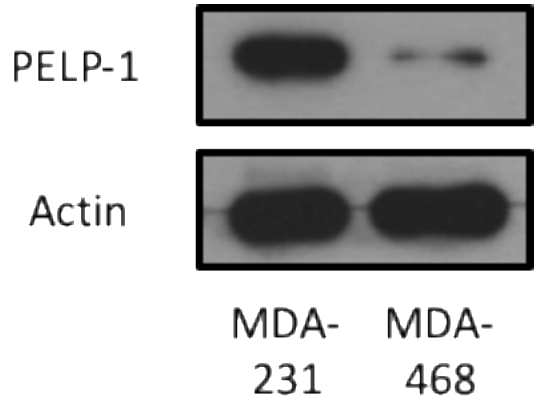

a.

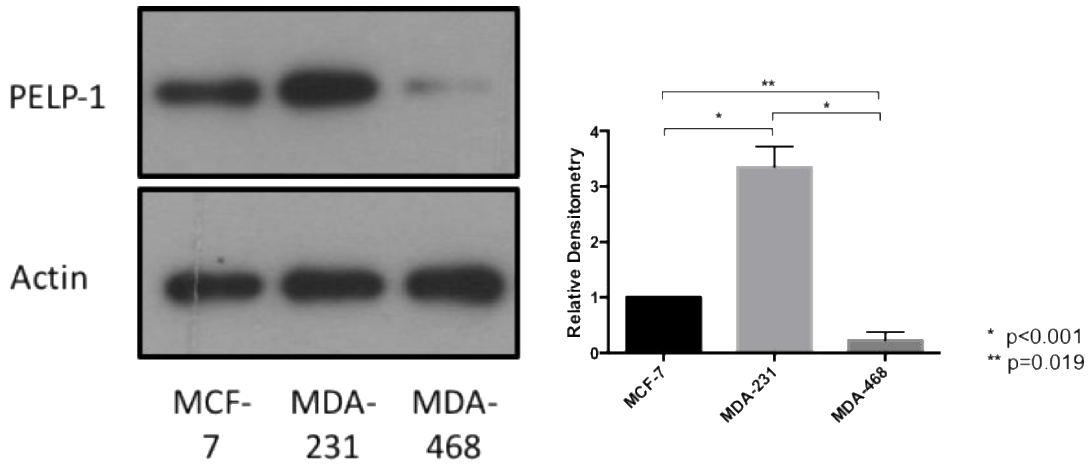

b.

Figure 3.50 – The variability in basal PELP-1 expression amongst the MDA-MB-231, MDA-MB-468 and MCF-7 breast cancer cell lines. Western Blot Analysis of total PELP-1 and Actin expression in MCF-7, MDA-MB-231 and MDA-MB-468 breast cancer cell lines grown under control conditions for 6 days. Differences in expression were assessed formally by densitometry. Total PELP-1 expression is significantly higher amongst MDA-MB-231, as compared to (a.) MDA-MB-468 cells and (b.) MCF-7 cells.

3.4.3 Optimization of siRNA transfection and subsequent knockdown of PELP-1 in TNBC cell lines

Prior to investigating the effect of PELP-1 suppression in TNBC, optimization of the siRNA transfection procedure using anti-PELP-1 siRNA, was required.

As used previously, a 72-hour lipid-based transfection system was utilized using Dharmafect smartpool® PELP-1 siRNA (Methods 2.26). Transfection was optimized using a range of concentrations of siRNA (100nm, 150nm, 200nm) to determine a dose that would achieve efficient knockdown of PELP-1 expression, assessed by Western blotting. Results demonstrated that PELP-1 knockdown was achieved in MDA—MB-231 cells at all doses (Figure 3.51), while in MDA-MB-468 cells (Figure 3.52), higher doses of 150nm or 200nm were required. Subsequently, all experimental transfection procedures with MDA-MB-231 and MDA-MB-468 cells were performed using the minimum required dose of PELP-1 siRNA (i.e. 100nm for MDA-MB-231 cells and 150nm for MDA-MB-468 cells) to make best use of resources and avoid potential siRNA toxicity with higher doses.

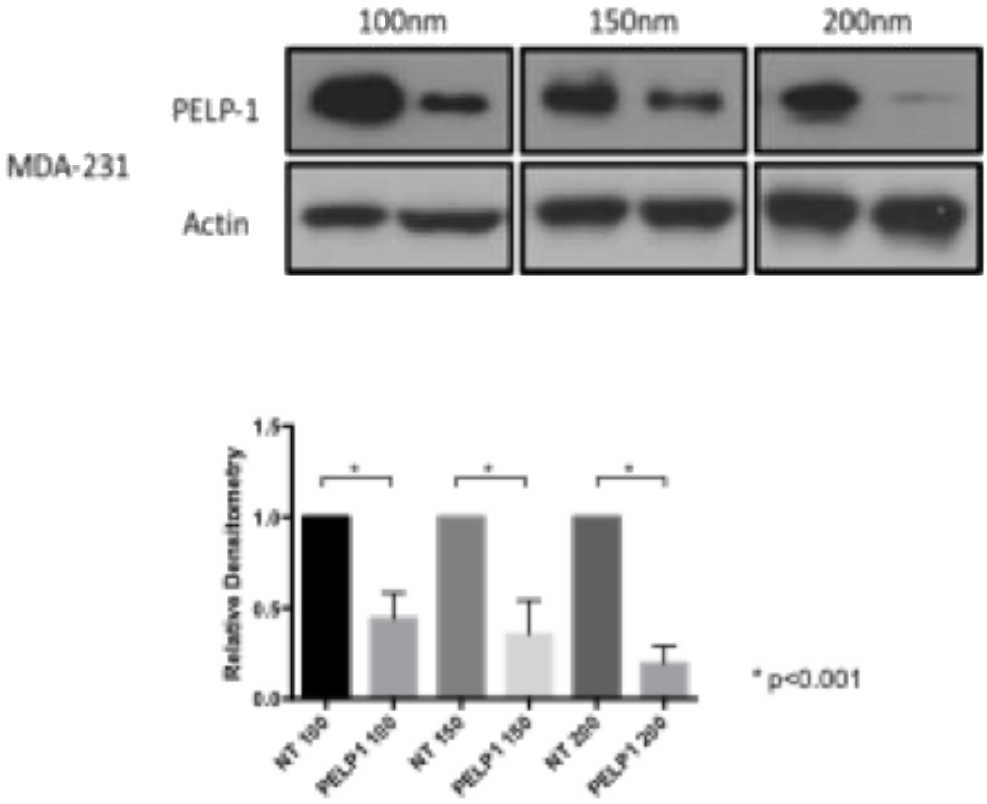

Figure 3.51 – Dose effect of PELP-1 siRNA on PELP-1 expression in MDA-MB-231 cells. Western blotting and densitometry data demonstrating the expression of PELP-1 and Actin in MDA-MB-231 cells, 72 hours after NT and PELP-1 siRNA transfection, using 100nm, 150nm and 200nm dose of siRNA respectively. PELP-1 expression is suppressed using 100nm, 150nm and 200nm dose of CDH1 siRNA in MDA-MB-231 cells. Differences in expression were assessed formally by densitometry.

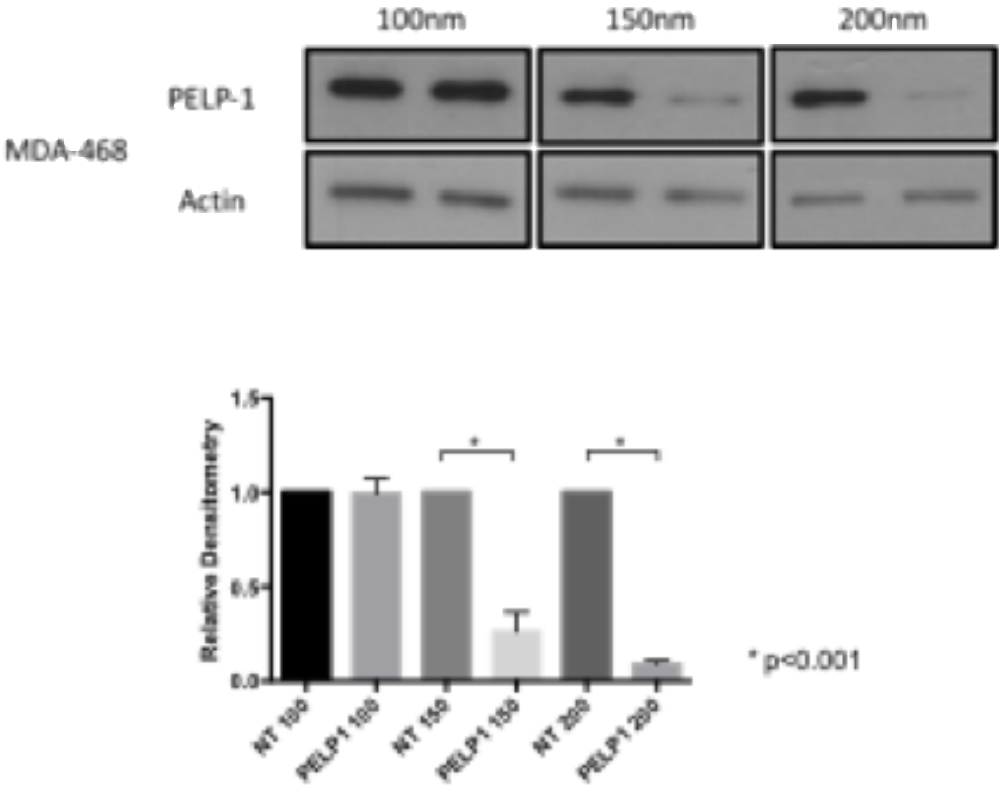

Figure 3.52 – Dose effect of PELP-1 siRNA on PELP-1 expression in MDA-MB-468 cells. Western blotting and densitometry data demonstrating the expression of PELP-1 and Actin in MDA-MB-468 cells, 72 hours after NT and PELP-1 siRNA transfection, using 100nm, 150nm and 200nm dose of siRNA respectively. PELP-1 expression is suppressed using 150nm and 200nm dose of CDH1 siRNA in MDA-MD-468 cells. Differences in expression were assessed formally by densitometry.

3.4.4 PELP-1 knockdown suppresses invasion in MDA-MB-231 cells, but not MDA-MB-468 breast cancer cells

To explore whether PELP-1 contributed to the invasive nature of MDA-MB-231 cells, these cells were treated with PELP-1 siRNA prior to performing the trans-well invasion chamber assay, as previously described.

When using this assay however, the initial seeding density of cells into the upper chamber of each wells insert was lowered in the case of MDA-MB-231 (from 50,000 cells/insert to 10,000 cells/insert) to account for the more aggressive phenotype and allow for a more accurate counting of invasive cells at the end of the assay. Meanwhile, the seeding density for MDA-MB-468 cells was left unchanged, given its relatively less aggressive phenotype.

Results from this assay showed that while the baseline invasion of MDA-MB-231 cells was much higher than that previously seen in the MCF-7 cell line, there was a significant suppression of invasion in PELP-1 deficient MDA-MB-231 cells as compared to controls (Figure 3.53a; $p=0.002$). In contrast, while MDA-MB-468 cells were relatively less invasive as compared to MDA-MB-231 cells, PELP-1 suppression had no effect on invasion in this cell line (Figure 3.53b).

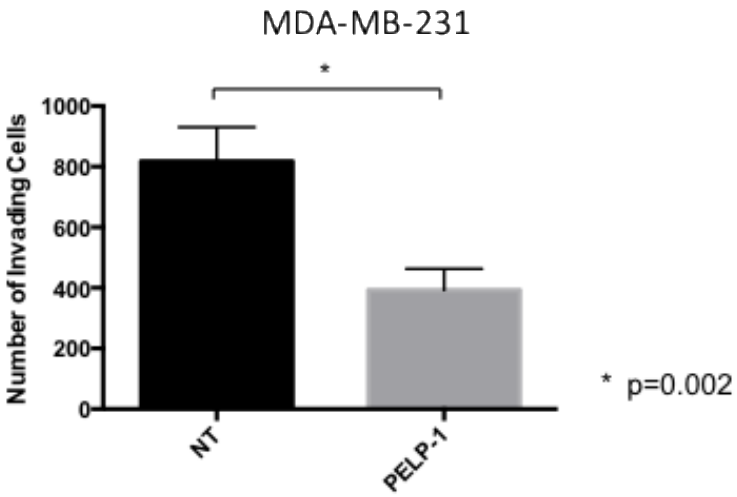

a.

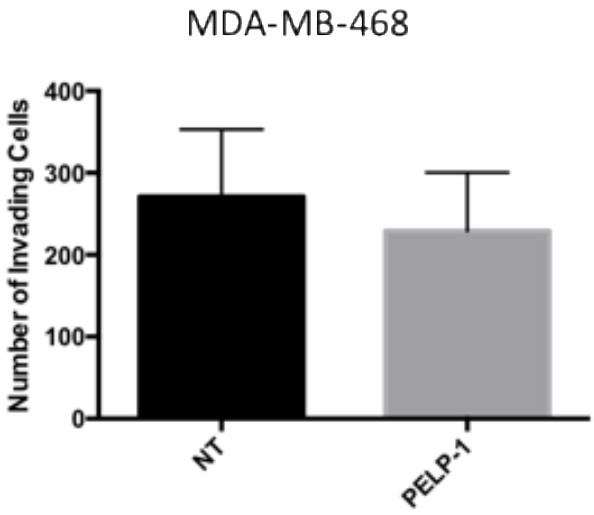

b.

Figure 3.53 – The effect of PELP-1 siRNA treatment on cell invasion in MDA-MB-231 and MDA-MB-468 cells. MDA-MB-231 and MDA-MB-468 cells were treated with non-targeting (NT) or PELP-1 targeting (PELP-1) siRNA for 72 hours, before assessing their invasive capacity. PELP-1 knockdown (a.) suppresses invasion in MDA-MB-231 but (b.) not MDA-MB-468 breast cancer cells. The graphs show the results for the mean of three separate experiments.

3.4.5 PELP-1 suppression reduces invasion in 3D cell culture in MDA-231 cells, but not MDA-468 cells

The role of PELP-1 in cell invasion in a 3D context was further investigated in both TNBC cell lines using the Matrigel®-based spheroid and "fried egg" assays. The extent of invasion was measured by visualization (bright field microscopy) of the periphery of the spheroids. At the end of the experiment, cells were harvested from the 3D cultures, lysed and probed for PELP-1 protein using Western blotting.

Results confirmed that PELP-1 knockdown suppressed invasion amongst MDA-MB-231 cells compared to the control by up to a 3-fold difference ($p<0.001$, Figures 3.54a and 3.54b). Unlike the MDA-231 cell line however, MDA-468 cells tended to form more friable spheroids, which could not be transferred from the ULA-plate to Matrigel® coated wells because of resultant spheroid fracture. As a result, the "Fried Egg" assay was deemed unsuitable for use in this cell line and instead the original 3D spheroid assay was employed. Invasion was subsequently determined through visualization by light microscopy, by assessing the relative change in area of each spheroid during the 6-day period of the experiment. Results demonstrated that, while invasion appeared less conspicuous compared to MDA-231 cells, invasion was demonstrated over the 6-day period using this assay (Figure 3.55a). No significant difference in invasion could be demonstrated however, when comparing wild-type MDA-468 cells and PELP-1 knockdown counterparts over this same time-period (Figure 3.55b).

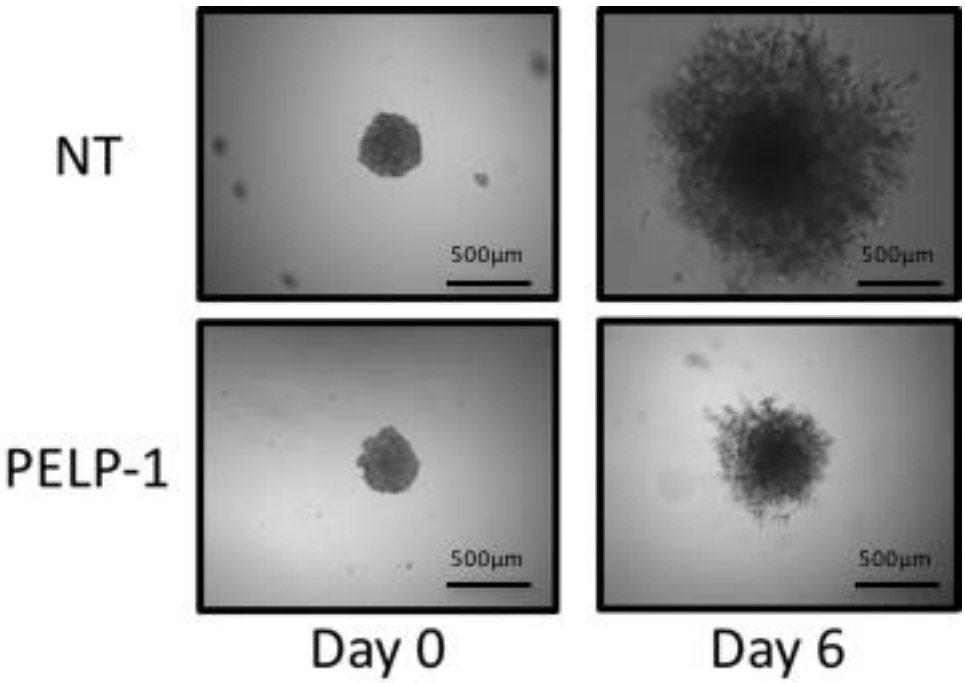

a.

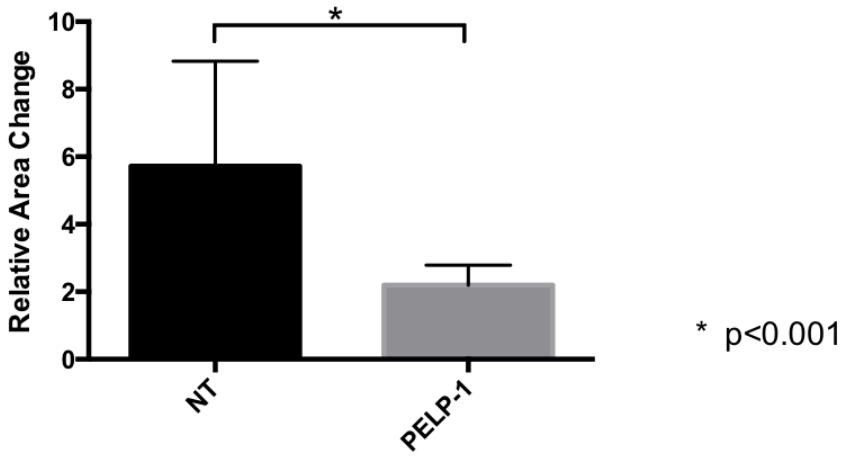

b.

Figure 3.54 – The effect of PELP-1 siRNA treatment on MDA-MB-231 cells in 3D cell culture. MDA-MB-231 cells were treated with non-targeting (NT) or PELP-1 targeting (PELP-1) siRNA for 72 hours, before assessing their invasive capacity within 3D cell culture. Invasion was assessed by a relative change in area of the spheroid. PELP-1 suppression reduces invasion in 3D cell culture of MDA-MB-231 cells. The graphs show the results for the mean of three separate experiments.

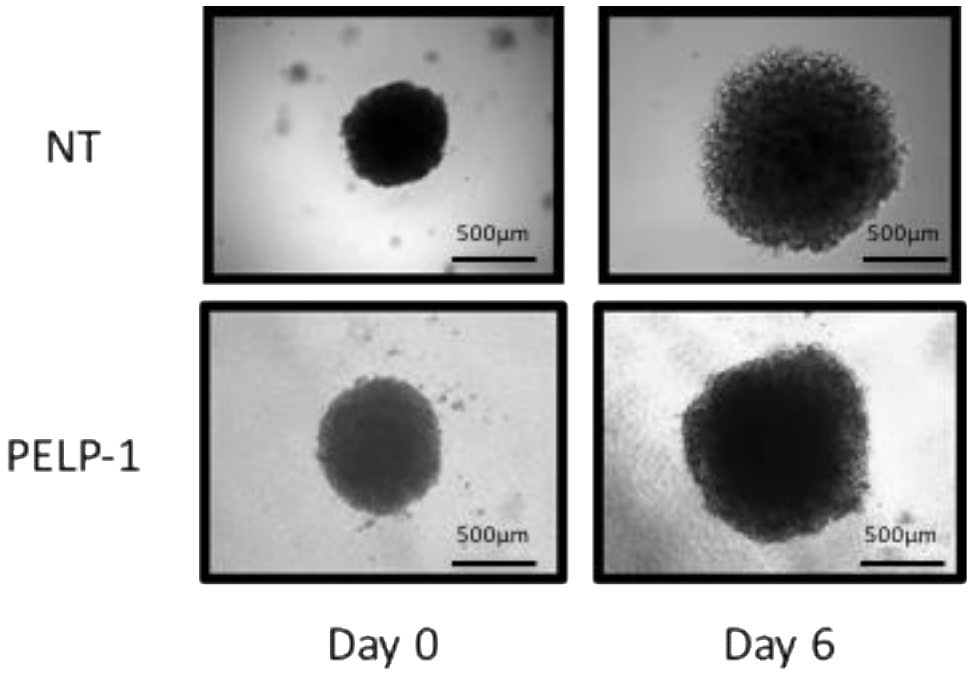

a.

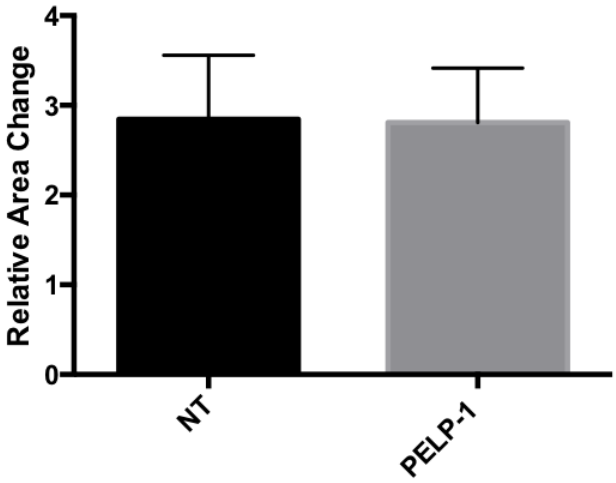

b.

Figure 3.55 - The effect of PELP-1 siRNA treatment on MDA-MB-468 cells in 3D cell culture. MDA-MB-468 cells were treated with non-targeting (NT) or PELP-1 targeting (PELP-1) siRNA for 72 hours, before assessing their invasive capacity within 3D cell culture. Invasion was assessed by a relative change in area of the spheroid. PELP-1 suppression has no effect on invasion in 3D cell culture on MDA-MB-468 cells. The graphs show the results for the mean of three separate experiments.

3.4.6 Exploring PELP-1 signaling in TNBC

The data in previous chapters suggested that PELP-1 may play an important role in cellular invasive responses induced by endocrine agents in ER+ breast cancer cells. This may occur through modulation of signaling pathways involving Src. To begin to explore mechanistically how PELP-1 might regulate cellular invasion in TNBC cell models an immunoblotting approach was taken.

Initially, changes in signaling previously elicited by PELP-1 knockdown in ER positive cell lines were re-examined. These included the key cellular proteins Src kinase, ERK and AKT, known to play a role in the non-genomic functions of PELP-1. Changes in total and phosphorylated expression of these proteins were therefore examined in MDA-MB-231 and MDA-MB-468 cells treated in with non-targeting (NT) or anti-PELP-1 (PELP-1) siRNA for 72 hours (Figures 3.56, 3.57 and 3.58). Results demonstrated reduced expression of pSrc in MDA-MB-231 cells with PELP-1 knockdown, while no significant difference in expression was observed in MDA-MB-468 cells. Meanwhile both total and phosphorylated ERK 1/2 and AKT expression was unaltered by PELP-1 suppression in both MDA-MB-231 and MDA-MB-468 cell lines.

In addition to the proteins of interest highlighted above, other targets concerned with the regulation of alternative functions of PELP-1 were investigated, including expression of FAK and STAT3, whose expression was found to be influenced by PELP-1 in ER+ cell lines. Again, changes in total and phosphorylated expression of these proteins were examined in MDA-MB-231 and MDA-MB-468 cells treated in with non-targeting (NT) or anti-PELP-1 (PELP-1) siRNA for 72 hours (Figures 3.59 and 3.60). Results demonstrated that expression of phosphorylated FAK and STAT3 were reduced by PELP-1 suppression in the MDA-MB-231 cells. Meanwhile in the MDA-MB-468 cell line there was no significant difference in total or phosphorylated FAK and STAT3 expression when comparing wild-type cells with their PELP-1 knockdown counterparts.

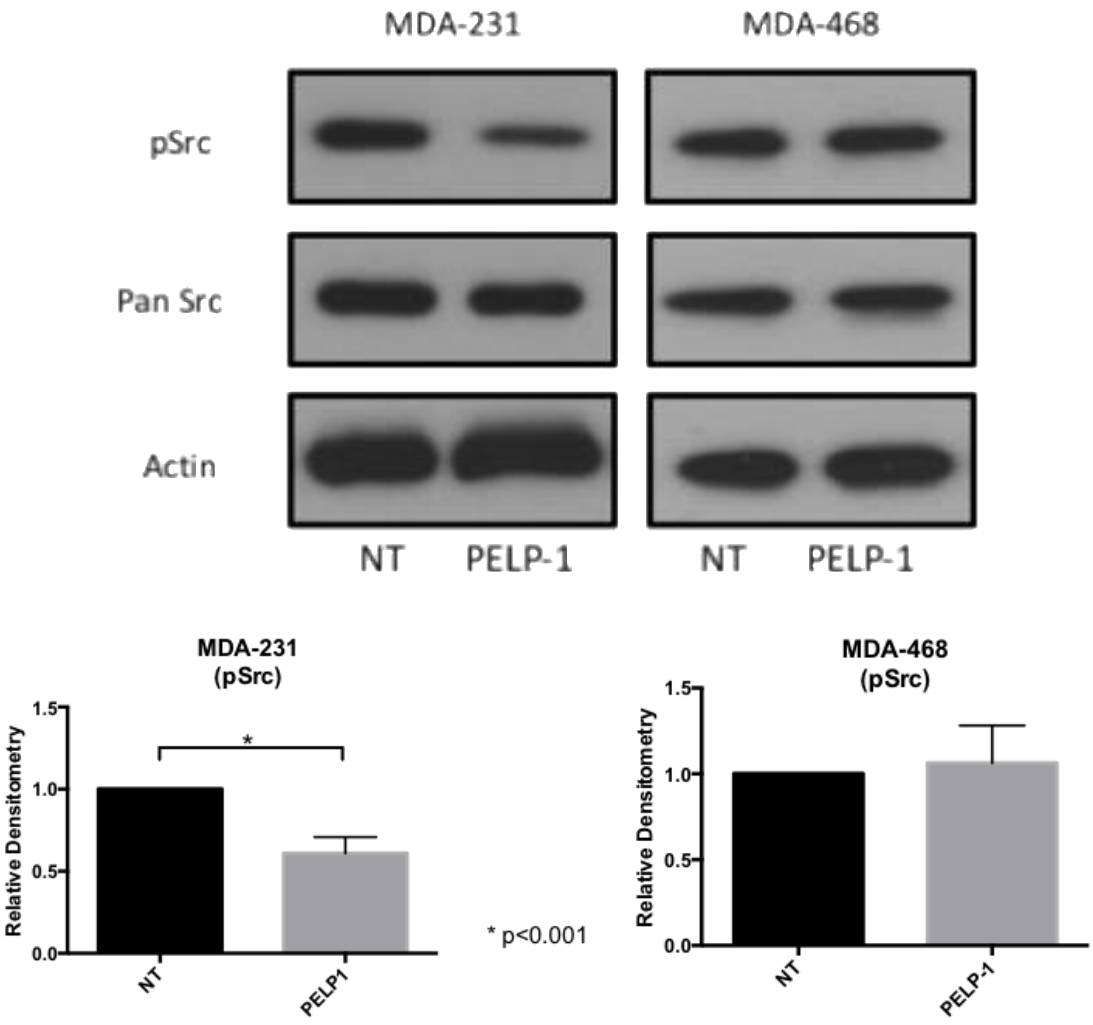

Figure 3.56 – Src expression in MDA-MB-231 and MDA-MB-468 cells treated with PELP-1 siRNA. Western Blot analysis of pSrc, total Src and Actin expression in MDA-MB-231 and MDA-MB-468 cells, with and without PELP-1 suppression. Differences in expression were assessed formally by densitometry. PELP-1 knockdown suppresses Src expression in MDA-MB-231, but not MDA-MB-468 cells.

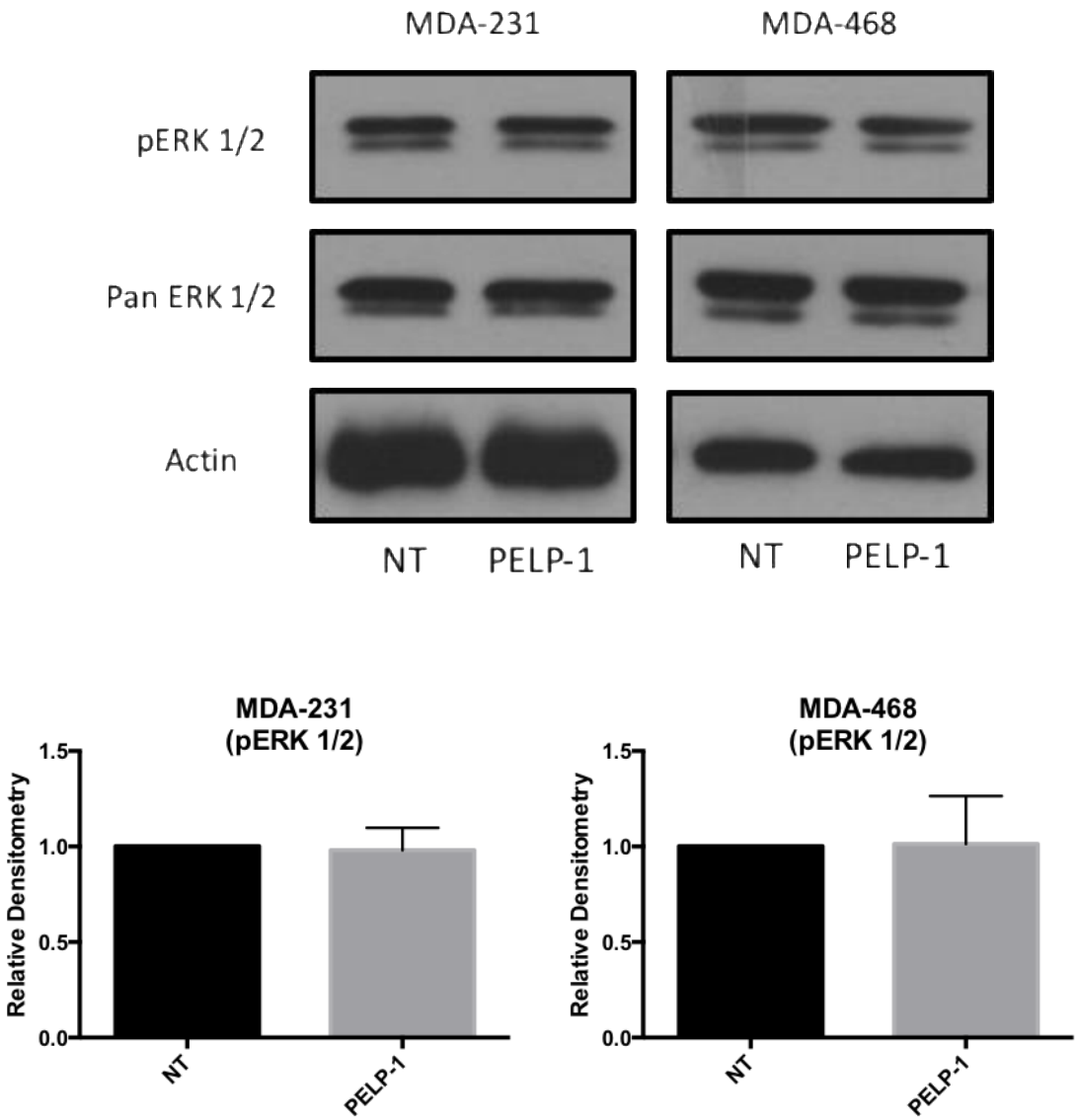

Figure 3.57 – ERK 1/2 expression in MDA-MB-231 and MDA-MB-468 cells treated with PELP-1 siRNA. Western Blot analysis of pERK 1/2, total ERK 1/2 and Actin expression in MDA-MB-231 and MDA-MB-468 cells, with and without PELP-1 suppression. Differences in expression were assessed formally by densitometry. PELP-1 knockdown has no effect on ERK 1/2 expression in MDA-MB-231 and MDA-MB-468 cells.

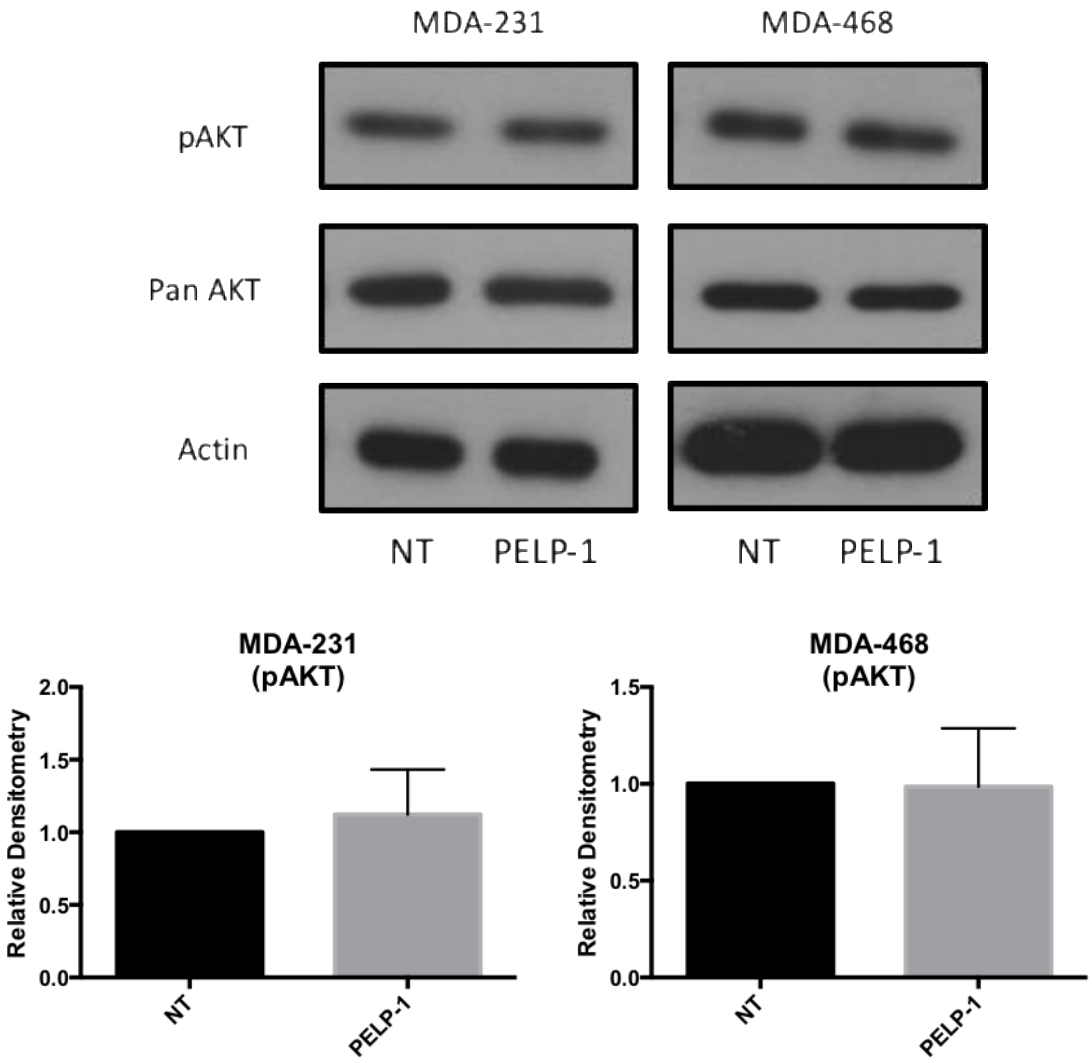

Figure 3.58 – AKT expression in MDA-MB-231 and MDA-MB-468 cells treated with PELP-1 siRNA. Western Blot analysis of pAKT, total AKT and Actin expression in MDA-MB-231 and MDA-MB-468 cells, with and without PELP-1 suppression. Differences in expression were assessed formally by densitometry. PELP-1 knockdown has no effect on AKT expression in MDA-MB-231 and MDA-MB-468 cells.

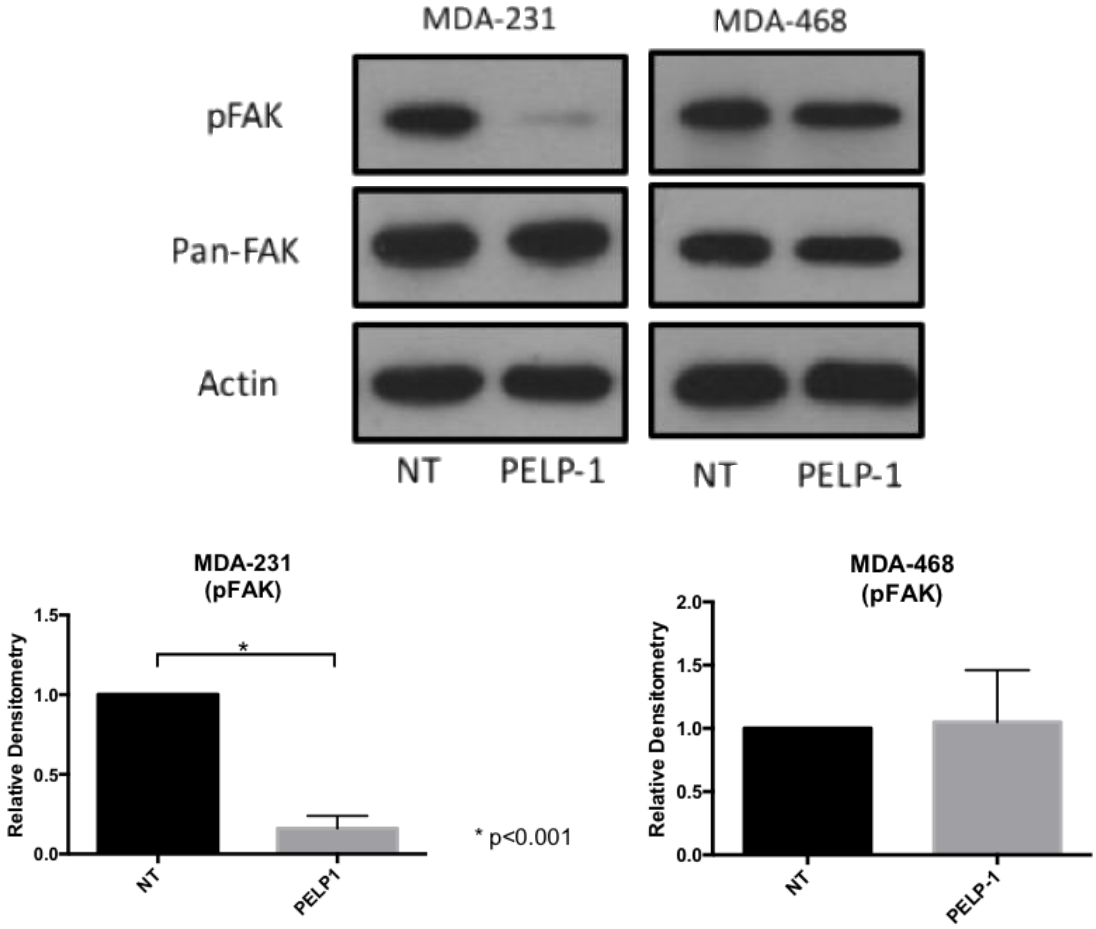

Figure 3.59 – FAK expression in MDA-MB-231 and MDA-MB-468 cells treated with PELP-1 siRNA. Western Blot analysis of pFAK, total FAK and Actin expression in MDA-MB-231 and MDA-MB-468 cells, with and without PELP-1 suppression. Differences in expression were assessed formally by densitometry. PELP-1 knockdown suppresses FAK expression in MDA-MB-231, but not MDA-MB-468 cells.

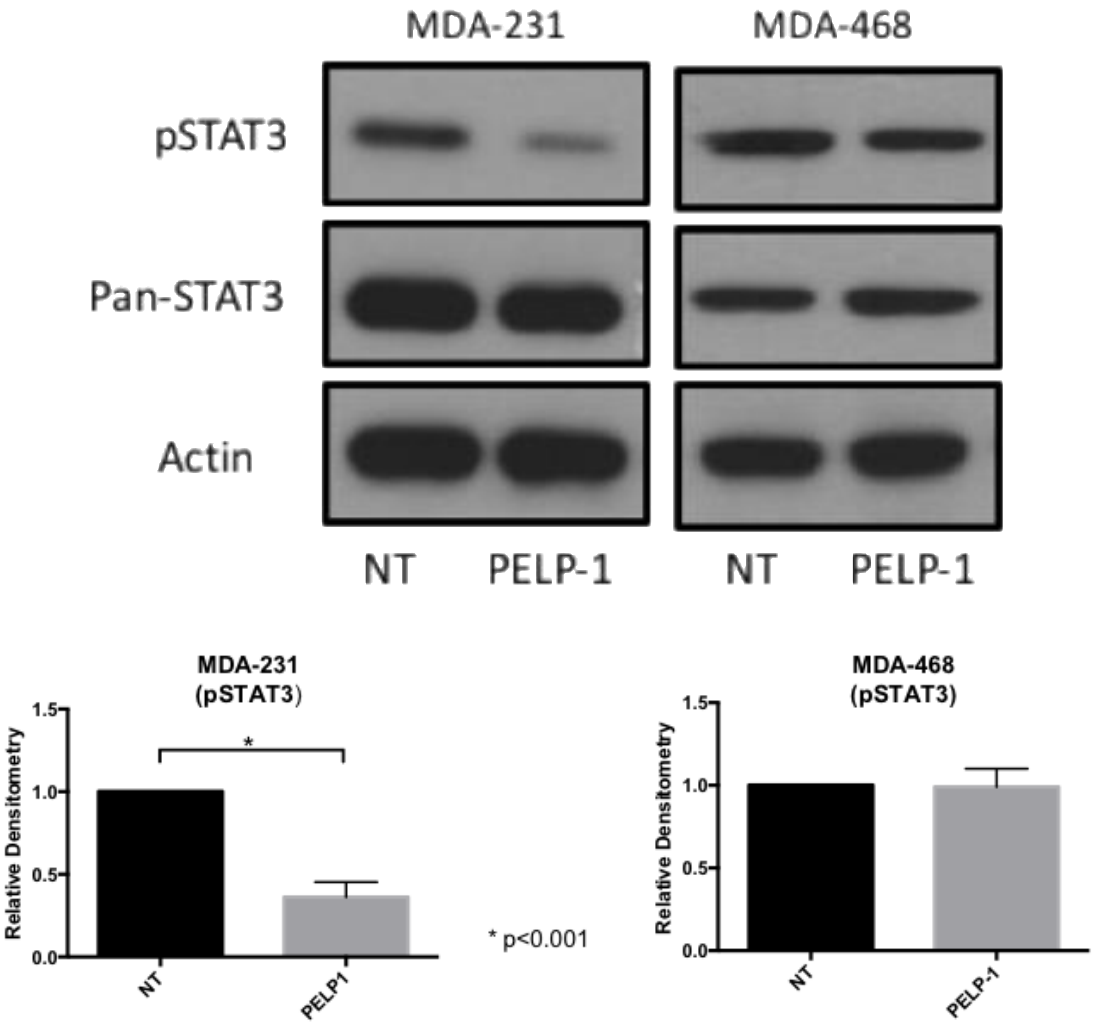

Figure 3.60 – STAT3 expression in MDA-MB-231 and MDA-MB-468 cells treated with PELP-1 siRNA. Western Blot analysis of pSTAT3, total STAT3 and Actin expression in MDA-MB-231 and MDA-MB-468 cells, with and without PELP-1 suppression. Differences in expression were assessed formally by densitometry. PELP-1 knockdown suppresses STAT3 expression in MDA-MB-231, but not MDA-MB-468 cells.

3.4.7 Discussion

Breast cancers that demonstrate lack of expression of ER, PR and HER2, so called triple-negative cancers (TNBC), represent approximately 15% of all cases (358). Based on the Stanford "intrinsic" system of breast cancer classification (359), the term TNBC is often used clinically as a surrogate for the basal-like subtype, as triple-negative tumors make up approximately 80% of this group (360). These triple negative cancers tend to be more aggressive than their hormone responsive counterparts, and are more likely to be poorly differentiated, of higher histological grade, and associated with a higher rate of recurrence and reduced overall survival (361-363). Population based data has also determined that a higher proportion of TNBC tends to affect younger pre-menopausal women, and is associated with increasing parity and shorter duration of breast feeding (364). Within these limits, TNBC can be thought of as a heterogeneous group of tumors, although several biological markers may help predict response to treatment and guide prognosis. These include loss of androgen receptor and E-cadherin, along with expression of basal cytokeratins, P-cadherin, p53 and EGFR (365).

In addition to the known functions of PELP-1 in relation to the ER, there are several of the proteins functions that act in an ER-independent fashion. Studies have shown that PELP1 functions as a co-regulator for a number of nuclear receptors, such as ERb, ERR, GR, and AR (366). Within the nuclear compartment, PELP1 interacts with histones and therefore plays a role in chromatin remodeling (367). PELP1 may also couple nuclear receptors to cytosolic signaling axes, such as Src-MAPK, PI3K-Akt, and EGFR/Her2, outside of its interaction with the ER (366). In addition, the expression of PELP-1 remains present in ER negative tumors (314, 339) and it may therefore be possible that expression has a significant effect on the cell phenotype in this breast cancer subtype.

PELP-1 expression was found to be variable across a panel of ER+ cell lines previously, and it might therefore be expected that its expression across ER negative cell lines would also be non-uniform. Basal expression of PELP-1 among MDA-MB-231 cells was significantly higher compared to MDA-MB-468. It was also

interesting to note that in comparison to the MCF-7 cell line, expression was significantly higher in MDA-MB-231, but lower in MDA-468. Given that PELP-1 expression has been associated clinically with a higher histological, tumour grade, higher incidence of nodal metastasis and poorer survival (368-370), this pattern perhaps depicts the relative aggressiveness, in terms of behavior, for each these cell lines. Variability of PELP-1 expression amongst different breast cancer cell lines have been reported by others (309), and although poorly understood this variability in expression may dictate the cellular events that control cell behavior.

Findings in this chapter demonstrated that PELP-1 suppression in MDA-MB-231 cells resulted in a significant reduction in invasion. This finding has been reported both in-vitro and in-vivo by others previously (342), whereby PELP-1 signaling was found to confer advantages to cell migration and invasion in ER-negative cell lines. Interestingly, this paper also demonstrates a growth advantage in MDA-MB-231 cells exhibiting PELP-1 expression, although this has not been demonstrated in the results of this chapter in either of the ER negative cell lines assessed here.

In correlation with results from the 2D Boyden chamber invasion assay, PELP-1 suppression was also found to inhibit invasion in MDA-MB-231, but not MDA-MB-468 cells, in 3D cell culture. Confirmation of these results within a 3D environment was important within the context of this work for several reasons as in addition to individual internal cell signalling events, external biophysical and biochemical cues play an important role in cell behaviour (371-374). As such cells can therefore behave differently when grown in a 3D as opposed to a 2D monolayer environment (375-377).

As compared to culture within a 2D monolayer, cells cultured within a 3D extracellular matrix (ECM) may bind to surrounding adhesive molecules, such as fibronectin or laminin. As such, cells are therefore supported by the surrounding ECM network on all surfaces, as opposed to its basal surface only (378). As a result, cells tend to form smaller focal adhesion complexes when grown in 3D cell culture (375) and therefore exhibit differences in adherence and migration (374-376). Cell migration across a 2D surface consists of 3 processes: (i) protrusion of the leading cell edge (ii) contraction of the cell body and (iii) detachment of the

trailing edge. In 3D culture however, the biophysics of tissues require cellular strategies to overcome matrix resistance, such as changing cell shape or ECM degradation, through protease secretion (376). Therefore, in addition to adhesion and tractile forces, matrix stiffness is also a key factor that influences cell movement in 3D (376, 379-381). Indeed, others have shown that in conditions where biochemical parameters, such as matrix ligand and receptor levels are held constant, cell movement tends to increase in conditions of increased matrix stiffness (379, 382). These findings would fit with the experience gained from the optimization of the invasion assay in this work, whereby there was a tendency for cell invasion to be more pronounced (amongst MDA-MB-231 cells particularly) with increasing matrix stiffness.

Matrix stiffness and cellular binding sites also play an important role in cell proliferation, as cells are required to anchor themselves within the ECM to create sufficient traction to divide (383, 384). Results from others imply that optimum matrix stiffness for proliferation is likely to be cell type dependent, as glioma cells appeared to grow faster in stiffer substrates (382) while fibroblasts preferred softer substrates (379, 385).

While research into the function of PELP-1 in the context of ER negative disease is relatively less well understood, it may therefore be assumed from these findings that it may still play an important, albeit not essential, role in the regulation of key cellular processes in cancer cell survival and metastases development. Indeed, studies have demonstrated no significant difference in PELP-1 expression between ER positive and ER negative tumors, but that its expression may implicate a more aggressive phenotype (314). To understand the mechanisms that may implicate PELP-1 in producing this phenotype, some of the key cellular pathways involved in metastasis development have been evaluated. PELP-1 suppression had a negative effect on cellular Src signaling, in similar fashion to ER+ cell lines, although in contrast MAPK and AKT signaling remained unaffected. Also, in a similar fashion to ER positive cell lines, PELP-1 suppression affected signaling involving STAT3 and FAK.

Interestingly, while these changes were observed in MDA-MB-231 cells, which exhibited high basal expression of PELP-1, MDA-MB-468 cells, which lower basal expression of the protein, were unaffected. These findings appear novel in the literature and are therefore currently poorly understood, but may implicate alternative mechanisms governing cellular functions in each cell line. As such, it may be possible that in cell lines lacking intrinsic PELP-1 expression, alternative cellular controls are in place that negate the need for PELP-1 mediated regulation. Clearly further work is required to demonstrate such events.

Studies have previously indicated that nuclear receptor interacting co-regulators, may play a role in cellular proliferation and metastases development in ER-negative breast tumors, through modulation of target gene transcription (386, 387). Although PELP-1 was initially described as an ER co-regulator (330), more recent studies have described PELP-1 as a more generic co-regulator for several nuclear receptors, such as the ER, PR, AR, and transcription factors, such as E2F, FHL2 and STAT3 (366). This larger scope of action for PELP-1 may therefore suggest that its deregulation may result in more widespread cellular response than perhaps initially anticipated.

Others have previously demonstrated that PELP-1 plays a crucial role in the expression of several genes involved in EMT and metastases development (342), such as MMP9 and MMP2, TWIST, SNAIL and Zeb. Outside of EMT itself, PELP-1 interacts with histones and histone-modifying enzymes, and therefore has action in chromatin remodeling at specific target genes (311). PELP-1 also modulates the function of metastasis-associated antigens 1 and 3 (MTA1 and MTA3), which are both implicated in invasion in human breast cancer (388). In addition, as previously mentioned in the last chapter, studies demonstrate that PELP-1 interacts with several proteins involved into cytoskeletal remodeling, including Src (313) and PI3K (344). Interestingly, while these latter signaling changes have previously been described in ER+ breast and ovarian tumors, we show that at least in relation to Src, similar findings may be found in ER negative disease.

Overall, findings within this chapter complies with the growing body of evidence that implicate PELP-1 as an important regulator of invasion in ER-negative, as well as ER+ breast cancer. Signaling behind this phenomenon is likely to be complex, utilizing the role of PELP-1 as nuclear receptor and transcription factor co-regulator, but appears to act, in part through changes in Src, STAT3 and FAK signaling. While similar findings would need to be replicated in both animal and human models, the potential of these results could identify PELP-1 as a key target for future therapies in both ER positive and ER negative breast cancer.

4.0 General Discussion

Endocrine therapy remains a key mode of treatment for ER+ breast cancer, in both the adjuvant and metastatic setting (82). Although several new endocrine agents have been developed over the last 30 to 40 years, such as the third-generation aromatase inhibitors (113), many of the original drugs developed for these purposes, including tamoxifen, remain in mainstay use. In the UK, tamoxifen remains the first-line endocrine agent of choice, in both the adjuvant and metastatic setting for pre-menopausal patients with ER+ disease, and is routinely given to patients for a minimum of 5 years after diagnosis in the adjuvant setting (82). More recently the use of tamoxifen has broadened with evidence suggesting better outcomes with prolonged use in the adjuvant setting for up to 10 years after diagnosis (389, 390), and potential use as a prophylactic drug in cancer prevention in high risk groups (391, 392) . Alongside these developments our understanding of breast cancer is currently going through a period of evolution, whereby rather than classifying the disease by histological criteria, new genomic techniques, such as next generation sequencing, real-time reverse transcriptase PCR (RT-PCR) and microarrays, have allowed tumours to be classified more accurately on a molecular basis (393).

This greater understanding of breast cancer, alongside the introduction of screening programs, and advances in surgical and oncological treatments have all contributed to improved breast cancer survival over the last 30 years (394). Despite this, disease progression and relapse remain as common findings in ER+ disease (2), either after the completion of adjuvant endocrine therapy (395) or whilst patients are still taking prescribed endocrine treatment. Indeed the risk of recurrence appears highest around 2-3 years after the time of curative surgery (396). Whilst relapse of ER+ disease is often related to the development of true hormone resistance (127), this need not always necessarily be the case. Indeed, the clinical response to endocrine therapy is known to be variable and can be dependent on the type of endocrine agent used (114). As a result, it may be possible that some methods of endocrine therapy are superior to others, based upon tumour biology, with some types of endocrine agent even exhibiting an adverse response (134).

Such observations were previously described by the BCMPG (133, 134), who demonstrated a pro-invasive response to tamoxifen in ER+ breast cancer cell lines, in the setting of a low E-cadherin environment. Indeed, this work has confirmed these findings, but has been able to go one stage further and demonstrate a pro-invasive response with tamoxifen that is independent of E-cadherin status, albeit the invasive response is augmented in an E-cadherin deficient environment. Similar findings have been demonstrated by others previously (135, 136), although the significance of such findings have remained unclear.

In addition to tamoxifen, this work has also demonstrated similar findings when using the pure ER antagonist, fulvestrant, while culture of cells in estrogen-deprived conditions, mimicking conditions of aromatase inhibitor use, did not demonstrate the same pro-invasive phenotype. These results would suggest that it is likely to be the antagonistic actions of tamoxifen on the ER resulting in any adverse cellular events, whilst also pointing towards the possibility of some ER+ breast cancers that may be better treated with aromatase inhibitors, as opposed to ER-targeting agents.

Despite these findings, the cellular mechanisms leading to this adverse cell response were unclear and therefore warranted further investigation. Pertinent to this investigation was to decipher whether: (i) the combined effect of E-cadherin loss and endocrine treatment activates specific pro-invasive pathways that are not activated in the context of either E-cadherin loss or endocrine treatment alone, or (ii) endocrine treatments activate signalling pathways that govern cell invasion but the consequence of this are not fully seen until the physical barrier to invasion (i.e. cadherin-mediated cell-cell adhesion) is removed. Findings from these investigations appeared to show strong evidence for the involvement of Src kinase in the underlying signalling responsible for this process, a finding replicated by the BCMPG previously (133, 134).

In addition to Src kinase itself, further evaluation of Src-mediated signalling pathways revealed several Src substrates, such as ERK 1/2, FAK and STAT3, were also over-expressed in response to tamoxifen therapy, implicating their involvement in the underlying process. Interestingly, these elements are known

to exhibit control over some critical cell invasion processes, including regulation of MMP synthesis (235), which aids ECM degradation, and stimulation of the semaphorin pathway (232), which guide cytoskeletal movements. Data shown here also demonstrates that both these pathways also contain members that demonstrate upregulated expression with tamoxifen treatment. While all the above elements are known to be important in cancer cell invasion or migration, their role as part of a combined response to tamoxifen treatment appear novel.

Interestingly, none of the pathways interrogated in this work demonstrated a significant association with E-cadherin expression, despite previous findings that Src itself may be relatively over-expressed in E-cadherin deficient MCF-7 cells treated with tamoxifen, when compared with either E-cadherin deficient cells or tamoxifen treated MCF-7 cells alone (133, 134). This was despite the interrogation of EMT markers and several intracellular kinases that have previously been shown to have an association with E-cadherin expression (121-123). Indeed, several of these elements appeared to, contrastingly, be associated with changes in expression based on tamoxifen therapy. This may indicate an overriding role of ER signalling and hence Src expression on these pathways. To prove this, it would be interesting to reassess the expression of proteins in some of these pathways following the introduction of a pharmacological Src inhibitor, and this should be the scope for further work. Given these findings however, it would appear E-cadherin itself does not play a significant role in the cellular mechanics governing endocrine-induced invasion but that its loss provides a physical means by which stimulated cells may invade more easily

It is important to stress at this point that while absent E-cadherin expression is a hallmark of lobular carcinoma (397), the E-cadherin deficient breast cancer model that has been created during this project should not be considered as a model for lobular breast cancer as such. This is because, in addition to absent E-cadherin expression, lobular carcinomas exhibit a variety of additional variations in gene expression when compared with ductal carcinomas, including differing expression in ER (398), AKT and Src (399), as well as changes in other markers related to angiogenesis and hormone dependence (400). Instead this model

should be considered to represent a subset of ductal carcinomas that exhibit aberrant E-cadherin expression, which have been found to account for up to 50% of ductal tumours in some studies (401).

While these findings would appear to indicate that ER-targeted endocrine therapies are a poor means of treating ER+ breast cancer, the clinical results achieved by tamoxifen and fulvestrant therapy would suggest otherwise (98-100). Indeed, rather than an adverse response from ER-targeted therapies being a generic feature across all ER+ breast cancers, it would appear more likely that this would affect a smaller subset of ER+ tumours. Indeed, a similar pro-invasive response to tamoxifen was not seen amongst an alternative ER+ cell line (T47D), while an absence of the previously seen pro-invasive signalling changes was also evident.

Given the above, an exploration into factors that may differentiate the cellular response to tamoxifen between different ER+ cell lines, was conducted. This focussed on identifying: (i) key molecular differences between MCF-7 and T47D cells, (ii) elements related to ER and Src kinase signalling and (iii) elements with a known existing role in cancer cell invasion/migration. Following a literature review the ER co-receptor, PELP-1, was identified as a potential target, given its known role in regulating Src-mediated invasion/migration (402), and the fact that it is relatively highly expressed in MCF-7 cells, as compared to the T47D cell line (309). Interestingly, data from this thesis corroborates these findings, while also noting that the knockdown of PELP-1 in MCF-7 cells appears to reverse the previously seen pro-invasive/pro-migratory effects of tamoxifen, both in the presence of E-cadherin deficiency. In line with these effects, PELP-1 suppression also appeared to reverse the pattern of Src-mediated signalling in these cells. While others have observed the relationship between PELP-1 expression and cellular invasion (316), this specific function of PELP-1 in relation to ER-targeted treatments would appear novel.

PELP-1 is a large multi-domain protein involved in modulating several signalling pathways (308). Importantly, PELP-1 contains several PXXP motifs, allowing its

interaction with the SH3 domain of Src, while having a separate binding site for interaction with the ER (Figure 4.1). This, essentially enhances the ability of ER and Src to interact via SH2 domain linkage (350). While this may enhance Src-mediated signalling in PELP-1 expressed ER+ cells under normal conditions, it was interesting to assess whether the presence of PELP-1 further modulates this interaction between Src and the ER, with respect to the binding of tamoxifen or other ER-targeted treatments. Such hypotheses could include increased ER-mediated Src activation via PELP-1 association, or indeed aberrant Src activation through PELP-1 alone when the ER is inactivated/downregulated by ligand binding. If so, such mechanisms could potentially explain the enhanced Src-mediated signalling in PELP-1 expressed cell lines with such treatment, and the resultant pro-invasive effects on the cell. While some evidence of co-localisation between the ER and PELP-1 has been observed in this thesis, to assess these hypotheses further, a more detailed investigation into this relationship would be required to identify and observe the interactions of these PELP-1, Src and the ER under different treatment conditions.

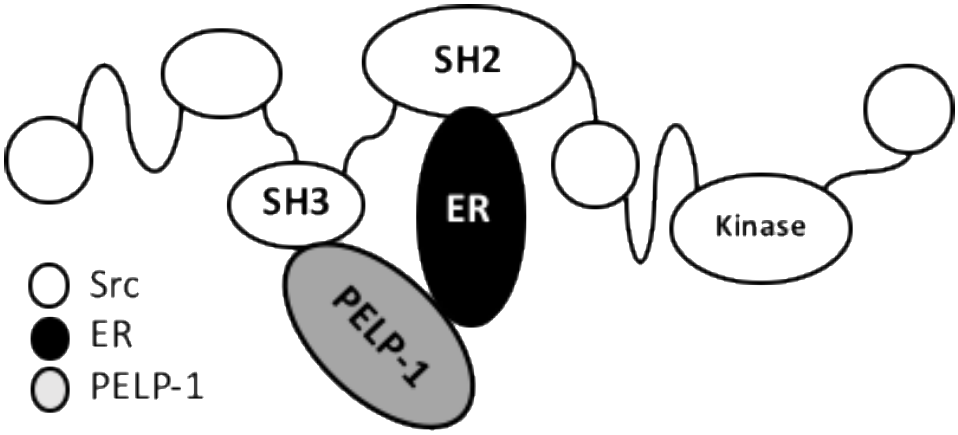

Figure 4.1 – Conformational relationship between the ER, PELP-1 and Src kinase. Adapted from (350). PELP-1 functions as an ER co-regulator by interacting with both the ER and the SH3 subunit of Src kinase.

It is recognised that the view of PELP-1 expression being the sole determinant of adverse cellular response to endocrine treatments is probably too simplistic, and that other signalling elements are also likely to be involved. As such, perhaps a more realistic hypothesis is that PELP-1 is just one part of a more widespread molecular profile that may help predict response to various endocrine therapies. Indeed, in a similar fashion to predictive gene testing tools, such as Oncotype DX© and MammaPrint©, which are used to assess the likely benefit of adjuvant chemotherapy based on tumour biology (403), it may be possible to devise such similar tools for adjuvant endocrine treatments.

In addition to its potential use as a prognostic marker, PELP-1 may act as a possible therapeutic target for future therapies. Indeed, findings within this thesis, alongside those of others (342), have identified PELP-1 to also be a regulator of invasion in TNBC, indicating a potential wider application for targeted therapies, outside of ER+ disease alone. Despite this, there are currently no pharmacological agents that directly target PELP-1 itself. One problem of therapeutic targeting of PELP-1 is potential toxicity because, although PELP-1 is prominent in breast cancer cells, it is still found in normal breast tissue (308). As such, more selective targeting of PELP-1 within tumour cells themselves would provide better specificity of treatment. In line with this, nano-liposomal formulations of anti-PELP-1 siRNA have been shown to reduce tumour growth and the development of tumour nodules in ovarian and breast xenograft models (345, 404). Given the lack of an agent directly targeting PELP-1 itself, an alternative approach may be to target specific PELP-1-coupled signalling pathways. Data in this thesis showed that Src was activated in response to endocrine treatment is a PELP-1 dependent manner. Thus, targeting the ER-PELP-1-Src axis might be fruitful, as has been demonstrated previously with dasatinib in PELP-1-mediated hormone resistant tumours (405). Similarly, the CDK2 inhibitor roscovitine, which downregulates expression of the ER and PELP-1, has the potential to abolish the growth of PELP-1 driven, hormone resistant cells (406). Rapamycin and AZD8055, both mTOR inhibitors, also suppressed proliferation in breast cancer cells in-vitro and within xenograft models, which overexpress PELP-1 (315). Meanwhile PR antagonists may also play a role in treating a subset of PELP-1 deregulated ER, PR positive

breast cancer (407). Finally, inhibition of KDM1 (345, 408) and arginine methyltransferases (409) may also be promising therapeutic agents for targeting PELP-1. Another approach in targeting PELP-1 is exhibited via peptidomimetics to inhibit prostate cancer proliferation by blocking the interactions of PELP-1 with the AR in vitro and in xenografts (410).

Outside of the findings and overall conclusions of this thesis, there is a recognition of some of the potential limitations in the current data, including areas where future work would enhance current knowledge. Initially, this thesis aimed to explore the invasive response of ER+ cancer cells to endocrine agents in the presence and absence of E-cadherin expression. E-cadherin loss was induced by siRNA transfection, resulting in a temporal loss of expression. While this method met the requirements for the purposes of the designed experiments, it would have been interesting to have explored the possibility of more stable knockdown of E-cadherin, either via shRNA or even CRISPR technology. A similar rationale could also have been implemented when later examining PELP-1 and combined PELP-1/ E-cadherin knockdown effects. In addition, a contrasting approach could have been taken by assessing if a pro-invasive phenotype could be induced by endocrine treatments in cells that are naturally deficient in PELP-1 (i.e. T47D), following upregulated PELP-1 expression through plasmid transfection. It is also accepted that this work has concentrated on luminal A and TNBC. As a result, exploration of adverse endocrine response and PELP-1 signalling in relation to HER2+ disease has played a limited role. As such, it would be interesting to assess the role of HER2 signalling, particularly in relation to its cross-talk with the ER, as data from this thesis seems to suggest that the pro-invasive response to ER-targeting treatment is not observed in ER+/HER2+ cell lines (i.e. BT474 and MDA-MB-361), despite these cell lines exhibiting a strong basal expression of PELP-1. Assessing cell invasion in the context of 3D cell culture has played a lesser role in this thesis than initially anticipated. This is because of the relative difficulty in adapting and optimizing a 3D cell culture invasion assay for use in ER+ cell lines. As such, while the effect of PELP-1 suppression on cell invasion in 2D cell culture was mirrored in the 3D cell culture for TNBC, similar findings cannot be assumed

for ER+ disease. The continued development of an appropriate 3D invasion assay to explore PELP-1 mediated invasion in ER+ disease would therefore be of merit.

Finally, this research has concentrated on working with immortalised cell lines to develop and manipulate breast cancer cell models for experimental purposes. While this approach is valid, there is a known limitation as to how well changes seen in these models correlate with disease clinically. As such, future work to test the hypotheses generated by this research in animal models and human tissue samples would undoubtedly help strengthen the validity of results demonstrated in this work.

In terms of the validity of this work from a clinical perspective, the BCMPG has retrospectively examined a series of clinical breast cancers from the Adjuvant Breast Cancer trial (411) and the Nottingham 2000 series (412) as part of a larger collaboration. This data suggests that patients with ductal cancers, lacking E-cadherin expression and treated with tamoxifen, demonstrate poor overall 5-year survival as compared to E-cadherin expressing tumours (133). While this data points to the possibility of a differential clinical response to tamoxifen based on E-cadherin expression, perhaps a more interesting analysis would be to assess the outcomes of patients with low E-cadherin tumours, comparing those treated with agents that target the ER (i.e. tamoxifen) with those that suppress circulating estrogen (i.e. ovarian suppression or aromatase inhibition). Of equal interest would be to assess the outcome of patients treated with tamoxifen therapy based on the intrinsic PELP-1 expression of the tumour to validate the hypothesis of PELP-1 being a key determinant of adverse endocrine response.

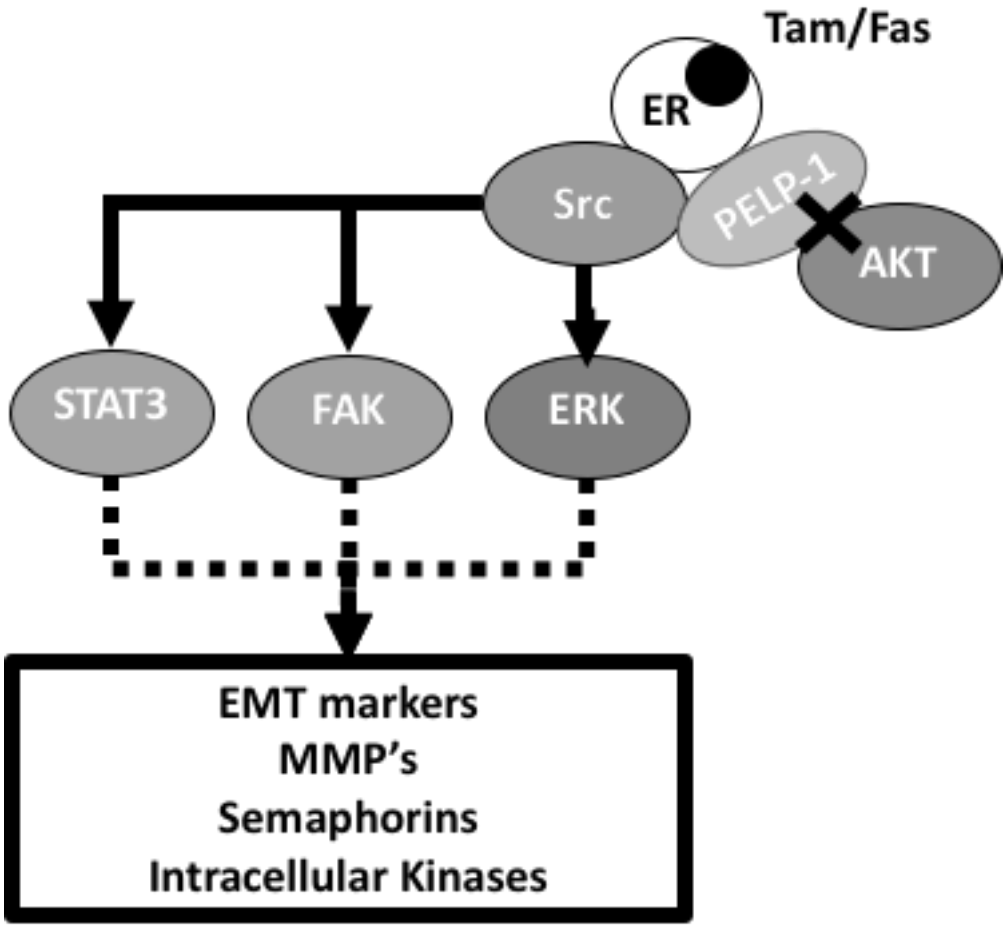

Figure 4.2 – Diagram demonstrating possible signalling cascade governing adverse cellular response to ER-targeting agents. PELP-1 regulates the relationship between ligand-bound ER with Src and AKT respectively, resulting in increased Src expression and decreased AKT expression. This results in downstream activation of elements, such as STAT3, FAK and AKT, which in turn regulate the expression of other key proteins and signalling cascades related to cell invasion and migration.

5.0 Conclusion(s) and future work

In conclusion, this pre-clinical data supports the hypothesis that patients with ER+ breast cancers that also exhibit a high basal expression of PELP-1, and who receive ER-targeted agents (tamoxifen and fulvestrant), may develop an adverse phenotype that could have an impact on disease recurrence and survival.

Given that current trends in breast cancer are moving towards more personalised therapy based on individual tumour biology, measures that help predict response to treatment is likely to be of benefit in either aiding treatment decisions or as part of outcome prognostication. PELP-1 and/or E-cadherin may thus represent important biological predictive markers for further evaluation in clinical tissue.

Following on from this thesis, future work could take place in several forms. Firstly, in terms of work that utilizes immortalised cell lines, it would be useful to explore a wider selection of ER+ cell lines to determine if other cell lines also exhibit the same adverse response to ER-targeting agents described in MCF-7 cells. In addition, ongoing development of 3D cell culture models is also warranted, particularly to assess invasion in ER+ cell lines, building upon some of the work that has been included here. Outside of in-vitro culture, it would also be useful to explore the findings of this thesis in-vivo, using xenograft models, by assessing the effects of endocrine therapy on tumour progression in the setting of E-cadherin and PELP-1 modulation. Demonstrating a response to endocrine therapies similar to that described here in such a model would ultimately add further weight to the findings of this thesis. Finally, to determine a clinical relevance to the role of PELP-1 and E-cadherin in relation to endocrine therapy, it would be ideal to assess any independent effect these markers may have on disease free survival amongst a cohort of patients with ER+ breast cancer, comparing those treated with ER-targeted (tamoxifen) or estrogen suppressive (ovarian suppression/AI) therapies, respectively.

6.0 References

1. Ferlay J, Soerjomataram I, Ervik M, Dikshit R, Eser S, Mathers C, et al. GLOBOCAN 2012 v1.1, Cancer Incidence and Mortality Worldwide: IARC CancerBase No. 11: WHO; 2012 [Available from: http://globocan.iarc.fr/].

2. World Cancer Research Fund International. Breast cancer statistics 2015 [Available from: http://www.wcrf.org/].

3. Cancer Research UK. Breast Cancer Statistics 2013 [Available from: http://www.cancerresearchuk.org/health-professional/cancer-statistics/statistics-by-cancer-type/breast-cancer].

4. McPherson K, Steel CM, Dixon JM. Breast cancer—epidemiology, risk factors, and genetics. BMJ. 2000;321(7261):624-8.

5. Gierisch JM, Coeytaux RR, Urrutia RP, Havrilesky LJ, Moorman PG, Lowery WJ, et al. Oral contraceptive use and risk of breast, cervical, colorectal, and endometrial cancers: a systematic review. Cancer Epidemiol Biomarkers Prev. 2013;22(11):1931-43.

6. Jones ME, Schoemaker MJ, Wright L, McFadden E, Griffin J, Thomas D, et al. Menopausal hormone therapy and breast cancer: what is the true size of the increased risk? British journal of cancer. 2016;115(5):607-15.

7. Paul A, S P. The breast cancer susceptibility genes (BRCA) in breast and ovarian cancers. Front Biosci. 2014;19:605-18.

8. Arpino G, Pensabene M, Condello C, Ruocco R, Cerillo I, Lauria R, et al. Tumor characteristics and prognosis in familial breast cancer. 16. 2016;924.

9. Moynahan ME, Chiu JW, Koller BH, M J. BRCA1 controls homology-directed DNA repair. Mol Cell. 1999;4(4):511-8.

10. King MC, Marks JH, JB M. Breast and ovarian cancer risks due to inherited mutations in BRCA1 and BRCA2. Science. 2003;302(5645):643-6.

11. Graf C, N W. Physical Activity in the Prevention and Therapy of Breast Cancer. Breast Care. 2010;5(6):389-94.

12. Howell A, Anderson AS, Clarke RB, Duffy SW, Evans DG, Garcia-Closas M, et al. Risk determination and prevention of breast cancer. Breast Cancer Res. 2014;14(446).

13. Bleyer A, Gilbert-Welch H. Effect of Three Decades of Screening Mammography on Breast-Cancer Incidence. N Engl J Med 2012;367:1998-2005.

14. Weigelt B, Horlings HM, Kreike B, Hayes MM, Hauptmann M, Wessels LF, et al. Refinement of breast cancer classification by molecular characterization of histological special types. J Pathol. 2008;216(2):141-50.

15. Vajpeyi R. WHO Classification of Tumours: Pathology and Genetics of Tumours of the Breast and Female Genital Organs. J Clin Pathol. 2005;58(6):671-2.

16. Dai X, Li T, Bai Z, Yang Y, Liu X, Zhan J, et al. Breast cancer intrinsic subtype classification, clinical use and future trends. . American Journal of Cancer Research. 2015;5(10):2929-43.

17. Cho N. Molecular subtypes and imaging phenotypes of breast cancer. Ultrasonography. 2016;35(4):281-8.

18. Sørlie T, Perou CM, Tibshirani R, Aas T, Geisler S, Johnsen H, et al. Gene expression patterns of breast carcinomas distinguish tumor subclasses with clinical implications. Proc Natl Acad Sci USA. 2001;98(19):10869-74.

19. Arteaga CL, Sliwkowski MX, Osborne CK, Perez EA, Puglisi F, Gianni L. Treatment of HER2-positive breast cancer: current status and future perspectives. Nat Rev Clin Oncol. 2011;9(1):16-32.

20. Perez EA, Romond EH, Suman VJ, Jeong JH, Davidson NE, Geyer CE, et al. Four-year follow-up of trastuzumab plus adjuvant chemotherapy for operable human epidermal growth factor receptor 2-positive breast cancer: joint analysis of data from NCCTG N9831 and NSABP B-31. J Clin Oncol. 2011;29(25):3366-73.

21. Prat A, Pineda E, Adamo B, Galván P, Fernández A, Gaba L, et al. Clinical implications of the intrinsic molecular subtypes of breast cancer. Breast. 2015;24(Suppl 2):S26-S35.

22. Coates AS, Winer EP, Goldhirsch A, Gelber RD, Gnant M, Piccart-Gebhart M, et al. Tailoring therapies: improving the management of early breast cancer: St Gallen International Expert Consensus on the Primary Therapy of Early Breast Cancer Ann Oncol. 2015;26(8):1533-46.

23. Baselga J, Perez EA, Pienkowski T, Bell R. Adjuvant trastuzumab: a milestone in the treatment of HER-2-positive early breast cancer. Oncologist. 2006;11(Suppl 1):4-12.

24. Untch M, Konecny GE, Paepke S, vonMinckwitz G. Current and future role of neoadjuvant therapy for breast cancer. Breast 2014;23(5):526-37.

25. Liedtke C, Mazouni C, Hess KR, André F, Tordai A, Mejia JA, et al. Response to neoadjuvant therapy and long-term survival in patients with triple-negative breast cancer. J Clin Oncol. 2008;26(8):1275-81.

26. Schneeweiss A, Chia S, Hickish T, Harvey V, Eniu A, Hegg R, et al. Pertuzumab plus trastuzumab in combination with standard neoadjuvant anthracycline-containing and anthracycline-free chemotherapy regimens in patients with HER2-positive early breast cancer: a randomized phase II cardiac safety study (TRYPHAENA). Ann Oncol. 2013;24(9):2278-84.

27. Ng CK, Schultheis AM, Bidard FC, Weigelt B, Reis-Filho JS. Breast cancer genomics from microarrays to massively parallel sequencing: paradigms and new insights. J Natl Cancer Inst. 2015;107(5).

28. Zografos GC, Michalopoulos NV, Zagouri F. Hormone Therapies. Anticancer Therapeutics: John Wiley & Sons, Ltd; 2008. p. 159-86.

29. Lipovka Y, Konhilas JP. The complex nature of oestrogen signalling in breast cancer: enemy or ally? Bioscience reports. 2016;36(3):e00352.

30. Simpson E. Sources of estrogen and their importance. J Steroid Biochem Mol Biol. 2003;86(3-5):225-30.

31. Thomas MP, Potter BV. The structural biology of oestrogen metabolism. J Steroid Biochem Mol Biol. 2013;137:27-49.

32. Bulun SE, Lin Z I, mir G, Amin S, Demura M, Yilmaz B, et al. Regulation of Aromatase Expression in Estrogen-Responsive Breast and Uterine Disease: From Bench to Treatment. Pharmacological Reviews 2005;57(3):359-83.

33. Yager JD, Davidson NE. Estrogen carcinogenesis in breast cancer. N Engl J Med. 2006;354(3):270-82.

34. Key T, Appleby F, Barnes I, Reeves G. Endogenous sex hormones and breast cancer in postmenopausal women: reanalysis of nine prospective studies. Journal of the National Cancer Institute. 2002;94(8):606-16.

35. Yager JD, Davidson NE. Estrogen carcinogenesis in breast cancer. N Engl J Med 2017. 2006;354(3):270-82.

36. Collaborative Group on Hormonal Factors in Breast Cancer. Breast cancer and hormone replacement therapy: collaborative reanalysis of data from 51 epidemiological studies of 52 705 women with breast cancer and 108 411 women without breast cancer. Lancet. 1997;350(9084):1047-59.

37. Davies C, Godwin J, Gray R, Clarke M, Cutter D, Darby S, et al. Relevance of breast cancer hormone receptors and other factors to the efficacy of adjuvant tamoxifen: patient-level meta-analysis of randomised trials. The Lancet. 2011;378(9793):771-84.

38. Eisen A, Trudeau M, Shelley W, Messersmith H, Pritchard KI. Aromatase inhibitors in adjuvant therapy for hormone receptor positive breast cancer: a systematic review. Cancer Treat Rev. 2008;34(2):157-74.

39. Ramaul R, Rakha E, Robertson J, Ellis I. Breast Surgery. Dixon JM, editor. Edinburgh: Elsevier; 2014.

40. Onitilo AA, Engel JM, Greenlee RT, Mukesh BN. Breast Cancer Subtypes Based on ER/PR and Her2 Expression: Comparison of Clinicopathologic Features and Survival. Clinical Medicine & Research. 2009;7((1-2)):4-13.

41. Ascenzi P, Bocedi A, Marino M. Structure–function relationship of estrogen receptor a and b: Impact on human health. Molecular Aspects of Medicine. 2006;27(4):299–402.

42. Girdler F, Brotherick I. The oestrogen receptors (ERα and ERβ) and their role in breast cancer: a review. The Breast. 2000;9(4):194-200.

43. Mosselman S, Polman J, Dijkema R. ERβ: identification and characterization of a novel human estrogen receptor. FEBS Lett. 1996;392(1):49-53.

44. Pennie WD, Aldridge TC, Brooks AN. Differential activation by xenoestrogens of ER alpha and ER beta when linked to different response elements. J Endocrinol. 1998;158(3):R11-R4.

45. Pace P, Taylor J, Suntharalingam S. Human estrogen receptor β binds DNA in a manner similar to and dimerizes with estrogen receptor α. J Biol Chem. 1997;272(41):25832-8.

46. Imamov O, Shim GJ, Warner M, Gustafsson JA. Estrogen receptor beta in health and disease. Biol Reprod. 2005;73(5):866-71.

47. Holst F, Stahl PR, Ruiz C, Hellwinkel O, Jehan Z, Wendland M, et al. Estrogen receptor alpha (ESR1) gene amplification is frequent in breast cancer. Nat Genet. 2007;39(5):655-60.

48. Ali S, Coombes RC. Estrogen receptor alpha in human breast cancer: occurrence and significance. J Mammary Gland Biol Neoplasia. 2000;5(3):271-81.

49. McInerney EM, Weis KE, Sun J, Mosselman S, Katzenellenbogen BS. Transcription activation by the human estrogen receptor subtype b (ER b) studied with ERa and ERb receptor chimeras. Endocrinology 1998. 139(11):4513–22.

50. Klinge C. Estrogen receptor interaction with estrogen response elements. Nucleic Acids Res. 2001;29(14):2905–19.

51. Edwards D. The role of coactivators and corepressors in the biology and mechanism of action of steroid hormone receptors. J Mammary Gland Biol Neoplasia. 2000;5(3):307-24.

52. Laperrière D, Rozendaal M, Mader S. Retinoic acid receptor, alpha: RARA; 2010 [Available from: http://www.cisreg.ca/cgi-bin/tfe/articles.pl?tfid=337].

53. Hall JM, Couse JF, Korach KS. The multifaceted mechanisms of estradiol and estrogen receptor signaling. J Biol Chem. 2001;276(40):36869-72.

54. Begam AJ, Jubie S, Nanjan MJ. Estrogen receptor agonists/antagonists in breast cancer therapy: A critical review. Bioorg Chem 2017;71:257-74.

55. Bjornstrom L, Sjoberg M. Mechanisms of Estrogen Receptor Signaling: Convergence of Genomic and Nongenomic Actions on Target Genes. Molecular Endocrinology 2005;19(4):833-42.

56. Christopoulos PF, Msaouel P, Koutsilieris M. The role of the insulin-like growth factor-1 system in breast cancer. Molecular Cancer. 2015;14:43.

57. Sabbah M, Courilleau D, Mester J, Redeuilh G. Estrogen induction of the cyclin D1 promoter: involvement of a cAMP response-like element. Proc Natl Acad Sci USA. 1999;96(20):11217-22.

58. Marino M, Galluzzo P, Ascenzi P. Estrogen Signaling Multiple Pathways to Impact Gene Transcription. Current Genomics. 2006;7(8):497-508.

59. Knüpfer H, Preiss R. Significance of interleukin-6 (IL-6) in breast cancer (review). Breast Cancer Res Treat. 2007;102(2):129-35.

60. Kahlert S, Nuedling S, van Eickels M, Vetter H, Meyer R, Grohe C. Estrogen receptor rapidly activates the IGF-1 receptor pathway. J Biol Chem. 2000;275(24):18447-53.

61. Farach-Carson M, Davis P. Steroid hormone interactions with target cells: cross talk between membrane and nuclear pathways. J Pharmacol Exper Therap 2003;30(3):839-45.

62. Barzi A, Lenz AM, Melissa J. Molecular Pathways: Estrogen Pathway in Colorectal Cancer. Clinical Cancer Research. 2013;19(21):5842–8.

63. Tai W, Mahato R, K C. The role of HER2 in cancer therapy and targeted drug delivery. J Control Release. 2010;146(3):264-75.

64. King CR, Kraus MH, Aaronson SA. Amplification of a novel v-erbB-related gene in a human mammary carcinoma. Science. 1985;229(4717):974-6.

65. Pietras RJ, Arboleda J, Reese DM, Wongvipat N, Pegram MD, Ramos L, et al. HER-2 tyrosine kinase pathway targets estrogen receptor and promotes hormone-independent growth in human breast cancer cells. Oncogene. 1995;10(12):2345-46.

66. Bazley LA, Gullick WJ. The epidermal growth factor receptor family. Endocr Relat Cancer. 2005;12(Suppl 1):17-27.

67. Rubin I, Yarden Y. The basic biology of HER2. Ann Oncol. 2001;12(Suppl 1):3-8.

68. Shou J, Massarweh S, Osborne CK, Wakeling AE, Ali S, Weiss H, et al. Mechanisms of tamoxifen resistance: increased estrogen receptor-HER2/neu cross-talk in ER/HER2-positive breast cancer. J Natl Cancer Inst. 2004;96(12):926-35.

69. Lin SY, Makino K, Xia W, Matin A, Wen Y, Kwong KY, et al. Nuclear localization of EGF receptor and its potential new role as a transcription factor. Nat Cell Biol. 2001;3(9):802-8.

70. Gutierrez C, Schiff R. HER 2: Biology, Detection, and Clinical Implications. Archives of pathology & laboratory medicine. 2011;135(1):55-62.

71. Atlas of Genetics and Cytogenetics in Oncology and Haematology. ERBB2 [http://atlasgeneticsoncology.org/Genes/ERBB2ID162ch17q11.html]: Atlas of Genetics and Cytogenetics in Oncology and Haematology; 2018.

72. Nahta R, Yu D, Hung MC, Hortobagyi GN, Esteva FJ. Mechanisms of disease: understanding resistance to HER2-targeted therapy in human breast cancer. Nat Clin Pract Oncol. 2006;3(5):269-80.

73. Barok M, Joensuu H, J I. Trastuzumab emtansine: mechanisms of action and drug resistance. Breast Cancer Res. 2014;16(2):209.

74. Martin M, S L-T. Emerging Therapeutic Options for HER2-Positive Breast Cancer. Am Soc Clin Oncol Educ Book. 2016;35:e64-70.

75. Jordan V. Tamoxifen: a most unlikely pioneering medicine. Nat Rev Drug Discov. 2003;2(3):205-13.

76. Harper MJK, Walpole AL. A new derivative of triphenylethylene: effect on implantation and mode of action in rats. Journal of reproduction and fertility. 1967;13(1):101-19.

77. Klopper A, Hall M. New synthetic agent for the induction of ovulation: preliminary trials in women. Br Med J. 1971;1(5741):152-4.

78. Lunan CB, Klopper A. Antioestrogens: a review. Clin Endocrinol (Oxf). 1975;4(5):551-72.

79. Tzukerman MT, Esty A, Santiso-Mere D, Danielian P, Parker MG, Stein RB, et al. Human estrogen receptor transactivational capacity is determined by both cellular and promoter context and mediated by two functionally distinct intramolecular regions. Mol Endocrinol. 1994;8(1):21-30.

80. Watanabe T, Inoue S, Ogawa S, Ishii Y, Hiroi H, Ikeda K, et al. Agonistic effect of tamoxifen is dependent on cell type, ERE-promoter context, and estrogen receptor subtype: functional difference between estrogen receptors alpha and beta. Biochem Biophys Res Commun. 1997;236(1):140-5.

81. Gobbi S, Rampa A, Belluti F, Bisi A. Nonsteroidal Aromatase Inhibitors for the Treatment of Breast Cancer: An Update. Anti-Cancer Agents in Medicinal Chemistry. 2014;14(1):54-65.

82. NICE. Early and locally advanced breast cancer: diagnosis and treatment. 2017.

83. Leake R. Side Effects of Adjuvant Tamoxifen BMJ : British Medical Journal. 1991;303(6809):1061.

84. Early Breast Cancer Trialists' Collaborative Group. Tamoxifen for early breast cancer: an overview of the randomised trials. Lancet. 1998;351(9114):1451-67.

85. Fisher B, Costantino J, Redmond C, Poisson R, Bowman D, Couture J, et al. A randomized clinical trial evaluating tamoxifen in the treatment of patients with node-negative breast cancer who have estrogen-receptor-positive tumors. The New England journal of medicine. 1989;320(8):479-84.

86. Fisher B, Dignam J, Bryant J, DeCillis A, Wickerham DL, Wolmark N, et al. Five versus more than five years of tamoxifen therapy for breast cancer patients with negative lymph nodes and estrogen receptor-positive tumors. Journal of the National Cancer Institute. 1996;88(21):1529-42.

87. Davies C, Pan H, Godwin J, Gray R, Arriagada R, Raina V, et al. Long-term effects of continuing adjuvant tamoxifen to 10 years versus stopping at 5 years after diagnosis of oestrogen receptor-positive breast cancer: ATLAS, a randomised trial. Lancet. 2013;381(9869):805-16.

88. Clemons M, Danson S, Howell A. Tamoxifen ('Nolvadex'): a review: Antitumour treatment. Cancer Treat Rev. 2002;28(4):165-80.

89. Litherland S, Jackson IM. Antioestrogens in the management of hormone-dependent cancer. Cancer Treat Rev. 1988;15(3):183-94.

90. Robertson J. Faslodex (ICI 182, 780), a novel estrogen receptor downregulator—future possibilities in breast cancer. The Journal of steroid biochemistry and molecular biology. 2001;79(1):209-12.

91. Pink JJ, Jordan VC. Models of estrogen receptor regulation by estrogens and antiestrogens in breast cancer cell lines. Cancer research. 1996;56(10):2321-30.

92. Dauvois S, White R, Parker MG. The antiestrogen ICI 182780 disrupts estrogen receptor nucleocytoplasmic shuttling. Journal of cell science. 1993;106(4):1377-88.

93. Howell A, Osborne CK, Morris C, Wakeling AE. ICI 182,780 (Faslodex™). Cancer. 2000;89(4):817-25.

94. Osborne CK, Wakeling A, Nicholson RI. Fulvestrant: an oestrogen receptor antagonist with a novel mechanism of action. Br J Cancer. 2004;90(Suppl 1):S2-S6.

95. DeFriend DJ, Anderson E, Bell J, Wilks DP, West CM, Mansel RE, et al. Effects of 4-hydroxytamoxifen and a novel pure antioestrogen (ICI 182780) on the clonogenic growth of human breast cancer cells in vitro. Br J Cancer. 1994;70(2):204-11.

96. Osborne CK, Coronado-Heinsohn EB, Hilsenbeck SG, McCue BL, Wakeling AE, McCleland RA, et al. Comparison of the Effects of a Pure Steroidal antiestrogen With Those of Tamoxifen in a Model of Human Breast Cancer. JNCI: Journal of the National Cancer Institute. 1995;87(10):746-50.

97. NICE. Fulvestrant for the treatment of locally advanced or metastatic breast cancer. Breast cancer: NICE; 2011.

98. Mittal R, Chaudhry N, Pathania S, Mukherjee TK. Mechanistic Insight of Drug Resistance with Special Focus on Iron in Estrogen Receptor Positive Breast Cancer. Curr Pharm Biotechnol. 2014;15(12):1141-57.

99. Howell A, DeFriend D, Robertson J, Blamey R, Walton P. Response to a specific antioestrogen (ICI 182780) in tamoxifen-resistant breast cancer. The Lancet. 1995;345(8941):29-30.

100. Howell A, DeFriend DJ, Robertson JF, Blamey RW, Anderson L, Anderson E, et al. Pharmacokinetics, pharmacological and anti-tumour effects of the specific anti-oestrogen ICI 182780 in women with advanced breast cancer. Br J Cancer. 1996;74(2):300-8.

101. Robertson JF, Nicholson RI, Bundred NJ, Anderson E, Rayter Z, Dowsett M, et al. Comparison of the short-term biological effects of 7alpha-[9-(4,4,5,5,5-pentafluoropentylsulfinyl)-nonyl]estra-1,3,5, (10)-triene-3,17beta-diol (Faslodex) versus tamoxifen in postmenopausal women with primary breast cancer. Cancer Res. 2001;61(18):6739-46.

102. Jerusalem G, Petruzelka L, Torres R. Final overall survival: fulvestrant 500mg vs 250mg in the randomized CONFIRM trial. J Natl Cancer Inst. 2013;106(1).

103. Robertson JF, Lindemann JP, Llombart-Cussac A, Rolski J, Feltl D, Dewar J, et al. Fulvestrant 500 mg versus anastrozole 1 mg for the first-line treatment of advanced breast cancer: follow-up analysis from the randomized 'FIRST'study. Breast Cancer Res Treat. 2012;136(2):503-11.

104. Howell A, Robertson JF, Abram P, Lichinitser MR, Elledge R, Bajetta E, et al. Comparison of Fulvestrant Versus Tamoxifen for the Treatment of Advanced Breast Cancer in Postmenopausal Women Previously Untreated With Endocrine Therapy: A Multinational, Double-Blind, Randomized Trial. Journal of Clinical Oncology. 2004;22(9):1605-13.

105. Nathan MR, Schmid P. A Review of Fulvestrant in Breast Cancer. Oncology and Therapy. 2017;5(1):17-29.

106. Slamon DJ, Neven P, Chia S, Fasching PA, De Laurentiis M, Im SA, et al. Phase III Randomized Study of Ribociclib and Fulvestrant in Hormone Receptor-Positive, Human Epidermal Growth Factor Receptor 2-Negative Advanced Breast Cancer: MONALEESA-3. J Clin Oncol. 2018;36(24):2465-72.

107. Loibl S, Turner NC, Ro J, Cristofanilli M, Iwata H, Im SA, et al. Palbociclib Combined with Fulvestrant in Premenopausal Women with Advanced Breast Cancer and Prior Progression on Endocrine Therapy: PALOMA-3 Results. Oncologist. 2017;22(9):1028-38.

108. Simpson ER, Mahendroo MS, Means GD, Kilgore MW, Hinshelwood MM, Graham-Lorence S, et al. Aromatase cytochrome P450, the enzyme responsible for estrogen biosynthesis. Endocr Rev. 1994;15(3):342-55.

109. Kümler I, Knoop AS, Jessing CA, Ejlertsen B, Nielsen DL. Review of hormone-based treatments in postmenopausal patients with advanced breast cancer focusing on aromatase inhibitors and fulvestrant. ESMO Open. 2016;1(4):e000062.

110. Brueggemeier RW, Hackett JC. Aromatase inhibitors in the treatment of breast cancer. Endocr Rev. 2005;26(3):331-45.

111. James VH, McNeill JM, Lai LC, Newton CJ, Ghilchik MW, Reed MJ. Aromatase activity in normal breast and breast tumor tissues: in vivo and in vitro studies. Steroids. 1987;50(1-3):269-79.

112. Miller WR, O'Neill J. The importance of local synthesis of estrogen within the breast. Steroids. 1987;50(4-6):537-48.

113. Cardoso F, Bischoff J, Brain E, Zotano ÁG. A review of the treatment of endocrine responsive metastatic breast cancer in postmenopausal women. Cancer Treat Rev. 2013;39(5):457-65.

114. Early Breast Cancer Trialists' Collaborative Group. Aromatase inhibitors versus tamoxifen in early breast cancer: patient-level meta-analysis of the randomised trials. Lancet 2015 386(1001):1341-52.

115. Schiavon G, Smith IE. Endocrine Therapy for Advanced/ Metastatic Breast Cancer. Hematology/Oncology Clinics of North America. 2013;27(4):715-36.

116. Nabholtz J. Long-term safety of aromatase inhibitors in the treatment of breast cancer. Therapeutics and Clinical Risk Management. 2008;4(1):189-204.

117. McGuire WL, Horwitz KB, Pearson OH, Segaloff A. Current status of estrogen and progesterone receptors in breast cancer. Cancer. 1977 39(Suppl 6):2934-47.

118. Chia S, Gradishar W, Mauriac L, Bines J, Amant F, Federico M, et al. Double-blind, randomized placebo controlled trial of fulvestrant compared with exemestane after prior nonsteroidal aromatase inhibitor therapy in postmenopausal women with hormone receptor-positive, advanced breast cancer: results from EFECT. Journal of Clinical Oncology 2008 26(10):1664-70.

119. Ellis MJ, Llombart-Cussac A, Feltl D, Dewar JA, Jasiówska M, Hewson N, et al. Fulvestrant 500mg Versus Anastrozole 1mg for the rst-line treatment of advanced breast cancer: overall survival analysis from the phase II rst study. Journal of Clinical Oncology 2015;33(32):3781-7.

120. Luqmani YA, N A-E. Overcoming Resistance to Endocrine Therapy in Breast Cancer: New Approaches to a Nagging Problem. Med Princ Pract. 2016;25(Suppl 2):28-40.

121. Osborne CK, Schiff R. Mechanisms of endocrine resistance in breast cancer. Annu Rev Med. 2011;62:233-47.

122. Sighoko D, Liu J, Hou N, Gustafson P, Huo D. Discordance in hormone receptor status among primary, metastatic, and second primary breast cancers: biological difference or misclassi cation? . Oncologist 2014;19(6):529-601.

123. Cancer Genome Atlas Network. Comprehensive molecular portraits of human breast tumours. Nature 2012 490(7418):61-70.

124. Toy W, Shen Y, Won H, Green B, Sakr RA, Will M, et al. ESR1 ligand-binding domain mutations in hormone-resistant breast cancer. Nature Genetics 2013 45 (12):1439–45.

125. Murphy CG, Dickler MN. Endocrine resistance in hormone-responsive breast cancer: mechanisms and therapeutic strategies. Endocr Relat Cancer. 2016;23(8):337-52.

126. Miller TW, Rexer BN, Garrett JT, Arteaga CL. Mutations in the phosphatidylinositol 3-kinase pathway: role in tumor progression and therapeutic implications in breast cancer. Breast Cancer Research. 2011 13(6):224.

127. Fan W, Chang J, Fu P. Endocrine therapy resistance in breast cancer: current status, possible mechanisms and overcoming strategies. Future Medicinal Chemistry. 2015;7(12):1511-9.

128. Watts CK, Brady A, Sarcevic B, deFazio A, Musgrove EA, Sutherland RL. Antiestrogen inhibition of cell cycle progression in breast cancer cells in associated with inhibition of cyclin-dependent kinase activity and decreased retinoblastoma protein phosphorylation. Molecular Endocrinology 1995 9(12):1804-13.

129. Kaufman B, Mackey JR, Clemens MR, Bapsy PP, Vaid A, Wardley A, et al. Trastuzumab plus anastrozole versus anastrozole alone for the treatment of postmenopausal women with human epidermal growth factor receptor 2-positive, hormone receptor-positive metastatic breast cancer: results from the randomized phase III TAnDEM study. J Clin Oncol. 2009;27(33):5529-37.

130. Guest SK, Ribas R, Pancholi S, Nikitorowicz-Buniak J, Simigdala N, Dowsett M, et al. Src Is a Potential Therapeutic Target in Endocrine-Resistant Breast Cancer Exhibiting Low Estrogen Receptor-Mediated Transactivation PLoS ONE. 2016;11(6):e0157397.

131. Hiscox S, Morgan L, Green TP, Barrow D, Gee J, Nicholson RI. Elevated Src activity promotes cellular invasion and motility in tamoxifen resistant breast cancer cells. Breast Cancer Res Treat. 2006;97(3):263-74.

132. Hiscox S, Jordan NJ, Morgan L, Green TP, Nicholson RI. Src kinase promotes adhesion-independent activation of FAK and enhances cellular migration in tamoxifen-resistant breast cancer cells. Clinical & experimental metastasis. 2007;24(3):157-67.

133. Borley A. E-cadherin Loss and Anti-oestrogen Induced Invasion in Oestrogen-Receptor Positive Breast cancer [MD]: Cardiff University; 2011.

134. Borley AC, Hiscox S, Gee J, Smith C, Shaw V, Barrett-Lee P, et al. Anti-oestrogens but not oestrogen deprivation promote cellular invasion in intercellular adhesion-deficient breast cancer cells. Breast cancer research : BCR. 2008;10(6):R103.

135. Lymperatou D, Giannopoulou E, Koutras AK, Kalofonos HP. The exposure of breast cancer cells to fulvestrant and tamoxifen modulates cell migration differently. Biomed Res Int. 2013;2013:147514.

136. Mathew AC, Rajah TT, Hurt GM, Abbas Abidi SM, Dmytryk JJ, Pento JT. Influence of antiestrogens on the migration of breast cancer cells using an in vitro wound model. Clinical & experimental metastasis. 1997;15(4):393-9.

137. Acconcia F, Barnes CJ, Kumar R. Estrogen and tamoxifen induce cytoskeletal remodeling and migration in endometrial cancer cells. Endocrinology. 2006;147(3):1203-12.

138. Nilsson UW, Garvin S, Dabrosin C. MMP-2 and MMP-9 activity is regulated by estradiol and tamoxifen in cultured human breast cancer cells. Breast cancer research and treatment. 2007;102(3):253-61.

139. Wang Q, Jiang J, Ying G, Xie XQ, Zhang X, Xu W, et al. Tamoxifen enhances stemness and promotes metastasis of ERα36+ breast cancer by upregulating ALDH1A1 in cancer cells. Cell Res. 2018 28
(3):336-58.

140. Platet N, Cathiard AM, Gleizes M, Garcia M. Estrogens and their receptors in breast cancer progression: a dual role in cancer proliferation and invasion. Critical reviews in oncology/hematology. 2004;51(1):55-67.

141. van Roy F, Berx G. The cell-cell adhesion molecule E-cadherin. Cell Mol Life Sci. 2008;65(23):3756-88.

142. Takeichi M. Functional correlation between cell adhesive properties and some cell surface proteins. The Journal of cell biology. 1977;75(2):464-74.

143. Tian X, Liu Z, Niu B, Zhang J, Tan TK, Lee SR, et al. E-cadherin/β-catenin complex and the epithelial barrier. J Biomed Biotechnol. 2011;2011:567305.

144. Wheelock MJ, Jensen PJ. Regulation of keratinocyte intercellular junction organization and epidermal morphogenesis by E-cadherin. The Journal of Cell Biology. 1992;117(2):415-25.

145. Jeanes A, Gottardi CJ, Yap AS. Cadherins and cancer: how does cadherin dysfunction promote tumor progression? Oncogene. 2008;27(55):6920-9.

146. Ashaie MA, Chowdhury EH. Cadherins: The Superfamily Critically Involved in Breast Cancer. Curr Pharm Des. 2016;22(5):616-38.

147. Memorial University of Newfoundland. Principles of Cell Biology (BIOL2060) 2018 [Available from: http://www.mun.ca/biology/desmid/brian/BIOL2060/BIOL2060-17/CB17.html].

148. Schackmann RC, Klarenbeek S, Vlug EJ, Stelloo S, van-Amersfoort M, Tenhagen M, et al. Loss of p120-catenin induces metastatic progression of breast cancer by inducing anoikis resistance and augmenting growth factor receptor signaling. Cancer research. 2013;73(15):4937-49.

149. Bajpai S, Feng Y, Krishnamurthy R, Longmore GD, Wirtz D. Loss of α-catenin decreases the strength of single E-cadherin bonds between human cancer cells. J Biol Chem. 2009;284(27):18252-9.

150. Geyer FC, Lacroix-Triki M, Savage K, Arnedos M, Lambros MB, MacKay A, et al. β-Catenin pathway activation in breast cancer is associated with triple-negative phenotype but not with CTNNB1 mutation. Mod Pathol. 2011;24(2):209-31.

151. López-Knowles E, Zardawi SJ, McNeil CM, Millar EK, Crea P, Musgrove EA, et al. Cytoplasmic localization of β-catenin is a marker of poor outcome in breast cancer patients. Cancer Epidemiol Biomarkers Prev. 2010;19(1):301-9.

152. Berx G, Van Roy F. Involvement of members of the cadherin superfamily in cancer. Cold Spring Harb Perspect Biol. 2009;1(6).

153. Yang SZ, Kohno N, Yokoyama A, Kondo K, Hamada H, Hiwada K. Decreased E-cadherin augments β-catenin nuclear localization: Studies in breast cancer cell lines. International Journal of Oncology. 2001 18(3):541-8.

154. Chen A, Beetham H, Black MA, Priya R, Telford BJ, Guest J, et al. E-cadherin loss alters cytoskeletal organization and adhesion in non-malignant breast cells but is insufficient to induce an epithelial-mesenchymal transition. BMC Cancer. 2014;14:552.

155. Son H, Moon A. Epithelial-mesenchymal transition and cell invasion. Toxicol Res. 2010;26(4):245-52.

156. Heerboth S, Housman G. EMT and tumor metastasis. Clin Transl Med. 2015;4:6.

157. Kashiwagi S, Yashiro M, Takashima T, Nomura S, Noda S, Kawajiri H, et al. Significance of E-cadherin expression in triple-negative breast cancer. Br J Cancer. 2010;103(2):249-55.

158. Li DM, Feng YM. Signaling mechanism of cell adhesion molecules in breast cancer metastasis: potential therapeutic targets. Breast cancer research and treatment. 2011;128(1):7-21.

159. Pećina-Šlaus N. Tumor suppressor gene E-cadherin and its role in normal and malignant cells. Cancer Cell Int. 2003;3(1):17.

160. Palacios F, Tushir JS, Fujita Y, D'Souza-Schorey C. Lysosomal targeting of E-cadherin: a unique mechanism for the down-regulation of cell-cell adhesion during epithelial to mesenchymal transitions. Mol Cell Biol. 2005;25(1):389-402.

161. Dhasarathy A, Phadke D, Mav D, Shah RR, Wade PA. The transcription factors Snail and Slug activate the transforming growth factor-beta signaling pathway in breast cancer. PloS one. 2011;6(10):e26514.

162. Lo HW, Hsu SC, Xia W, Cao X, Shih JY, Wei Y, et al. Epidermal growth factor receptor cooperates with signal transducer and activator of transcription 3 to induce epithelial-mesenchymal transition in cancer cells via up-regulation of TWIST gene expression. Cancer Res. 2007;67(19):9066-76.

163. Hardy KM, Booth BW, Hendrix MJC. ErbB/EGF signaling and EMT in mammary development and breast cancer. J Mammary Gland Biol Neoplasia. 2010;15(2):191-9.

164. Guarino M. Src signaling in cancer invasion. Journal of cellular physiology. 2010;223(1):14-26.

165. Martin G. The hunting of the Src. Nature reviews Molecular cell biology. 2001;2(6):467-75.

166. Yeatman TJ. A renaissance for SRC. Nat Rev Cancer. 2004;4(6):470-80.

167. Summy JM, Gallick GE. Src family kinases in tumor progression and metastasis. Cancer Metastasis Rev. 2003;22(4):337-58.

168. Roskoski R. Src protein-tyrosine kinase structure and regulation. Biochemical and biophysical research communications. 2004;324(4):1155-64.

169. Boggon TJ, Eck MJ. Structure and regulation of Src family kinases. Oncogene volume 2004;23(48):7918-27.

170. Jacobs C, Rübsamen H. Expression of pp60c-src protein kinase in adult and fetal human tissue: high activities in some sarcomas and mammary carcinomas. Cancer Res. 1983;43(4):1696-702.

171. Verbeek BS, Vroom TM, Slot SS, Kalff AE, Geertzema JG, Hennipman A, et al. c Src protein expression is increased in human breast cancer. An immunohistochemical and biochemical analysis. The Journal of pathology. 1996;180(4):383-8.

172. Morgan L, Gee J, Pumford S, Farrow L, Finlay P, Robertson J, et al. Elevated Src kinase activity attenuates Tamoxifen response in vitro and is associated with poor prognosis clinically. Cancer Biol Ther. 2009;8(16):1550-8.

173. Herynk MH, Beyer AR, Cui Y, Weiss H, Anderson E, Green TP, et al. Cooperative action of tamoxifen and c-Src inhibition in preventing the growth of estrogen receptor–positive human breast cancer cells. Mol Cancer Ther. 2006;5(12):3023-31.

174. Boonyaratanakornkit V, Edwards DP. Receptor mechanisms of rapid extranuclear signalling initiated by steroid hormones. Essays in biochemistry. 2004;40:105-20.

175. Finn R. Targeting Src in breast cancer. Annals of Oncology. 2008;19(8):1379-86.

176. Mukhopadhyay D, Tsiokas L, Zhou XM, Foster D, Brugge JS, Sukhatme VP. Hypoxic induction of human vascular endothelial growth factor expression through c-Src activation. Nature. 1995;375(6532):577-81.

177. Pal S, Datta K, Mukhopadhyay D. Central role of p53 on regulation of vascular permeability factor/vascular endothelial growth factor (VPF/VEGF) expression in mammary carcinoma. Cancer Res. 2001;61(18):6952-7.

178. Nills D, Minton S, Cox C, Bowman T, Gritsko T, Garcia R, et al. Activation of stat3 in primary tumors from high-risk breast cancer patients is associated with elevated levels of activated SRC and survivin expression. Clinical Cancer Research. 2006;12(1):20-8.

179. Tan M, Li P, Sun M, Yin G, Yu D. Upregulation and activation of PKC alpha by ErbB2 through Src promotes breast cancer cell invasion that can be blocked by combined treatment with PKC alpha and Src inhibitors. Oncogene. 2006;25(23):3286-95.

180. González L, Agulló-Ortuño MT, García-Martínez JM, Calcabrini A, Gamallo C, Palacios J, et al. Role of c-Src in human MCF7 breast cancer cell tumorigenesis. Journal of Biological Chemistry. 2006;281(30):20851-64.

181. Gutwein P, Oleszewski M, Mechtersheimer S, Agmon-Levin N, Krauss K, Altevogt P. Role of Src kinases in the ADAM-mediated release of L1 adhesion molecule from human tumor cells. J Biol Chem. 2000;275(20):15490-7.

182. Finn RS, Dering J, Ginther C, Wilson CA, Glaspy P, Tchekmedyian N, et al. Dasatinib, an orally active small molecule inhibitor of both the src and abl kinases, selectively inhibits growth of basal-type/"triple-negative" breast cancer cell lines growing in vitro. Breast Cancer Res Treat. 2007;105(3):319-26.

183. Huang F, Reeves K, Han X, Fairchild C, Platero S, Wong TW, et al. Identification of candidate molecular markers predicting sensitivity in solid tumors to dasatinib: rationale for patient selection. Cancer Res. 2007;67(5):2226-38.

184. Lombardo LJ, Lee FY, Chen P, Norris D, Barrish JC, Behnia K, et al. Discovery of N-(2-chloro-6-methyl- phenyl)-2-(6-(4-(2-hydroxyethyl)-piperazin-1-yl)-2-methylpyrimidin-4- ylamino)thiazole-5-carboxamide (BMS-354825), a dual Src/Abl kinase inhibitor with potent antitumor activity in preclinical assays. J Med Chem. 2004;47(27):6658-61.

185. Cancer Research UK. A trial looking at saracatinib in post menopausal women with advanced breast cancer (ARISTACAT) [https://www.cancerresearchuk.org/about-cancer/find-a-clinical-trial/a-trial-looking-saracatinib-post-menopausal-women-advanced-breast-cancer-aristacat - undefined]: Cancer Research UK; 2018

186. Duval K, Grover H, Han LH, Mou Y, Pegoraro AF, Fredberg J, et al. Modeling Physiological Events in 2D vs. 3D Cell Culture. Physiology. 2017;32(4):266-77.

187. Edmondson R, Broglie JJ, Adcock AF, Yang L. Three-dimensional cell culture systems and their applications in drug discovery and cell-based biosensors. Assay Drug Dev Technol. 2014;12(4):207-18.

188. Burdick JA, Vunjak-Novakovic G. Engineered microenvironments for controlled stem cell differentiation. Tissue Eng Part A. 2009;15(2):205-19.

189. Scadden D. The stem-cell niche as an entity of action. Nature. 2006;441(7097):1075-9.

190. Corning. Corning Matrigel Matrix 2018 [cited 2018 17th May 2018]. [Available from: https://www.corning.com/emea/en/products/life-sciences/products/surfaces/matrigel-matrix.html].

191. Chitcholtan K, Asselin E, Parent S, Sykes PH, Evans JJ. Differences in growth properties of endometrial cancer in three dimensional (3D) culture and 2D cell monolayer. Exp Cell Res. 2013 319(1):75-87.

192. Mabry KM, Payne SZ, Anseth KS. Microarray analyses to quantify advantages of 2D and 3D hydrogel culture systems in maintaining the native valvular interstitial cell phenotype. Biomaterials. 2016;74:31-41.

193. Pineda ET, Nerem RM, Ahsan T. Differentiation patterns of embryonic stem cells in two- versus three-dimensional culture. Cells Tissues Organs. 2013;197(5):399-410.

194. Gangadhara S, Smith C, Barrett-Lee P, Hiscox S. 3D culture of Her2+ breast cancer cells promotes AKT to MAPK switching and a loss of therapeutic response. BMC cancer. 2016;16:345.

195. Grinnell F. Fibroblast biology in three-dimensional collagen matrices. Trends Cell Biol. 2003;13(5):264-9.

196. Gjorevski N, Piotrowski AS, Varner VD, Nelson CM. Dynamic tensile forces drive collective cell migration through three-dimensional extracellular matrices. Sci Rep. 2015;13(5):11458.

197. Vinci M, Box C, Eccles SA. Three-dimensional (3D) tumor spheroid invasion assay. J Vis Exp. 2015(99):e52686.

198. Frasor J, Stossi F, Danes JM, Komm B, Lyttle CR, Katzenellenbogen BS. Selective estrogen receptor modulators: discrimination of agonistic versus antagonistic activities by gene expression profiling in breast cancer cells. Cancer research. 2004;64(4):1522-33.

199. Gee JM, Harper ME, Hutcheson IR, Madden TA, Barrow D, Knowlden JM, et al. The antiepidermal growth factor receptor agent gefitinib (ZD1839/Iressa) improves antihormone response and prevents development of resistance in breast cancer in vitro. Endocrinology. 2003;144(11):5105-17.

200. Shaw VE, Gee J, McClelland RA, Morgan H, Rushmere N, Nicholson RI. Identification of anti-hormone induced genes as potential therapeutic targets in breast cancer. Cancer Res. 2007;65(Suppl 9):874.

201. Corso G, Intra M, Trentin C, Veronesi P, Galimberti V. CDH1 germline mutations and hereditary lobular breast cancer. Familial cancer. 2016.

202. Gould Rothberg, E. B, Bracken, Michael B. E-cadherin immunohistochemical expression as a prognostic factor in infiltrating ductal carcinoma of the breast: a systematic review and meta-analysis. Breast cancer research and treatment. 2006;100(2):139-48.

203. Park D, Kåresen R, Axcrona U, Noren T, Sauer T. Expression pattern of adhesion molecules (E-cadherin, alpha-, beta-, gamma-catenin and claudin-7), their influence on survival in primary breast carcinoma, and their corresponding axillary lymph node metastasis. APMIS. 2007;115(1):52-65.

204. Onder TT, Gupta PB, Mani SA, Yang J, Lander ES, Weinberg RA. Loss of E-cadherin promotes metastasis via multiple downstream transcriptional pathways. Cancer research. 2008;68(10):3645-54.

205. Herzig M, Savarese F, Novatchkova M, Semb H, Christofori G. Tumor progression induced by the loss of E-cadherin independent of beta-catenin/Tcf-mediated Wnt signaling. Oncogene. 2007;26(16):2290-8.

206. Shibata T, Kokubu A, Sekine S, Kanai Y, Hirohashi S. Cytoplasmic p120ctn regulates the invasive phenotypes of E-cadherin-deficient breast cancer. The American journal of pathology. 2004;164(6):2269-78.

207. Pennisi PA, Barr V, Nunez NP, Stannard B, Le Roith D. Reduced expression of insulin-like growth factor I receptors in MCF-7 breast cancer cells leads to a more metastatic phenotype. Cancer research. 2002;62(22):6529-37.

208. Maynadier M, Nirdé P, Ramirez JM, Cathiard AM, Platet N, Chambon M, et al. Role of estrogens and their receptors in adhesion and invasiveness of breast cancer cells. Advances in experimental medicine and biology. 2008;617:485-91.

209. Paredes J, Stove C, Stove V, Milanezi F, Van Marck V, Derycke L, et al. P-cadherin is up-regulated by the antiestrogen ICI 182,780 and promotes invasion of human breast cancer cells. Cancer research. 2004;64(22):8309-17.

210. Rochefort H, Platet N, Hayashido Y, Derocq D, Lucas A, Cunat S, et al. Estrogen receptor mediated inhibition of cancer cell invasion and motility: an overview. J Steroid Biochem Mol Biol. 1998;65((1-6)):163-8.

211. Garcia M, Derocq D, Platet N, Bonnet S, Brouillet JP, Touitou I, et al. Both estradiol and tamoxifen decrease proliferation and invasiveness of cancer cells transfected with a mutated estrogen receptor. J Steroid Biochem Mol Biol. 1997;61(1-2):11-7.

212. Hayashido Y, Lucas A, Rougeot C, Godyna S, Argraves WS, Rochefort H. Estradiol and fibulin‐1 inhibit motility of human ovarian‐and breast‐cancer cells induced by fibronectin. Int J Cancer. 1998;75(4):654-8.

213. Kolodgie FD, Jacob A, Wilson PS, Carlson GC, Farb A, Verma A, et al. Estradiol attenuates directed migration of vascular smooth muscle cells in vitro. American Journal of Pathology. 1996;148(3):969-76.

214. Long BJ, Rose DP. Invasive capacity and regulation of urokinase-type plasminogen activator in estrogen receptor (ER)-negative MDA-MB-231 human breast cancer cells, and a transfectant (S30) stably expressing ER. Cancer Lett. 1996;99(2):209-15.

215. Platet N, Garcia M. A new bioassay using transient transfection for invasion-related gene analysis. Invasion Metastasis. 1998;18(4):198-208.

216. Platet N, Cunat S, Chalbos D. Unliganded and liganded estrogen receptors protect against cancer invasion via different mechanisms. Mol Endocrinol. 2000;14(7):999-1009.

217. Platet N, Prévostel C, Derocq D, Joubert D, Rochefort H, Garcia M. Breast cancer cell invasiveness: correlation with protein kinase C activity and differential regulation by phorbol ester in estrogen receptor‐positive and‐negative cells. Int J Cancer. 1998;75(5):750-6.

218. Albini A, Graf J, Kitten GT. 17 beta-estradiol regulates and v-Ha-ras transfection constitutively enhances MCF7 breast cancer cell interactions with basement membrane. Proc Natl Acad Sci USA 1986;83(21):8182-6.

219. Thompson EW, Reich R, Shima TB, Albini A, Graf J, Martin GR, et al. Differential regulation of growth and invasiveness of MCF-7 breast cancer cells by antiestrogens. Cancer Res. 1988;48(23):6764-8.

220. Aka JA, Lin SX. Comparison of functional proteomic analyses of human breast cancer cell lines T47D and MCF7. PLoS One. 2012;7(2):e31532.

221. Hennequin LF, Allen J, Breed J, Curwen J, Fennell M, Green TP, et al. N-(5-Chloro-1,3-benzodioxol-4-yl)-7-[2-(4-methylpiperazin-1-yl)ethoxy]-5-(tetrahydro-2H-pyran-4-yloxy)quinazolin-4-amine, a Novel, Highly Selective, Orally Available, Dual-Specific c-Src/Abl Kinase Inhibitor. Journal of Medicinal Chemistry 2006;49(22):6465-88.

222. Maik-Rachline G, Seger R. The ERK cascade inhibitors: Towards overcoming resistance. Drug resistance updates : reviews and commentaries in antimicrobial and anticancer chemotherapy. 2016;25:1-12.

223. Duncia JV, Santella JB, Higley CA, Pitts WJ, Wityak J, Frietze WE, et al. MEK inhibitors: The chemistry and biological activity of U0126, its analogs, and cyclization products. Bioorganic & Medicinal Chemistry Letters. 1998;8(20):2839-44.

224. Fresno Vara JA, Casado E, deCastro J, Cejas P, Belda-Iniesta C, González-Barón M. PI3K/Akt signalling pathway and cancer. Cancer Treat Rev. 2004;30(2):193-204.

225. Yoeli-Lerner M, Yiu GK, Rabinovitz I, Erhardt P, Jauliac S, Toker A. Akt blocks breast cancer cell motility and invasion through the transcription factor NFAT. Mol Cell. 2005;20(4):539-50.

226. Panigrahi AR, Pinder SE, Chan SY, Paish EC, Robertson JFR, Ellis IO. The role of PTEN and its signalling pathways, including AKT, in breast cancer; an assessment of relationships with other prognostic factors and with outcome. The Journal of Pathology. 2004;204(1):93-100.

227. Richardson PG, Eng C, Kolesar J, Hideshima T, Anderson KC. Perifosine, an oral, anti-cancer agent and inhibitor of the Akt pathway: mechanistic actions, pharmacodynamics, pharmacokinetics, and clinical activity. Expert opinion on drug metabolism & toxicology. 2012;8(5):623-33.

228. Liu F, Gu LN, Shan BE, Geng CZ, Sang MX. Biomarkers for EMT and MET in breast cancer: An update. Oncology Letters. 2016;12(6):4869-76.

229. Zhan T, Rindtorff N, Boutros M. Wnt signaling in cancer. Oncogene. 2017;36(11):1461.

230. Fang D, Chen H, Zhu JY, Wan W, Teng Y, Ding HF, et al. Epithelial-Mesenchymal Transition of Ovarian Cancer Cells Is Sustained by Rac1 through Simultaneous Activation of MEK1/2 and Src Signaling Pathways. Oncogene. 2017;36(11):1546-58.

231. Neufeld G, Mumblat Y, Smolkin T, Toledano S, Nir-Zvi I, Ziv K, et al. The role of the semaphorins in cancer. Cell adhesion & migration. 2016;10(6):652-74.

232. Hota PK, Buck M. Plexin structures are coming: opportunities for multilevel investigations of semaphorin guidance receptors, their cell signaling mechanisms, and functions. Cell Mol Life Sci. 2012;69(22):3765-805.

233. Alto LT, Terman JR. Semaphorins and their Signaling Mechanisms. Methods in molecular biology. 2017;1493:1-25.

234. Radisky ES, Raeeszadeh‐Sarmazdeh M, Radisky DC. Therapeutic Potential of Matrix Metalloproteinase Inhibition in Breast Cancer. Journal of Cellular Biochemistry. 2017;118(11):3531-48.

235. Reddy KB, Nabha SM, Atanaskova N. Role of MAP kinase in tumor progression and invasion. Cancer Metastasis Rev. 2003;22(4):395-403.

236. Tengn TS, Lin B, Manser E, Ng DCH, X C. Stat3 promotes directional cell migration by regulating Rac1 activity via its activator βPIX. Journal of Cell Science. 2009;122(22):4510-159.

237. Chung J, Uchida E, Grammer TC, Blenis J. STAT3 serine phosphorylation by ERK-dependent and -independent pathways negatively modulates its tyrosine phosphorylation. Molecular and Cellular Biology. 1997;17(11):6508-16.

238. Kamran MZ, Patil P, Gude RP. Role of STAT3 in Cancer Metastasis and Translational Advances. Biomed Res Int. 2013;2013:1-15.

239. Zhang J, Kalyankrishna S, Wislez M, Thilaganathan N, Saigal B, Wei W, et al. SRC-family kinases are activated in non-small cell lung cancer and promote the survival of epidermal growth factor receptor-dependent cell lines. Am J Pathol 2007; 170(1):366-76.

240. Masaki T, Igarashi K, Tokuda M, Yukimasa S, Han F, YJ J, et al. pp60c-src activation in lung adenocarcinoma. Eur J Cancer 2003; 39(10):1447-55.

241. Masaki T, Shiratori Y, Okada H, Nishioka M, Taniguchi K, Hatanaka Y, et al. pp60c-src activation in gastric carcinoma: a preliminary study. Am J Gastroenterol 2000;95(3):837-8.

242. Summy JM, GE G. Src family kinases in tumor progression and metastasis. Cancer Metast Rev. 2003 22(4):337-58.

243. Frame M. Src in cancer: deregulation and consequences for cell behavior. Biochim Biophys Acta 2002;1602(2):114-30.

244. González L, Agulló-Ortuño MT, García-Martínez JM, Calcabrini A, Gamallo C, Palacios J, et al. Role of c-Src in human MCF7 breast cancer cell tumorigenesis J Biol Chem 2006;281(30):20851-64.

245. Park JH, Lee MY, Han HJ. A potential role for caveolin-1 in estradiol-17beta-induced proliferation of mouse embryonic stem cells: Involvement of Src, PI3K/Akt and MAPKs pathways. Int J Biochem Cell Biol 2009 41(3):659-65.

246. Madak-Erdogan Z, Kieser KJ, Kim SH, Komm B, Katzenellenbogen JA, Katzenellenbogen BS. Nuclear and extranuclear pathway inputs in the regulation

of global gene expression by estrogen receptors. Mol Endocrinol 2008;22(9):2116-27.

247. Boonyaratanakornkit V, McGowan E, Sherman L, Mancini MA, Cheskis BJ, Edwards DP. The role of extra-nuclear signaling actions of progesterone receptor in mediating progesterone regulation of gene expression and the cell cycle Mol Endocrinol 2007;27(2):359-75.

248. Kim H, Laing M, Muller W. c-Src-null mice exhibit defects in normal mammary gland development and ERalpha signaling. Oncogene 2005;24(36):5629-36.

249. Fan P, Wang J, Santen RJ, Yue W. Long-term treatment with Tamoxifen facilitates trans-location of estrogen receptor alpha out of the nucleus and enhances its interaction with EGFR in MCF-7 breast cancer cells. Cancer Res 2007;67(3):1352-60.

250. Cowell LN, Graham JD, Bouton AH, Clarke CL, O'Neill GM. Tamoxifen treatment promotes phosphorylation of the adhesion molecules, p130Cas/BCAR1, FAK and Src, via an adhesion-dependent pathway. Oncogene 2006;25(58):7597–607.

251. Pratt SJ, Epple H, Ward M, Feng Y, Braga VM, Longmore GD. The LIM protein Ajuba influences p130Cas localization and Rac1 activity during cell migration. J Cell Biol 2005 168(5):813–24.

252. Song RXD, McPherson RA, Adam L. Linkage of rapid estrogen action to MAPK activation by ERα-Shc association and Shc pathway activation. Molecular Endocrinology. 2002;16(1):116-27.

253. Plotnikov A, Zehorai E, Procaccia S, Seger R. The MAPK cascades: Signaling components, nuclear roles and mechanisms of nuclear translocation. Biochimica et Biophysica Acta. 2011;1813(9):1619–163.

254. Bi R, Broutman G, Foy MR, Thompson RF, Baudry M. The tyrosine kinase and mitogen-activated protein kinase pathways mediate multiple effects of estrogen in hippocampus. Proc Natl Acad Sci USA 2000;97(7):3602–7.

255. Migliaccio A, Domenico DM, Castoria G. Tyrosine kinase/p21ras/MAP-kinase pathway activation by estradiol-receptor complex in MCF-7 cells. The EMBO Journal. 1996;15(6):1292-300.

256. Lenormand P, Brondello JM, Brunet A, Pouyssegur J. Growth factor-induced p42/p44 MAPK nuclear translocation and retention requires both MAPK activation and neosynthesis of nuclear anchoring proteins. J Cell Biol 1998;142(3):625–33.

257. Adachi M, Fukuda M, Nishida E. Nuclear export of MAP kinase (ERK) involves a MAP kinase kinase (MEK)-dependent active transport mechanism J Cell Biol. 2000;148; 849–56.

258. Hartmann G, Weidner KM, Schwarz H, Birchmeier W. The motility signal of scatter factor/hepatocyte growth factor mediated through the receptor tyrosine kinase met requires intracellular action of Ras. J Biol Chem. 1994;269(35):21936–9.

259. Klemke RL, Yebra M, Bayna EM, Cheresh DA. Receptor tyrosine kinase signaling required for integrin alpha v beta 5-directed cell motility but not adhesion on vitronectin. J Cell Biol 1994;127(3):859–66.

260. Klemke RL, Cai S, Giannini AL, Gallagher PJ, deLanerolle P, Cheresh DA. Regulation of cell motility by mitogen-activated protein kinase. J Cell Biol. 1997;137(2):481–92.

261. Krueger JS, Keshamouni VG, Atanaskova N, Reddy KB. Temporal and quantitative regulation of mitogen-activated protein kinase (MAPK) modulates cell motility and invasion. Oncogene 2001;20 (31):4209–18.

262. Sivaraman VS, Wang H, Nuovo GJ, Malbon CC. Hyperexpression of mitogen-activated protein kinase in human breast cancer. J Clin Invest 1997;99(7):1478–83.

263. Adeyinka A, Nui Y, Cherlet T, Snell L, Watson PH, Murphy LC. Activated mitogen-activated protein kinase expression during human breast tumorigenesis and breast cancer progression. Clin Cancer Res 2002;8:1747–53.

264. Miller TW, Rexer BN, Garrett JT, Arteaga CL. Mutations in the phosphatidylinositol 3-kinase pathway: role in tumor progression and therapeutic implications in breast cancer. Breast Cancer Res 2011;13(6):224.

265. Miller TW, Balko JM, Arteaga CL. Phosphatidylinositol 3-kinase and antiestrogen resistance in breast cancer. J Clin Oncol 2011;29(33):4452–61.

266. Simoncini T, Hafezi-Moghadam A, Brazil DP, Ley K, Chin WW, Liao JK. Interaction of oestrogen receptor with the regulatory subunit of phosphatidylinositol-3-OH kinase. Nature 2000;407(6803):538–41.

267. Miller TW, Perez-Torres M, Narasanna A. Loss of phosphatase and tensin homologue deleted on chromosome 10 engages ErbB3 and insulin-like growth factor-I receptor signaling to promote antiestrogen resistance in breast cancer. Cancer Res 2009;69(10):4192–201.

268. Generali D, Fox SB, Brizzi MP. Down-regulation of phosphatidylinositol 3'-kinase/AKT/molecular target of rapamycin metabolic pathway by primary

letrozole-based therapy in human breast cancer. Clin Cancer Res 2008;14(9):2673–80.

269. Baselga J, Semiglazov V, van Dam P. Phase II randomized study of neoadjuvant everolimus plus letrozole compared with placebo plus letrozole in patients with estrogen receptor-positive breast cancer. J Clin Oncol 2009;27(16):2630–367.

270. Chakravarty D, Nair SS, Santhamma B, Nair BC, Wang L, Bandyopadhyay A, et al. Extranuclear functions of ER impact invasive migration and metastasis by breast cancer cells. Cancer Res. 2010;70(10):4092-101.

271. Roy S, Vadlamudi R. Role of Estrogen Receptor Signaling in Breast Cancer Metastasis. International Journal of Breast Cancer. 2012;19:1-8.

272. Vicente-Manzanares M, Webb DJ, Horwitz AR. Cell migration at a glance. Journal of Cell Science. 2005;118(21):4917–9.

273. Shi Q, D B. A novel mode for integrin-mediated signaling: tethering is required for phosphorylation of FAK Y397 Molecular Biology of the Cell. 2003;14(10):4306-15.

274. Cary LA, Han DC, Polte TR, Hanks SK, Guan JL. Identification of p130(Cas) as a mediator of focal adhesion kinase-promoted cell migration. The Journal of Cell Biology. 1998;140(1):211-21.

275. Webb DJ, Donais K, Whitmore LA, Thomas SM, Turner CE, Parsons JT, et al. FAK-Src signalling through paxillin, ERK and MLCK regulates adhesion disassembly. Nature Cell Biology. 2004;6(2):154-61.

276. Tai YL, Chen LC, Shen TL. Emerging Roles of Focal Adhesion Kinase in Cancer. BioMed Research International. 2015;1:1-13.

277. McLean GW, Carragher NO, Avizienyte E, Evans J, Brunton VG, Frame MC. The role of focal-adhesion kinase in cancer—a new therapeutic opportunity. Nature Reviews Cancer 2005;5(7):505-15.

278. Yilmaz M, Christofori G. EMT, the cytoskeleton, and cancer cell invasion Cancer and Metastasis Reviews. 2009;28(1-2):15-33.

279. Krugmann S, Jordens I, Gevaert K, Driessens M, Vandekerckhove J, Hall A. Cdc42 induces filopodia by promoting the formation of an IRSp53:Mena complex Current Biology. 2001;11(21):1645-55.

280. Ridley A. Rho GTPases and actin dynamics in membrane protrusions and vesicle trafficking. Trends in Cell Biology. 2006;16:522-9.

281. Lim Y, Han I, Jeon J, Park H, Bahk YY, Oh ES. Phosphorylation of focal adhesion kinase at tyrosine 861 is crucial for ras transformation of fibroblasts. The Journal of Biological Chemistry. 2004;279(28):29060-5.

282. Avizienyte E, Frame MC. Src and FAK signalling controls adhesion fate and the epithelial-to- mesenchymal transition. Current Opinion in Cell Biology. 2005;17(5):542-7.

283. Serrels A, Canel M, Brunton VG, Frame MC. Src/FAK-mediated regulation of E-cadherin as a mechanism for controlling collective cell movement: insights from in vivo imaging. Cell Adhesion & Migration. 2011;5(4):360-5.

284. Levy D. Physiological significance of STAT proteins: investigations through gene disruption in vivo Cellular and Molecular Life Sciences 1999;55(12):1599-67.

285. Huang S. Regulation of metastases by signal transducer and activator of transcription 3 signaling pathway: clinical implications Clinical Cancer Research. 2007;13(5):1362-6.

286. Yu CL, Meyer DJ, Campbell GS, Larner AC, Carter-Su C, Schwartz J, et al. Enhanced DNA-binding activity of a Stat3-related protein in cells transformed by the Src oncoprotein Science. 1995;269(5220):81-3.

287. Ng DC, Lin BH, Lim CP, Huang G, Zhang T, Poli V, et al. Stat3 regulates microtubules by antagonizing the depolymerization activity of stathmin. Journal of Cell Biology. 2006;172(2):245-57.

288. Reddy KB, Krueger JS, Kondapaka SB, Diglio CA. Mitogen-activated protein kinase (MAPK) regulates the expression of progelatinase B (MMP-9) in breast epithelial cells. Int J Cancer 1999;82 (2):268–73.

289. Overall CM, Lopez-Otin C. Strategies for mmp inhibition in cancer: innovations for the post-trial era. Nat Rev Cancer 2002;2(9):657–72.

290. Treps L, Le Guelte A, Gavard J. Emerging roles of Semaphorins in the regulation of epithelial and endothelial junctions. Tissue Barriers. 2013 1(1):e23272.

291. Christensen CR, Klingelhofer J, Tarabykina S, Hulgaard EF, Kramerov D, Lukanidin E. Transcription of a novel mouse semaphorin gene, M-semaH, correlates with the metastatic ability of mouse tumor cell lines. Cancer Res 1998;58(6):1238-44.

292. Capparuccia L, Tamagnone L. Semaphorin signaling in cancer cells and in cells of the tumor microenvironment–two sides of a coin. J Cell Science. 2009;122(11):1723-36.

293. Oka H, Shiozaki H, Kobayashi K, Inoue M, Tahara M, Kobayashi T, et al. Expression of E-cadherin cell adhesion molecules in human breast cancer tissues and its relationship to metastasis. Cancer research. 1993;53(7):1696-701.

294. Schipper JH, Frixen UH, Behrens J, Unger A, Jahnke K, Birchmeier W. E-Cadherin expression in squamous cellcarcinomas of head and neck: inverse correlation with tumor differentiation and lymph node metastasis. Cancer Res 1991;51((23)):6328–37.

295. Umbas R, Isaacs WB, Bringuier PP. Decreased E-cadherin expression is associated with poor prognosis in patients with prostate cancer Cancer Res. 1994;54(14):3929–33.

296. Wildenberg GA, Dohn MR, Carnahan RH, Davis MA, Lobdell NA, Settleman J, et al. p120-catenin and p190RhoGAP regulate cell-cell adhesion by coordinating antagonism between Rac and Rho. Cell. 2006;127(5):1027–39.

297. Vasioukhin V, Bauer C, Degenstein L, Wise B, Fuchs E. Hyperproliferation and defects in epithelial polarity on conditional ablation of a-catenin in skin. Cell 2001;104(4):605–17.

298. Nelson WJ, Nusse R. Convergence of Wnt, B-catenin, and cadherin pathways. Science 2004;303(5663):1483–7.

299. Perez-Moreno M, Fuchs E. Catenins: keeping cells from getting their signals crossed Dev Cell 2006;11(5):601–12.

300. Wildenberg GA, Dohn MR, Carnahan RH, Davis MA, Lobdell NA, Settleman J, et al. p120-Catenin and p190RhoGAP Regulate Cell-Cell Adhesion by Coordinating Antagonism between Rac and Rho. Cell 2006;127 (5):1027-39.

301. Nelson WJ, Nusse R. Convergence of Wnt, β-Catenin, and Cadherin Pathways. Science. 2004 303(5663):1483–7.

302. Yoshiura K, Kanai Y, Ochiai A, Shimoyama Y, Sugimura T, Hirohashi S. Silencing of the E-cadherin invasion-suppressor gene by CpG methylation in human carcinomas Proc Natl Acad Sci USA. 1995;92(16):7416–9.

303. Bolos V, Peinado H, Perez-Moreno MA, Fraga MF, Esteller M, Cano A. The transcription factor Slug represses E-cadherin expression and induces epithelial to mesenchymal transitions: a comparison with Snail and E47 repressors. J Cell Sci 2003;116:499–511.

304. Batlle E, Sancho E, Franci C. The transcription factor snail is a repressor of E-cadherin gene expression in epithelial tumour cells. Nat Cell Biol 2000;2(2):84–9.

305. Yang J, Mani SA, Donaher JL, Ramaswamy S, Itzykson RA, Come C, et al. Twist, a master regulator of morphogenesis, plays an essential role in tumor metastasis. Cell 2004;117(7):927–39.

306. Huber MA, Kraut N, Beug H. Molecular requirements for epithelial-mesenchymal transition during tumor progression. Curr Opin Cell Biol 2005;17(5):548–58.

307. NCBI. Pubmed: NCBI; 2018 [Available from:https://www.ncbi.nlm.nih.gov/].

308. Sareddy GR, Vadlamudi RK. PELP1: structure, biological function and clinical significance. Gene. 2016;585(1):128-34.

309. Vadlamudi RK, Wang RA, Mazumdar A, Kim Y, Shin J, Sahin A, et al. Molecular cloning and characterization of PELP1, a novel human coregulator of estrogen receptor α. J Biol Chem. 2001;276(41):38272-9.

310. Choi Y, Ko J, Shin J. The Transcriptional Corepressor, PELP1, Recruits HDAC2 and Masks Histones Using Two Separate Domains. Journal of Biological Chemistry. 2004;279(49):50930-41.

311. Nair SS, Mishra SK, Yang Z, Balasenthil S, Kumar R, Vadlamudi RK. Potential Role of a Novel Transcriptional Coactivator PELP1 in Histone H1 Displacement in Cancer Cells. Cancer Research. 2004;64(18):6416-23.

312. Chakravarty D, Tekmal R, Vadlamudi RK. PELP1: A novel therapeutic target for hormonal cancers. IUBMB Life. 2010;62(3):162-9.

313. Vadlamudi RK, Manavathi B, Balasenthil S, Nair SS, Yang Z, Sahin AA, et al. Functional implications of altered subcellular localization of PELP1 in breast cancer cells. Cancer Res. 2005;65(17):7724-32.

314. Rajhans R, Nair S, Holden AH, Kumar R, Tekmal RR. Oncogenic potential of the nuclear receptor coregulator proline-, glutamic acid–, leucine-rich protein 1/modulator of the nongenomic actions of the estrogen receptor. Cancer research. 2007;67(11):5505-12.

315. Gonugunta VK, Sareddy GR, Krishnan SR, Cortez V, Roy SS, Tekmal RR, et al. Inhibition of mTOR signaling reduces PELP1-mediated tumor growth and therapy resistance. Mol Cancer Ther. 2014;13(6):1578-88.

316. Ravindranathan P, Lange CA. Minireview: Deciphering the Cellular Functions of PELP1. Mol Endocrinol. 2015;29(9):1222-9.

317. Vadlamudi RK, Balasenthil S, Broaddus RR, Gustafsson JA, Kumar R. Deregulation of estrogen receptor coactivator proline-, glutamic acid-, and leucine-rich protein-1/modulator of nongenomic activity of estrogen receptor in human endometrial tumors. J Clin Endocrinol Metab. 2004;89(12):6130-8.

318. Vadlamudi RK, Balasenthil S, Sahin AA, Kies M, Weber RS, Kumar R, et al. Novel estrogen receptor coactivator PELP1/MNAR gene and ERβ expression in salivary duct adenocarcinoma: potential therapeutic targets. Human pathology. 2005;36(6):670-5.

319. Yang L, Ravindranathan P, Ramanan M, Kapur P, Hammes SR, Hsieh JT, et al. Central role for PELP1 in nonandrogenic activation of the androgen receptor in prostate cancer. Mol Endocrinol. 2012;26(4):550-61.

320. Słowikowski BK, Gałęcki B, Dyszkiewicz W, Jagodziński PP. Increased expression of proline-, glutamic acid-and leucine-rich protein PELP1 in non-small cell lung cancer. Biomed Pharmacother. 2015;73:97-101.

321. Kashiwaya K, Nakagawa H, Hosokawa M, Mochizuki Y, Ueda K, Piao L, et al. Involvement of the tubulin tyrosine ligase-like family member 4 polyglutamylase in PELP1 polyglutamylation and chromatin remodeling in pancreatic cancer cells. Cancer Res. 2010;70(10):4024-33.

322. Krishnan SR, Nair BC, Sareddy GR, Roy SS, Natarajan M, Suzuki T, et al. Novel role of PELP1 in regulating chemotherapy response in mutant p53-expressing triple negative breast cancer cells. Breast cancer research and treatment. 2015;150(3):487-99.

323. Zhang Y, Dai J, McNamara KM, Bai B, Shi M, Chan MS, et al. Prognostic significance of proline, glutamic acid, leucine rich protein 1 (PELP1) in triple-negative breast cancer: a retrospective study on 129 cases. BMC Cancer. 2015;15:699.

324. Cortez V, Samayoa C, Zamora A, Martinez L, Tekmal RR, Vadlamudi RK. PELP1 overexpression in the mouse mammary gland results in the development of hyperplasia and carcinoma. Cancer Res. 2014;74(24):7395-405.

325. Kumar R, Zhang H, Holm C, Vadlamudi RK, Landberg G, Rayala SK. Extranuclear coactivator signaling confers insensitivity to tamoxifen. Clinical Cancer Research. 2009;15(12):4123-30.

326. Girard BJ, Regan Anderson TM, Welch SL, Nicely J, Seewaldt VL, Ostrander JH. Cytoplasmic PELP1 and ERRgamma protect human mammary epithelial cells from Tam-induced cell death. PLoS ONE 2015;10(3):e0121206.

327. Popov VM, Zhou J, Shirley LA, Quong J, Yeow WS, Wright JA, et al. The Cell Fate Determination Factor DACH1 Is Expressed in Estrogen Receptor-α–Positive Breast Cancer and Represses Estrogen Receptor-α Signaling. Cancer Res. 2009 69(14):5752–60.

328. Kefalopoulou Z, Tzelepi V, Zolota V, Grivas PD, Christopoulos C, Kalofonos H, et al. Prognostic value of novel biomarkers in astrocytic brain tumors: nuclear receptor co-regulators AIB1, TIF2, and PELP1 are associated with high tumor grade and worse patient prognosis. J Neuro-Oncol 2012;106(1):23–31.

329. Grivas PD, Tzelepi V, Sotiropoulou-Bonikou G, Kefalopoulou Z, Papavassiliou AG, Kalofonos H. Expression of ERalpha, ERbeta and co-regulator PELP1/MNAR in colorectal cancer: prognostic significance and clinicopathologic correlations. Cell Oncol. 2009;31(3):235–47.

330. Vadlamudi RK, Wang RA, Mazumdar A, Kim Y, Shin J, Sahin A, et al. Molecular cloning and characterization of PELP1, a novel human coregulator of estrogen receptor α. Journal of Biological Cancer. 2001;12(41): 38272-9.

331. Gonugunta VK, Nair BC, Rajhans R, Sareddy GR, Nair SS, Vadlamudi RK. Regulation of rDNA transcription by proto-oncogene PELP1. PloS one. 2011;6(6):e21095.

332. Malovannaya A, Lanz RB, Jung SY, Bulynko Y, Le NT, Chan DW, et al. Analysis of the human endogenous coregulator complexome. Cell. 2011;145(5):787-99.

333. Fanis P, Gillemans N, Aghajanirefah A, Pourfarzad F, Demmers J, Esteghamat F, et al. Five friends of methylated chromatin target of protein-arginine-methyltransferase [prmt]-1 (chtop), a complex linking arginine methylation to desumoylation. Mol Cell Proteomics. 2012;11(11):1263-73.

334. Nagpal JK, Nair S, Chakravarty D, Rajhans R, Pothana S, Brann DW, et al. Growth factor regulation of estrogen receptor coregulator PELP1 functions via protein kinase A pathway. Mol Cancer Res. 2008;6(5):851-61.

335. Sareddy GR, Zhang Q, Wang R, Scott E, Zou Y, O'Connor JC, et al. Proline-, glutamic acid-, and leucine-rich protein 1 mediates estrogen rapid signaling and neuroprotection in the brain. Proc Natl Acad Sci USA. 2015;112(48):E6673-82.

336. Nair BC, Nair SS, Chakravarty D, Challa R, Manavathi B, Yew PR, et al. Cyclin-Dependent Kinase–Mediated Phosphorylation Plays a Critical Role in the Oncogenic Functions of PELP1. Cancer Res. 2010;70(18):7166-75.

337. Nair BC, Krishnan SR, Sareddy GR, Mann M, Xu B, Natarajan M, et al. Proline, glutamic acid and leucine-rich protein-1 is essential for optimal p53-mediated DNA damage response. Cell Death Differ. 2014;21(9):1409-18.

338. Manavathi B, Nair SS, Wang RA, Kumar R, Vadlamudi RK. Proline-, glutamic acid-, and leucine-rich protein-1 is essential in growth factor regulation of signal transducers and activators of transcription 3 activation. Cancer Res. 2005;65(13):5571-7.

339. Habashy HO, Powe DG, Rakha EA, Ball G, Macmillan RD, Green AR, et al. The prognostic significance of PELP1 expression in invasive breast cancer with emphasis on the ER-positive luminal-like subtype. Breast cancer research treatment. 2010;120(3):603-12.

340. Rajhans R, Nair HB, Nair SS, Cortez V, Ikuko K, Kirma NB, et al. Modulation of in situ estrogen synthesis by proline-, glutamic acid-, and leucine-rich protein-1: potential estrogen receptor autocrine signaling loop in breast cancer cells. Mol Endocrinol. 2008;22(4):649–64.

341. Vadlamudi RK, Rajhans R, Chakravarty D, Nair BC, Nair SS, Evans DB, et al. Regulation of aromatase induction by nuclear receptor coregulator PELP1. J Steroid Biochem Mol Biol. 2010;118(4-5):211-8.

342. Roy S, Chakravarty D, Cortez V, DeMukhopadhyay K, Bandyopadhyay A, Ahn JM, et al. Significance of PELP1 in ER-negative breast cancer metastasis. Mol Cancer Res. 2012;10(1):25-33.

343. Wan J, Li X. PELP1/MNAR suppression inhibits proliferation and metastasis of endometrial carcinoma cells. Oncol Rep. 2012;28(6):2035-42.

344. Dimple C, Nair SS, Rajhans R, Pitcheswara PR, Liu J, Balasenthil S, et al. Role of PELP1/MNAR signaling in ovarian tumorigenesis. Cancer Res. 2008;68(12):4902-9.

345. Cortez V, Mann M, Tekmal S, Suzuki T, Miyata N, Rodriguez-Aguayo C, et al. Targeting the PELP1-KDM1 axis as a potential therapeutic strategy for breast cancer. Breast Cancer Research. 2012;14(4):108.

346. Balasenthil S, Vadlamudi RK. Functional Interactions between the Estrogen Receptor Coactivator PELP1/MNAR and Retinoblastoma Protein. Journal of Biological Chemistry. 2003;278(24):22119-27.

347. Rayala SK, Mascarenhas J, Vadlamudi RK, Kumar R. Altered localization of a coactivator sensitizes breast cancer cells to tumor necrosis factor-induced apoptosis. Mol Cancer Ther. 2006;5(2):230–7.

348. Haas D, White SN, Lutz LB, Rasar M, Hammes SR. The modulator of nongenomic actions of the estrogen receptor (MNAR) regulates transcription-independent androgen receptor-mediated signaling: evidence that MNAR participates in G protein-regulated meiosis in Xenopus laevis oocytes. Mol Endocrinol 2005;19(8):2035–46.

349. Unni E, Sun S, Nan B, McPhaul MJ, Cheskis B, Mancini MA, et al. Changes in androgen receptor non-genotropic signaling correlate with transition of LNCaP cells to androgen independence. Cancer Res. 2004;64(19):7156–68.

350. Wong C, McNally C, Nickbarg E, Komm BS, Cheskis BJ. Estrogen receptor-interacting protein that modulates its nongenomic activity-crosstalk with Src/Erk phosphorylation cascade. Proceedings of the National Academy of Sciences. 2002;99(23):14783-8.

351. Joung I, Strominger JL, Shin J. Molecular cloning of a phosphotyrosine-independent ligand of the p56lck SH2 domain Proc Natl Acad Sci USA. 1996 93 (12):5991-5.

352. Rayala SK, Hollander PD, Balasenthil S, Molli PR, Bean AJ, Vadlamudi RK, et al. Hepatocyte growth factor-regulated tyrosine kinase substrate (HRS) interacts with PELP1 and activates MAPK. J Biol Chem. 2006;281(7):4395–403.

353. Boonyaratanakornkit V. Scaffolding proteins mediating membrane-initiated extra-nuclear actions of estrogen receptor. Steroids. 2011;76(9):877–84.

354. Song RX, Santen RJ. Membrane initiated estrogen signaling in breast cancer Biol Reprod 2006;75(1):9-16.

355. Manavathi B, Kumar R. Steering estrogen signals from the plasma membrane to the nucleus: two sides of the coin J Cell Physiol 2006 207(3):594-604.

356. Manavathi B, Nair SS, Wang RA, Kumar R, Vadlamudi RK. Proline-, glutamic acid-, and leucine-rich protein-1 is essential in growth factor regulation of signal transducers and activators of transcription 3 activation Cancer Res 2005 65(13):5571-7.

357. Xiaofeng Z, Jun-Lin G. Focal adhesion kinase and its signaling pathways in cell migration and angiogenesis. Adv Drug Deliv Rev. 2011 63(8):610–5.

358. Chacón RD, Costanzo MV. Triple-negative breast cancer. Breast Cancer Res. 2010;12(Suppl 2):S3.

359. Perou CM, Sorlie T, Eisen MB, van-de-Rijn M. Molecular portraits of human breast tumours. Nature. 2000;406(6797):747-52.

360. Bartsch R, Ziebermayr R, Zielinski CC, Steger GG. Triple-negative breast cancer. Wien Med Wochenschr. 2010;160:7-8.

361. Kinne DW, Butler JA, Kimmel M, Flehinger BJ, Menendez-Botet C, Schwartz M. Estrogen receptor protein of breast cancer in patients with positive nodes. High recurrence rates in the postmenopausal estrogen receptor-negative group. Archives of Surgery. 1987 122(11):1303-6.

362. Parl FF, Schmidt BP, Dupont WD, Wagner RK. Prognostic significance of estrogen receptor status in breast cancer in relation to tumor stage, axillary node metastasis, and histopathologic grading. Cancer. 1984;54(10):2237-42.

363. Pichon MF, Broet P, Magdelenat H, Delarue JC, Spyratos F, Basuyau JP, et al. Prognostic value of steroid receptors after long-term follow-up of 2257 operable breast cancers. British Journal of Cancer. 1996;3(12):1545-51.

364. Anders CK, Carey LA. Biology, metastatic patterns, and treatment of patients with triple-negative breast cancer. Clin Breast Cancer. 2009;9(Suppl 2):S73-S81.

365. Rakha EA, Abd El Rehim D, Pinder SE, Lewis SA, Ellis IO. E‐cadherin expression in invasive non‐lobular carcinoma of the breast and its prognostic significance. Histopathology. 2005;46(6):685-93.

366. Vadlamudi RK, Kumar R. Functional and biological properties of the nuclear receptor coregulator PELP1/MNAR. Nucl Recept Signal. 2007;5:e004.

367. Nair SS, Nair BC, Cortez V, Chakravarty D, Metzger E, Schüle R, et al. PELP1 is a reader of histone H3 methylation that facilitates oestrogen receptor‐α target gene activation by regulating lysine demethylase 1 specificity. EMBO Rep. 2010;11(6):438-44.

368. Girard BJ, Daniel AR, Lange CA, Ostrander JH. PELP1: A review of PELP1 interactions, signaling, and biology. Mol Cell Endocrinol. 2014;382(1):642-51.

369. Zhang Y, Dai J, McNamara KM, Bai B, Shi M, Chan MS, et al. Prognostic significance of proline, glutamic acid, leucine rich protein 1 (PELP1) in triple-negative breast cancer: a retrospective study on 129 cases. BMC Cancer. 2015;15:699.

370. Habashy HO, Powe DG, Rakha EA, Ball G, Macmillan RD, Green AR, et al. The prognostic significance of PELP1 expression in invasive breast cancer with emphasis on the ER-positive luminal-like subtype. Breast Cancer Res Treat. 2010;120(3):603-12.

371. Griffith LG, Swartz MA. Capturing complex 3D tissue physiology in vitro. Nature Reviews Molecular Cell Biology. 2006;7
(3):211–24.

372. Hebner C, Weaver VM, Debnath J. Modeling morphogenesis and oncogenesis in three-dimensional breast epithelial cultures. Annual Review of Pathology-Mechanisms of Disease 2008;3:313–39.

373. Pampaloni F, Reynaud EG, Stelzer EHK. The third dimension bridges the gap between cell culture and live tissue Nature Reviews Molecular Cell Biology 2007;8(10):839–45.

374. Cukierman E, Pankov R, Yamada KM. Cell interactions with three-dimensional matrices. Current Opininions in Cell Biolology. 2002;14(5):633–9.

375. Cukierman E, Pankov R, Stevens DR, Yamada KM. Taking cell-matrix adhesions to the third dimension. Science. 2001;294(5547):1708–12.

376. Friedl P, Brocker EB. The biology of cell locomotion within three-dimensional extracellular matrix. Cellular and Molecular Life Sciences. 2000;57(1):41–64.

377. Fischbach C, Kong HJ, Hsiong SX, Evangelista MB, Yuen W, Mooney DJ. Cancer cell angiogenic capability is regulated by 3D culture and integrin engagement. Proc Natl Acad Sci USA 2009;106(2):399–404.

378. Kim BJ, Zhao S, Bunaciu RP, Yen A, Wu M. A 3D in situ cell counter reveals that breast tumor cell (MDA-MB-231) proliferation rate is reduced by the collagen matrix density. Biotechnol Prog. 2015 31(4):990-6.

379. Zaman MH, Trapani LM, Siemeski A, MacKellar D, Gong HY, Kamm RD, et al. Migration of tumor cells in 3D matrices is governed by matrix stiffness along with cell-matrix adhesion and proteolysis. Proc Natl Acad Sci USA. 2006;103(29):10889–94.

380. Wolf K, Alexander S, Schacht V, Coussens LM, vonAndrian UH, vanRheenen J, et al. Collagen-based cell migration models in vitro and in vivo. Seminars in Cell & Developmental Biology. 2009;20(8):931–41.

381. Gobin AS, West JL. Cell migration through defined, synthetic extracellular matrix analogues. Faseb Journal. 2002;16(3):751–3.

382. Ulrich TA, Pardo EMD, Kumar S. The Mechanical Rigidity of the Extracellular Matrix Regulates the Structure, Motility, and Proliferation of Glioma Cells Cancer Research. 2009;69(10):4167–74.

383. Park CC, Zhang H, Paravicini M, Gray JW, Baehner F, Park CJ, et al. Beta(1) integrin inhibitory antibody induces apoptosis of breast cancer cells, inhibits growth, and distinguishes malignant from normal phenotype in three dimensional cultures and in vivo Cancer Research. 2006;66(3):1526–35.

384. Bott K, Upton Z, Schrobback K, Ehrbar M, Hubbell JA, Lutolf MP, et al. The effect of matrix characteristics on fibroblast proliferation in 3D gels. Biomaterials. 2010;31(32):8454–64.

385. Tan PS, Teoh SH. Effect of stiffness of polycaprolactone (PCL) membrane on cell proliferation. Materials Science & Engineering C-Biomimetic and Supramolecular Systems. 2007;27(2):304–8.

386. O'Malley BW, Kumar R. Nuclear receptor coregulators in cancer biology Cancer Res 2009;69(21):8217–22.

387. Lydon JP, O'Malley BW. Minireview: steroid receptor coactivator-3: a multifarious coregulator in mammary gland metastasis. Endocrinology. 2011;152(1):19–25.

388. Mishra SK, Mazumdar A, Vadlamudi RK, Li F, Wang RA, Yu W. MICoA, a novel metastasis-associated protein 1 (MTA1) interacting protein coactivator, regulates estrogen receptor-alpha transactivation functions. J Biol Chem 2003;278(21):19209–19.

389. Davies C, Pan H, Godwin J, Gray R, Arriagada R, Raina V, et al. Long-term effects of continuing adjuvant tamoxifen to 10 years versus stopping at 5 years after diagnosis of oestrogen receptor-positive breast cancer: ATLAS, a randomised trial. The Lancet. 2013;381(9869):805-16.

390. Petrelli F, Coinu A, Cabiddu M, Ghilardi M, Lonati V, Barni S. Five or more years of adjuvant endocrine therapy in breast cancer: a meta-analysis of published randomised trials. Breast Cancer Res Treat. 2013;140(2):233-40.

391. Cuzick J, Sestak I, Cawthorn S, Hamed H, Holli K, Howell A, et al. Tamoxifen for prevention of breast cancer: extended long-term follow-up of the IBIS-I breast cancer prevention trial. The Lancet Oncology. 2015;16(1):67-75.

392. Nazarali SA, Narod SA. Tamoxifen for women at high risk of breast cancer. Breast Cancer (Dove Med Press). 2014;6:29-36.

393. DeAbreu FB, Schwartz GN, Wells WA. Personalized therapy for breast cancer. Clin Genet. 2014;86(1):62-7.

394. Siegel RL, Miller KD, Jemal A. Cancer statistics, 2015. CA Cancer J Clin. 2015;65(1):5-29.

395. Pan H, Gray R, Braybrooke J, Davies C, Taylor C, McGale P, et al. 20-Year Risks of Breast-Cancer Recurrence after Stopping Endocrine Therapy at 5 Years. N Engl J Med. 2017;377(19):1836-46.

396. Gerber B, Freund M, Reimer T. Recurrent Breast Cancer. Dtsch Arztebl Int. 2010;107(6):85–91.

397. Da-Silva L, Parry S, Reid L, Keith P, Waddell N, Kossai M, et al. Aberrant expression of E-cadherin in lobular carcinomas of the breast. Am J Surg Pathol. 2008 32(5):773-83.

398. Huang B, Omoto Y, Iwase H, Yamashita H, Toyama T, Coombes RC, et al. Differential expression of estrogen receptor α, β1, and β2 in lobular and ductal breast cancer. Proc Natl Acad Sci USA. 2014 111(5):1933-8.

399. Ciriello G, Gatza ML, Beck AH, Wilkerson MD, Rhie SK, Pastore A, et al. Comprehensive molecular portraits of invasive lobular breast cancer. Cell. 2015;163(2):506-19.

400. Coradini D, Pellizzaro C, Veneroni S, Ventura L, Daidone MG. Infiltrating ductal and lobular breast carcinomas are characterised by different interrelationships among markers related to angiogenesis and hormone dependence. Br J Cancer. 2002;87(10):1105-11.

401. Jiang WG, Mansel RE. E-cadherin complex and its abnormalities in human breast cancer. Surg Oncol. 2000 9(4):151-71.

402. Brann DW, Zhang QG, Wang RM, Mahesh VB. PELP1—a novel estrogen receptor-interacting protein. Mol Cell Endocrinol. 2008;290(1-2):2-7.

403. Győrffy B, Hatzis C, Sanft T, Hofstatter E, Aktas B, Pusztai L. Multigene prognostic tests in breast cancer: past, present, future. Breast Cancer Res. 2015 27(17):11.

404. Chakravarty D, Roy SS, Babu CR. Therapeutic targeting of PELP1 prevents ovarian cancer growth and metastasis. Clin Cancer Res. 2011;17 (8):2250–9.

405. Vallabhaneni S, Nair BC, Cortez V. Significance of ER-Src axis in hormonal therapy resistance. Breast Cancer Res Treat 2011;130(2):377–85.

406. Nair BC, Vallabhaneni S, Tekmal RR, Vadlamudi RK. Roscovitine confers tumor suppressive effect on therapy-resistant breast tumor cells. Breast Cancer Res. 2011;13(3):80.

407. Daniel AR, Gaviglio AL, Knutson TP, Ostrander JH, D'Assoro AB, Ravindranathan P, et al. Progesterone receptor-B enhances estrogen responsiveness of breast cancer cells via scaffolding proteins Oncogene 2015;34 (4):506–15.

408. Bennani-Baiti I. Integration of ERalpha-PELP1-HER2 signaling by LSD1 (KDM1A/AOF2) offers combinatorial therapeutic opportunities to circumventing hormone resistance in breast cancer. Breast Cancer Res. 2012;14(5):112.

409. Mann M, Cortez V, Vadlamudi R. PELP1 oncogenic functions involve CARM1 regulation Carcinogenesis 2013;34(7):1468–75.

410. Bartlett DL, Liu Z, Sathaiah M. Oncolytic viruses as therapeutic cancer vaccines. Mol Cancer. 2013;12(1):103.

411. Adjuvant Breast Cancer Trials Collaborative Group. Ovarian ablation or suppression in premenopausal early breast cancer: results from the international adjuvant breast cancer ovarian ablation or suppression randomized trial. J Natl Cancer Inst. 2007 99(7):516-25.

412. Habashy HO, Powe DG, Staka CM, Rakha EA, Ball G, Green AR, et al. Transferrin receptor (CD71) is a marker of poor prognosis in breast cancer and can predict response to tamoxifen. Breast Cancer Res Treat 2010;119(2):283-93.

7.0 Appendix

7.1 Cell lysis buffer to obtain total soluble protein

Component	**Mass/Volume for 100ml Lysis Buffer**	**Final Concentration**
Tris Base	0.61g	50mM
EGTA	0.19g	5mM
NaCl	0.87g	150mM
Trixton X-100	1ml	1% (v/v)
H_2O	100ml	-

- Final solution was adjusted to pH 7.7 and stored at 4°C
- Protease inhibitors were added to the cell lysis buffer immediately before use

7.2 Protease inhibitors used in conjunction with cell lysis buffer

Inhibitor	**Stock Conc.**	**Solvent**	**Volume in 10ml cell lysis buffer**	**Final Conc.**
Sodium Orthovanadate	100mM	H_2O	200µl	2mM
PMSF	100mM	Isopropranol	100µl	1mM
Sodium Fluoride	2.5M	H_2O	100µl	25mM
Sodium Molybdate	1M	H_2O	100µl	10mM
Phenylarsinine	20mM	Chloroform	10µl	20µM
Leupeptin	5mg/ml	H_2O	20µl	10µg/ml
Apoprotinin	2mg/ml	H_2O	40µl	8µg/ml

7.3 BSA standard curve for Bio-Rad® micro-assay procedure (96-well plate) – based on the Bradford Assay

BSA Conc. (mg/ml)	**Volume (µl) of BSA Stock (1mg/ml)**	**Volume of dH_2O (µl)**
0	0	400
5	2	398
10	4	396
15	6	394
20	8	392
25	10	390

7.4 Excel spreadsheet used to calculate standard curve and stock protein concentration of samples as part of the Bio-Rad Micro assay procedure

BSA Standard Line

OD (595nm)

Protein conc. (µg/ml)

Delete values in table columns headed 1, 2 and 3 and replace with new values for your standards and samples. Do not delete values in any other column as there may be formulas attached. These values should update automatically when you enter your raw data.
Similarly, the chart above should also update. Use the chart only as as a guide to assess whether you need to discard any of the points. All the protein calculations are based on the line of best fit (regression analysis) and not on the Excel chart above.

Protein conc (µg/ml)	OD (595nm)					
	1	2	3	Mean	Corrected	Protein blank
0	0.311	0.293		0.302	0.000	0.302
5	0.362	0.366		0.364	0.062	0.302
10	0.411	0.413		0.412	0.110	0.302
15	0.44	0.48		0.460	0.158	0.302
20	0.482	0.484		0.483	0.181	0.302
25	0.522	0.531		0.527	0.225	0.302
30				#DIV/0!	#DIV/0!	0.302

Mean OD - the average of 3 replicate readings
Corrected OD - the mean OD minus the OD for the protein blank.
The mean ODs are corrected so that the standard line passes through the origin

To calculate **the slope** of the standard line use the following equation:

$b = \Sigma xy - (\Sigma x \Sigma y)/n$
$\Sigma x^2 - (\Sigma x)^2/n$

Protein conc(µg/ml)	OD (corrected)					
x	y	xy	$(\Sigma x \Sigma y)/n$	x^2	$(\Sigma x)^2/n$	b (slope)
0	0.000	0.00		0.00		
5	0.062	0.31		25.00		
10	0.110	1.10		100.00		
15	0.158	2.37		225.00		
20	0.181	3.62		400.00		
25	0.225	5.61		625.00		
30	#DIV/0!	#DIV/0!		900.00		
75	0.736	13.01	9.19	1375.00	937.5	0.0087
Σx	Σy	Σxy	$(\Sigma x \Sigma y)/n$	Σx^2	$(\Sigma x)^2/n$	b

Sample No	Sample Identifier	OD (595nm)			Mean OD_{595nm}	Corrected	Protein blank	Slope of Standard Line (b)	Diluted Protein conc (µg/ml) 1/400 dil	Stock Protein conc (µg/µl)
		1	2	3						
1	NT 100	0.627	0.656		0.642	0.340	0.302	0.0087	38.90	15.56
2	P 100	0.674	0.653		0.663	0.367	0.302	0.0087	41.99	16.80
3	NT 150	0.663	0.688		0.676	0.374	0.302	0.0087	42.79	17.12
4	P150	0.651	0.68		0.666	0.364	0.302	0.0087	41.64	16.66
5	NT200	0.673	0.688		0.681	0.379	0.302	0.0087	31.91	12.76
6	P200	0.559	0.584		0.572	0.270	0.302	0.0087	30.88	12.35
7	NT100TAM	0.454	0.479		0.467	0.165	0.302	0.0087	18.85	7.54
8	P100TAM	0.442	0.463		0.453	0.151	0.302	0.0087	17.24	6.90

7.5 SDS-PAGE Running Buffer

Component	**Mass/Volume for 1L Running Buffer**	**Final Conc.**
Tris Base	3.03g	0.25M
Glycine	14.4g	1.92M
SDS	1g	0.1% (v/v)
H_20	1L	-

- Final solution was adjusted to pH 8.3 and stored at room temperature

7.6 Laemmli 4x Sample Loading Buffer

Component	**Mass/Volume for 10ml of Loading Buffer**
SDS	800mg
Glycerol	4ml
0.5M Stacking gel buffer (pH 6.8)	4.8ml
dH_20	1.2
Bromophenol Blue	0.001 – 0.002% (w/v)

- 3.08mg of DTT was added and dissolved per ml of loading buffer immediately before use

7.7 Western Blot Transfer Buffer

Component	**Mass/Volume for 1L of Transfer Buffer**	**Final Conc.**
Tris Base	3.03g	0.25M
Glycine	14.4g	1.92M
Methanol	200ml	20% (v/v)
H_20	800ml	-

- Transfer Buffer was made and used immediately for Western Blotting

7.8 Tris-buffered saline (TBS)

Component	**Mass/Volume for 1L of TBS**	**Final Conc.**
Tris Base	1.21g	10mM
NaCl	5.8g	100nM
H_20	1L	-

7.9 Tris-buffered saline with Tween (TBST)

Component	**Mass/Volume for 1L of TBST**	**Final Conc.**
Tris Base	1.21g	10mM
NaCl	5.8g	100nM
Tween 20	0.5ml	0.05% (v/v)
H_20	1L	-

7.10 SDS-PAGE Gel Components

Stacking Gel

Reagent	**Volume**
dH_20	6.1ml
Tris-HCL Buffer (Ph6.8)	2.5ml
30% Acrylamide	1.3ml
10% SDS	100µl
10% APS	50µl
TEMED	10µl

- The table provides volumes needed to make enough solution for 2 gels

Resolving Gel

Reagent	**% Gel**						
	5%	**7.5%**	**10%**	**12%**	**17%**	**18%**	**20%**
dH_20	11.2ml	9.6ml	8ml	6.6ml	3ml	2.4ml	1ml
Tris-HCL Buffer (Ph8.8)	5ml	5ml	5ml	5ml	5ml	5ml	5ml
30% Acrylamide	3.4ml	5ml	6.8ml	8ml	11.6ml	12.2ml	13.6ml
10% SDS	200µl	200µl	200µl	200µl	200µl	200µl	200µl
10% APS	200µl	200µl	200µl	200µl	200µl	200µl	200µl
TEMED	12µl	12µl	12µl	12µl	12µl	12µl	12µl

- The table provides volumes needed to make enough solution for 2 gels

7.11 Volumes for 3D Cell Culture

					3D Embedded		3D on-top
	No. Wells	Diameter (mm)	Area (cm^2)	Medium Volume (µl)	Matrix Coat (µl)	Matrix Plate (µl)	Matrix Coat (µl)
Dish	-	60	28.3	5000	250	3600	850
Plates	6	35	9.6	2000	120	1200	500
	24	16	2.0	500	50	300	120
	48	10	0.75	200	30	150	80
	96	6	0.26	60	5	75	15

7.12 siRNA Transfection Reagents

- **100nm working solution**

	Tube A			Tube B		Tubes A + B		
Required Volume (ml)	siRNA (µl)	x1 siRNA Buffer (µl)	WRPMI (µl)	WRPMI (µl)	Lipid (µl)	Total Volume A + B (µl)	Experimental Medium (µl) 1:5 dilution	Final Volume (µl)
1	5	45	50	98.4	1.6	200	800	1000
2	10	90	100	196.8	3.2	400	1600	2000
3	15	135	150	295.2	4.8	600	2400	3000
4	20	180	200	393.6	6.4	800	3200	4000
5	25	225	250	492	8	1000	4000	5000
6	30	270	300	590.4	9.6	1200	4800	6000
7	35	315	350	688.8	11.2	1400	5600	7000
8	40	360	400	787.2	12.8	1600	6400	8000
9	45	405	450	885.6	14.4	1800	7200	9000
10	50	450	500	984	16	2000	8000	100000

- **150nm working solution**

	Tube A			Tube B		Tubes A + B		
Required Volume (ml)	siRNA (µl)	x1 siRNA Buffer (µl)	WRPMI (µl)	WRPMI (µl)	Lipid (µl)	Total Volume A + B (µl)	Experimental Medium (µl)	Final Volume (µl)
1	7.5	67.5	25	97.6	2.4	200	800	1000
2	15	135	50	195.2	4.8	400	1600	2000
3	22.5	202.5	75	292.8	7.2	600	2400	3000
4	30	270	100	390.4	9.6	800	3200	4000
5	37.5	328.5	125	488	12	1000	4000	5000
6	45	405	150	585.6	14.4	1200	4800	6000
7	52.5	472.5	175	683.2	16.8	1400	5600	7000
8	60	540	200	780.8	19.2	1600	6400	8000
9	67.5	607.5	225	878.4	21.6	1800	7200	9000
10	75	675	250	976	24	2000	8000	100000

- **200nm working solution**

	Tube A			**Tube B**		**Tubes A + B**		
Required Volume (ml)	**siRNA (µl)**	**x1 siRNA Buffer (µl)**	**WRPMI (µl)**	**WRPMI (µl)**	**Lipid (µl)**	**Total Volume A + B (µl)**	**Experimental Medium (µl)**	**Final Volume (µl)**
1	10	90	0	97.6	2.4	200	800	1000
2	20	180	0	195.2	4.8	400	1600	2000
3	30	270	0	292.8	7.2	600	2400	3000
4	40	360	0	390.4	9.6	800	3200	4000
5	50	450	0	488	12	1000	4000	5000
6	60	540	0	585.6	14.4	1200	4800	6000
7	70	630	0	683.2	16.8	1400	5600	7000
8	80	720	0	780.8	19.2	1600	6400	8000

7.13 siRNA Target Sequences

7.13.1 Dharmacon™, L-003877-00-0005, ON-TARGET plus Human CDH1 (999) siRNA– SMARTpool

ON-TARGETplus SMARTpool siRNA J-003877-08, CDH1
Target Sequence: GGCCUGAAGUGACUCGUAA
Mol. Wt: 13,444.8 (g/mol)
Ext. Coeff: 366,057 (L/mol.cm)

ON-TARGETplus SMARTpool siRNA J-003877-09, CDH1
Target Sequence: GAGAACGCAUUGCCACAUA
Mol. Wt: 13,429.9 (g/mol)
Ext. Coeff: 368,905 (L/mol.cm)

ON-TARGETplus SMARTpool siRNA J-003877-10, CDH1
Target Sequence: GGGACAACGUUUAUUACUA
Mol. Wt: 13,399.9 (g/mol)
Ext. Coeff: 383,679 (L/mol.cm)

ON-TARGETplus SMARTpool siRNA J-003877-11, CDH1
Target Sequence: GACAAUGGUUCUCCAGUUG
Mol. Wt: 13,429.9 (g/mol)
Ext. Coeff: 369,628 (L/mol.cm)

7.13.2 Dharmacon™, L-004463-00-0005, ON-TARGET plus Human PELP-1 (27043) siRNA – SMARTpool

ON-TARGETplus SMARTpool siRNA J-004463-05, PELP-1

Target Sequence: GACCAAGGUGUAUGCGAUA

Mol. Wt: 13,429.9 (g/mol)

Ext. Coeff: 372,821 (L/mol.cm)

ON-TARGETplus SMARTpool siRNA J-004463-06, PELP-1

Target Sequence: GAGGAUUUGACAGUUAUUA

Mol. Wt: 13,384.9 (g/mol)

Ext. Coeff: 386,527 (L/mol.cm)

ON-TARGETplus SMARTpool siRNA J-004463-07, PELP-1

Target Sequence: GUAAUGCACGUCUCAGUUC

Mol. Wt: 13,429.8 (g/mol)

Ext. Coeff: 370,863 (L/mol.cm)

ON-TARGETplus SMARTpool siRNA J-004463-08, PELP-1

Target Sequence: GCGAGAAGAUAGCCUUGAG

Mol. Wt: 13,444.8 (g/mol)

Ext. Coeff: 364,722 (L/mol.cm)

7.14 Plasmid DNA transfection reagents

Container	Surface area (cm^2)	Typical total volume of medium (ml)	Starting volume of FuGENE 6 Reagent (µl)		Starting mass of DNA (µg)		Approximate total volume of complex (µl)
			µl Amount	µl Range	µg Amount	µg Range	
96 well (1 well)	0.3	0.1–0.2	0.15	0.1–0.3	0.05	0.03–0.06	5
24 well (1 well)	1.9	0.5–2.0	0.6	0.6–1.8	0.2	0.2–0.4	20
12 well (1 well)	3.8	0.5–1.0	1.5	1.2–3.6	0.5	0.4–0.8	50
35 mm dish	8	2.0	3.0	3.0–9.0	1.0	1.0–2.0	100
6 well (1 well)	9.4	2.0	3.0	3.0–9.0	1.0	1.0–2.0	100
60 mm dish	21	4.0–6.0	6.0	6.0–20.0	2.0	2.0–4.5	200
10 cm dish	55	10.0	18.0	17.0–51.0	6.0	5.6–11.0	600
T-25 flask	25	5.0–7.0	7.5	7.5–24.0	2.5	2.5–5.3	250
T-75 flask	75	15.0–30.0	24.0	24.0–72.0	8.0	8.0–16.0	800

7.15 List of proteins identified by literature review with differences in molecular expression between MCF-7 and T47D cell lines.

- Phosphoserine phosphatase
- Heat shock protein beta-1
- Peroxiredoxin-4
- Protein CDV3 homolog
- N(G),N(G)-dimethylarginine dimethylaminohydrolase 2
- Uncharacterized protein EIF4E
- cDNA FLJ76387
- N(G),N(G)-dimethylarginine dimethylaminohydrolase 2
- Prohibitin
- Glutathione S-transferase Mu 2
- 5′(3′)-deoxyribonucleotidase
- 17β-Hydroxysteroid dehydrogenase 10
- Protein-L-isoaspartate(D-aspartate) O-methyltransferase
- Cathepsin B
- Heat shock protein
- Nicotinate-nucleotide pyrophosphorylase
- Malate dehydrogenase
- L-lactate dehydrogenase A chain
- cDNA, FLJ93804
- Proteasome subunit alpha type-2
- Ras-related protein Rab-7a
- Beta-hexosaminidase subunit beta chain A
- StAR-related lipid transfer protein 5
- Molybdenum cofactor synthesis protein 2 large subunit
- RAB1B protein
- cDNA FLJ75516, highly similar to Xenopus tropicalis ubiquitin C, mRNA
- cDNA, FLJ92406
- Heme-binding protein 1
- RNA polymerase II subunit A C-terminal domain phosphatase SSU72
- cDNA FLJ78235
- Proteasome subunit beta type-4
- Glutathione S-transferase theta-2
- Proteasome subunit beta type-3
- NADH dehydrogenase flavoprotein 2, mitochondrial
- Brain type mu-glutathione S-transferase(3095)
- Farnesyltranstransferase
- Splicing factor
- Actin, cytoplasmic 1
- EF-hand domain-containing protein D
- 3-hydroxyisobutyrate dehydrogenase, mitochondri
- STIP1 homology and U box-containing protein 1
- Heterogeneous nuclear ribonucleoproteins A2/B1

- 39S ribosomal protein L3
- Cathepsin D
- cDNA, FLJ92320
- Uncharacterized protein PSME2
- Inositol monophosphatase
- Chloride intracellular channel protein 1
- Density-regulated protein
- Heat shock 70 kDa protein 1
- A-kinase anchor protein 3
- Caspase-3 subunit p12
- Nuclear protein Hcc-1
- Guanine nucleotide-binding protein subunit beta-2-like 1
- G1/S-specific cyclin-D3
- ATP synthase subunit gamma
- Carbonyl reductase [NADPH] 1
- Electron transfer flavoprotein subunit alpha
- Voltage-dependent anion-selective channel protein 1
- Pyrroline-5-carboxylate reductase
- FK506-binding protein 5
- Vacuolar ATP synthase subunit B, brain isoform
- cDNA FLJ75447, highly similar to Homo sapiens peptidase D, mRNA
- Tubulin beta chain
- Uncharacterized protein WARS
- Cytosolic non-specific dipeptidase
- Adenylyl cyclase-associated protein 2
- Translation initiation factor eIF-2B subunit gamma
- Charged multivesicular body protein 2a(4364)
- Desmoplakin
- Junction plakoglobin
- Oligoribonuclease, mitochondrial(2399)
- Ras-related protein Rab-5C
- Cell division control protein 2 homolog
- 2,4-dienoyl-CoA reductase
- Elongation factor Ts
- cDNA FLJ76011
- Destrin
- Cofilin-1(4492)
- Pyridoxine 5'-phosphate oxidase
- Isopentenyl-diphosphate Delta-isomerase 1
- Calcyphosin
- Protein S100-A14
- Calmodulin-like 5
- NADP-dependent malic enzyme
- T-complex protein 1 subunit alpha
- Prolyl 4-hydroxylase subunit alpha-1
- Heterogeneous nuclear ribonucleoprotein K
- Triosephosphate isomerase

- Protein ETHE1
- Heterogeneous nuclear ribonucleoprotein H3
- Aflatoxin B1 aldehyde reductase member 2
- Glycerol-3-phosphate dehydrogenase 1-like
- Heterogeneous nuclear ribonucleoprotein D-like
- Latexin
- Proteasome activator complex subunit 1
- cDNA, FLJ96310
- cDNA, FLJ94267
- NAD-dependent deacetylase sirtuin-3
- SH3 domain-binding glutamic acid-rich-like
- Myosin regulatory light chain 2
- Profilin
- Cellular retinoic acid-binding protein 1
- TRM112-like protein
- Chromobox protein homolog 3
- BH3-interacting domain death agonist p11
- Proline-, glutamic acid- and leucine-rich protein 1
- Chromobox protein homolog 5
- Beta-galactosidase
- REST corepressor 1
- Nitrilase homolog 2
- Reticulocalbin-1(1904)
- Human P37 AUF1
- cAMP response element-binding protein
- Coiled-coil domain-containing protein
- CHD9 protein
- Transcriptional repressor NF-X1
- MHC class I antigen
- Probable global transcription activator
- Thioredoxin-dependent peroxide reductase, mitochondrial
- Transgelin-2
- Interleukin-10
- Telomerase-binding protein EST1A
- Bullous pemphigoid antigen 1
- cDNA, FLJ94446
- Cytochrome c-releasing factor 21

7.16 Supplemental Files

- **Supplemental File 1 – Time lapse microscopy of spheroid invasion assay using the MCF-7 cell line.** MCF-7 cells were seeded into ULA round bottom wells (5.000 cells/well) to form spheroids before being embedded in a Matrigel® matrix. Spheroids were imaged by time lapse microscopy at 5-minute time intervals for 72 hours.

- **Supplemental File 2 – Time lapse microscopy of spheroid invasion assay using the MDA-MD-231 cell line.** MDA-MB-231 cells were seeded into ULA round bottom wells (5.000 cells/well) to form spheroids before being embedded in a Matrigel® matrix. Spheroids were imaged by time lapse microscopy at 5-minute time intervals for 72 hours.

- **Supplemental File 3 – Time lapse microscopy of "fried-egg" invasion assay using the MDA-MD-231 cell line.** MDA-MB-231 cells were seeded into ULA round bottom wells (5.000 cells/well) to form spheroids before being transferred to Matrigel® membrane. Spheroids were imaged by time lapse microscopy at 5-minute time intervals for 72 hours.

- **Supplemental File 4 – Time lapse microscopy of spheroid formation using MCF-7 cells.** MCF-7 cells were seeded into ULA round bottom wells (5.000 cells/well) and imaged using time lapse microscopy at 5-minute time intervals for 72 hours.

- **Supplemental File 5 – Time lapse microscopy of spheroid formation using T47D cells.** T47D cells were seeded into ULA round bottom wells (5.000 cells/well) and imaged using time lapse microscopy at 5-minute time intervals for 72 hours.

- **Supplemental File 6 – Time lapse microscopy of spheroid formation using BT474 cells.** BT474 cells were seeded into ULA round bottom wells (5.000 cells/well) and imaged using time lapse microscopy at 5-minute time intervals for 72 hours.